

## PDF hosted at the Radboud Repository of the Radboud University Nijmegen

The following full text is a publisher's version.

For additional information about this publication click this link.

<http://hdl.handle.net/2066/205871>

Please be advised that this information was generated on 2023-04-13 and may be subject to change.

# Stargardt disease

Clinical, genetic and psychological characteristics

Nathalie M. Bax

The work presented in this thesis was carried out within the Radboud Institute for Health Sciences.

Research described in this thesis was financially supported by Stichting A.F. Deutman Researchfonds Oogheelkunde; Nederlandse Oogonderzoek Stichting; Gelderse Blindenstichting; Deutsche Forschungsgemeinschaft; BONFOR GEROK Program, Faculty of Medicine, University of Bonn; the National Institute for Health Research Biomedical Research Centre at Moorfields Eye Hospital National Health Service Foundation Trust and UCL Institute of Ophthalmology; Fight for Sight; The Macular Society; Moorfields Eye Hospital Special Trustees; Moorfields Eye Charity; the Foundation Fighting Blindness; Retina UK; and by the following foundations that contributed through Uitzicht: Stichting MD fonds, Landelijke Stichting voor Blinden en Slechtienden, and Oogfonds.

All funding organizations had no role in the design or conduct of this research. They provided unrestricted grants.

©2019, Nathalie M. Bax, Nijmegen, the Netherlands

No other parts of this publication may be reproduced or transmitted in any form without prior written permission by the copyright holder.

Cover design:	Nathalie M. Bax
Lay-out:	Theo Hafmans Fotografie
Photograph of the author:	DUTZU Photography
Printed by:	Ipskamp Printing B.V.
ISBN:	978-94-028-1641-9

# Stargardt disease

Clinical, genetic and psychological characteristics

## PROEFSCHRIFT

ter verkrijging van de graad van doctor  
aan de Radboud Universiteit Nijmegen  
op gezag van de rector magnificus prof. dr. J.H.J.M. van Krieken,  
volgens besluit van het college van decanen  
in het openbaar te verdedigen op  
donderdag 29 augustus 2019  
om 14.30 uur precies

door

**Nathalie Martine Bax**  
geboren op 14 mei 1984  
te Gouda

**Promotoren:**

prof. dr. C.B. Hoyng  
prof. dr. F.P.M. Cremers

**Manuscriptcommissie:**

prof. dr. J.A.M. Smeitink  
prof. dr. M.M. van Genderen (UMC Utrecht)  
prof. dr. S.M. Downes (University of Oxford, Verenigd Koninkrijk)

**Paranimfen**

Charlotte de Bie  
Anne-Fleur Klandermans

*"To suppose that the eye with all its inimitable contrivances for adjusting the focus to different distances, for admitting different amounts of light, and for the correction of Spherical and chromatic aberration, could have been formed by natural selection, seems, I freely confess, absurd in the highest degree. When it was first said that the sun stood still and the world turned round, the common sense of mankind declared the doctrine false; but the old saying of Vox populi, vox Dei, as every philosopher knows, cannot be trusted in science. Reason tells me, that if numerous gradations from a simple and imperfect eye to one complex and perfect can be shown to exist, each grade being useful to its possessor, as is certain the case; if further, the eye ever varies and the variations be inherited, as is likewise certainly the case; and if such variations should be useful to any animal under changing conditions of life, then the difficulty of believing that a perfect and complex eye could be formed by natural selection, though insuperable by our imagination, should not be considered as subversive of the theory. How a nerve comes to be sensitive to light, hardly concerns us more than how life itself originated; but I may remark that, as some of the lowest organisms, in which nerves cannot be detected, are capable of perceiving light, it does not seem impossible that certain sensitive elements in their sarcode should become aggregated and developed into nerves, endowed with this special sensibility."*

*"On the Origin of Species", 1859*

*Charles Darwin*

# Stargardt disease

Clinical, genetic and psychological characteristics

CHAPTER 1	<b>Introduction</b>	9
CHAPTER 2	<b>Clinical characteristics of Stargardt disease</b>	45
2.1	Early-onset Stargardt disease Stanley Lambertus, Ramon A.C. van Huet, <a href="#">Nathalie M. Bax</a> , Lies H. Hoefsloot, Frans P.M. Cremers, Camiel J.F. Boon, B. Jeroen Klevering, and Carel B. Hoyng <i>Ophthalmology</i> 2015;122(2):335-44	47
2.2	The absence of fundus abnormalities in Stargardt disease <a href="#">Nathalie M. Bax</a> , Stanley Lambertus, Frans P.M. Cremers, B. Jeroen Klevering, and Carel B. Hoyng <i>Graefe's Archive for Clinical and Experimental Ophthalmology</i> , 2019;257(6):1147-1157	67
2.3	Foveal sparing in Stargardt disease Ramon A.C. van Huet*, <a href="#">Nathalie M. Bax*</a> , S. Carla Westeneng- Van Haften, Muhamed Muhamed, Marijke N. Zonneveld- Vrieling, Lies H. Hoefsloot, Frans P.M. Cremers, Camiel J.F. Boon B. Jeroen Klevering, and Carel B. Hoyng <i>Investigative Ophthalmology and Visual Science</i> 2014;55(11):7467-78 *shared first authors	87
2.4	Foveal sparing in central retinal dystrophies <a href="#">Nathalie M. Bax</a> , Dyon Valkenburg, Stanley Lambertus, B. Jeroen Klevering, Camiel J.F. Boon, Frank G Holz, Frans P.M. Cremers, Monika Fleckenstein, Moritz Lindner*, and Carel B. Hoyng* <i>Investigative Ophthalmology and Visual Science, In Press</i> *shared last authors	111
2.5	Asymmetric inter-eye progression in Stargardt disease Stanley Lambertus, <a href="#">Nathalie M. Bax</a> , Joannes M.M. Groenewoud, Frans P.M. Cremers, Gert Jan van der Wilt, B. Jeroen Klevering, Thomas Theelen, and Carel B. Hoyng <i>Investigative Ophthalmology and Visual Science</i> 2016;57(15):6824- 6830	139

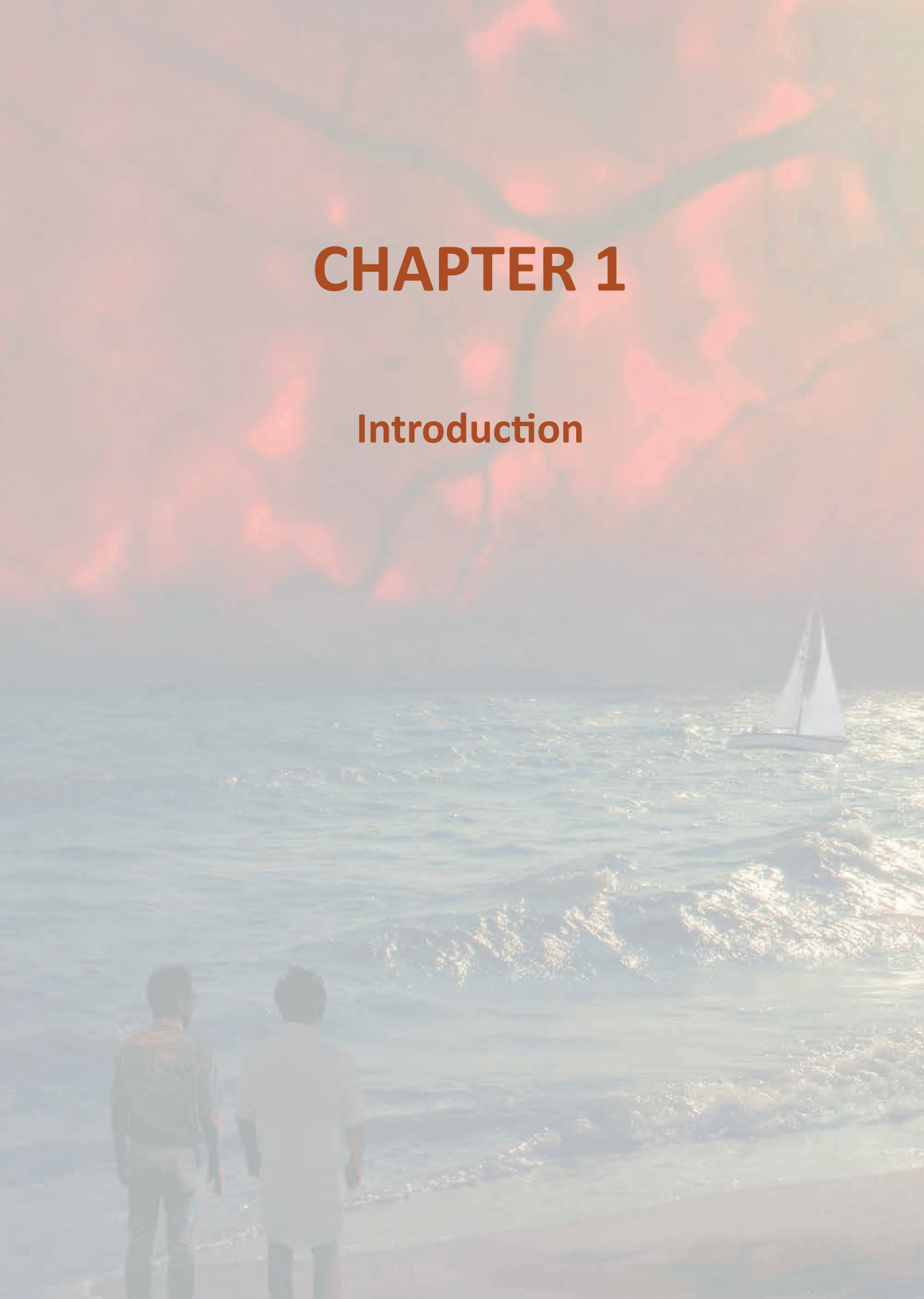
CHAPTER 3	<b>Identification, registry and functional assessment of <i>ABCA4</i> variants</b>	159
3.1	In silico functional meta-analysis of 5,962 <i>ABCA4</i> variants in 3,928 retinal dystrophy cases. Stéphanie S. Cornelis, <a href="#">Nathalie M. Bax</a> , Jana Zernant, Rando Allikmets, Lars G. Fritsche, Johan T. den Dunnen, M. Ajmal, Carel B. Hoyng, and Frans P.M. Cremers <i>Human Mutation 2017;38(4):400-408</i>	161
3.2	Heterozygous deep-intronic variants and deletions in <i>ABCA4</i> in persons with retinal dystrophies and one exonic <i>ABCA4</i> variant. <a href="#">Nathalie M. Bax</a> *, Riccardo Sangermano*, Susanne Roosing*, Alberta A. Thiadens, Lies H. Hoefsloot, L. Ingeborgh van den Born, Milan Phan, B. Jeroen Klevering, S. Carla Westeneng-van Haaften, Terry A. Braun, Marijke N. Zonneveld-Vrieling, Ilse J. de Wijs, Merve Mutlu, Ed M. Stone, Anneke I. den Hollander, Caroline C.W. Klaver, Carel B. Hoyng, and Frans P.M. Cremers <i>Human Mutation 2015;36(1):43-7</i> *shared first authors	207
3.3	Photoreceptor progenitor mRNA analysis reveals exon skipping resulting from the <i>ABCA4</i> c.5461-10T →C mutation in Stargardt disease. Riccardo Sangermano, <a href="#">Nathalie M. Bax</a> , Miriam Bauwens, L. Ingeborgh van den Born, Elfride de Baere, Alex Garanto, Rob W. Collin, Angélique S. Goercharn-Ramlal, Anke H. den Engelsman-van Dijk, Karl Rohrschneider, Carel B. Hoyng, Frans P.M. Cremers, Silvia Albert <i>Ophthalmology 2016;123(6):1375-85.</i>	223
CHAPTER 4	<b>Quality of life in Stargardt patients</b>	255
	Quality of life in Stargardt patients <a href="#">Nathalie M. Bax</a> , Stanley Lambertus, Lena Ye, Petronella J.M. van den Wittenboer, B. Jeroen Klevering, Chris M. Verhaak, Carel B. Hoyng <i>Submitted for publication</i>	
CHAPTER 5	<b>Discussion</b>	277
CHAPTER 6	<b>Epilogue</b>	299
	Summary	300
	Samenvatting	303
	List of publications	306
	PhD portfolio	310
	Curriculum Vitae	312
	Acknowledgements/ Dankwoord	313





# CHAPTER 1

## Introduction



## 1.1 General introduction

### The human retina

- Anatomical landmarks*
- Anatomy of the retina*
- Retinal processes*
- Retinal imaging*
- Retinal function tests*

### Retinal dystrophies

- Classification of retinal dystrophies*
- Rod-cone dystrophies*
- Cone and cone-rod dystrophies*
- Macular dystrophies*

## 1.2 Introduction to Stargardt disease

### Stargardt disease

- History*
- Clinical characteristics*
- ABCA4 function*

### Missing heritability in Stargardt disease

- Stargardt-like phenotypes due to mutations in other genes*
- Structural variants*
- Misinterpreted variants*
- Frequent coding variants*
- Non-coding variants*

### Quality of life in Stargardt disease patients

## 1.3 Aims and outline of this thesis

## 1.1 General introduction

The eye is a very fascinating organ that we share with many species. Every eye of each species has evolved to optimize its survival in their natural habitat, resulting in a diversity of eye types. The human eye has evolved to see objects from a distance, but also enables detailed nearby vision. We can see colors and details by daylight, as well as some colors and details in nightfall. The anatomical structure of the human eye is depicted in [Figure 1](#).

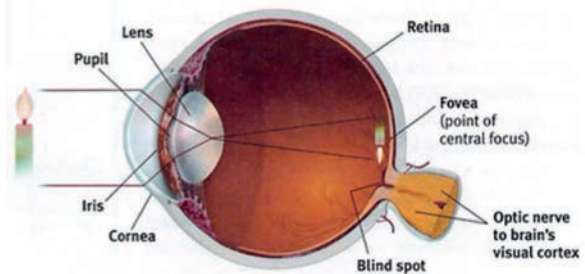


**Figure 1.** (Adapted from Pascal Goetgheluck/Science source).

## The human retina



### Anatomical landmarks

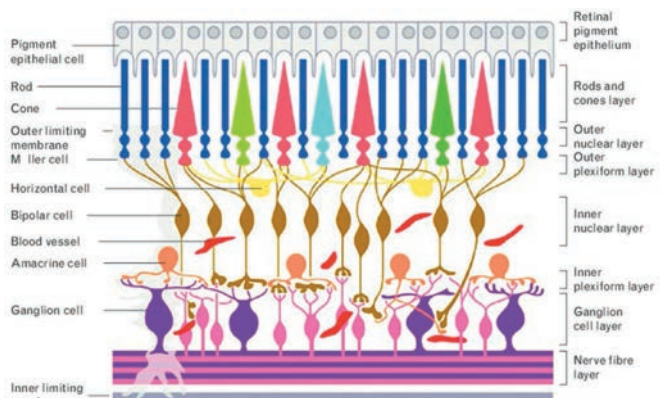
The retina is a complex transparent tissue that covers the inside of the back two-thirds of the eyeball. The anterior and posterior retina are divided by the equator, and the ora serrata is the junction between the retina and ciliary body. The macula, optic nerve and the vascular arcades complete the posterior pole.

**Figure 2:** Topography of the posterior pole of the retina. Color fundus photograph with overlaying grid chart to define the subfields of the macula and size/ degrees.

### Anatomy of the retina

The retina is formed embryonically from neural tissue and is connected to the brain by the optic nerve. The retina consists of several layers as depicted in [Figure 3](#).

**Figure 3:** Adapted from Lober et al, 2016 [1].



The photoreceptor layer and retinal pigment epithelium layer will be discussed in further detail below.

### Photoreceptor cells

There are two types of photoreceptor cells: rods and cones. They are differentiated structurally by their distinctive shapes and functionally by their sensitivity to different frequencies and intensities of light.

The rods are the most numerous (92 million) and have the highest concentration in the mid-peripheral retina [2]. Rod photoreceptor cells contain rhodopsin [3]. They are most sensitive in dim illumination and are responsible for night and peripheral vision. Dysfunction of the rods will result in poor night vision and peripheral field loss.

The cones are fewer in number (4.6 million) and have their highest concentration at the fovea [2]. They are most sensitive in bright light and mediate day vision, color vision, and central visual acuity. There are three different cones that allow for color vision: the S (“blue”) cones, the M (“green”) cones, and the L (“red”) cones. The S cones contain iodopsin that is most sensitive to short-wavelength light, while iodopsin in M and L cones are sensitive to medium- and long-wavelength light [4, 5].

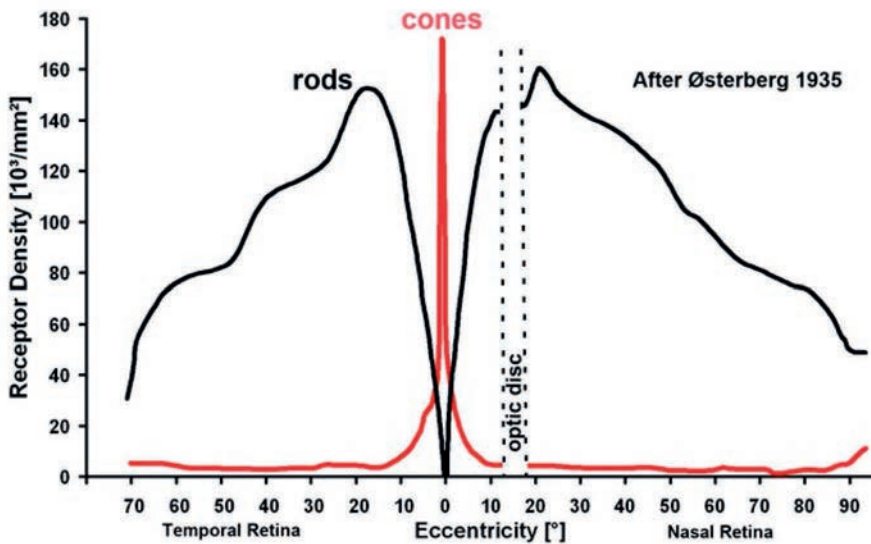


Figure 4: Distribution of rod and cone photoreceptors in the retina, adapted from Osterberg 1935 [6].

### ***Retinal pigment epithelium***

The retinal pigment epithelium (RPE) is composed of a single layer of hexagonal cells. The cells consist of an outer non-pigmented basal element containing the nucleus, and an inner pigmented apical section containing melanosomes. The cell base is in contact with Bruch's membrane, and at the cell apices, multiple thread-like villous processes that extend between the outer segments of the photoreceptors. At the posterior pole, particularly at the fovea, RPE cells are taller and thinner, more regular in shape and contain more numerous and larger melanosomes than in the periphery. The RPE cells and intervening tight junctional complexes (zonula occludentes) constitute the outer blood-retinal barrier, preventing extracellular fluid leaking into the subretinal space from the choriocapillaris. The RPE cells actively pump ions and water out of the subretinal space. Its integrity, and that of Bruch's membrane, is important for continued adhesion between the two, thought to be due to a combination of osmotic and hydrostatic forces, possibly with the aid of hemidesmosomal attachments. Another function is facilitation of photoreceptor turnover by phagocytosis and lysosomal degradation of outer segments following shedding, and preservation of an optimal retinal milieu. Maintenance of the outer blood-retinal barrier is a key factor, as are the inward transport of metabolites and the outward transport of metabolic waste products. The RPE also is involved in storage, metabolism, and 'recycling of vitamin A in the visual cycle'. Finally, the dense RPE pigment serves to absorb stray light. Adapted from Kanski et al [7].

### ***Retinal processes***

There are two important processes to transform light into an electrical signal: the phototransduction cascade and the visual cycle.

### ***Phototransduction cascade***

This is the process by which the photoreceptors transduce the energy of an absorbed photon into a neuronal signal. The phototransduction cascade occurs in the photoreceptor outer segments. The membranous discs of the outer segment contain a photosensitive pigment, a membrane protein that comprises of an opsin protein (green, red or blue opsin in cones, and rhodopsin in rods) containing an 11-*cis*-retinal chromophore. If a light photon reaches the retina, it activates rhodopsin by transforming the 11-*cis*-retinal into all-*trans*-retinal. The activated rhodopsin (metarhodopsin II) induces the activation of transducin, which – when bound to GTP – then activates cGMP specific phosphodiesterase (PDE). The activated PDE $\alpha$  and - $\beta$  subunit hydrolyze cGMP to 5-GMP. The following decline of cytoplasmic cGMP leads to the closure of cGMP channels in the plasma membrane and sodium is not able to enter the cell uninterrupted. This

leads to hyperpolarization of the cell. Because of hyperpolarization of the plasma membrane, voltage-gated calcium channels at the synaptic terminal will close. Consequently, the intracellular calcium concentration reduces abruptly, which leads to the inhibition of neurotransmitter (glutamate) release. Concomitantly, in the dark there is a continuous release of neurotransmitters, and at the same time activation of the photoreceptor induces a decrease of neurotransmitter release [8, 9].

Succeeding activation of the phototransduction cascade, utilized molecules are transposed into their initial form during the recapture phase [10]. Metarhodopsin II is inactivated through phosphorylation by rhodopsin kinase and by connecting to arrestin which results in free opsin and all-*trans*-retinal. Then, activated transducin and PDE are deactivated by a complex of GTP-ase accelerator protein; RGS9-1 and G $\beta$ 5L, which together stimulate GTP hydrolysis. From this GTP, cGMP is synthesized by guanylate cyclase enzymes (GC-1 and GC-2) and as a consequence cGMP concentration is raised to “dark situation levels”. The final result is an outer segment in dark state, in which the cation channels are open, the photoreceptor is depolarized, neurotransmitter is constantly released from the synaptic terminal, all proteins involved in the phototransduction cascade are adjusted for the following activation, and all-*trans*-retinal is set to be recycled in the visual cycle.

### **Visual cycle**

The rod visual cycle is a recycle device which occurs in the RPE and photoreceptor outer segment, where it recycles “consumed” all-*trans*-retinal into 11-*cis*-retinal that can be re-utilized in the phototransduction cascade [11]. As a result of inactivation of the phototransduction cascade, all-*trans*-retinal disseminates from the opsin into the disc membranes of the photoreceptor outer segment, is then transferred to the cytoplasmic space facilitated by the ABCR protein in the disc membrane, and converted into all-*trans*-retinol (vitamin A) by retinol dehydrogenase (RDH12). Subsequently, Vitamin A is released into the interphotoreceptor matrix, which is accelerated by interphotoreceptor retinoid-binding protein (IRBP), a protein localized in the interphotoreceptor matrix that binds all-*trans*-retinol. All-*trans*-retinol is then absorbed by the RPE cells, facilitated by cellular retinol-binding protein-1 (CRBP1). RPE cells are also able to absorb vitamin A from blood in the choroidal circulation. In the RPE cell, all-*trans*-retinol is esterified by lecithin retinol acyl transferase (LRAT) into all-*trans*-retinyl ester, which is the stable and non-cytotoxic storage form of vitamin A. As a result, RPE-specific 65-kDA protein (RPE65) isomerizes all-*trans*-retinyl ester into 11-*cis*-retinol, and – since free 11-*cis*-retinol inhibits the isomerization

of more all-*trans*-retinyl ester – it then connects to cellular retinal-binding protein (CRALBP), and may be temporarily removed from the chemical equilibrium by conversion into 11-*cis*-retinyl by LRAT. 11-*cis*-retinol is subsequently oxidized into 11-*cis*-retinal, catalyzed by 11-*cis*-retinol dehydrogenase (RDH5), and then released from the RPE cell into the interphotoreceptor matrix, again facilitated by IRBP. Eventually, 11-*cis*-retinal is absorbed by the photoreceptor, where it connects to opsin to form the photoactive rhodopsin and the phototransduction cascade can start again. The rod photoreceptors are fully dependent on the visual cycle in the RPE for the regeneration of 11-*cis*-retinal. Notably, the visual pigment regeneration in cones is 2000-fold higher than in rods, and the maximum throughput of the visual cycle is too slow to explain the sustained photosensitivity of cones in bright light. Supported by these observation, a new pathway for regeneration of visual pigment was discovered in which part of the visual cycle in cones takes place in the Müller cells, instead of RPE cells [12]. The existence of this alternative visual cycle may function in conjunction with the visual cycle in RPE cells, to provide visual chromophores to the cone in the high rate that is required for daylight vision (Figure 5).

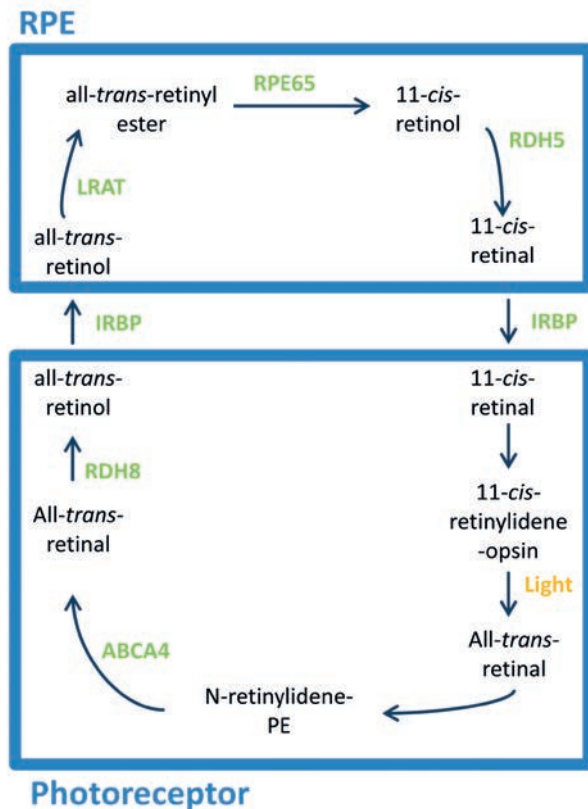


Figure 5: Visual cycle. Adjusted from Sears AE, Bernstein PS, Cideciyan AV, et al. [13]



### Retinal imaging

Both retinal imaging and functional assessment are necessary to help ophthalmologists obtain the right diagnoses.

*Fundus autofluorescence (FAF):* a non-invasive imaging technique, which provides a topographical map of lipofuscin distribution within the RPE. This technique uses short-wavelength light to excite lipofuscin, which autofluoresces. FAF can reveal metabolic changes at the level of the RPE.

*Fluorescein angiography (FA):* involves photographic surveillance of the passage of fluorescein through the retinal and choroidal circulations following intravenous injection.

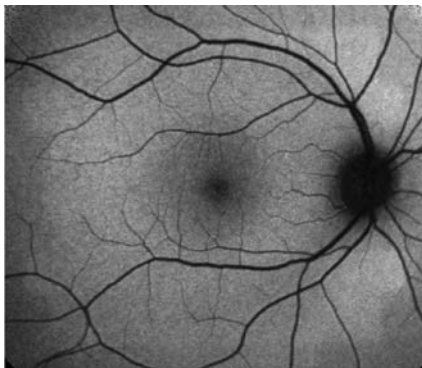


**Figure 6:** Fundus autofluorescence of a normal retina



**Figure 7:** Fluorescein angiography of a normal retina

*Optical coherence tomography (OCT):* a non-invasive, non-contact imaging system which provides high resolution cross-sectional images of the retina, optic nerve head, and vitreous. Imaging of the anterior segment is also possible.

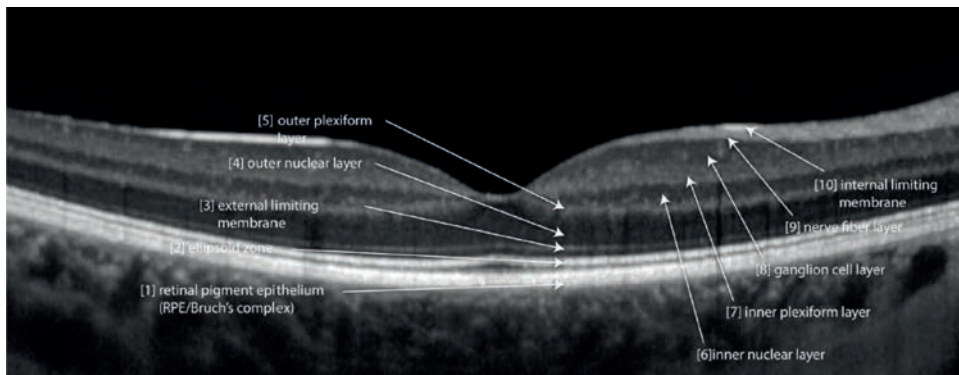


**Figure 8:** Spectral-domain optical coherence tomography of the retina. A horizontal scan through the fovea reveals several hyperreflective layers, which correlate with anatomical structures of the retina.

### Retinal function tests

*Visual field testing:* measures sensitivity to light stimuli in both the central and peripheral visual fields. A region with decreased light sensitivity surrounded by a zone of relatively normal sensitivity is called a scotoma. Dynamic perimetry (e.g., Goldmann perimetry) can be used to define the peripheral visual field (and its borders) by confrontation of a moving light stimulus into the visual field; this technique can also be used to roughly locate a relative or absolute central scotoma. Static perimetry (e.g., Humphrey visual field testing) measures the sensitivity of the retina within the central visual field by applying several non-moving spots of light of varying brightness.

*Color vision:* several tests are available to measure any deficiency in color vision. Color vision test contains the function of three populations of retinal cones; blue (tritan), green (deuteron) and red (protan).

*Electroretinography (ERG):* is the record of an action potential produced by the retina when it is stimulated by light of adequate intensity. A light stimulus is followed by an initial negative “a-wave”, which arises from the photoreceptors. Then follows a “b-wave”, which arises from the Müller and bipolar cells. In dark-adapted conditions (scotopic), a weak flash is used to stimulate the rods, followed by a very bright flash, which stimulates rods and cones. After exposing the eye to light-adapted conditions, an intense flash is utilized to measure the photopic potential arising from the cones, and the cone-derived flicker response is obtained using a 30 Hz white light flicker stimulus. The International Society for Clinical Electrophysiology of Vision (ISCEV) provides a standardized classification for ERG [14].

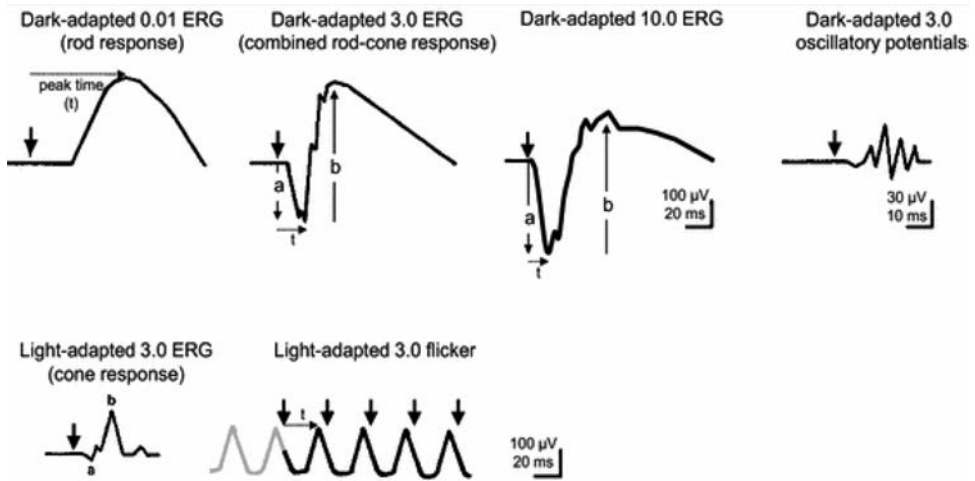


*Figure 9: The diagram of the six basic ERGs defined by the ISCEV Standard depicted. These waveforms are only given as examples and are not intended to indicate minimum, maximum or typical values. Bold arrowheads indicate the stimulus flash; solid arrows illustrate a-wave and b-wave amplitudes dotted arrows exemplify how to measure time-to-peak ( $t$ , implicit time or peak time). Adapted from ISCEV standards [14].*

## Retinal dystrophies

Retinal dystrophies (RDs) consist of a group of rare, degenerative conditions of the retina, affecting about 1:2000 individuals, and thereby the leading cause of vision loss in persons between 15 and 45 years old [15-17]. Retinal dystrophies account for ~5% of blindness worldwide, in which blindness is defined by the World Health Organization (WHO) as visual field smaller than 10 degrees and/or in the best eye a visual acuity of <20/400 (Snellen). Retinal dystrophies can be isolated or syndromic, the progression of disease differs from nearly stable to progressive, and the mode of inheritance can be autosomal dominant, autosomal recessive, X-linked or digenic. There is a wide clinical and genetic heterogeneity, caused by mutations in >261 different genes [18]. See [Figure 10](#)

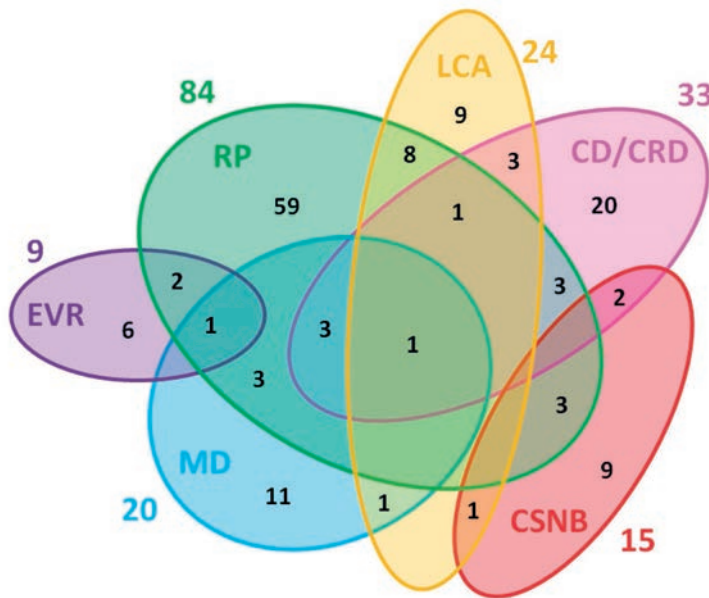


**Figure 10:** Genetic overlap between non-syndromic monogenic retinal diseases. Clinical diagnoses are indicated by colored circles. In the overlapping areas are the number of genes implicated in different phenotypes. Colored numbers outside the circles represent the total number of genes associated with these phenotypes. RP, retinitis pigmentosa; CNSB, congenital stationary night blindness; LCA Leber congenital amaurosis, CD/CRD, cone and cone-rod dystrophy; MD, macular degeneration; EVR exudative vitreoretinopathies. With permission from Khan et al. 2019 [18].

The genes involved encode proteins that have a variety functions in development and homeostasis of the retina. Mutations within the same gene may cause various disease phenotypes, even amongst affected persons within the same family. These genes encode proteins involved in retinal cellular structures, photo-transduction, the visual cycle, and photoreceptor structure or gene regulation ([Figures 11](#) and [12](#)).

**Figure 11:** Schematic representation of the roles of the non-syndromic cone disorder-associated proteins in the human retina. Schematic representation of five major functionalities of human cone photoreceptor cells (PC), Müller cells and the RPE. The locations and functions of proteins involved in non-syndromic CDs are depicted in different colors. Proteins which are relevant for the different cellular processes and not mutated in CDs are given in black lettering. Some CD-associated proteins are not shown in this figure either because of their wide-spread localization in the retina (EFEMP1, FSCN2, HMCN1), or because they localize to structures not shown (TIMP3). Panel A. The retinoid cycle taking place in cone photoreceptor cells and the RPE. Upon photoactivation (indicated by a lightning symbol), 11-cis-retinal is converted into all-trans-retinal and dissociates from activated cone opsins, OPN1LW and OPN1MW (activated opsins indicated by an asterisk). All-trans-retinal is then recycled to 11-cis-retinal via several enzymatic steps in the RPE. Transport of all-trans-retinal is mediated by ABCA4. Panel B. Retinoid cycle in cones and Müller cells. Upon photoactivation, isomerization of 11-cis to all-trans-retinal in a cone opsin takes place. After dissociation, all-trans-retinal is reduced to all-trans-retinol by RDH8 and then released from the cone outer segment into the interphotoreceptor matrix where it is bound by IRBP and taken up by the Müller cells. All-trans-retinol is isomerized by dihydroceramide desaturase-1 (DES1) to 11-cis-retinol, 9-cis-retinol and 13-cis-retinol, of which 11-cis-retinol is subsequently bound to cellular retinal-binding protein (CRALBP). The interphotoreceptor retinoid-binding protein (IRBP) transports 11-cis-retinol to the cone outer segments. 9-cis-retinol diffuses directly to the interphotoreceptor matrix and into cone outer segments, and together with 11-cis-retinol is oxidized by an unknown retinal dehydrogenase to 9/11-cis-retinal which subsequently is combined with apo-opsin to form a new chromophore. Panel C. Developmental and structural proteins. Three transcription factors mutated in non-syndromic CDs are CRX, NR2E3 and RAX2. Other proteins important in the morphogenesis and structure of the cone photoreceptor cell are EYS, IMPG1, PRPH2, PROM1, and PCDH21. Panel D. The phototransduction cascade in cone photoreceptor cells. Upon activation, amplification of the signal is mediated by the  $\alpha$ -subunit of transducin and the  $\alpha 0$ - and  $\gamma$ -subunits of cone phosphodiesterase, encoded by PDE6C and PDE6H. This results in closure of the cGMP-gated channel composed of CNGA3 and CNGB3, a hyperpolarization of the cell and a reduction in glutamate release at the synaptic region. The KCNV2 gene encodes a voltage-gated potassium channel subunit together with other channel components and regulated the potassium current in the cell and affects its excitability potential. PDE6 and transducin subunits are marked as alpha (a), alpha' ( $\alpha 0$ ), beta (b), and gamma ( $\gamma$ ). Panel E. CD-associated proteins involved in transport processes in the cone photoreceptor cell. ALPL1 is a chaperone of the putative farnesylated protein PDE6C. Farnesylated proteins are marked with a red zig-zag icon. C8orf37, RAB28, RIMS1, and TULP1, based on immunolocalisation studies, act predominantly in transport processes toward and at the base of the connecting cilium, whereas RPGR and RRGRI1 act throughout the connecting cilium. UNC119 is responsible for ciliary delivery of myristoylated proteins as well as the dissociation of transducin in separate subunits in mice. ATP, adenosine-triphosphate; GTP, guanosine-5 $\alpha$ -triphosphate; GDP, guanosine diphosphate; GMP, guanosine monophosphate; cGMP, cyclic GMP; IRBP, interphotoreceptor retinal binding protein, the product of RBP3; Mill, metarhodopsin II; P, phosphorylation; RAL, retinal; RE, retinyl esters; REH, retinyl ester hydrolase; ROL, retinol. Adapted from Roosing et al, 2014 [19].



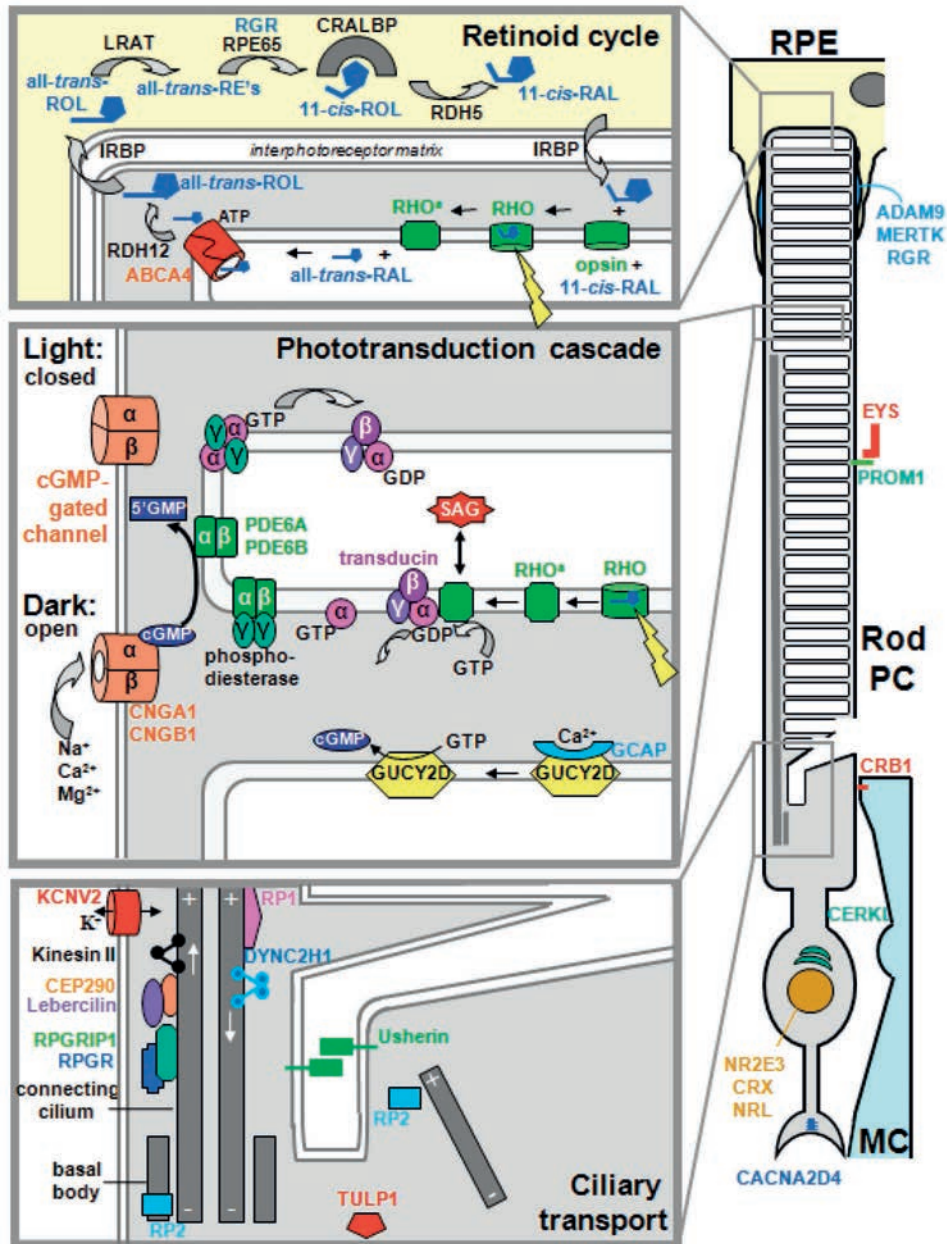


**Figure 12:** Schematic representation of three major processes in human rod photoreceptor cells and the RPE. Upper panel: The retinoid cycle taking place in rod photoreceptor cells (PC) and the RPE. Upon photactivation, 11-cis-retinal is converted into all-trans-retinal and dissociates from activated rhodopsin. The all-trans-retinal is then recycled to produce more 11-cis-retinal via several enzymatic steps in the RPE. ABCA4 mediates transport of all-trans-retinal to the outside of the photoreceptor outer segment disks. The localization and function of proteins involved in AR and XL nonsyndromic retinal dystrophies are depicted, with the exception of GCAP, a critical Ca<sup>2+</sup>-binding interactor of

*GUCY2D, which is mutated in autosomal dominant CRD (<http://www.sph.uth.tmc.edu/Retnet/home.htm>). CRALBP, protein product of RLBP1; IRBP, protein product of RBP3; RAL, retinal; RE, retinyl esters; RHO<sup>o</sup>, photoactivated rhodopsin; ROL, retinol. Middle panel: The phototransduction cascade in rod PCs. Upon photoactivation, amplification of the signal is mediated through the  $\alpha$ -subunit of transducin and phosphodiesterase, which results in closure of the cGMP-gated channel, hyperpolarization of the cell, and reduced glutamate release at the synapse. SAG, arrestin. Lower panel: Ciliary transport along the connecting cilium. Kinesin II family motors mediate transport toward the outer segments; cytoplasmic dynein 2/1b (DYNC2H1) is involved in transport processes from the outer segments toward the inner segments. The precise roles of CEP290, Lebercilin, RPGR, RPGRIP1, and RP1 in ciliary transport processes are not yet known. AIPL1 (not indicated in this figure) is a chaperone for proteins that are farnesylated. For IDH3B and PRCD, the exact cellular functions are not known. ADAM9, MERTK, and RGR are secreted by the RPE and localize in the interphotoreceptor matrix. The CNGA3, CNGB3, GNAT2, and PDE6C genes are specifically expressed in cone PCs and therefore not indicated in this figure. At the right side, a Müller cell (MC) connects to the photoreceptor cell with the transmembrane protein CRB1. Usherin, protein product of USH2A. Adapted from Den Hollander et al, 2011 [20].*

### *Classification of retinal dystrophies*

There are several types of retinal dystrophies, representing a spectrum of cone-dominated (e.g. cone dystrophy, achromatopsia) or rod-dominated disorders (e.g. retinitis pigmentosa), and disorders that can show as either cone- or rod-dominated (e.g. Leber congenital amaurosis). In addition, the sub-classification is based on age of onset, clinical characteristics, and the natural course of disease.

### *Rod-cone dystrophies*

Rod-cone dystrophies includes mainly the spectrum of all retinitis pigmentosa (RP) entities. RP comprise the most widely recognized group of patients with inherited retinal disorders, with a worldwide prevalence of 1:4000 [21]. It should be regarded as a phenotypic description of several related dystrophies of the photoreceptors and the RPE. All Mendelian patterns of inheritance have been found in these disorders. Patients with X-linked RP (5-15% of RP patients) have a more severe disease course compared to patients with autosomal recessive RP (50-60% of RP patients), and RP patients with an autosomal dominant inheritance (30-40% of RP patients), have the best long-term prognosis according to a spared central vision [16, 22, 23].

By definition, RP is a progressive disorder. Both rod and, in most types, cone photoreceptors are affected early in the course of disease. Eventually, loss of photoreceptor elements leads to widespread atrophy of most of the retinal layers. Although the clinical findings may be highly variable, these patients typically demonstrate night blindness, difficulty with dark adaptation and progressive loss



of the peripheral visual field early in the course of their disease. The characteristic ophthalmoscopic findings of this retinopathy include hyperpigmentation in the form of “bone spicules” that alternate with atrophic regions, attenuation of retinal arterioles, and waxy pallor of the optic nerve head. The ERG is the most critical diagnostic test for RP because it provides an objective measure of rod and cone function across the retina. The full-field ERG typically shows a marked reduction of both rod- and cone-mediated responses, although rod loss predominates. In the later stages of the disease, cone and rod tracings often become non-recordable [24, 25]. Visual field testing is useful for follow-up care of patients with RP and typically starts with isolated scotomas in mid-peripheral zones, which progressively coalesce to form a partial or complete ring scotoma [21, 26-29].

RP is usually isolated, but may occur as a part of a syndrome. Some of the well-known syndromes include: Usher syndrome, Bardet-Biedl syndrome, Senior-Loken syndrome, abetaproteinemia (Bassen-Kornzweig syndrome), peroxisomal disorders (e.g. Zellweger syndrome or Refsum disease), and mitochondrial disorders (e.g. Kearns-Sayre, or Maternally Inherited Diabetes and Deafness, abbreviated as “MIDD”).

Besides the large group that is referred to as RP, a few other peripheral retinal degenerations with primarily or initial involvement of rod photoreceptors have been discerned. These diseases, such as Bietti crystalline dystrophy, gyrate atrophy and choroideremia, all display a unique fundus appearance that enables a separate clinical classification. In addition, RP seems to be one of the most common underlying diseases in patients with secondary retinal vasoproliferative tumors [30].

### *Cone and cone-rod dystrophies*

In general, cone dystrophy (CD) presents in the 2<sup>nd</sup> decade of life. Symptoms are pronounced photophobia, day blindness and progressive loss of visual acuity. Color vision abnormalities, commonly of the red-green type, are present at an early disease stage. A subtle nystagmus can be noticed in these patients. Fundus abnormalities include mostly a bull’s eye maculopathy, or granular pigment alterations in the posterior pole. Rarely, a central atrophy of RPE with exposure of the larger choroidal vessels may be found. Visual field testing shows central scotomas, sometimes with relative central sparing; the peripheral visual field remains unaffected. The ERG shows loss of the cone-mediated responses with normal rod-mediated responses. A substantial number of patients that are initially diagnosed with progressive CD will eventually progress to a cone-rod dystrophy

(CRD), with abnormalities in the rod mediated ERG recordings and mostly night blindness. Many cases of progressive CD are sporadic. In patients with a family history, autosomal dominant inheritance is most common, although autosomal recessive and X-linked forms may occur [31, 32].

In patients with CRD, the rod photoreceptors are also affected, but their symptoms are overshadowed by the abnormalities of the cones, especially in the early stages of the disorder. The initial symptoms therefore resemble progressive CD and most patients do not develop night blindness until the later stages of disease. In addition to the macular abnormalities described in CD, midperipheral fundus abnormalities could be observed, indicative of a more widespread retinal degeneration. These abnormalities include mild attenuation of the retinal vessels, and mild bone spicules or dust-like pigmentations. Atrophy of the RPE may occur in the macula, but may extend beyond the vascular arcades. Initially, the visual field demonstrates a central scotoma; eventually, partial ringscotomas and large paracentral scotomas may be found, as well as mild peripheral constriction. The ERG is crucial in the diagnosis and typically shows a more severe reduction in cone-mediated responses compared with rod-mediated responses. Nevertheless, some patients demonstrate equally reduced cone and rod ERG recordings, despite an otherwise typical presentation. Most cases with CRD are either isolated or inherited in an autosomal recessive fashion, but all inheritance patterns have been identified [32-36].

### *Macular dystrophies*

A variety of dystrophies, principally located at the macula, can be distinguished according to fundus appearance and inheritance pattern. Despite the term “macular dystrophies”, which suggest localized pathology, many of these disorders are at a molecular level panretinal diseases, in which the macular region shows greater susceptibility to the degeneration. This can be argued for Stargardt disease (STGD1), as well for Best disease, where the EOG abnormalities also indicate a more widespread retinal dysfunction [37]. The majority of the macular dystrophies demonstrate an autosomal inheritance, with X-linked juvenile retinoschisis and STGD1 as the most important exceptions. Among the most renowned autosomal dominant macular dystrophies are Best disease (vitelliform macular dystrophy), adult-onset vitelliform macular dystrophy, the pattern dystrophies, autosomal dominant drusen, central areolar choroidal dystrophy (CACD), and Sorsby fundus dystrophy. Although these disorders are all characterized by loss of central vision and atrophy of the macula and underlying RPE, they are highly heterogeneous with regard to the clinical findings and the underlying genetic cause [38, 39].

I will continue on the most common macular dystrophy: Stargardt disease (STGD1).

## 1.2 Introduction to Stargardt disease

### Stargardt disease

#### History

The remarkable clinical variations of macular dystrophies were already noted in 1917 by Karl B. Stargardt (1875-1927). He proposed to separate these clinical entities into different groups, based on the clinical presentation and ophthalmoscopic appearance [40].

Eight years earlier (1909), he described the clinical features in seven patients at ages 12-20 years, from two families. The disease was coined Stargardt disease, and initially was also known as fundus flavimaculatus. The patients had good vision in early childhood, but had progressive loss of central vision between the age of 8 and 15 years. In the posterior pole, slight pigment changes with yellow-white spots were observed, and a fairly well-defined, central atrophic lesion. In some patients, a broad ring of several yellow-white spots evolved around this area. Retinal vessels and retinal periphery remained quite normal. In [Figure 13](#) and [14](#), fundus images of two Stargardt patients, drawn and described by Karl Stargardt in 1909 are depicted [41].



**Figure 13:** Fundus drawing of Stargardt disease patient. This girl started to have complaints of visual loss at the age of 14 years. At the age of 20 years, she had a visual acuity of 0.08 (right eye), and 0.16 (left eye). In the macula were grayish-yellow flecks were described with pigment lesions. Near the arteries and vena temporalis inferior, some little yellow-white flecks were seen.

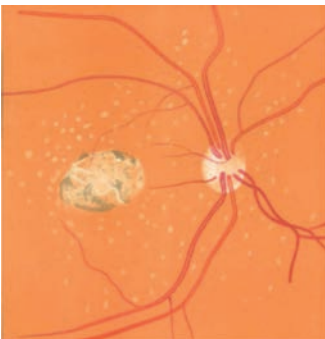


**Figure 14:** Fundus drawing of Stargardt disease patient. This boy started to have complaints of visual loss at the age of 13 years. At the age of 18 years, he was only able to reach a visual acuity of finger counting at 4 meters. With funduscopy, a grayish heart-shaped lesion with a quite sharp border was seen. Near this lesion and the optic nerve, there were lots of small, yellow-white flecks.

### Clinical characteristics

Presently, STGD1 is the most prevalent inherited disease that causes visual impairment in childhood and young adults, with an estimated prevalence of 1:10,000 [42]. It is an autosomal recessive retinal dystrophy due to mutations in the *ABCA4* gene [43]. Both sexes are equally affected. The disease typically presents within the first two decades of life, even though initial symptoms can also appear as late as the seventh decade. It is typically characterized by a progressive bilateral loss of central vision causing blurry vision. Peripheral vision is usually unaffected. Most patients also have impaired color vision. Photophobia may be present. A timeline of three STGD1 patients are reported in [Figure 15](#).

However, STGD1 has a wide clinical heterogeneity. Ranging from an early age of onset with a cone-rod phenotype in progressed disease, to a late disease onset with a foveal sparing phenotype [44, 45]. As a consequence, STGD1 patients could present with a range of phenotypes at consultation to an ophthalmologist. In [Figure 16](#), several STGD1 patients are described with a wide clinical heterogeneity.

In recent years, considerable advances have been made in our understanding of the clinical phenotypes, natural history and molecular genetics of STGD1. Due to the phenotypic spectrum, several classifications have been proposed. Van Driel et al. (1998) and Maugeri et al. (1999) first proposed a classification based on the expected residual function of the *ABCA4* protein by the severity of mutations, extending the putative associations of *ABCA4* mutations from the presumed mildest phenotype of age-related macular degeneration (one *ABCA4* variant) to more severe phenotypes such as cone-rod dystrophy and RP, the latter carrying two severe *ABCA4* variants (see [Figure 17](#)) [46, 47]. The AMD-association [48, 49] in later studies has not been confirmed [50, 51].

Fishman et al. (1999) differentiated three clinical phenotypes: 1) an atrophic-appearing macular lesion with localized perifoveal flecks, 2) diffuse flecks, and 3) extensive atrophic-appearing changes of the retinal pigment [52]. Lois et al. recognized three patterns based on electrophysiological attributes: 1) severe pattern ERG abnormality with normal scotopic and full-field ERGs, 2) additional loss of photopic function, and 3) loss of both photopic and scotopic function [53].

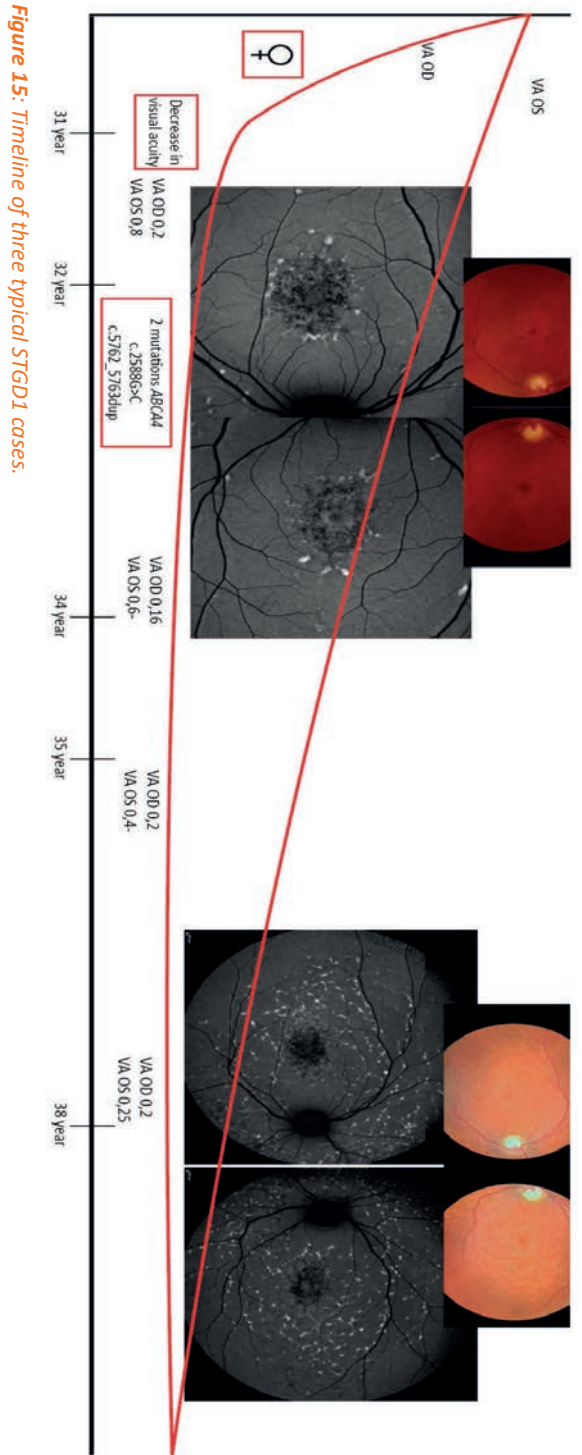
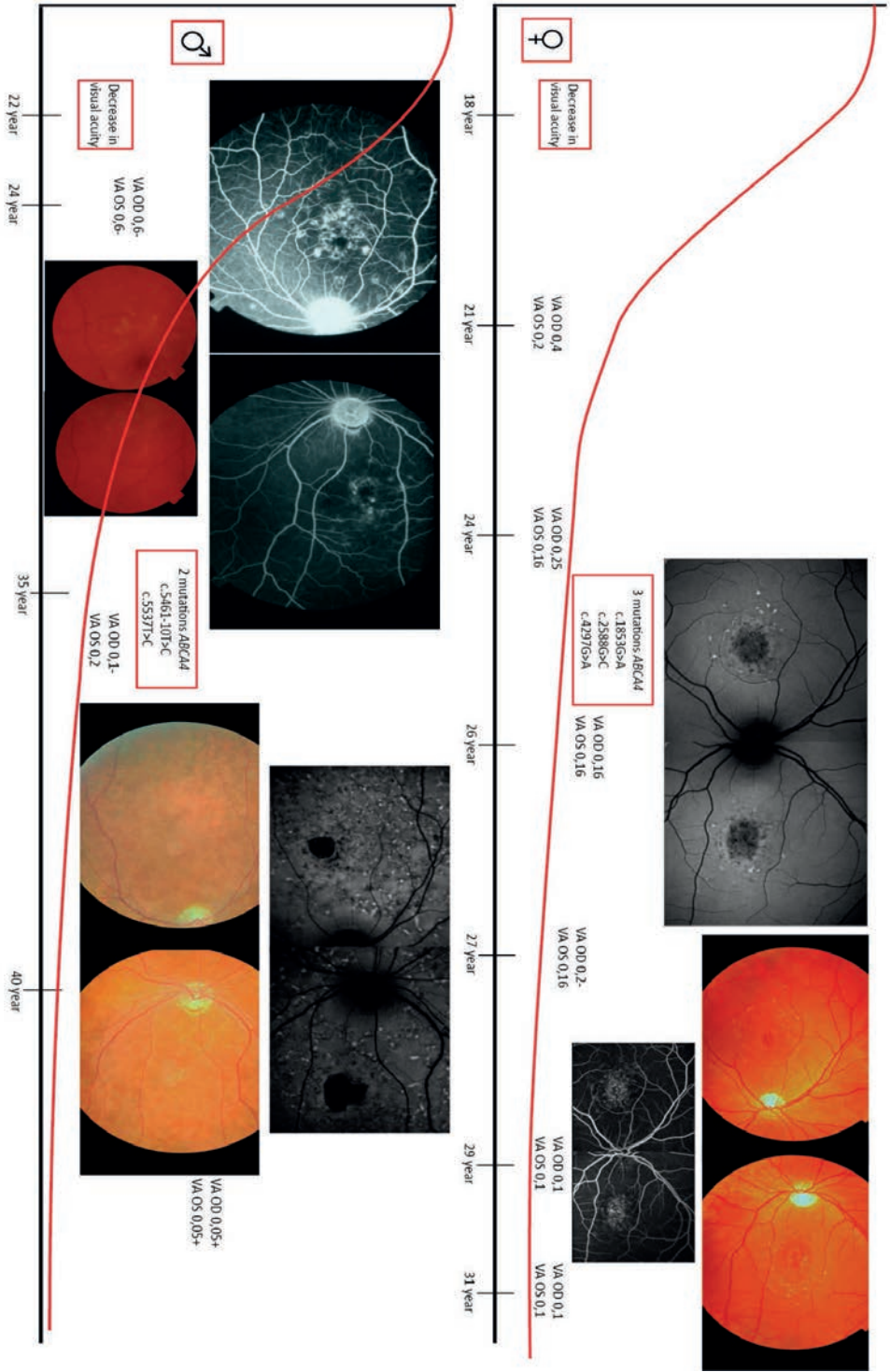
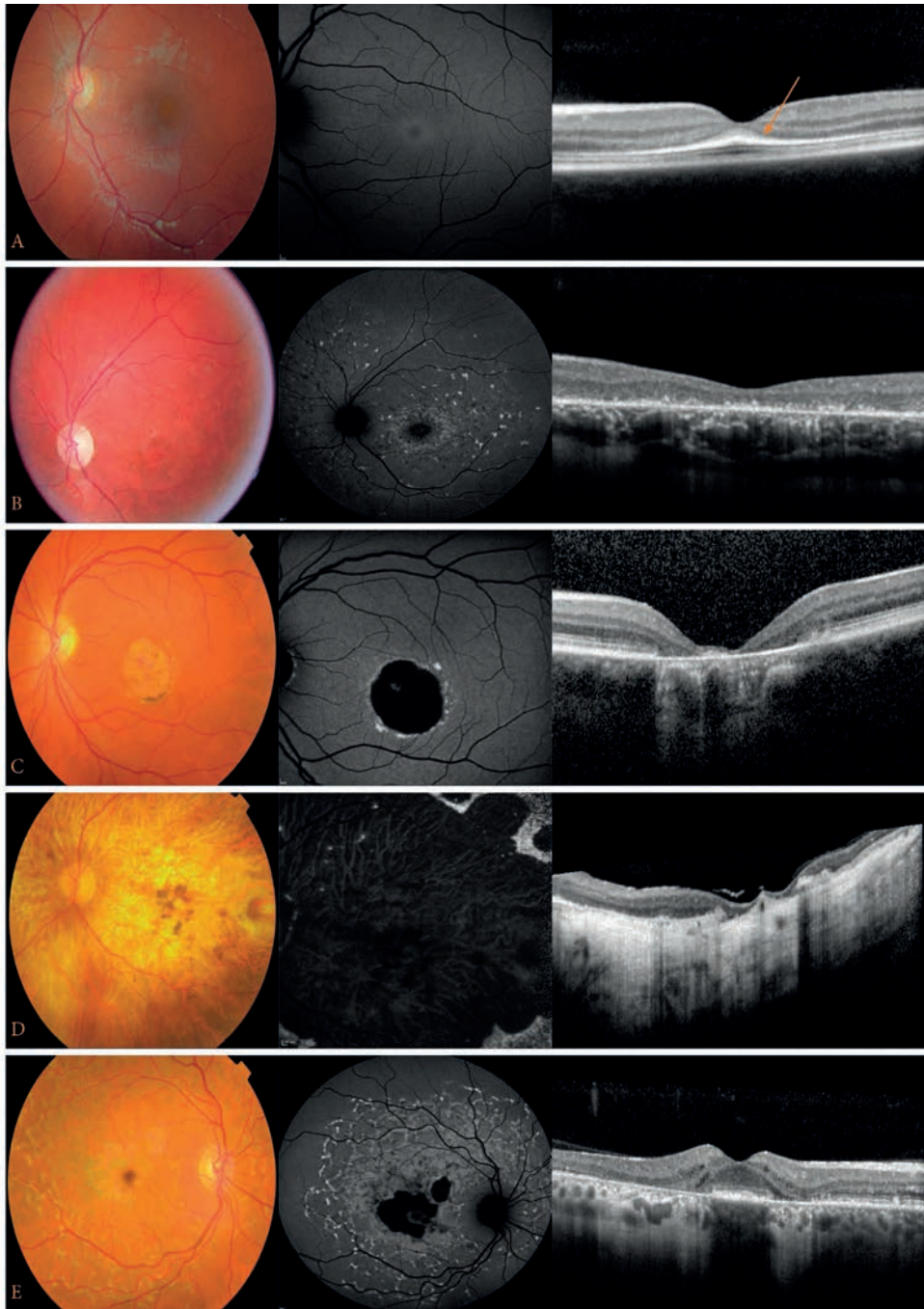


Figure 15: Timeline of three typical STGD1 cases.

1





**Figure 16:** Retinal imaging from five different STGD1 cases with a wide clinical heterogeneity. Images contains (from left to right) Color fundus photo, Fundus autofluorescence, and OCT-scan. Best corrected visual acuity (BCVA) is given in Snellen.

*A: A 7-year-old boy with complaints of decrease of visual acuity. Imaging from first visit; no abnormalities were shown in color fundus photo or autofluorescence, but on OCT a thickened ILM was noticed (orange arrow). BCVA 0.6 in both eyes. STGD1 was diagnosed 2 years later, confirmed with 2 ABCA4 mutations (c.2947A>G (p.(Thr983Ala)); c.5461-10T>C (p.[Thr1821Valfs, Thr1821Aspfs])).*

*B: A young woman from 21 years old, start to have complaints of visual loss at age 16 years. Central choroiretinal atrophy with central to midperipheral lipofuscine flecks is seen on fundus photography. Her visual acuity was 0.1. Two ABCA4 mutations were detected: c.2588G>C (p.[Gly863Ala, Gly863del]) and c.768G>T (p.Val256=).*

*C: A 40-year-old woman started to have visual acuity complaints at 24 years. Images are not showing the “typical” fundus flecks diffuse in macula or midperiphery, but central choroiretinal atrophy surrounding with just some lipofuscine flecks. Her visual acuity was 0.2 in both eyes. Only 1 ABCA4 mutation was found: c.1822T>A (p.(Phe608Ile)). No mutations in other genes could be detected.*

*D: A woman at age 66 years old. She started to have complaints of visual loss at 18 years. Images showing choroiretinal atrophy of the macula to midperipheral. BCVA was hand movement at 3 meter. Two ABCA4 mutations were found: c.5381C>A (p.(Ala1794Asn)) and c.4539+2001G>A (p?).*

*E: A 49-years-old man, started to have visual complaints at age 44. Imaging present the typical pisciform fundus flecks in macula and midperiphery. Central choroiretinal atrophy, but with a spared foveal island, as confirmed at OCT-scan. Visual acuity was 1.0 in both eyes. Diagnose was confirmed with two ABCA4 mutations: c.5461-10T>C (p.[Thr1821Valfs, Thr1821Aspfs]) and c.4685T>C (p.(Ile1562Thr)).*

Phenotype	ABCA4 activity							
	Normal		AMD		STGD1		CRD	RP
ABCA4 mutation 1		mild	moderate	severe	moderate	severe	severe	severe
ABCA4 mutation 2					moderate	mild	moderate	severe

**Figure 17:** Initial genotype-phenotype correlation model based on the severity of ABCA4 variants.

Unfortunately, in clinical settings, despite these well-defined classifications, it may happen that patients get several diagnoses because of different stages of disease during life. For example, based on the classification of Lois et al, patients may get the diagnosis “cone dystrophy” and may develop during life to a “cone-rod dystrophy”. Furthermore, the present classifications offer an “in time” diagnosis, instead of a single diagnosis that is informative with respect to clinical course, which could help the patient to answer personal questions, like: “Am I able to continue my present work for the next 10 years?”, or “Am I able to see my children growing up?” etcetera. Currently, the ophthalmologist identifies a variety of phenotypes of STGD1, and it is hard to provide good counseling.



### ABCA4 Function

STGD1 has only been associated with variants in the ATP-binding cassette transporter type A4 (*ABCA4*) gene [43] which encodes a multidomain transmembrane protein located at the rim of the disc membrane in the outer segment of photoreceptors [54, 55] (Figure 18A). Low expression of this gene has also been found in keratinocytes, fibroblasts and recently in human and murine RPE [56, 57]. *ABCA4* acts as a flippase for 11-*cis* and *all-trans* isomers of N-retinylidene-phosphatidylethanolamine across disc membranes, thereby facilitating the removal of retinal products from the disc membranes and preventing the accumulation of potentially toxic bisretinoid compounds (e.g. A2E) in photoreceptor and RPE cells (Figure 18B). The visual cycle in STGD1 is depicted in Figure 19.

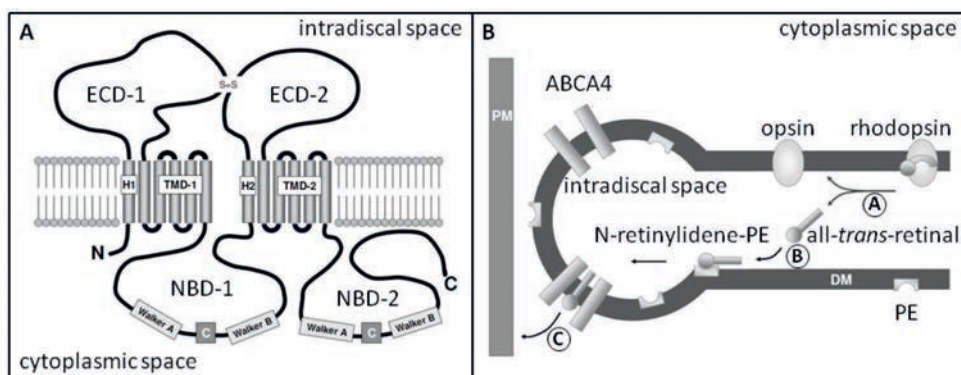


**Figure 18.** Protein domain structure and function of *ABCA4*. **A.** Topological model for the *ABCA4* protein. (ECD) exocyttoplasmic domain; (H1 or H2) first transmembrane segment; (TMD) transmembrane domain; (NBD) nucleotide binding domain. The two Walker motifs (A and B) and the C region which lies between them are the hallmark of ABC transporter superfamily members. Figure adapted with permission from Bungert et al. 2001 [58]. **B.** Proposed function of the *ABCA4* protein. A. All-*trans*-retinal is released by the photoactivated rhodopsin. B. All-*trans*-retinal enters the hydrophobic disc membrane (DM) and reacts to form a Schiff base with the amine of a phosphatidylethanolamine (PE), a phospholipid found on the DM outer segment. C. All-*trans*-retinal or the N-retinylidene-PE complex is transported by *ABCA4* to the cytoplasmic side. All-*trans*-retinal is then reduced by all-*trans*-retinol dehydrogenase and transported to the RPE (not shown). (PM) plasma membrane.

### Missing heritability in STGD1

Until recently, approximately 25% of STGD1 patients were missing a complete genetic diagnosis. The majority of whom only carries one pathogenic *ABCA4* variant. This large number of mono-allelic STGD1 patients is larger than for any other monogenic retinal dystrophy. This was consistently observed in many studies regardless the ethnic background of the patients [59–66], which argues against genetic heterogeneity of STGD1. The missing heritability for STGD1 could be explained by:

### STGD1-like phenotypes due to mutations in other genes

Before the causing gene of STGD1 was elucidated, all Stargardt-like phenotypes were called: “Stargardt disease”. With techniques to find the underlying genes, scientists were able to differentiate four types of Stargardt-like diseases. Therefore, the “1” in STGD refers to the causing *ABCA4* mutations in what we know presently as Stargardt disease. Variants in peripherin 2 (*PRPH2*) have been associated with autosomal dominant multifocal pattern dystrophy, but also were found in genetically unsolved STGD patients. The variable expressivity and penetrance of the *PRPH2* variants combined with the peculiar type and distribution of the flecks, strongly resembling the ones observed in the fundus flavimaculatus phenotype of STGD1, are the two major causes for misdiagnosis [67]. STGD3 is caused by variants in *ELOVL4* (elongation of very long chain fatty acids protein 4) gene, and STGD4 is associated with variants in the *PROM1* (prominin 1) gene. STGD3 and STGD4 are well known to be associated with rare autosomal dominant forms of Stargardt-like dystrophies [68-70].

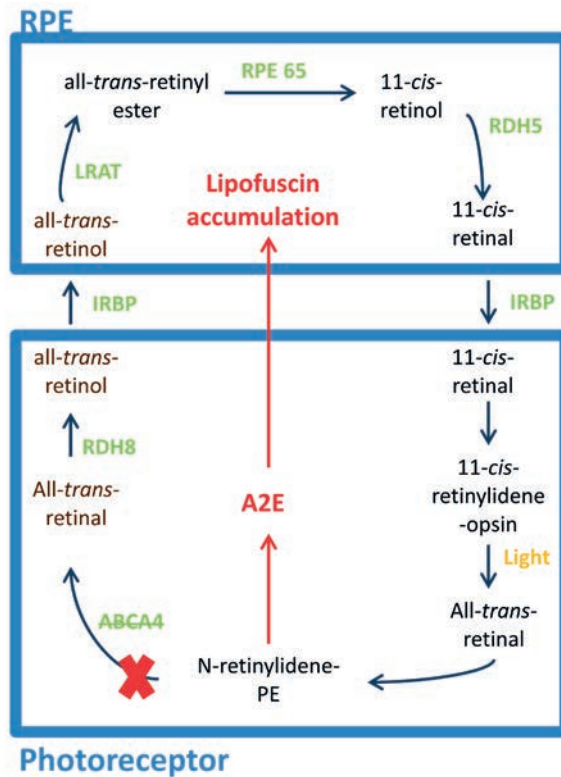


**Figure 19:** Visual cycle in STGD1. Adjusted from Sears AE, Bernstein PS, Cideciyan AV, et al. Towards Treatment of Stargardt Disease: Workshop Organized and Sponsored by the Foundation Fighting Blindness [13]

To date, modifiers associated with STGD1 have not been reported. However, since a synergistic effect of pathologic *ABCA4* sequence variations with an autosomal dominant form of Stargardt disease (STGD3) has already been demonstrated [71], it is very likely that variants in other genes may play a role in *ABCA4*-associated disease and contribute to ameliorating or worsening the clinical outcome of the disease.

### *Structural variations*

Heterozygous deletions or duplications spanning one or more *ABCA4* exons will not be detected using standard PCR-based mutation analyses methods and therefore may explain a percentage of the unsolved STGD1 cases. Likewise, inversions and sizeable insertions also would be missed. Currently, only a few studies reported on a systematic analysis of copy-number variants (CNVs) in *ABCA4*, either by Southern blot analysis [47, 72] or by NGS [73]. CNVs were detected only in a very small proportion (~1%) of STGD1 cases and it therefore has been generally accepted that they do not represent a major cause of missing heritability.

### *Misinterpreted variants*

Non-canonical splice site (NCSS) variants are exonic or intronic variants located at the splice donor sites (SDSs) or splice acceptor sites (SASs). Intronic NCSS variants are mostly situated at positions +3 to +6 downstream of exons or at positions -14 to -3 upstream of exons. Exonic NCSS variants almost invariably are found within the first or the last two nucleotides of an exon [74]. These variants are often overlooked, their effect on splicing is not assayed and often classified as variants of unknown significance (VUS) or even non disease-causing.

Synonymous variants, which usually occur in the third base of a codon, can be misinterpreted as they do not alter the protein sequence. However, only a few synonymous variants have been predicted to alter the strength of the splice site identified and/or to be significantly enriched in STGD1 patients [75, 76].

### *Frequent coding variants*

Coding variants having a high allele frequency (AF) in healthy persons could be incorrectly deemed not to be associated with the disease. Even though rare genetic disorders usually are due to unique sequence changes, there are exceptions. Variants with an AF  $\geq 0.01$  are normally discharged from further analyses, but a comparison of the carrier frequency between non-affected and affected individuals may still suggest a possible role for these variants in disease [77]. For example, the *ABCA4* variant c.5603A>T (p.Asn1868Ile) was previously

considered benign due to the high AF of 0.066 in the non-Finnish European population (<http://gnomad.broadinstitute.org>). In a recent study of Zernant et al (2017), this common variant accounted for 15% of the *ABCA4* alleles in STGD1 patients, which was three to four times more frequent than expected [78].

### Non-coding variants

A major fraction of deleterious variants could be located in the non-coding sequences of *ABCA4*, constituting 94.5% of the 128-kb sized gene, and therefore cannot be detected by exonic sequencing. Unraveling the role of deep-intronic variants in human disease-associated genes is a recent research field, and for STGD1 the first work that clearly aimed to identify and functionally prove the effect of novel non-coding variants in *ABCA4* was published in 2013 [79]. By performing haplotype analysis in a group of 28 unrelated mono-allelic STGD1 probands, Braun and colleagues identified three *ABCA4* haplotypes (H1-3) shared among ten families. The fact that 64% of the unsolved samples shared no haplotype and that not more than four patients shared the same disease-haplotype, suggested that highly recurrent deep-intronic variants were not present among unsolved STGD1 patients. Deep sequencing of mRNA extracted from human donor retina showed that 5% of *ABCA4* transcripts carried minor alternate exons, each observed in less than 1% of the total mRNA. Sequencing of genomic regions containing these alternate exons in the 28 unsolved STGD1 patients revealed five deep-intronic variants (c.5196+1137G>A, c.5196+1216C>A, c.5196+1056A>G, c.4539+2001G>A, c.4539+2028C>T) some of which were located in splice sites or the predicted alternate exons. All variants were present in *trans* with the first pathogenic *ABCA4* variant in unsolved patients. The effect of c.5196+1137G>A, c.5196+1216C>A and c.5196+1056A>G variants was tested by employing RNA from patient-derived keratinocytes and RT-PCR studies revealed the generation of pseudoexons (PEs) in intron 36, while for c.4539+2001G>A and c.4539+2028C>T, functional studies were not performed. Although this was not a systematic analysis of non-coding variants, it paved the way for more complete studies of non-coding elements in *ABCA4* [73].

The predicted *ABCA4* promoter sequence has been investigated only in two studies [73]; **Chapter 3.3**), but to date the rare non-coding variants identified have not yet been further characterized [73].

## Quality of life in Stargardt disease patients

Currently, the quality of life is determined as a significant outcome for measuring the impact of disease, and for estimating the efficacy of treatment. Literature suggests that visual impairment is related to loss in quality of life [80-84]; visually impaired patients frequently have high levels of anxiety and periods of depression [82, 85, 86]. These patients are also at increased risk of accidental injuries, which can worsen existing chronic health conditions [87, 88]. Moreover, blindness is the third most feared of all chronic disorders, after cancer and AIDS/HIV, by Americans [89].

To date, quality of life studies which assess visual impairment are mainly focused on elderly patients, and many are not specified for retinal dystrophies [81, 88, 90-93]. To our knowledge, besides from RP in general [94-99], we know little about the quality of life in patients with retinal dystrophies, for example STGD1.

Knowledge of quality of life in STGD1 patients can gain insight about the impact of the disease on daily functioning. These data are important to provide outcome measures and indicators of cost effectiveness for emerging clinical trials, such as gene augmentation (trial number NCT01367444, NCT01736592), and small molecule drugs (trial number NCT02402660) [100, 101].

### 1.3 Aims and outline of this thesis

STGD1 is one of the most common causes of blindness in young people. Clinically, the phenotype is extremely heterogeneous. Little is known about the natural course and staging of disease. No useful classification of subtypes is available and the underlying genetic causes have only been partially elucidated. Therefore, this thesis contains three main goals that are addressed in the following chapters:

Chapter 2: To define subtypes and genotype-phenotype correlations through describing clinical characteristics of STGD1.

Chapter 3: Identification, registry and functional assessment of *ABCA4* variants.

Chapter 4: Information about quality of life in STGD1 patients.

The overarching goal is to understand the natural course and staging of disease enabling the ophthalmologist a better counseling and to provide a more accurate diagnosis and prognosis for the patient. Furthermore, it is important to select uniform cohorts in upcoming and ongoing trials to provide correct outcome measurements.

## References

1. Lorber, B., W.K. Hsiao, and K.R. Martin, *Three-dimensional printing of the retina*. *Curr Opin Ophthalmol*, 2016. **27**(3): p. 262-7.
2. Curcio, C.A., et al., *Human photoreceptor topography*. *J Comp Neurol*, 1990. **292**(4): p. 497-523.
3. Aminoff, M.J.D., R.B., *Encyclopedia of the neurological sciences* 2014: p. 441.
4. Roorda, A. and D.R. Williams, *The arrangement of the three cone classes in the living human eye*. *Nature*, 1999. **397**(6719): p. 520-2.
5. Solomon, S.G. and P. Lennie, *The machinery of colour vision*. *Nat Rev Neurosci*, 2007. **8**(4): p. 276-86.
6. Osterberg, *Topography of the layer of rods and cones in the human retina*. *Acta Ophthalmol*, 1935. **6**: p. 1-106.
7. kanski, J.J.B., B., *Clinical Ophthalmology; a systematic approach; 7th edition*. 2011: p. 594-595.
8. Jindrova, H., *Vertebrate phototransduction:activation, recovery, and adaptation*. *Physiol Res*,1998. **47**(3):p.155-68.
9. Yau, K.W., *Phototransduction mechanism in retinal rods and cones. The Friedenwald Lecture*. *Invest Ophthalmol Vis Sci*, 1994. **35**(1): p. 9-32.
10. Burns, M.E. and D.A. Baylor, *Activation, deactivation, and adaptation in vertebrate photoreceptor cells*. *Annu Rev Neurosci*, 2001. **24**: p. 779-805.
11. Travis, G.H., et al., *Diseases caused by defects in the visual cycle: retinoids as potential therapeutic agents*. *Annu Rev Pharmacol Toxicol*, 2007. **47**: p. 469-512.
12. Mata, N.L., et al., *Isomerization and oxidation of vitamin a in cone-dominant retinas: a novel pathway for visual-pigment regeneration in daylight*. *Neuron*, 2002. **36**(1): p. 69-80.
13. Sears, A.E., et al., *Towards Treatment of Stargardt Disease: Workshop Organized and Sponsored by the Foundation Fighting Blindness*. *Transl Vis Sci Technol*, 2017. **6**(5): p. 6.
14. McCulloch, D.L., et al., *ISCEV Standard for full-field clinical electroretinography (2015 update)*. *Doc Ophthalmol*, 2015. **130**(1): p. 1-12.
15. Rattner, A., H. Sun, and J. Nathans, *Molecular genetics of human retinal disease*. *Annu Rev Genet*, 1999. **33**: p. 89-131.
16. Hamel, C., *Retinitis pigmentosa*. *Orphanet J Rare Dis*, 2006. **1**: p. 40.
17. Krumpaszy, H.G., et al., *Blindness incidence in Germany. A population-based study from Wurttemberg-Hohenzollern*. *Ophthalmologica*, 1999. **213**(3): p. 176-82.
18. Khan, M., et al., *Identification and Analysis of Genes Associated with Inherited Retinal Diseases*. *Methods Mol Biol*, 2019. **1834**: p. 3-27.
19. Roosing, S., et al., *Causes and consequences of inherited cone disorders*. *Prog Retin Eye Res*, 2014. **42**: p. 1-26.
20. den Hollander, A.I., et al., *Lighting a candle in the dark: advances in genetics and gene therapy of recessive retinal dystrophies*. *J Clin Invest*, 2010. **120**(9): p. 3042-53.
21. Pagon, R.A., *Retinitis pigmentosa*. *Surv Ophthalmol*, 1988. **33**(3): p. 137-77.
22. Bunker, C.H., et al., *Prevalence of retinitis pigmentosa in Maine*. *Am J Ophthalmol*, 1984. **97**(3): p. 357-65.
23. Grover, S., et al., *Visual acuity impairment in patients with retinitis pigmentosa*. *Ophthalmology*, 1996. **103**(10): p. 1593-600.
24. Mantyjarvi, M. and K. Tuppurainen, *Clinical symptoms at different ages in autosomal dominant retinitis pigmentosa. A family study in three generations*. *Ophthalmologica*, 1994. **208**(1): p. 23-8.
25. Alexander, K.R. and G.A. Fishman, *Prolonged rod dark adaptation in retinitis pigmentosa*. *Br J Ophthalmol*, 1984. **68**(8): p. 561-9.

26. Verbakel, S.K., et al., *Non-syndromic retinitis pigmentosa*. *Prog Retin Eye Res*, 2018. **66**: p. 157-186.
27. Marmor, M.F., *Visual acuity and field loss in retinitis pigmentosa*. *Arch Ophthalmol*, 1991. **109**(1): p. 13-4.
28. Marmor, M.F., *Visual loss in retinitis pigmentosa*. *Am J Ophthalmol*, 1980. **89**(5): p. 692-8.
29. Marmor, M.F., *The electroretinogram in retinitis pigmentosa*. *Arch Ophthalmol*, 1979. **97**(7): p. 1300-4.
30. Shields, C.L., et al., *Retinal vasoproliferative tumors: comparative clinical features of primary vs secondary tumors in 334 cases*. *JAMA Ophthalmol*, 2013. **131**(3): p. 328-34.
31. Goodman, G., H. Ripps, and I.M. Siegel, *Cone Dysfunction Syndromes*. *Arch Ophthalmol*, 1963. **70**: p. 214-31.
32. Krill, A.E., A.F. Deutman, and M. Fishman, *The cone degenerations*. *Doc Ophthalmol*, 1973. **35**(1): p. 1-80.
33. Berson, E.L., P. Gouras, and R.D. Gunkel, *Progressive cone degeneration, dominantly inherited*. *Arch Ophthalmol*, 1968. **80**(1): p. 77-83.
34. Berson, E.L., P. Gouras, and R.D. Gunkel, *Progressive cone-rod degeneration*. *Arch Ophthalmol*, 1968. **80**(1): p. 68-76.
35. Szlyk, J.P., et al., *Clinical subtypes of cone-rod dystrophy*. *Arch Ophthalmol*, 1993. **111**(6): p. 781-8.
36. Yagasaki, K. and S.G. Jacobson, *Cone-rod dystrophy. Phenotypic diversity by retinal function testing*. *Arch Ophthalmol*, 1989. **107**(5): p. 701-8.
37. Klevering, B.J., et al., *The spectrum of retinal phenotypes caused by mutations in the ABCA4 gene*. *Graefes Arch Clin Exp Ophthalmol*, 2005. **243**(2): p. 90-100.
38. Chung, M. and A.J. Lotery, *Genetics update of macular diseases*. *Ophthalmol Clin North Am*, 2002. **15**(4): p. 459-65.
39. Michaelides, M., D.M. Hunt, and A.T. Moore, *The genetics of inherited macular dystrophies*. *J Med Genet*, 2003. **40**(9): p. 641-50.
40. K., S., *Über familiäre Degeneration in de Makulagegend des Auges mit und ohne psychischen Störungen*. *Arch f Psych und Nervenkr*, 1917(58): p. 852-887.
41. Stargardt, K., *Über familiäre, progressive Degeneration in der Makulagegend des Auges*. *Graefes Arch Clin Exp Ophthalmol*, 1909(71): p. 534-550.
42. Blacharski, P., *Retinal dystrophies and degenerations*. Newsome DA (ed), 1988: p. 135-159.
43. Allikmets, R., et al., *A photoreceptor cell-specific ATP-binding transporter gene (ABCR) is mutated in recessive Stargardt macular dystrophy*. *Nat Genet*, 1997. **15**(3): p. 236-46.
44. Klevering, B.J., et al., *Phenotypic spectrum of autosomal recessive cone-rod dystrophies caused by mutations in the ABCA4 (ABCR) gene*. *Investigative Ophthalmology & Visual Science*, 2002. **43**(6): p. 1980-5.
45. Westeneng-van Haafden, S.C., et al., *Clinical and genetic characteristics of late-onset Stargardt's disease*. *Ophthalmology*, 2012. **119**(6): p. 1199-210.
46. van Driel, M.A., et al., *ABCR unites what ophthalmologists divide(s)*. *Ophthalmic Genet*, 1998. **19**(3): p. 117-22.
47. Maugeri, A., et al., *The 2588G-->C mutation in the ABCR gene is a mild frequent founder mutation in the Western European population and allows the classification of ABCR mutations in patients with Stargardt disease*. *Am J Hum Genet*, 1999. **64**(4): p. 1024-35.
48. Allikmets, R., et al., *Mutation of the Stargardt disease gene (ABCR) in age-related macular degeneration*. *Science*, 1997. **277**(5333): p. 1805-7.
49. Allikmets, R., *Further evidence for an association of ABCR alleles with age-related macular degeneration. The International ABCR Screening Consortium*. *Am J Hum Genet*, 2000. **67**(2): p. 487-91.
50. Stone, E.M., et al., *Allelic variation in ABCR associated with Stargardt disease but not age-related macular degeneration*. *Nat Genet*, 1998. **20**(4): p. 328-9.



51. Guymer, R.H., et al., *Variation of codons 1961 and 2177 of the Stargardt disease gene is not associated with age-related macular degeneration*. Arch Ophthalmol, 2001. **119**(5): p. 745-51.
52. Fishman, G.A., et al., *Variation of clinical expression in patients with Stargardt dystrophy and sequence variations in the ABCR gene*. Arch Ophthalmol, 1999. **117**(4): p. 504-10.
53. Lois, N., et al., *Phenotypic subtypes of Stargardt macular dystrophy-fundus flavimaculatus*. Arch Ophthalmol, 2001. **119**(3): p. 359-69.
54. Sun, H. and J. Nathans, *Stargardt's ABCR is localized to the disc membrane of retinal rod outer segments*. Nat Genet, 1997. **17**(1): p. 15-6.
55. Molday, L.L., A.R. Rabin, and R.S. Molday, *ABCR expression in foveal cone photoreceptors and its role in Stargardt macular dystrophy*. Nat Genet, 2000. **25**(3): p. 257-8.
56. Lenis, T.L., et al., *Complement modulation in the retinal pigment epithelium rescues photoreceptor degeneration in a mouse model of Stargardt disease*. Proc Natl Acad Sci U S A, 2017. **114**(15): p. 3987-3992.
57. Aukrust, I., et al., *The intronic ABCA4 c.5461-10T>C variant, frequently seen in patients with Stargardt disease, causes splice defects and reduced ABCA4 protein level*. Acta Ophthalmol, 2017. **95**(3): p. 240-246.
58. Bungert, S., L.L. Molday, and R.S. Molday, *Membrane topology of the ATP binding cassette transporter ABCR and its relationship to ABC1 and related ABCA transporters: identification of N-linked glycosylation sites*. J Biol Chem, 2001. **276**(26): p. 23539-46.
59. Zernant, J., et al., *Analysis of the ABCA4 gene by next-generation sequencing*. Invest Ophthalmol Vis Sci, 2011. **52**(11): p. 8479-87.
60. Chacon-Camacho, O.F., et al., *ABCA4 mutational spectrum in Mexican patients with Stargardt disease: Identification of 12 novel mutations and evidence of a founder effect for the common p.A1773V mutation*. Exp Eye Res, 2013. **109**: p. 77-82.
61. Riveiro-Alvarez, R., et al., *Outcome of ABCA4 disease-associated alleles in autosomal recessive retinal dystrophies: retrospective analysis in 420 Spanish families*. Ophthalmology, 2013. **120**(11): p. 2332-7.
62. Bocquet, B., et al., *Relative frequencies of inherited retinal dystrophies and optic neuropathies in Southern France: assessment of 21-year data management*. Ophthalmic Epidemiol, 2013. **20**(1): p. 13-25.
63. Miraldi Utz, V., et al., *Predictors of visual acuity and genotype-phenotype correlates in a cohort of patients with Stargardt disease*. Br J Ophthalmol, 2014. **98**(4): p. 513-8.
64. Zaneveld, J., et al., *Comprehensive analysis of patients with Stargardt macular dystrophy reveals new genotype-phenotype correlations and unexpected diagnostic revisions*. Genet Med, 2015. **17**(4): p. 262-70.
65. Xin, W., et al., *Identification of Genetic Defects in 33 Proband with Stargardt Disease by WES-Based Bioinformatics Gene Panel Analysis*. PLoS One, 2015. **10**(7): p. e0132635.
66. Scieczynska, A., et al., *Next-generation sequencing of ABCA4: High frequency of complex alleles and novel mutations in patients with retinal dystrophies from Central Europe*. Exp Eye Res, 2016. **145**: p. 93-99.
67. Boon, C.J., et al., *Mutations in the peripherin/RDS gene are an important cause of multifocal pattern dystrophy simulating STGD1/fundus flavimaculatus*. Br J Ophthalmol, 2007. **91**(11): p. 1504-11.
68. Stone, E.M., et al., *Clinical features of a Stargardt-like dominant progressive macular dystrophy with genetic linkage to chromosome 6q*. Arch Ophthalmol, 1994. **112**(6): p. 765-72.
69. Kniazeva, M., et al., *A new locus for autosomal dominant stargardt-like disease maps to chromosome 4*. Am J Hum Genet, 1999. **64**(5): p. 1394-9.
70. Zhang, K., et al., *A 5-bp deletion in ELOVL4 is associated with two related forms of autosomal dominant macular dystrophy*. Nat Genet, 2001. **27**(1): p. 89-93.

71. Zhang, K., et al., *The ABCR gene in recessive and dominant Stargardt diseases: a genetic pathway in macular degeneration*. Genomics, 1999. **60**(2): p. 234-7.
72. Yatsenko, A.N., et al., *An ABCA4 genomic deletion in patients with Stargardt disease*. Hum Mutat, 2003. **21**(6): p. 636-44.
73. Zernant, J., et al., *Analysis of the ABCA4 genomic locus in Stargardt disease*. Hum Mol Genet, 2014. **23**(25): p. 6797-806.
74. Shapiro, M.B. and P. Senapathy, *RNA splice junctions of different classes of eukaryotes: sequence statistics and functional implications in gene expression*. Nucleic Acids Res, 1987. **15**(17): p. 7155-74.
75. Webster, A.R., et al., *An analysis of allelic variation in the ABCA4 gene*. Invest Ophthalmol Vis Sci, 2001. **42**(6): p. 1179-89.
76. Cornelis, S.S., et al., *In Silico Functional Meta-Analysis of 5,962 ABCA4 Variants in 3,928 Retinal Dystrophy Cases*. Hum Mutat, 2017. **38**(4): p. 400-408.
77. Schulz, H.L., et al., *Mutation Spectrum of the ABCA4 Gene in 335 Stargardt Disease Patients From a Multicenter German Cohort-Impact of Selected Deep Intronic Variants and Common SNPs*. Invest Ophthalmol Vis Sci, 2017. **58**(1): p. 394-403.
78. Zernant, J., et al., *Frequent hypomorphic alleles account for a significant fraction of ABCA4 disease and distinguish it from age-related macular degeneration*. J Med Genet, 2017. **54**(6): p. 404-412.
79. Braun, T.A., et al., *Non-exomic and synonymous variants in ABCA4 are an important cause of Stargardt disease*. Hum Mol Genet, 2013. **22**(25): p. 5136-45.
80. Seland, J.H., et al., *Visual impairment and quality of life in the older European population, the EUREYE study*. Acta Ophthalmol, 2011. **89**(7): p. 608-13.
81. Crews, J.E., et al., *The Association of Health-Related Quality of Life with Severity of Visual Impairment among People Aged 40-64 Years: Findings from the 2006-2010 Behavioral Risk Factor Surveillance System*. Ophthalmic Epidemiol, 2016. **23**(3): p. 145-53.
82. Augustin, A., et al., *Anxiety and depression prevalence rates in age-related macular degeneration*. Invest Ophthalmol Vis Sci, 2007. **48**(4): p. 1498-503.
83. Finger, R.P., et al., *The impact of the severity of vision loss on vision-related quality of life in India: an evaluation of the IND-VFQ-33*. Invest Ophthalmol Vis Sci, 2011. **52**(9): p. 6081-8.
84. Hamblion, E.L., A.T. Moore, and J.S. Rahi, *The health-related quality of life of children with hereditary retinal disorders and the psychosocial impact on their families*. Invest Ophthalmol Vis Sci, 2011. **52**(11): p. 7981-6.
85. van der Aa, H.P., et al., *Major depressive and anxiety disorders in visually impaired older adults*. Invest Ophthalmol Vis Sci, 2015. **56**(2): p. 849-54.
86. Casten, R.J. and B.W. Rovner, *Update on depression and age-related macular degeneration*. Curr Opin Ophthalmol, 2013. **24**(3): p. 239-43.
87. Ivers, R.Q., et al., *Visual impairment and risk of hip fracture*. Am J Epidemiol, 2000. **152**(7): p. 633-9.
88. Crews, J.E. and V.A. Campbell, *Vision impairment and hearing loss among community-dwelling older Americans: implications for health and functioning*. Am J Public Health, 2004. **94**(5): p. 823-9.
89. PR, L., *Testimony before: Departments of Labor, Health, and Human Services, and Related Agencies. 1st U.S. Congress House Committee on Appropriations for 1993.*, D.C.G.P.O. Washington, 1992, Editor. 1992: pt 8A, 1317-30.
90. van der Aa, H.P., et al., *Stepped care for depression and anxiety in visually impaired older adults: multicentre randomised controlled trial*. BMJ, 2015. **351**: p. h6127.
91. Matamoros, E., et al., *Quality of Life in Patients Suffering from Active Exudative Age-Related Macular Degeneration: The EQUADE Study*. Ophthalmologica, 2015. **234**(3): p. 151-9.
92. Cimarolli, V.R., et al., *Anxiety and depression in patients with advanced macular degeneration: current perspectives*. Clin Ophthalmol, 2016. **10**: p. 55-63.

93. Jivraj, J., et al., *Prevalence and impact of depressive symptoms in patients with age-related macular degeneration*. *Can J Ophthalmol*, 2013. **48**(4): p. 269-73.
94. Sainohira, M., et al., *Quantitative analyses of factors related to anxiety and depression in patients with retinitis pigmentosa*. *PLoS One*, 2018. **13**(4): p. e0195983.
95. Anil, K. and G. Garip, *Coping strategies, vision-related quality of life, and emotional health in managing retinitis pigmentosa: a survey study*. *BMC Ophthalmol*, 2018. **18**(1): p. 21.
96. Levinson, J.D., et al., *Physical Activity and Quality of Life in Retinitis Pigmentosa*. *J Ophthalmol*, 2017. **2017**: p. 6950642.
97. Chaumet-Riffaud, A.E., et al., *Impact of Retinitis Pigmentosa on Quality of Life, Mental Health, and Employment Among Young Adults*. *Am J Ophthalmol*, 2017. **177**: p. 169-174.
98. Azoulay, L., et al., *Threshold levels of visual field and acuity loss related to significant decreases in the quality of life and emotional states of patients with retinitis pigmentosa*. *Ophthalmic Res*, 2015. **54**(2): p. 78-84.
99. Prem Senthil, M., J. Khadka, and K. Pesudovs, *Seeing through their eyes: lived experiences of people with retinitis pigmentosa*. *Eye (Lond)*, 2017. **31**(5): p. 741-748.
100. Cohn, D.E., et al., *A cost-utility analysis of NRG Oncology/Gynecologic Oncology Group Protocol 218: incorporating prospectively collected quality-of-life scores in an economic model of treatment of ovarian cancer*. *Gynecol Oncol*, 2015. **136**(2): p. 293-9.
101. Tosh, J., et al., *A review of generic preference-based measures of health-related quality of life in visual disorders*. *Value Health*, 2012. **15**(1): p. 118-27.





A large, bright yellow sun or moon is positioned in the upper left quadrant of the image. The sky is filled with soft, pink and orange clouds, suggesting a sunset or sunrise. The bottom of the image shows a body of water with gentle waves, and a faint silhouette of a mountain range is visible in the distance.

# **CHAPTER 2**

## **Clinical characteristics of Stargardt disease**



## CHAPTER 2.1

### Early-onset Stargardt disease: phenotypic and genotypic characteristics

*“In its natural course, early-onset Stargardt disease initially presents with variable full-field electroretinographic abnormalities and fundusoscopic findings. As this retinal degeneration progresses, the spectrum of phenotypes eventually converges, causing profound chorioretinal atrophy and severe vision loss.”*

2

Stanley Lambertus  
Ramon A.C. van Huet  
Nathalie M. Bax  
Lies H. Hoefsloot  
Frans P.M. Cremers  
Camiel J.F. Boon  
B. Jeroen Klevering  
Carel B. Hoyng

Ophthalmology. 2015 Feb;122(2):335-44.doi: 10.1016/j.opthta.2014.08.032.

The authors thank L. Ye, MD and P.J.M. van den Wittenboer, MD for their contribution, without which this study could not have been completed.



**OBJECTIVE:** To describe the phenotype and genotype of patients with early-onset Stargardt disease.

**DESIGN:** Retrospective cohort study.

**PARTICIPANTS:** Fifty-one Stargardt patients with age at onset  $\leq 10$  years.

**METHODS:** We reviewed patient medical records for age at onset, medical history, initial symptoms, best-corrected visual acuity (BCVA), ophthalmoscopy, fundus photography, fundus autofluorescence (FAF), fluorescein angiography (FA), spectral-domain optical coherence tomography (SD-OCT), and full-field electroretinography (ffERG). The *ABCA4* gene was screened for mutations.

**MAIN OUTCOME MEASURES:** Age at onset, BCVA, fundus appearance, FAF, FA, SD-OCT, ffERG, and presence of *ABCA4* mutations.

**RESULTS:** The mean age at onset was 7.2 years (range, 1–10). The median times to develop BCVA of 20/32, 20/80, 20/200, and 20/500 were 3, 5, 12, and 23 years, respectively. Initial ophthalmoscopy in 41 patients revealed either no abnormalities or foveal retinal pigment epithelium (RPE) changes in 10 and 9 patients, respectively; the other 22 patients had foveal atrophy, atrophic RPE lesions, and/or irregular yellow-white fundus flecks. On FA, there was a “dark choroid” in 21 out of 29 patients. In 14 out of 50 patients, foveal atrophy occurred before flecks developed. On FAF, there was centrifugal expansion of disseminated atrophic spots, which progressed to the eventual profound chorioretinal atrophy. Spectral-domain OCT revealed early photoreceptor damage followed by atrophy of the outer retina, RPE, and choroid. On ffERG in 26 patients, 15 had normal amplitudes, and 11 had reduced photopic and/or scotopic amplitudes at their first visit. We found no correlation between ffERG abnormalities and the rate of vision loss. Thirteen out of 25 patients had progressive ffERG abnormalities. Finally, genetic screening of 44 patients revealed  $\geq 2$  *ABCA4* mutations in 37 patients and single heterozygous mutations in 7.

**CONCLUSIONS:** In early-onset Stargardt, initial ophthalmoscopy can reveal no abnormalities or minor retinal abnormalities. Yellow-white flecks can be preceded by foveal atrophy and may be visible only on FAF. Although ffERG is insufficient for predicting the rate of vision loss, abnormalities can develop. Over time, visual acuity declines rapidly in parallel with progressive retinal degeneration, resulting in profound chorioretinal atrophy. Thus, early-onset Stargardt lies at the severe end of the spectrum of *ABCA4*-associated retinal phenotypes.

## Introduction

Stargardt disease (STGD1) is the most prevalent inherited juvenile-onset retinal dystrophy, with a mean age at onset of 15.2 years.<sup>1,2</sup> The inheritance pattern of STGD1 is autosomal recessive, and the disease is characterized by the presence of irregular yellow-white fundus flecks in the posterior pole.<sup>2-4</sup> Over time, the disease progresses to include macular depigmentation and chorioretinal atrophy. Typical STGD1 patients have normal—or near-normal—panretinal cone and rod function on full-field electroretinography (ffERG); however, progressive abnormalities in photopic and scotopic amplitudes have been reported.<sup>5-7</sup> Blockage of choroidal fluorescence (the so-called dark choroid sign) on fluorescein angiography is present in 80% of STGD1 patients.<sup>8-10</sup> The aforementioned yellow-white fundus flecks are hyperautofluorescent on fundus autofluorescence (FAF), presumably owing to an accumulation of lipofuscin fluorophores in the retinal pigment epithelium (RPE).<sup>11,12</sup> Spectral-domain optical coherence tomography (SD-OCT) can reveal changes in the outer nuclear layer, as well as photoreceptor loss, RPE abnormalities, and a general thinning of the retina.<sup>13</sup>

Mutations in the *ABCA4* gene have been associated with a spectrum of retinal diseases ranging from mild phenotypes (e.g., late-onset STGD1 with relatively preserved visual function) to severe, early-onset retinitis pigmentosa accompanied by a rapid loss of central and peripheral photoreceptors.<sup>14-16</sup> The *ABCA4* gene encodes the retinal-specific ATP-binding cassette transporter (ABCR).<sup>17</sup> *ABCA4* is expressed in both cones and rods. In rod cells, the ABCR protein is localized at the rim of the outer segment discs, where ABCR transports *all-trans*-retinal from the lumen of the outer segment disc to the cytoplasm of the photoreceptor cell.<sup>18</sup> The accumulation of *all-trans*-retinal—and its toxic derivatives—eventually results in the death of RPE cells and photoreceptor cells.<sup>19-21</sup> The *ABCA4* gene has high mutation heterogeneity; >700 distinct mutations have been identified to date, with a wide range of effects on ABCR protein function. A model to correlate the phenotype with the functional severity of the *ABCA4* mutation has been proposed.<sup>22,23</sup> According to this model, STGD1 results from mild to moderate ABCR impairment.

Among patients who are diagnosed with STGD1, the disease has remarkably wide clinical variability with respect to the general course of the disease, the retinal features, and the electrophysiologic findings.<sup>5,8,14,15</sup> Stargardt disease has both genetic and clinical overlap with cone-rod dystrophy, and this may cause confusion among general ophthalmologists; indeed, diagnosing STGD1 can be challenging at an early age. Therefore, obtaining an accurate description of the full

spectrum of *ABCA4*-associated retinal dystrophies—including STGD1—is essential for providing appropriate patient counseling and adequate disease management, and may have important implications for selecting patients to participate in gene therapy trials. Although clinical features of STGD1 patients with a very young onset have been described in heterogeneous cohorts,<sup>5,7,24,25</sup> there is lack of studies concerning the natural history of these patients. Herein, we have provided a comprehensive description of the initial and longitudinal clinical and genetic characteristics of a large number of patients with early-onset Stargardt, which we defined as an age at onset  $\leq 10$  years.

## Methods

### Patients and Genetic Analysis

The database of the Department of Ophthalmology at Radboud university medical center (Nijmegen, The Netherlands) contains 426 patients with a clinical diagnosis of STGD1. For 258 of these patients, the *ABCA4* gene was analyzed by the Department of Human Genetics at Radboud university medical center (Nijmegen, The Netherlands). Known mutations were screened using the arrayed-primer extension microarray (Asper Biotech, Tartu, Estonia), and exon duplications and/or deletions were detected using multiplex ligation-dependent probe amplification (MRC-Holland P151/P152). If no mutations or only a single heterozygous mutation was identified, the exons and intron–exon boundaries were sequenced using the Sanger method to screen for mutations in the other allele. All identified mutations were confirmed using Sanger sequencing. In total, 199 patients contained  $\geq 1$  mutation in the *ABCA4* gene. Age at onset of disease was defined as the age at which symptoms were first noticed by the patient. If this information was not available, we used the patient’s age at which he or she first visited an ophthalmologist.

In this study, we included 51 patients with an age at onset of  $\leq 10$  years and one of the following criteria:  $\geq 2$  *ABCA4* mutations ( $n = 37$ ); 1 *ABCA4* mutation and the presence of yellow-white flecks ( $n = 7$ ); or in the absence of *ABCA4* analysis, the presence of yellow-white flecks, and either a dark choroid or an atrophic macular lesion ( $n = 7$ ).

This study was approved by the Institutional Ethics Committee and was performed in accordance with the Declaration of Helsinki. All patients provided informed consent before giving a blood sample and receiving additional ophthalmologic examinations.

## Clinical Evaluation

We defined the duration of disease as the time interval between the patient's age at onset (defined as described) and the age at the last visit. Best-corrected visual acuity (BCVA) was measured using a Snellen chart, then transformed into the logarithm of the minimum angle of resolution (logMAR) for subsequent analysis. A logMAR value of 1.9, 2.3, or 2.7 was assigned to the patient's ability to count fingers, detect hand movements, or perceive light, respectively.<sup>26</sup> Fundus characteristics were documented for 41 patients using fundus photography (Topcon TRC-50IX, Topcon Corporation, Tokyo, Japan). Fundus autofluorescence was performed in 32 patients using a confocal scanning laser ophthalmoscope (cSLO; Spectralis, Heidelberg Engineering, Heidelberg, Germany) fitted with an optically pumped solid-state laser (488-nm excitation). Atrophic chorioretinal lesions outside the fovea were stratified into 2 groups: (1) A patchy pattern consisting of mild disseminated hypoautofluorescent spots and (2) sharply demarcated chorioretinal atrophic lesions with an absence of autofluorescence; the extent of these lesions was then classified as either (1) lesions that were limited to the posterior pole, or (2) lesions that extended beyond the vascular arcades. Cross-sectional images were obtained for 30 patients using SD-OCT (Spectralis, Heidelberg Engineering). Fluorescein angiography (Topcon TRC-50IX, Topcon Corporation; Spectralis, Heidelberg Engineering) was performed in 32 patients to determine the presence or absence of the "dark choroid" sign. Full-field ERG was performed in 43 patients in accordance with the guidelines established by the International Society for Clinical Electrophysiology of Vision (ISCEV)<sup>27</sup> using either Dawson-Trick-Litzkow electrodes or contact lens electrodes together with the RETI-port system (Roland Consults, Stasche & Finger GmbH, Brandenburg an der Havel, Germany). Dawson-Trick-Litzkow and contact lens electrodes have similarly high signal stability.<sup>28</sup> Based on the ffERG results, the patients were assigned to 3 groups as described previously<sup>5</sup>: Group 1 consisted of patients with normal ffERG amplitudes, group 2 consisted of patients with reduced photopic amplitude (<5% of normal range, <78  $\mu$ V [B-wave]) and normal scotopic amplitude, and group 3 consisted of patients with reduced photopic and scotopic amplitudes (<5% of normal range, <263  $\mu$ V [B-wave]).

## Statistical Analysis

Data were analyzed using SPSS version 20.0 (IBM Corp, Armonk, NY). Kaplan-Meier “survival” curves were used to analyze the interval between the age at onset and the age at which the following endpoints were achieved: Mild visual impairment ( $\geq 0.2$  logMAR; Snellen  $\leq 20/32$ ), moderate visual impairment ( $\geq 0.6$  logMAR; Snellen  $\leq 20/80$ ), severe visual impairment ( $\geq 1.0$  logMAR; Snellen  $\leq 20/200$ ), and blindness ( $\geq 1.4$  logMAR; Snellen  $\leq 20/500$ ).<sup>29</sup> Cox regression analysis was used to compare the fFERG groups. Differences with a *P* value of  $\leq 0.05$  were considered significant.

## Results

### Initial Clinical Characteristics

A total of 51 patients (28 men and 23 women) were included in this study. The mean ( $\pm$  standard deviation) age at onset was 7.2 ( $\pm 2.2$ ) years (median, 8; range, 1–10).

### Visual Acuity

In each case, the initial symptom of the disease was a decline in visual acuity noticed by the patient, the patient’s parents, or the school physician. Where available (*n* = 41 patients), the mean BCVA at the first visit to an ophthalmologist was 0.51 ( $\pm 0.36$ ) logMAR (median, 0.48; range, 0–1.15), Snellen 20/65. In 13 patients, the vision loss was initially unexplained. Six of these 13 patients were diagnosed with functional vision loss, and 6 other patients were diagnosed initially with cone–rod dystrophy. Of the 51 patients, 22 were diagnosed with STGD1  $\geq 3$  years after the initial symptoms appeared (range, 3–30).

### Retinal Features

Ophthalmoscopy performed at the first visit revealed no retinal abnormalities in 10 out of 41 patients. Nine additional patients had foveal RPE changes, and the remaining 22 patients had foveal atrophy, atrophic RPE lesions that were not limited to the fovea, and/or irregular yellow-white fundus flecks. Fluorescein angiography in 29 patients revealed an absence of choroidal fluorescence (the so-called dark choroid) in 21 patients. In patient 4, FAF revealed subtle hyperautofluorescence of the fovea, and SD-OCT revealed thickening of what appeared to be the external limiting membrane (Fig 1A<sub>1,2,3</sub>). One year later, this patient developed several small parafoveal hyperautofluorescent flecks with no apparent abnormalities on ophthalmoscopy (Fig 1B<sub>2</sub>).

### Electrophysiologic Findings

At their first visit, ffERG data were collected for 26 patients, and the patients were classified based on their findings. Group 1 (patients with normal photopic and scotopic amplitudes) contained 15 patients (58%), group 2 (patients with reduced photopic amplitude and normal scotopic amplitudes) contained 4 patients (15%), and group 3 (patients with reduced photopic and scotopic amplitudes) contained 6 patients (23%). One patient could not be classified into 1 of these 3 groups because only the scotopic amplitudes were reduced moderately, although no pigmentary retinopathy was observed. We found no correlation between the ffERG group classification at the first visit and progression toward mild visual impairment ( $P = 0.485$ ), moderate visual impairment ( $P = 0.309$ ), severe visual impairment ( $P = 0.203$ ), or blindness ( $P = 0.647$ ).

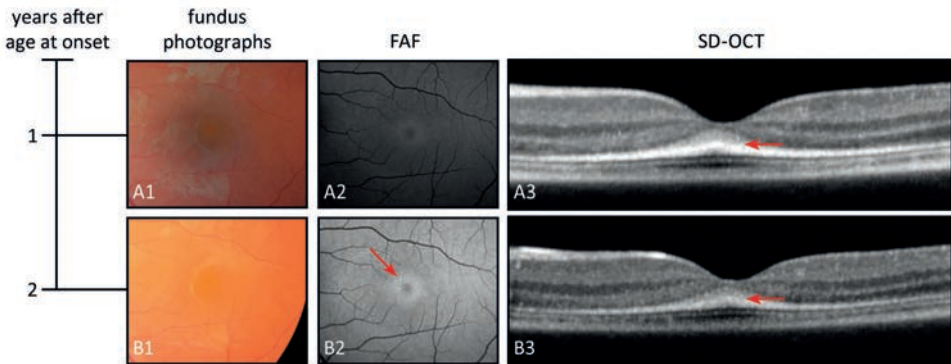


**Figure 1.** Retinal imaging of patient 4 (age at onset, 6 years; best-corrected visual acuity, 0.24 logarithm of the minimum angle of resolution; Snellen 20/35; ABCA4 genotype: p.Thr983Ala and c.5461-10T>C (p.?) at 7 (A<sub>1,2,3</sub>) and 8 (B<sub>1,2,3</sub>) years of age. Initially, only subtle foveal hyperautofluorescence was present (A<sub>2</sub>); 1 year later, small parafoveal hyperautofluorescent flecks were present (the arrow in B<sub>2</sub>), despite a lack of apparent abnormalities on ophthalmoscopy. Spectral-domain optical coherence tomography (SD-OCT) revealed foveal thickening of the band representing the external limiting membrane (the arrows in A<sub>3</sub>–B<sub>3</sub>). FAF = fundus autofluorescence.

### Natural Course

The mean disease duration was 17.1 ( $\pm 14.5$ ) years (median, 11; range, 0–56). The follow-up period ranged from a single examination in 3 patients to 47 years (mean, 12.4 $\pm$ 12.6; median, 9). The clinical and genetic characteristics of the patient cohort at the last examination are summarized in [Table 1](#).

28	9	19	0.72 (20/105)	Yes	NP	N	N	c.5461-10T>C	NI
29	1	28	1.90 (CF)	Yes	Yes	SR	N	c.5585-10T>C	NI
30	8	26	1.30 (20/400)	Yes	Yes	N	N	c.5312+1G>A	c.286A>G
31	10	22	1.90 (CF)	Yes	Yes	SR	N	c.2588G>C	c.4539+1G>T
32	9	15	0.80 (20/125)	Yes	Yes	NP	NP	c.2588G>C	c.4539+1G>T
33	7	18	1.15 (20/286)	Yes	NP	N	N	c.1957C>T, c.6320G>A, c.3449G>A	c.5537T>C
34	10	31	1.15 (20/286)	Yes	Yes	N	N	c.5461-10T>C	c.5537T>C
35	7	11	0.80 (20/125)	Yes	NP	N	N	c.818G>A	NI
36	7	7	0.80 (20/125)	No	Yes	N	N	c.872C>T, 4224G>T	c.2947A<G
37	8	22	1.15 (20/286)	Yes	NP	N	N	c.1822T>A	c.5882G>A
38	10	13	0.52 (20/67)	No	No	N	N	c.5882G>A	c.5882G>A
39	10	16	1.15 (20/286)	Yes	No	N	N	c.768G>T	c.1822T>A
40	5	24	1.30 (20/400)	Yes	Yes	MR	MR	c.768G>T	c.5461-10T>C
41	6	22	1.90 (CF)	Yes	Yes	ND	ND	c.1622T>C, 3113C>T	c.1622T>C, 3113C>T
42	10	22	1.30 (20/400)	Yes	Yes	MR	N	NP	
43	7	19	1.10 (20/250)	Yes	NP	N	N	NP	
44	8	19	1.00 (20/200)	Yes	NP	SR	N	NP	
45	5	15	1.00 (20/200)	Yes	Yes	MR	N	c.3335C>A	c.5461-10T>C
46	7	31	2.30 (HM)	Yes	No	ND	MR	c.1822T>A	c.5461-10T>C
47	9	20	0.85 (20/143)	Yes	NP	N	N	c.122G>A	c.286A>G
48	4	32	1.00 (20/200)	Yes	NP	NP	NP	c.5882G>A	NI
49	8	18	1.00 (20/200)	Yes	No	SR	ND	c.286A>G	c.286A>G
50	9	14	0.80 (20/125)	No	No	ND	SR	c.4773+1G>A	c.5461-10T>C
51	8	43	1.90 (CF)	Yes	No	ND	ND	c.768G>T	c.5113C>T

BCVA = best-corrected visual acuity; CF = counting fingers; del = deletion; dup = duplication; jfERG = full-field electroretinography; HM = hand movements;

logMAR = logarithm of the minimum angle of resolution; NI = not identified; NP = not performed.

\* Age, BCVA, and jfERG at last examination.

+ The abbreviations reflect the B-wave amplitude: N = normal (equal to or above the lower 5% of the range for a normal population: photopic  $\geq 78$   $\mu$ V, scotopic  $\geq 263$   $\mu$ V); MR = moderately reduced (1%-5% or normal range: photopic  $\geq 69$   $\mu$ V and  $< 78$   $\mu$ V, scotopic  $\geq 195$   $\mu$ V and  $< 263$   $\mu$ V); SR = severely reduced ( $< 1\%$  of normal range, photopic  $< 69$   $\mu$ V, scotopic  $< 195$   $\mu$ V); ND = not detectable (flat amplitudes).

‡ Mean age at onset of the total cohort is used.

§ In the patients' medical records fundus findings were described "in accordance with Stargardt," but no detailed description or imaging was made and thus were excluded from imaging analysis.

Table 1. Clinical and Genetic Characteristics of 51 Early-Onset Stargardt Patients

Patient	Age at Onset (y)	Age (y)*	BCVA [Snellen]*	(logMAR)	Fundus Findings		fERG±		Mutations	
					Flacks	Dark Chorioid	Photopic	Scotopic	Allele 1	Allele 2
1	7 <sup>1</sup>	18	0.30 (20/40)		Yes	Yes	NP	NP	c.2588G>C, c.6556G>C, c.1822T>A	
2	8	14	0.89 (20/155)		Yes	NP	NP	NP	c.5461-10T>C	c.5461-10T>C
3	6	17	1.90 (CF)		Yes	Yes	N	MR	c.5461-10T>C	c.5461-10T>C
4	6	8	0.20 (20/32)		Yes	Yes	MR	N	c.2947A>G	c.5461-10T>C
5	6	57	2.30 (HM)		Yes	Yes	ND	ND	c.768G>T	c.443-?_570+?del
6	9	10	0.40 (20/50)		Yes	Yes	SR	N	c.768G>T	NI
7	6	40	1.30 (20/400)		Yes	NP	NP	NP	c.5461-10T>C	c.5714+5G>A
8	4	35	1.90 (CF)		Yes	Yes	MR	N	c.4462T>C	c.2919-?_3328+?del
9	9	25	1.90 (CF)		Yes	Yes	NP	NP	c.768G>T	NI
10	3	36	1.90 (CF)		Yes	Yes	SR	SR	c.3813G>C	NI
11	5	52	2.30 (HM)		Yes	NP	MR	MR	c.6411T>A	NI
12	7	8	1.22 (20/333)		Yes	Yes	MR	MR	c.768G>T	c.5461-10T>C
13	7	7	0.33 (20/43)		Yes	Yes	MR	MR	NP	
14	9	17	1.15 (20/286)		Yes	No	N	N	c.3874C>T	c.6543_6578del
15	3	14	1.00 (20/200)		Yes	NP	N	N	c.4539+1G>T	c.768G>T
16	9	11	1.10 (20/250)		Yes	No	MR	N	NP	
17	10	47	1.90 (CF)		Yes	Yes	SR	SR	NP	
18	7	48	2.30 (HM)		Yes	NP	SR	SR	c.768G>T	c.5461-10T>C
19	6	43	1.90 (CF)		Yes	NP	SR	SR	c.768G>T	c.5461-10T>C
20	8	33	1.10 (20/250)		Yes	No	N	N	c.5161-5162delAC	c.5882G>A
21	8	64	1.90 (CF)		Yes	NP	ND	ND	c.2947A>G	c.4506C>A
22	8	31	1.90 (CF)		Yes	NP	SR	SR	NP	
23	9	51	1.90 (CF)		Yes	Yes	ND	ND	c.768G>T	c.5461-10T>C
24	3	19	1.00 (20/200)		Yes	No	ND	N	c.5461-10T>C	c.6320G>A
25	9	16	1.30 (20/400)		Yes	NP	MR	N	c.214G>A	c.5461-10T>C
26	5	10	1.10 (20/250)		Yes	NP	NP	NP	c.5762_5763dup	c.2919-?_3328+?del
27	10	31	0.40 (20/50)		NP <sup>‡</sup>	NP <sup>‡</sup>	NP	NP	c.455G>A	c.5461-10T>C



## Visual Acuity

A survival analysis yielded a median interval and 95% CI between age at onset and a decline in BCVA to mild visual impairment, moderate visual impairment, severe visual impairment, and blindness of 3 (95% CI, 1.1–4.9), 5 (95% CI, 2.2–7.8), 12 (95% CI, 9.3–14.7), and 23 (95% CI, 13.2–32.8) years, respectively (Fig 2). Mean patient age at the last recorded visit was 24.9 ( $\pm 14.0$ ) years (median, 20; range, 7–64), and mean BCVA was 1.29 ( $\pm 0.58$ ) logMAR (median, 1.15; range, 0.20–2.30), Snellen 20/386.

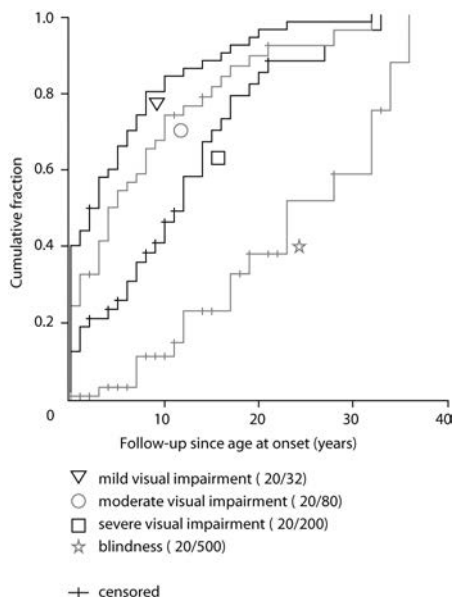


**Figure 2.** Kaplan-Meier curves showing the cumulative fraction in early-onset Stargardt with the following clinical endpoints: mild visual impairment ( $\geq 0.2$  logarithm of the minimum angle of resolution [logMAR]; Snellen  $\leq 20/32$ ; triangle), moderate visual impairment ( $\geq 0.6$  logMAR; Snellen  $\leq 20/80$ ; square), severe visual impairment ( $\geq 1.0$  logMAR; Snellen  $\leq 20/200$ ; circle), and blindness ( $\geq 1.4$  logMAR; Snellen  $\leq 20/500$ ; star). Censored observations are depicted as vertical bars.

## Retinal Features

We observed irregular yellow-white fundus flecks in 47 out of 50 patients. These flecks were not always evident at the first examination, but they developed within an average of 2.9 ( $\pm 4.1$ ) years (median, 0; range, 0–17) of the first visit. The location of these flecks varied among the patients: In 10 patients, the flecks were present exclusively in the central macula; in 17 patients, the flecks were scattered throughout the posterior pole, but did not extend beyond the vascular arcades; and the remaining 20 patients presented with a fundus flavimaculatus pattern with numerous flecks in the central and mid-peripheral retina. Foveal atrophy was reported in 38 patients and occurred within 1.9 ( $\pm 3.3$ ) years (median, 0; range, 0–13) of the initial visit. Finally, 14 patients developed foveal atrophy before the appearance of fundus flecks (Fig 3A<sub>1,2</sub>).

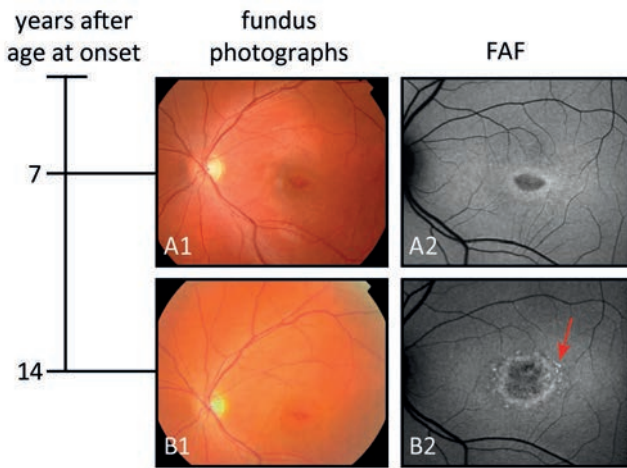


**Figure 3. Fundus photographs and autofluorescence (FAF) imaging of patient 37** (age at onset, 8 years; ABCA4 genotype: p.Phe608Ile and p.Gly1961Glu) at 15 (A<sub>1,2</sub>) and 22 years (B<sub>1,2</sub>) of age, showing isolated foveal pigment alterations and a hypoautofluorescent lesion (best-corrected visual acuity [BCVA], 0.52 logarithm of the minimum angle of resolution [logMAR], Snellen 20/66). Seven years later (B<sub>1,2</sub>), yellow-white parafoveal fundus flecks (the arrow in B<sub>2</sub>) developed (BCVA 1.15 logMAR; Snellen 20/283).

Long-term follow-up data revealed that the initial foveal atrophy progressed to more widespread chorioretinal atrophy. Over time, FAF imaging revealed centrifugal expansion of disseminated spots in 30 out of 32 patients with a mean timeframe of 9.8 ( $\pm 10.5$ ) years (median, 8; range, 0–40; Fig 4B<sub>2</sub>). These spots extended beyond the vascular arcades in 24 of these 30 patients with a mean of 11.2 ( $\pm 11.0$ ) years (median, 9.5; range, 0–40) after the first visit (Fig 4C<sub>2</sub>). In 22 out of 32 patients, the spots progressed to chorioretinal atrophic lesions after a mean period of 13.5 ( $\pm 12.3$ ) years (median, 10.5; range, 0–40; Fig 4C<sub>2</sub>–D<sub>2</sub>). In 11 of these 22 patients, the confluence of these lesions extended beyond the vascular arcades after a mean period of 23.0 ( $\pm 10.3$ ) years (median, 23; range, 5–40; Fig 4E<sub>2</sub>). The 11 patients who presented with the common phenotype of chorioretinal lesions beyond the vascular arcades at the final examination initially presented with flecks (n = 3), foveal atrophy (n = 4), or both flecks and atrophy (n = 4) at their first examination.

Over time, SD-OCT showed thinning of the outer nuclear layer and loss of the ellipsoid zone, which preceded loss of the RPE/Bruch's membrane complex. In addition, hyperreflective abnormalities in the outer retina were present (Fig 4A<sub>3</sub>). Progression occurred as an expanding loss of the outer nuclear layer, ellipsoid zone, RPE, and choriocapillaris (Fig 4B<sub>3</sub>–E<sub>3</sub>). Hyperreflective deposits in the inner layers of the fovea developed, corresponding with intraretinal pigmentations on fundus photography (Fig 4C<sub>1</sub>–C<sub>3</sub>).

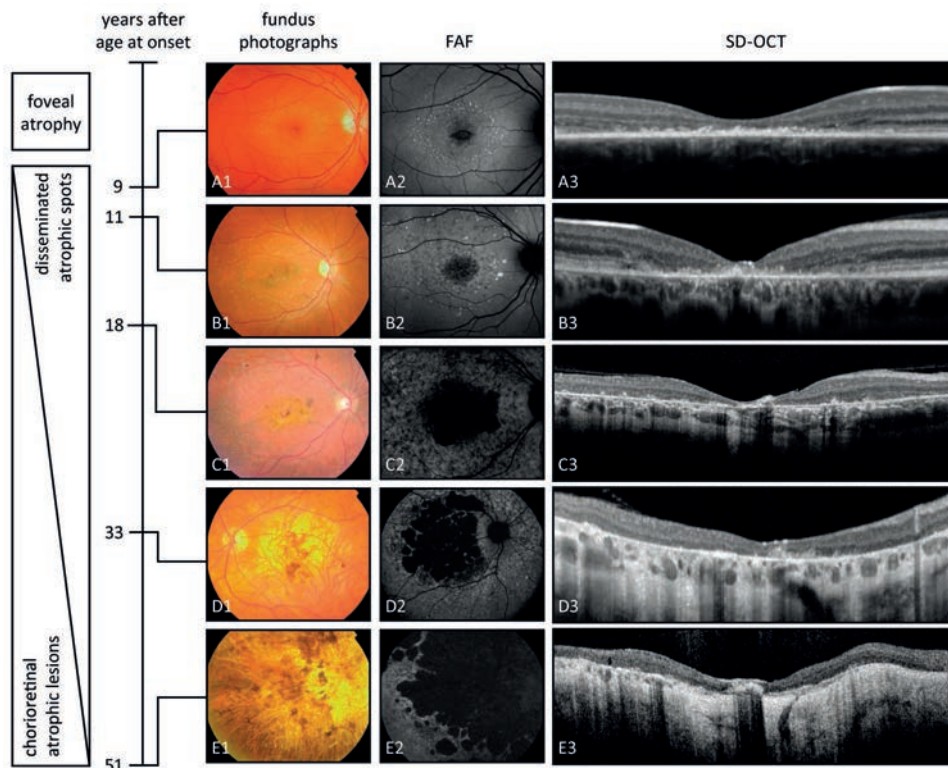


**Figure 4. Overview of the natural course of retinal disease in early-onset Stargardt based on findings obtained from 5 separate patients using fundus photography, autofluorescence (FAF), and spectral-domain optical coherence tomography (SD-OCT).** Early-onset Stargardt includes foveal atrophy and parafoveal hyperautofluorescent fundus flecks ( $A_{1,2}$ ) in an early disease stage. On SD-OCT, there is hyperreflective abnormalities in the outer retina, loss of the ellipsoid zone, and thinning of the outer nuclear layer ( $A_3$ ). The initial foveal atrophy and parafoveal flecks then extend centrifugally ( $B_{1,2}$ ), and disseminated hypoautofluorescent spots appear ( $B_2$ ). On SD-OCT, there is progression of the foveal atrophy, with thinning of the retinal pigment epithelium/Bruch's membrane complex ( $B_3$ ). Further in the course of the disease, the disseminated hypoautofluorescent spots become chorioretinal atrophic lesions, the central atrophy expands further ( $C_{1,2}$ ), and pigmentations ( $C_1$ ) are visible as hyperreflective deposits on SD-OCT ( $C_3$ ). Over time, confluence of these lesions evolves centrifugally ( $D_{1,2}$ ), extending beyond the vascular arcades ( $E_{1,2}$ ), with further retinal thinning and atrophy of the choriocapillaris ( $D_3$ – $E_3$ ) visible on SD-OCT.  $A_{1,2,3}$  Patient 1 at age 17;  $B_{1,2,3}$  patient 31 at age 22;  $C_{1,2,3}$  patient 40 at age 24;  $D_{1,2,3}$  patient 8 at age 36;  $E_{1,2,3}$  patient 5 at age 57.

### Electrophysiologic Findings

Follow-up data for 25 patients showed that 4 patients progressed from fERG group 1 to group 2 within a mean of 10.5 ( $\pm 4.4$ ) years (range, 7–16), and 9 patients progressed from group 1 to group 3 within a mean of 27.7 ( $\pm 14.4$ ) years (range, 3–47).

## Mutation Analysis

The *ABCA4* gene was screened for mutations in 44 of the 51 patients; the remaining 7 patients refused genetic analysis for personal reasons. In these 44 patients, mutations in the *ABCA4* gene were identified in 81 of the 88 alleles (92%). Thirty-three of these patients had 2 *ABCA4* mutations, 7 patients had 1 mutation, 3 patients had 3 mutations, and 1 patient had 4 mutations. In total, 37 distinct mutations were identified; these mutations are summarized in [Table 2](#). The c.768G>T mutation was identified in 25% of the 44 patients and accounted for 13% of all identified mutations. The c.5461-10T>C mutation was identified in 36% of the patients and accounted for 22% of all identified mutations. The most prevalent *ABCA4* mutation among Dutch patients with STGD1 (c.2588G>C)<sup>23</sup> was identified in only 4% of the alleles. [Table 3](#) summarizes the non-missense mutations that were identified in this study.

**Table 2.** *ABCA4* Mutations in Early-Onset Stargardt Patients

Mutation	Effect	Allele		References
		Frequency	Percentage	
c.122G>A	p.Trp41 <sup>±</sup>	1	1	35
c.214G>A	p.Gly72Arg	1	1	32
c.286A>G	p.Asn96Asp	4	5	36
c.443-?_570+?del	p.Arg149fs	1	1	This study
c.455G>A	p.Arg152Gln	1	1	32, 37
c.656G>C	p.Arg219Thr	1	1	38
c.768G>T	p.Val256Val/p.?	11	13	16, 23, 32, 39
c.818G>A	p.Trp273 <sup>±</sup>	1	1	This study
c.872C>T	p.Pro291Leu	1	1	34
c.1622T>C	p.Leu541Pro	2	2	1, 16, 32, 40
c.1822T>A	p.Phe608Ile	4	5	1, 23
c.1957C>T	p.Arg653Cys	1	1	32, 41
c.2588G>C	p.Gly863Ala/p.DelGly863	3	4	16, 18, 23, 32, 42
c.2919-?_3328+?del	p.Ser974_Gly1110delinsCys	2	2	23
c.2947A>G	p.Thr983Ala	3	4	34
c.3113C>T	p.Ala1038Val	2	2	16, 31, 32, 40, 43
c.3335C>A	p.Thr1112Asn	1	1	23
c.3449G>A	p.Cys1150Tyr	1	1	This study
c.3813G>C	p.Glu1271Asp	1	1	This study
c.3874C>T	p.Gln1292 <sup>±</sup>	1	1	34
c.4224G>T	p.Trp1408Cys	1	1	This study
c.4462T>C	p.Cys1488Arg	1	1	1, 8, 44, 45
c.4506C>A	p.Cys1502 <sup>±</sup>	1	1	34
c.4539+1G>T	p.?	3	4	1, 23, 43, 44
c.4773+1G>A	p.?	1	1	This study
c.5113C>T	p.Arg1705Trp	1	1	34
c.5161_5162del	p.Thr1721fs	1	1	23, 36
c.5312+1G>A	p.?	1	1	46
c.5461-10T>C	p.?	19	22	16, 23, 47
c.5537T>C	p.Ile1846Thr	1	1	23, 45
c.5585-10T>C	p.?	1	1	48
c.5714+5G>A	p.?	1	1	1, 23, 32, 41, 43
c.5762_5763dup	p.Ala1922fs	1	1	34
c.5882G>A	p.Gly1961Glu	5	6	18, 31, 32, 44, 49
c.6320G>A	p.Arg2107His	2	2	8, 31, 40, 45, 50
c.6411T>A	p.Cys2137 <sup>±</sup>	1	1	34
c.6543_6578del	p.Leu2182_Phe2193del	1	1	1

del = deletion; dup = duplication; fs = frame shift. References are shown for mutations that have been reported previously. \* Stop signal.

**Table 3.** Characteristics of the Non-missense ABCA4 Mutations Identified in our Cohort Study

Mutation	Protein Effect	SIFT	Polyphen-2	Grantham	PhyloP
c.3449G>A	p.Cys1150Tyr	Not tolerated	Benign	194	3.19
c.3813G>C	p.Glu1271Asp	Not tolerated	Possibly damaging	45	6.10
c.4224G>T	p.Trp1408Cys	Not tolerated	Probably damaging	215	5.86

*The outcome of 2 protein prediction programs (SIFT = tolerated or not tolerated; PolyPhen = benign, possibly damaging, probably damaging), together with Grantham (>60 pathogenic) and PhyloP conservation score (>2.5 pathogenic), were used to form the final conclusion. Mutations are proposed to be pathogenic when ≥2 categories point to pathogenicity.*

## Discussion

In this study, we examined the clinical and genetic characteristics of patients with early-onset Stargardt, a disease that lies within the spectrum of retinal phenotypes linked with mutations in the *ABCA4* gene. Whenever a spectrum of disorders contains overlapping phenotypes as the rule rather than an exception, any cutoff point used to define a particular disease within that spectrum will be arbitrary. Therefore, we arbitrarily defined “early-onset Stargardt” as occurring with an age at onset of ≤10 years of age; this definition enabled us to avoid including patients with a more typical STGD1 phenotype. Only 4% of the 51 patients in our early-onset Stargardt cohort had visual acuity of ≤0.30 logMAR, Snellen <20/40 (measured at age 8 and 18 years of age in these 2 patients), compared with 14% to 37% of patients with typical STGD1 and 59% of patients with late-onset STGD1.<sup>5,14,24</sup> Because patients with a relatively good visual acuity tended to return less often than those with progressive problems, these data may have overrepresented more severe cases. The majority of our patients for whom ffERG data were available developed abnormal ffERG amplitudes, consistent with a previous report by Fujinami et al.<sup>7</sup> However, we found no correlation between the ffERG group classifications (which were based on the nature of the ffERG abnormalities) at the age of onset and the speed of vision loss in this early-onset Stargardt cohort. This finding differs from STGD1 cohorts that included patients with later ages at onset.<sup>5,6</sup> Our findings indicate that early-onset Stargardt can be considered a distinct severe subtype of STGD1 that is characterized by early foveal abnormalities and the rapid loss of visual function; in contrast, in late-onset STGD1, foveal sparing is common, and visual acuity is often preserved to a relatively advanced age.<sup>14</sup>

## Diagnosis

The natural course of early-onset *ABCA4*-related retinal disease in our cohort reflects a broad clinical spectrum both at the time of onset and at follow-up, with varying degrees of ffERG abnormalities and yellow-white flecks and/or

atrophy at a variety of locations. Thus, each combination of electrophysiologic and fundusoscopic findings could be considered a unique phenotype at a specific time point. Moreover, these phenotypes changed during the course of the disease, suggesting progression of the disease. Because both fundusoscopic and electrophysiologic criteria have been proposed for establishing a descriptive diagnosis (e.g., Stargardt disease and cone-rod dystrophy), each individual patient can potentially receive several diagnoses at 1 time point and at follow-up. Importantly, receiving several diagnoses can be extremely confusing to both the patient and the referring ophthalmologist.

Nevertheless, we found that the spectrum of fundus presentations in this early-onset retinal dystrophy ultimately converges to a single clinical and functional endpoint that includes profound chorioretinal atrophy and severe vision loss. Therefore, we propose that one diagnosis of “early-onset Stargardt” should be given to patients with early-onset central retinal dystrophy and *ABCA4* gene mutations. This approach provides the patient with the benefit of receiving a single diagnosis throughout his or her entire life.

### Genotype–Phenotype Correlation

Because early-onset Stargardt can be considered a severe phenotype, severe combinations of mutations are expected in these patients. In our cohort, the c.768G>T and c.5461-10T>C mutations were significantly more prevalent (present in 25% and 36% of our patients, respectively) than in other STGD1 cohorts (8% and 5%, respectively).<sup>30,31</sup> The c.768G>T mutation is predicted to cause a splice defect that leads to nonsense-mediated decay owing to absence of the corresponding messenger RNA; this mutation is therefore considered to be a severe pathogenic mutation. In addition, a founder effect has been suggested for this mutation owing to the allele frequency of 8% among Dutch patients with STGD1.<sup>30</sup> On the other hand, the c.5461-10T>C mutation does not seem to be pathogenic, because heterologous expression of this mutation failed to reveal a splicing defect.<sup>32</sup> This mutation is rare among control patients, but is present in 5% of patients with general STGD1. Therefore, the c.5461-10T>C mutation may be in linkage disequilibrium with another, currently unidentified, severe pathogenic mutation.<sup>31</sup> Equally important, the most prevalent *ABCA4* mutation among Dutch patients with STGD1—c.2588G>C, which was reported in approximately one third of typical STGD1 cases<sup>33</sup>—was present in only 4% of the *ABCA4* alleles in our cohort of patients with early-onset Stargardt. To date, no homozygous carriers of this mutation have been identified,<sup>23</sup> supporting the hypothesis that this is a relatively mild mutation. The low prevalence of this presumably mild mutation in our cohort is consistent with a previously proposed genotype–phenotype model that correlates the degree of residual ABCR activity with the severity of the phenotype.<sup>17,23</sup>

We identified *ABCA4* mutations in all of our patients who received genetic screening; in contrast, the detection rate in routine clinical practice is 73%.<sup>34</sup> This difference can be explained—at least in part—by the inclusion criteria; patients who lacked a detected *ABCA4* mutation only would have been included if yellow-white flecks and either a dark choroid or an atrophic macular lesion were present. However, our database did not contain such patients who received genetic screening and had an early-onset disease. This finding supports the notion that early onset is highly predictive for identifying *ABCA4* mutations,<sup>34</sup> possibly because of the relatively higher percentage of severe mutations, which are more readily identified and/or recognized.

It remains unclear why the fovea is affected early in the course of STGD1 in some patients, whereas it can be spared—even for many decades—in other patients carrying compound heterozygous mutations, including 1 severe *ABCA4* mutation.<sup>14,15</sup> Other factors must therefore play a role in the development of foveal atrophy in early-onset Stargardt; possible factors can include pathogenic mutations or single nucleotide polymorphisms in genes other than *ABCA4*, as well as aberrant cellular processes. For example, the accumulation of *all-trans*-retinal in photoreceptor cells can directly increase cellular stress, thereby triggering apoptotic signaling pathways.<sup>35</sup> Next-generation sequencing of all retina-specific genes may help to identify the genetic factors that determine whether or not the fovea is involved early in the course of STGD1.

### Clinical Significance

Although diagnosing STGD1 at an early age is challenging, delaying diagnosis can have serious consequences. For example, 22 patients in our study did not receive the correct diagnosis for  $\geq 3$  years, and vision loss was initially unexplained in 13 patients. Recognizing early-onset Stargardt early in the disease course enables the timely start of potential measures—such as sunlight protection and low-vision counseling—and can prevent the inappropriate prescription of vitamin A supplements. Therefore, patients who are suspected of having early-onset Stargardt should be examined thoroughly using FAF and SD-OCT, particularly when no abnormalities (or mild foveal abnormalities) are present in a child with central vision loss that is otherwise unexplained. This diagnosis should also be confirmed by screening for the presence of *ABCA4* mutations. Finally, in light of future therapeutic options, such as gene therapy for treating *ABCA4*-related retinal disorders, obtaining a thorough understanding of the phenotypic spectrum and clinical course of STGD1 is essential for identifying the patients who will benefit most from these treatments.

## References

1. Lewis RA, Shroyer NF, Singh N, et al. Genotype/Phenotype analysis of a photoreceptor-specific ATP-binding cassette transporter gene, ABCR, in Stargardt disease. *Am J Hum Genet* 1999;64(2):422-34.
2. Stargardt K. Über familiäre, progressive Degeneration in der Maculagegend des Auges. *Graefes Arch Clin Exp Ophthalmol* 1909(71):534-50.
3. Franceschetti A. A special form of tapetoretinal degeneration: fundus flavimaculatus. *Trans Am Acad Ophthalmol Otolaryngol* 1965;69(6):1048-53.
4. Klevering BJ, Blankenagel A, Maugeri A, et al. Phenotypic spectrum of autosomal recessive cone-rod dystrophies caused by mutations in the ABCA4 (ABCR) gene. *Investigative Ophthalmology & Visual Science* 2002;43(6):1980-5.
5. Lois N, Holder GE, Bunce C, et al. Phenotypic subtypes of Stargardt macular dystrophy-fundus flavimaculatus. *Arch Ophthalmol* 2001;119(3):359-69.
6. Zahid S, Jayasundera T, Rhoades W, et al. Clinical phenotypes and prognostic full-field electroretinographic findings in Stargardt disease. *American Journal of Ophthalmology* 2013;155(3):465-73 e3.
7. Fujinami K, Lois N, Davidson AE, et al. A longitudinal study of stargardt disease: clinical and electrophysiologic assessment, progression, and genotype correlations. *American Journal of Ophthalmology* 2013;155(6):1075-88 e13.
8. Fishman GA, Stone EM, Grover S, et al. Variation of clinical expression in patients with Stargardt dystrophy and sequence variations in the ABCR gene. *Arch Ophthalmol* 1999;117(4):504-10.
9. Armstrong JD, Meyer D, Xu S, Elfervig JL. Long-term follow-up of Stargardt's disease and fundus flavimaculatus. *Ophthalmology* 1998;105(3):448-57; discussion 57-8.
10. Querques G, Leveziel N, Benhamou N, et al. Analysis of retinal flecks in fundus flavimaculatus using optical coherence tomography. *British Journal of Ophthalmology* 2006;90(9):1157-62.
11. Sparrow JR, Gregory-Roberts E, Yamamoto K, et al. The bisretinoids of retinal pigment epithelium. *Progress in Retinal and Eye Research* 2012;31(2):121-35.
12. Charbel Issa P, Barnard AR, Singh MS, et al. Fundus autofluorescence in the Abca4(-/-) mouse model of Stargardt disease--correlation with accumulation of A2E, retinal function, and histology. *Investigative Ophthalmology & Visual Science* 2013;54(8):5602-12.
13. Ergun E, Hermann B, Wirtitsch M, et al. Assessment of central visual function in Stargardt's disease/fundus flavimaculatus with ultrahigh-resolution optical coherence tomography. *Invest Ophthalmol Vis Sci* 2005;46(1):310-6.
14. Westeneng-van Haften SC, Boon CJ, Cremers FP, et al. Clinical and Genetic Characteristics of Late-onset Stargardt's Disease. *Ophthalmology* 2012;119(6):1199-210.
15. Fujinami K, Sergouniotis PI, Davidson AE, et al. Clinical and molecular analysis of stargardt disease with preserved foveal structure and function. *Am J Ophthalmol* 2013;156(3):487-501 e1.
16. Maugeri A, Klevering BJ, Rohrschneider K, et al. Mutations in the ABCA4 (ABCR) gene are the major cause of autosomal recessive cone-rod dystrophy. *Am J Hum Genet* 2000;67(4):960-6.
17. Klevering BJ, Deutman AF, Maugeri A, et al. The spectrum of retinal phenotypes caused by mutations in the ABCA4 gene. *Graefes Arch Clin Exp Ophthalmol* 2005;243(2):90-100.
18. Allikmets R, Singh N, Sun H, et al. A photoreceptor cell-specific ATP-binding transporter gene (ABCR) is mutated in recessive Stargardt macular dystrophy. *Nat Genet* 1997;15(3):236-46.
19. Molday LL, Rabin AR, Molday RS. ABCR expression in foveal cone photoreceptors and its role in Stargardt macular dystrophy. *Nat Genet* 2000;25(3):257-8.



20. Sun H, Smallwood PM, Nathans J. Biochemical defects in ABCR protein variants associated with human retinopathies. *Nat Genet* 2000;26(2):242-6.
21. Sparrow JR, Wu Y, Kim CY, Zhou J. Phospholipid meets all-trans-retinal: the making of RPE bisretinoids. *J Lipid Res* 2010;51(2):247-61.
22. van Driel MA, Maugeri A, Klevering BJ, et al. ABCR unites what ophthalmologists divide(s). *Ophthalmic Genet* 1998;19(3):117-22.
23. Maugeri A, van Driel MA, van de Pol DJ, et al. The 2588G-->C mutation in the ABCR gene is a mild frequent founder mutation in the Western European population and allows the classification of ABCR mutations in patients with Stargardt disease. *Am J Hum Genet* 1999;64(4):1024-35.
24. Rotenstreich Y, Fishman GA, Anderson RJ. Visual acuity loss and clinical observations in a large series of patients with Stargardt disease. *Ophthalmology* 2003;110(6):1151-8.
25. Burke TR, Yzer S, Zernant J, et al. Abnormality in the external limiting membrane in early Stargardt Disease. *Ophthalmic Genet* 2012.
26. Schulze-Bonsel K, Feltgen N, Burau H, et al. Visual acuities "hand motion" and "counting fingers" can be quantified with the freiburg visual acuity test. *Investigative Ophthalmology & Visual Science* 2006;47(3):1236-40.
27. Marmor MF, Fulton AB, Holder GE, et al. ISCEV Standard for full-field clinical electroretinography (2008 update). *Doc Ophthalmol* 2009;118(1):69-77.
28. Kuze M, Uji Y. Comparison between Dawson, Trick, and Litzkow electrode and contact lens electrodes used in clinical electroretinography. *Japanese Journal of Ophthalmology* 2000;44(4):374-80.
29. Colenbrander A. Visual standards: aspects and ranges of vision loss with emphasis on population surveys. Report prepared for the International Council of Ophthalmology (ICO) at the 29th International Congress of Ophthalmology, Sydney, 2002. San Francisco: Pacific Vision Foundation; 2002.
30. Cremers FP, Maugeri A, den Hollander AI, Hoyng CB. The expanding roles of ABCA4 and CRB1 in inherited blindness. *Novartis Found Symp* 2004;255:68-79; discussion -84, 177-8.
31. Webster AR, Heon E, Lotery AJ, et al. An analysis of allelic variation in the ABCA4 gene. *Invest Ophthalmol Vis Sci* 2001;42(6):1179-89.
32. Rivera A, White K, Stohr H, et al. A comprehensive survey of sequence variation in the ABCA4 (ABCR) gene in Stargardt disease and age-related macular degeneration. *Am J Hum Genet* 2000;67(4):800-13.
33. Maugeri A, Flothmann K, Hemmrich N, et al. The ABCA4 2588G>C Stargardt mutation: single origin and increasing frequency from South-West to North-East Europe. *Eur J Hum Genet* 2002;10(3):197-203.
34. Ernest PJ, Boon CJ, Klevering BJ, et al. Outcome of ABCA4 microarray screening in routine clinical practice. *Molecular Vision* 2009;15:2841-7.
35. Cideciyan AV, Swider M, Aleman TS, et al. ABCA4 disease progression and a proposed strategy for gene therapy. *Hum Mol Genet* 2009;18(5):931-41.
36. Papaioannou M, Ocaka L, Bessant D, et al. An analysis of ABCR mutations in British patients with recessive retinal dystrophies. *Invest Ophthalmol Vis Sci* 2000;41(1):16-9.
37. September AV, Vorster AA, Ramesar RS, Greenberg LJ. Mutation spectrum and founder chromosomes for the ABCA4 gene in South African patients with Stargardt disease. *Investigative Ophthalmology & Visual Science* 2004;45(6):1705-11.
38. Jaakson K, Zernant J, Kulm M, et al. Genotyping microarray (gene chip) for the ABCR (ABCA4) gene. *Hum Mutat* 2003;22(5):395-403.
39. Yatsenko AN, Shroyer NF, Lewis RA, Lupski JR. Late-onset Stargardt disease is associated with missense mutations that map outside known functional regions of ABCR (ABCA4). *Hum Genet* 2001;108(4):346-55.

40. Rozet JM, Gerber S, Souied E, et al. Spectrum of ABCR gene mutations in autosomal recessive macular dystrophies. *European Journal of Human Genetics* 1998;6(3):291-5.
41. Fumagalli A, Ferrari M, Soriani N, et al. Mutational scanning of the ABCR gene with double-gradient denaturing-gradient gel electrophoresis (DG-DGGE) in Italian Stargardt disease patients. *Human Genetics* 2001;109(3):326-38.
42. Allikmets R, Shroyer NF, Singh N, et al. Mutation of the Stargardt disease gene (ABCR) in age-related macular degeneration. *Science* 1997;277(5333):1805-7.
43. Cremers FP, van de Pol DJ, van Driel M, et al. Autosomal recessive retinitis pigmentosa and cone-rod dystrophy caused by splice site mutations in the Stargardt's disease gene ABCR. *Hum Mol Genet* 1998;7(3):355-62.
44. Stone EM, Webster AR, Vandenburgh K, et al. Allelic variation in ABCR associated with Stargardt disease but not age-related macular degeneration. *Nature Genetics* 1998;20(4):328-9.
45. Briggs CE, Rucinski D, Rosenfeld PJ, et al. Mutations in ABCR (ABCA4) in patients with Stargardt macular degeneration or cone-rod degeneration. *Invest Ophthalmol Vis Sci* 2001;42(10):2229-36.
46. Zernant J, Schubert C, Im KM, et al. Analysis of the ABCA4 gene by next-generation sequencing. *Invest Ophthalmol Vis Sci* 2011;52(11):8479-87.
47. Roberts LJ, Nossek CA, Greenberg LJ, Ramesar RS. Stargardt macular dystrophy: common ABCA4 mutations in South Africa--establishment of a rapid genetic test and relating risk to patients. *Mol Vis* 2012;18:280-9.
48. Lenassi E, Jarc-Vidmar M, Glavac D, Hawlina M. Pattern electroretinography of larger stimulus field size and spectral-domain optical coherence tomography in patients with Stargardt disease. *British Journal of Ophthalmology* 2009;93(12):1600-5.
49. Simonelli F, Testa F, de Crecchio G, et al. New ABCR mutations and clinical phenotype in Italian patients with Stargardt disease. *Investigative Ophthalmology & Visual Science* 2000;41(3):892-7.
50. Paloma E, Martinez-Mir A, Vilageliu L, et al. Spectrum of ABCA4 (ABCR) gene mutations in Spanish patients with autosomal recessive macular dystrophies. *Human Mutation* 2001;17(6):504-10.



## CHAPTER 2.2

### The absence of fundus abnormalities in Stargardt disease

*“A lack of obvious fundus abnormalities left an alarming number of children with Stargardt disease without the correct diagnosis. We hope that greater awareness of this subtype avoids misdiagnosis and years of inappropriate treatment.”*

Nathalie M. Bax  
Stanley Lambertus  
Frans P.M. Cremers  
B. Jeroen Klevering  
Carel B. Hoyng

*Graefe's Archive for Clinical and Experimental Ophthalmology, 2019  
Jun;257(6):1147-1157.*

**PURPOSE:** To raise awareness of Stargardt disease (STGD1) patients without fundus abnormalities.

**METHODS:** Medical records were evaluated for age at onset, initial symptoms and diagnosis, reason for delay of diagnosis, age at STGD1 diagnosis, best-corrected visual acuity (BCVA), ophthalmoscopy, fundus photography, fundus autofluorescence (FAF), fluorescein angiography (FA), spectral-domain optical coherence tomography (SD-OCT), full-field electroretinography (ffERG), color vision test, and the presence of *ABCA4* variants.

**RESULTS:** In 11.1% of our STGD1 cohort of 280 patients, no fundus abnormalities were observed at first ophthalmic consultation. The median age at onset was 8 years (range, 1-18). There was a median delay in diagnosis of 3 years (range, 0 – 19) in 27 out of 31 patients, which resulted in a median age at diagnosis of 12 years (range, 7-26). Patients were misdiagnosed with amblyopia, myopia, optic disk pathology, mental health problems, tension headache, neuritis bulbaris, and uveitis. Subtle abnormalities, such as lipofuscin accumulation, were seen on FAF at an earlier disease stage than in ophthalmoscopy. On SD-OCT, this included a thickened external limiting membrane. Color vision tests showed red-green insufficiency in 79% of patients. Reduced ERG amplitudes were only present in 26% (N=8), and a dark choroid sign in 65% of the patients. Visual acuity considerably fluctuated in the first 5 years after onset. The majority of the patients (65%) carried a least one variant with a severe effect on *ABCA4* function.

**CONCLUSIONS:** Childhood-onset STGD1 patients were diagnosed with a delay of median 3 years. The presence of accurate competence, equipment and the possibility for genetic screening is required, therefore we recommend to refer children with visual complaints without initial fundus abnormalities to a specialized ophthalmologic center. In particular, to diagnose patients at an early stage of disease is of increased importance with the advent of new therapeutic possibilities.

## Introduction

Stargardt disease (STGD1) is arguably the most common retinal dystrophy and affects 1:10000 people worldwide.<sup>1</sup> This autosomal recessive disease is caused by variants in the *ABCA4* gene that encodes for a retinal-specific ATP-binding cassette transporter protein. Dysfunction of the *ABCA4* protein leads to toxic accumulation of byproducts from the visual cycle in the photoreceptor cell and retina pigment epithelium (RPE), which eventually leads to irreversible damage of the outer retinal layers.<sup>2,3</sup>

Up to 5,962 variants in the *ABCA4* gene have been identified; the specific combinations of variants in conjunction with largely unknown modifying factors in each patient result in a highly heterogenic phenotype.<sup>4</sup> Patients with STGD1 present with progressive vision loss, which typically occurs in young adulthood, but early and late forms have been well recognized.<sup>5-7</sup> In general, the fundus picture is characterized by the presence of irregular yellow-white fundus flecks in the posterior pole. During the course of the disease, macular atrophy develops, sometimes with a 'beaten bronze' aspect; in other patients a bull's eye pattern can be observed. Lipofuscin accumulates in the outer retinal layers, which results in a 'dark choroid' on the fluorescein angiogram in approximately 80% of the patients.<sup>8-11</sup> In early forms with a disease onset  $\leq 10$  years of age, atrophy of the macula is a prominent and early feature; the yellow flecks may be absent or hardly notable.<sup>5,12,13</sup> The flecks are much more common in the classic form of STGD1 with an age of onset in the early teens, sometimes extending beyond the vascular arcades resulting in the fundus flavimaculatus phenotype.<sup>14,15</sup> Late-onset forms of the disease are characterized by atrophy of the retinal pigment epithelium, subtle flecks, and foveal sparing.<sup>6,16,17</sup>

The diagnosis of STGD1 can be challenging in early disease especially, as no apparent changes may be present on ophthalmoscopy despite the loss of visual function.<sup>5</sup> This lack of clinical signs in combination with the limited capabilities for expression in young children may delay the correct diagnosis. Not only is early identification of these patients essential for the emotional aspect of a timely diagnosis, it is also important in the light of emerging therapeutic options for STGD1 disease, such as gene augmentation (trial number NCT01367444, NCT01736592), stem cell therapy (trial number NCT01469832), and small molecule drugs (trial number NCT02402660).

In this study, we describe—in detail—the clinical and molecular genetic findings in a group of STGD1 patients, which presents without initial fundus abnormalities in ophthalmoscopy. We hope that a heightened awareness avoids misdiagnosis, such as functional visual loss in these children and, in worst case scenarios, years of inappropriate treatment.

## Methods

### Patients

The database with STGD1 patients of the Department of Ophthalmology, Radboud university medical center, (Nijmegen, the Netherlands) contains 280 patients of all ages and disease-onset, of whom one or more *ABCA4* variants could be identified. We included 31 patients who did not show obvious fundus abnormalities at the first presentation. This study was approved by the Institutional Ethics Committee and was performed in accordance with the Declaration of Helsinki.

### Clinical evaluation

We collected the clinical data from the medical records. These included age at onset, initial symptoms, initial diagnosis and examinations or therapy, age at STGD1 diagnosis, delay of diagnosis and reason for this delay, number of referrals before diagnosis, and general medical history. Age at onset was defined as the first manifestation of the disease, these symptoms could have been noticed by the patient, but also their family members and/or the school physician. If visual complaints of the patient was initially diagnosed due to stress or need for attention, we used the term “mental health issues”.

The standard ophthalmic examination included best-corrected visual acuity (BCVA) using Early Treatment Diabetic Retinopathy Study (ETDRS) or Snellen charts, slit-lamp biomicroscopy and detailed fundus examination. BCVA was transformed into the logarithm of the minimum angle of resolution (logMAR) for statistical analysis. For fundus photography, we used the Topcon TRC50IX (Topcon Corporation, Tokyo, Japan). Fluorescein angiography (FA) and cross-sectional images using spectral-domain optical coherence tomography (SD-OCT) centered at the macula were obtained with the Spectralis (HRA+OCT, Heidelberg Engineering, Heidelberg, Germany). Short-wave fundus autofluorescence imaging (FAF) ( $\lambda = 488$  nm, emission 500–700 nm) was performed using a confocal scanning laser ophthalmoscope (Spectralis HRA+OCT or HRA2, Heidelberg Engineering, Heidelberg, Germany). The field of view was set at 30°×30° or 55°×55°, centered at the macula. For evaluation of color vision we employed the Ishihara or Panel D-15 test. Full-field electroretinography (ERG) was performed using Dawson-Trick-Litzkow (DTL) electrodes and the RETI-port system (Roland Consults, Stasche & Finger GmbH, Brandenburg an der Havel, Germany). The recordings were performed in accordance with the guidelines of the International Society for Clinical Electrophysiology of Vision (ISCEV).<sup>18</sup> We grouped ERG results as described by Lois et al.<sup>19</sup> Group 1: patients with normal ERG responses; Group 2: patients with reduced photopic amplitudes (<5% of normal range) and Group 3: patients with reduced photopic and scotopic amplitudes (<5% of normal range).

### Genetic analysis

Genetic analysis of the *ABCA4* gene was performed at the Department of Human Genetics at the Radboud University Medical Center using arrayed primer extension analysis (APEX, Asper Biotech, Tartu, Estonia). If the Asper microarray screening revealed only one *ABCA4* variant, exon and intron-exon boundaries were sequenced in the *ABCA4* gene to identify additional variants. All variants were confirmed with Sanger sequencing. The following variants were defined as severe: protein-truncating, canonical splice-site variants, as well as deletions spanning at least one exon.

### Statistical analysis

We used SPSS version 22.0 (IBM Corp, Armonk, NY) for statistical data analysis, using descriptive statistics by median and range for continuous variables, and percentages for categorical variables. We employed Kaplan-Meier estimators to analyze the interval between age at onset and age at which four different visual endpoints were reached. These four points were based on the classification of visual impairment of the World Health Organization: (near-)normal to mild visual impairment  $\geq 0.2$  logMAR ( $\leq 20/32$  Snellen), moderate visual impairment  $\geq 0.6$  logMAR ( $\leq 20/80$  Snellen), severe visual impairment  $\geq 1.0$  logMAR ( $\leq 20/200$  Snellen), and blindness  $\geq 1.4$  logMAR ( $\leq 20/500$  Snellen).

## Results

### Clinical characteristics

In 31 of 280 (11.1%) STGD1 patients, no obvious fundus abnormalities were observed at the first ophthalmic consultation. The group consisted of 15 males and 16 females with six siblings from three different families, and 25 isolated cases. An overview of the clinical findings and the diagnostic process is given in [Table 1](#). In one-third of cases, symptoms of a decreased visual acuity were not noticed by the patient, but by the parents or a school physician. Age at onset occurred at a median age of 8 years (range, 1-18). In 87% of the patients, there was a delay in diagnosis: a median delay of 3 years (range, 0 -19), which resulted in a median age at diagnosis of 12 years (range, 7-26). The main reason for delayed STGD1 diagnosis was misdiagnosis, in particular amblyopia treated with occlusion therapy (6 patients) and mental health issues (5 patients). The majority of patients (94%) visited more than two hospitals before the correct diagnosis was made. All patients were finally diagnosed with STGD1 in tertiary referral centers. The first fundus abnormalities were observed at a median time of 3 years (range, 0.5-16) after first symptoms. These included central retinal pigment epithelium (RPE) alterations (43%), bull's eye maculopathy (33%), and/or parafoveal flecks (24%). Once these features had been observed, STGD1 was generally diagnosed relatively quickly in the majority of patients (median; 0.7 years, range; 0.1-3).



*ID= identification patient in this study, m= male, f= female, VA= visual acuity, BCVA= best-corrected visual acuity, RPE=retinal pigment epithelium.*

18	f	10	school physician	4	Other disease overshadowed STGD1	Diagnosis of optic drusen overshadowed STGD1	26	RPE alterations	20/200
19	f	9	patient	2	Wait and see	No diagnosis	12	Bull's eye	20/400
20	m	16	patient	2	Wait and see	No diagnosis	21	RPE alterations	20/70
21	f	9	school physician	2	Wrong diagnosis	Uveitis	10	RPE alterations	20/40
22	m	6	patient	2	No delay, due to timely referral to academic hospital	Immediate referral to academic center for addition examinations, because of extreme low VA (20/400 Snellen)	7	RPE alterations	20/400
23	f	11	patient	2	Wrong diagnosis	Tension headache, consulting neurologist	13	Central fundus flecks	20/125
24	m	3	school physician and family	2	Wrong diagnosis	Amblyopia, received occlusion therapy (decrease in VA due to lack of therapy)	9	Bull's eye	20/125
25	f	11	patient	2	Delayed referral	No diagnosis	13	Bull's eye	20/100
26	m	7	patient	2	Little delay, due to referral to academic hospital	Cone dystrophy	8	Bull's eye	20/125
27	f	8	patient	1	Wrong diagnosis	Mental health problem	11	RPE alterations	20/70
28	m	6	patient	2	Minor delay, due to timely referral to academic hospital	Cone dystrophy	7	Central fundus flecks	20/35
29	f	18	patient	2	Delayed referral	Cone dystrophy	20	Bull's eye	20/35
30	f	3	public health service	2	Wrong diagnosis	"Schoolight amblyopia"	12	Central fundus flecks	20/250
31	m	13	school physician	2	Minor delay, due to timely referral to academic hospital	Cone dystrophy	14	RPE alterations	20/70

**Table 1.** Clinical characteristics and diagnostic process in Stargardt disease (STGD1) patients without initial fundus abnormalities

ID	Gender	Age at onset (years)	Decreased VA noticed by	Number of other hospitals before correct diagnosis	Reason for delay of diagnosis	Initial diagnosis and examinations or therapy	Age at STGD1 diagnosis (years)	Fundus abnormalities at the time of diagnosis	BCVA at diagnosis (Snellen)
1	m	1	family	2	Wrong diagnosis	Mental health problem or unknown syndrome	14	Bull's eye	20/200
2	m	5	patient	2	Wrong diagnosis	Amblyopia with occlusion therapy	11	Bull's eye	20/125
3	f	16	family	2	Wrong diagnoses	Amblyopia with occlusion therapy. Retrobulbar optic neuritis. Neuro-imaging (CT) was performed (no abnormalities). Cone dystrophy	20	RPE alterations	20/100
4	m	7	patient	2	No delay (mother insisted on a referral to an academic hospital)	Cone dystrophy	7	RPE alterations	20/125
5	f	7	family	3	Wait and see	No diagnosis	26	Bull's eye	20/125
6	f	7	patient	3	Wrong diagnosis	Diagnosed with a mental health problem, in view of the variable VA between visits.	23	RPE alterations	20/30
7	f	9	patient	1	Wait and see	No diagnosis	15	Bull's eye	20/125
8	m	10	patient	2	Wrong diagnosis	Myopia	13	Central fundus flecks	20/35
9	m	4	patient	2	Wrong diagnoses	Initially, amblyopia with occlusion therapy. Complaints of headache lead to neuro-imaging (MRI) followed by physiotherapy. Eventually diagnosed with cone dystrophy. Mental health problem	8	RPE alterations	20/70
10	f	7	patient	2	Wrong diagnosis	Cone dystrophy	10	RPE alterations	20/20
11	m	6	public health service	2	Delayed referral to ophthalmologist	Cone dystrophy	8	RPE alterations	20/125
12	m	3	school physician	2	Wrong diagnosis	Amblyopia with occlusion therapy	10	Bull's eye	20/35
13	f	17	patient	2	Delayed referral to ophthalmologist	Cone dystrophy	20	Bull's eye	20/80
14	f	13	patient	2	Wrong diagnosis	Amblyopia with occlusion therapy. Also neuro-imaging (MRI) via neurologist.	15	RPE alterations	20/70
15	m	8	patient	2	Wrong diagnosis	Optic neuropathy. A brain MRI and lumbar puncture revealed no abnormalities.	10	RPE alterations	20/80
16	f	8	patient	3	Wrong diagnosis	Myopia	23	Central fundus flecks	20/35
17	m	15	patient	2	Wait and see	No diagnosis	18	Central fundus flecks	20/100

We could retrieve the BCVA at the first ophthalmic visit in 21 out of 31 patients; the median BCVA at that time was 20/32 Snellen (20/20 - 20/400). The median interval and 95% confidence interval (CI) between the age at onset and decline in BCVA to mild, moderate, severe visual impairment and blindness was 1 year (95% CI, 0.0 - 2.25), 4 years (95% CI, 3.1 - 4.9) and 12 years (CI 95% 7.8 – 16.2). One patient reached blindness 34 years after the first symptoms of onset at age 9. In many patients, the visual acuity findings were quite variable early in the course of the disease as shown in [Figure 1](#).

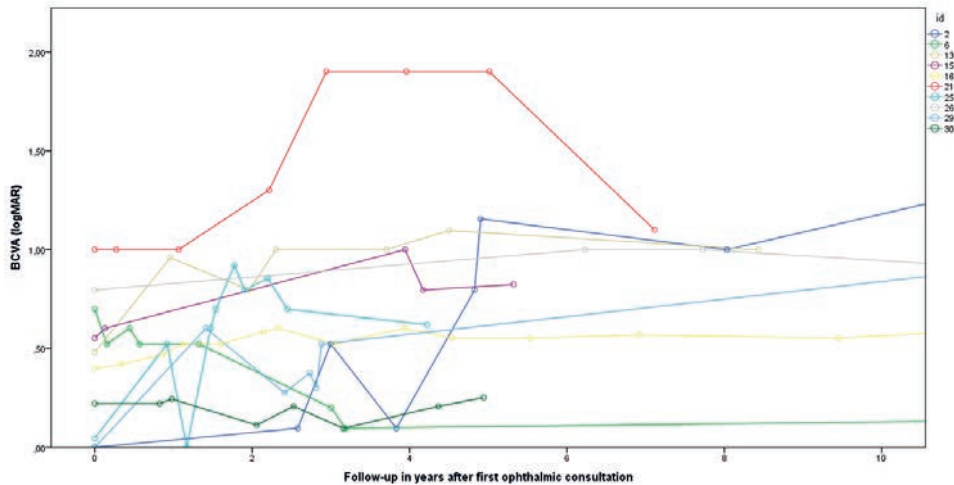


**Figure 1:** Course of the best-corrected visual acuity (BCVA) in logMAR in ten patients. The visual acuity varies greatly during the first five years after first ophthalmic consultation. LogMAR 0 = 20/20 Snellen, LogMAR 0.5 = 20/63 Snellen, LogMAR 1.00 = 20/200 Snellen, LogMAR 1.50 ≈ 20/630 Snellen, LogMAR 2.00 = 20/2000 Snellen. Each patient (ID= identification) is shown in a different color.

In 29 out of 31 patients, fundus flecks were eventually noticed at a median time of 3.5 years (range, 0.1 -16.5) after the initial ophthalmic consultation. In 17 patients (59%), subtle parafoveal flecks could be seen, in 5 patients (17%) flecks were noticed within the vascular arcades, and in 7 patients (24%) flecks extended to the periphery. In 2 patients, no fundus flecks were reported at any time during the course of the disease (follow-up time, 1 and 10 years).

In 23 of 31 patients, the first SD-OCT was performed at 9 years (range, 0.1-24) after disease onset. No SD-OCT scans were performed in the remaining 8 patients. All OCT scans showed abnormalities by disorganized or absent RPE. A thickened external limiting membrane (ELM) was seen in 2 patients (0.5 and 1 year after disease onset). A dark choroid was observed in 15 of 23 (65%) patients in whom

FA was performed. In 22 patients, the first FAF was performed 3.5 years (0.5-24) after onset. No atrophy was seen (median, 1 year after onset) in 5 patients, (peri)foveal atrophy in 9 (median, 4 years after onset), atrophy within the vascular arcades in 7 (median, 15 years after onset), and panretinal atrophy (15 years after onset) in 1. In 4 patients, abnormalities were seen on FAF, but were missed on ophthalmoscopy.

The first ERG was performed 2 years (0.1 – 27) after onset in 27 patients. Normal ERG recordings (Group 1) were present in 20 patients (74%), 2 years (0.1-21) after disease onset. We found Group 2 ERGs in 4 patients (15%) with 1 year (0.1 – 3.5) after onset, and Group 3 recordings in 3 patients (11%) with 18 years (6-27) after onset. Follow-up for ERG recordings was available in 21 patients. In 4 of these patients progressed from Group 1 to Group 2 (median time, 8 (7-16) years), 2 patients progressed from Group 2 to Group 3 (within 2 and 3 years), and 1 patient progressed from Group 1 to Group 3 in 6 years. In 17 patients color vision was tested. In 15 patients (79%) abnormalities were noticed, red-green defects in 14 patients and a blue-yellow defect in 1 patient.

Various imaging modalities of patient 28 and patient 21 are depicted respectively in [Figure 2](#) and [3](#).

### Genetic characteristics

Overall, genetic analysis was not performed at first visit, but with a median delay of five years (range, 0 - 30) after first visit. An overview of *ABCA4* variants in our cohort is described in [Table 2](#).

Variants in the *ABCA4* gene were identified in 59 of 62 alleles (95%). Three variants were found in one patient, two *ABCA4* variants in 27, and one variant in three. In total, 32 distinct variants were detected. The majority of the patients (65%) carried at least one variant with a severe effect on *ABCA4* function ([Table 2](#), in bold).

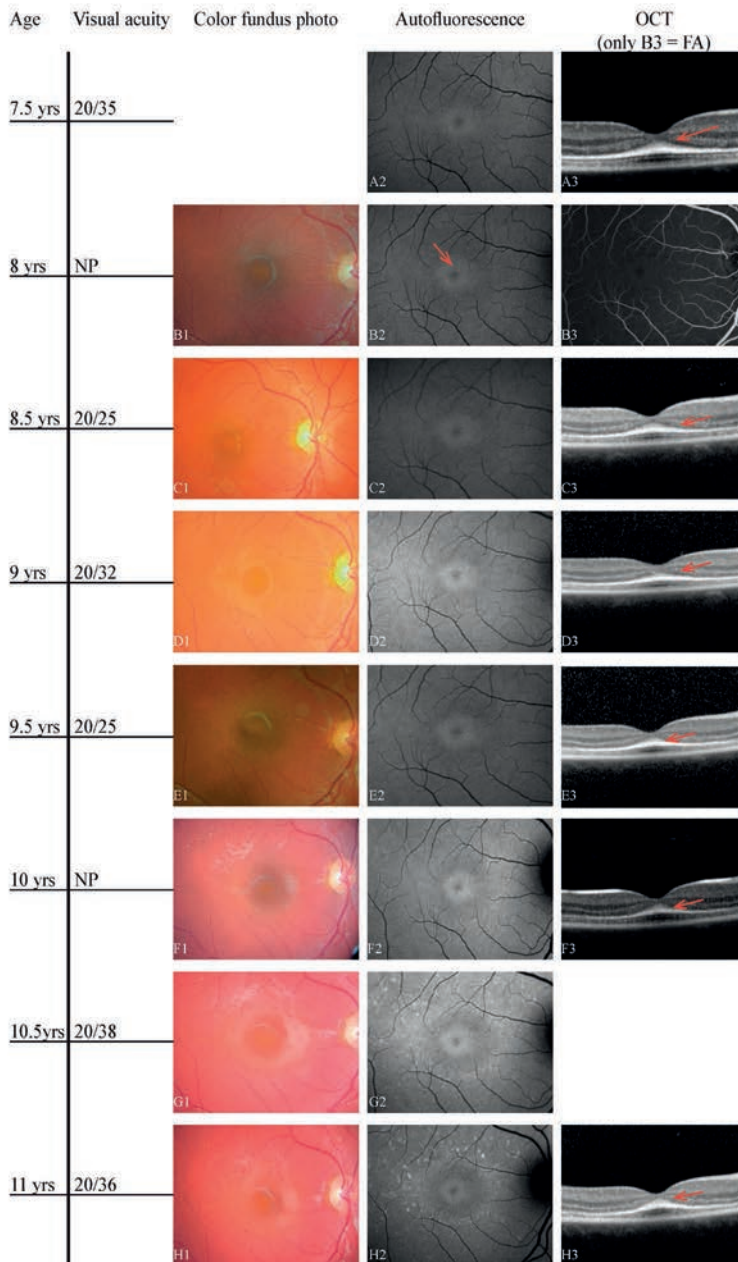


**Figure 2:** Three-and-a-half year follow-up in patient ID28. Age at onset at 6.5 years, one year later the fundus auto-fluorescence showed a perifoveal ring of hyper-fluorescence (A2), and on OCT a discrete thickening of the external limiting membrane can be seen (A3, red arrow). Only 6 months later, a subtle hyper-fluorescent perifoveal lesion developed as shown in B2, red arrow. Over time, the hyper-fluorescent flecks become more visible on autofluorescence imaging. In addition the flecks became noticeable on color fundus photographs. The thickened external limiting membrane remained present during the entire follow-up time (red arrows A3, C3, D3, E3, F3, H3).

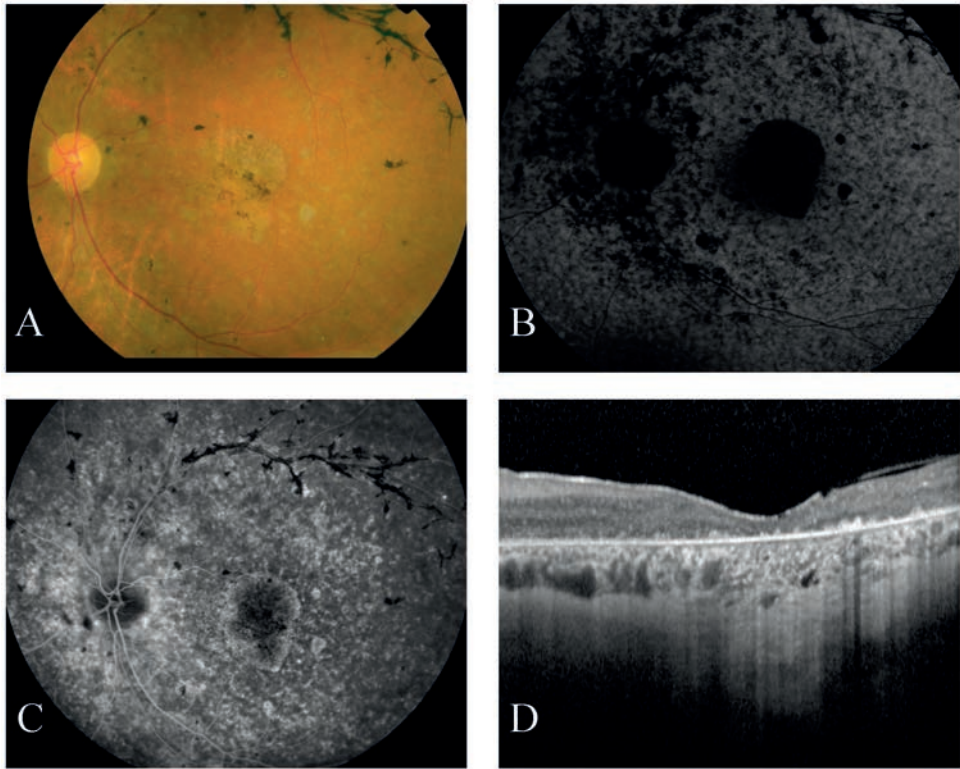


**Figure 3:** Multimodal imaging in ID21 at age 25, 15 years after the first symptoms. The visual acuity is now 20/1000 Snellen OU. Color fundus photography (A) shows attenuated retinal vessels (especially the veins), para-arteriolar pigmentations and diffuse chorioretinal atrophy. The fundus autofluorescence (B) shows widespread hypofluorescence, especially at the macula, indicative of RPE cell loss. The fluorescence angiogram (C) shows widespread granular hyperfluorescent lesions as result of RPE damage, and on the OCT (D) loss of the outer retinal layers, as well as the choriocapillaris, can readily be observed.

21	c.768G>T	p.(?)	Splice-site (non-canonical)	c.2919?_43328+?del	p.(Ser974Glnfs*64)	Frameshift; deletion
22	c.768G>T	p.(?)	Splice-site (non-canonical)	c.1804C>T	p.(Arg602Trp)	Missense
23	c.[1622T>C;3113C>T]	p.[Leu541Pro;Ala1038Val]	Missense; missense	c.6316C>T	p.(Arg2106Cys)	Missense
24	c.5714+5G>A	p.(?)	Splice-site (non-canonical)	c.3033-?_3364+?del	p.(?)	Frameshift; deletion
25	c.5714+5G>A	p.(?)	Splice-site (non-canonical)	c.3033-?_3364+?del	p.(?)	Frameshift; deletion
26	c.[872C>T;4224G>T]	p.[Pro291Leu;Trp1408Cys]	Missense; missense	c.2947A>G	p.(Thr983Ala)	Missense
27	c.768G>T	p.(?)	Splice-site (non-canonical)	c.5113C>T	p.(Arg1705Trp)	Missense
28	c.2947A>G	p.(Thr983Ala)	Missense	c.5461-10T>C	p.(Thr1821Valfs*13, Thr1821Aspfs*6)	Frameshift
29	c.768G>T	p.(?)	Splice-site (non-canonical)	c.872C>T	p.(Pro291Leu);	Missense
30	c.5461-10T>C	p.(Thr1821Valfs*13, Thr1821Aspfs*6)	Frameshift	c.6320G>A	p.(Arg2107His)	Missense
31	c.5882G>A	p.(Gly1961Glu)	Missense	c.4352+1G>A	p.(?)	Splice-site (canonical)

*In bold= mutations with a severe effect on ABCA4 function.*

**Table 2:** Variant, protein notation and type of variant in the ABCA4 gene of Stargardt disease patients without fundus abnormalities

ID	Variant 1	Protein	Type of variant	Variant 2	Protein	Type of variant
1	c.5585-10T>C	p.(?)	Splice-site (non-canonical)	+		
2	c.[1622T>C;3113C>T]	p.[Leu541Pro;Ala1038Val]	Missense, missense	c.[1622T>C;3113C>T]	p.[Leu541Pro;Ala1038Val]	Missense, missense
3	c.5882G>A	p.[Gly1961Glu]	Missense	c.3305A>T	p.[Asp1102Val]	Missense
4	c.4539+1G>T	p.(?)	Splice-site (canonical)	c.5762_5763dup	p.[Ala1922T;Pfs*18]	Frameshift
5	c.6089G>A	p.[Arg2030Gln]	Missense	c.5461-10T>C	p.[Thr1821Val;fs*13, Thr1821Asp;fs*6]	Frameshift
6	c.2588G>C	p.[Gly863Ala, Gly863del]	Missense, splice defect	+		
7	c.2588G>C	p.[Gly863Ala, Gly863del]	Missense, splice defect	c.4539+1G>T	p.(?)	Splice-site (canonical)
8	c.2588G>C	p.[Gly863Ala, Gly863del]	Missense, splice defect	c.4539+1G>T	p.(?)	Splice-site (canonical)
9	c.3259G>A	p.[Glu1087*]	Nonsense	c.4128+1G>A	p.(?)	Splice-site (canonical)
10	c.3259G>A	p.[Glu1087*]	Nonsense	c.4128+1G>A	p.(?)	Splice-site (canonical)
11	c.5762_5763dup	p.[Ala1922T;Pfs*18]	Frameshift	c.2919_?_3328+?del	p.[Ser974Gln;fs*64]	Frameshift, deletion
12	c.4539+1G>T	p.(?)	Splice-site (canonical)	c.768G>T	p.(?)	Splice-site (non-canonical)
13	c.3874C>T	p.[Gln1292*]	Nonsense	c.6320G>A	p.[Arg2107His]	Missense
14	c.5196+1137G>A	p.(?)	Deep-intronic, splicing	+		
15	c.5312+1G>A	p.(?)	Splice-site (canonical)	c.280A>G	p.[Asn96Asp]	Missense
16	c.5161_5162del	p.[Thr1721His;fs*65]	Frameshift	c.5882G>A	p.[Gly1961Glu]	Missense
17	c.3874C>T	p.[Gln1292*]	Nonsense	c.5196+1137G>A	p.(?)	Deep-intronic, splicing
18	c.5461-10T>C	p.[Thr1821Val;fs*13, Thr1821Asp;fs*6]	Frameshift	c.5537T>C	p.[Ile1846Thr]	Missense
19	c.214G>A	p.[Gly72Arg]	Missense	c.5461-10T>C	p.[Thr1821Val;fs*13, Thr1821Asp;fs*6]	Frameshift
20	c.4773+1G>A	p.(?)	Splice-site (canonical)	c.5537T>C	p.[Ile1846Thr]	Missense



## Discussion

A lack of obvious fundus abnormalities left a high number of children with STGD1 disease without the correct diagnosis. Instead, these patients underwent unnecessary investigations, such as psychic evaluations, brain MRIs or CTs, and lumbar punctures. Many of these children were treated for mental illness and/or amblyopia with pointless and possibly harmful treatments, including years of occlusion therapy.

In patients with adult-onset STGD1, initial ophthalmoscopic features typically include yellow-white flecks and central macular atrophy, and cases without fundus abnormalities have not been described.<sup>6</sup> In young children, the clinical presentation can be confusing for the general ophthalmologist. Fujinami et al noticed that one third of their child cohort (<17 years) initially had a normal fundus appearance.<sup>7</sup> Lambertus et al described a cohort of 41 STGD1 patients younger than 10 years, and 10 of these patients (24%) also did not have fundus abnormalities.<sup>5</sup> These studies show that the absence of readily observable fundus abnormalities in young STGD1 patients is not an isolated finding, but a relative common part of the clinical spectrum.

Recently, Khan et al. reported the earliest features of *ABCA4*-associated retinopathy.<sup>20</sup> In their study, they included 8 children (6 prospectively) to describe their ophthalmologic features. At the first visit, four children were asymptomatic and four had complaints of visual decline. In 6 out of 8 children, the central macula appeared normal or had an altered foveal reflex. This is similar to the findings in our study. In contrast, their study focused on the (most prospectively) appearance of abnormalities in *ABCA4*-related dystrophy even if they were asymptomatic. Our study is focused, retrospectively, on STGD1 patients initially without fundus abnormalities, despite having visual complaints. Besides the natural course of this phenotype, we describe the reasons of delay in diagnoses and to find similarities within this group of patients in order to provide recommendations for ophthalmologists in general. Therefore, this study is a contribution from another point of view of children with STGD1 which initially present without fundus abnormalities.

In our cohort, when fundus abnormalities did occur, these were often not the typical yellowish flecks but rather RPE alterations, often in a bull's eye pattern. A hypothesis for the absence of typical fundus flecks may lie in the relative high pathogenicity of *ABCA4* variants. As the majority of our cohort (65%) carried at least one severe variant, there may be little *ABCA4* function left in these patients,

leading to a very early manifestation of the disease. The built up of toxic A2E in RPE cells develops rapidly, thereby causing early cell death without the opportunity for lipofuscin to accumulate and subsequent fleck formation.

Blocking of the choroidal vessels on FA resulting a dark or silent choroid is frequently used as diagnostic marker for STGD1. The prevalence of this FA finding in STGD1 patients has been described in up to 86% of patients.<sup>21</sup> A dark choroid was present in 65% in our relatively small cohort. A correlation has been described between the presence of yellow-white fundus flecks and the appearance of dark choroid, which might account for the relative low percentage of patients with a dark choroid in this cohort.<sup>9,22</sup> FAF imaging is a relative new modality that may be used to identify early and subtle lipofuscin.<sup>23</sup> In addition, a thickened ELM on OCT may also serve as an early marker for STGD1.<sup>24</sup> However, in the study of Lee et al, this distinct ELM thickening was described to occur in all (26/26) cases. In our cohort, only 2/23 cases with performed OCT (0.5 and 1 year after disease onset), were observed to have this feature. The delay of performing an OCT (mean: 9 years after disease onset), could be an explanation of the difference in appearance of ELM thickening in both cohorts. Abnormal color vision was observed in 79% of our STGD1 patients, which corresponds with the previously reported percentages.<sup>25</sup>

Fluctuation of visual acuity in 10/31 children in the first 5 years of ophthalmic consultation suggests that visual acuity is an ambiguous symptom at early stages of STGD1. This could be explained by lowered reading performance due to ring scotomas that allow for good visual acuity, but cause visual field impairment.<sup>26</sup>

Although STGD1 is the most common juvenile macular dystrophy, it remains a relative rare disorder. Clinicians in a general ophthalmic practice may lack the experience to identify and interpret the subtle abnormalities in these young children. When we take into account the relative difficulty associated with the ophthalmic examination of (very) young children, the high number of misdiagnoses in the early-onset STGD1 patient group may not come as a surprise. Therefore, we want to make ophthalmologists aware of early findings in STGD1, especially appearing in children. First, visual acuity often fluctuates in these patients which should not automatically rule out the possibility of a photoreceptor disease. Second, a fundus photograph can be helpful in discerning very subtle fundus abnormalities and may be useful in follow-up. Third, non-invasive investigations such as OCT (thickening of the ELM), FAF (subtle lipofuscin accumulation) and color vision tests may help in the diagnostic process. FA is invasive, apart from the oral variant, but may also be less helpful in patients without fundus abnormalities in the light of the relative low percentage of dark choroids in these patients.

In children with visual disturbances, retinal dystrophies should be considered and ruled out when possible, even in the absence of fundus abnormalities on ophthalmoscopy, because STGD1 may be a cause of low vision in normal fundus. Instead of wait and see, we would recommend referring these children to a tertiary ophthalmic center and performing OCT and FAF to define early findings of STGD1. In addition, early identification may prove important in the light of emerging therapeutic options.

## References

1. Blacharski P (1988) Retinal dystrophies and degenerations. Newsome DA (ed): 135-159
2. Allikmets R, Shroyer NF, Singh N, Seddon JM, Lewis RA, Bernstein PS, Peiffer A, Zabriskie NA, Li Y, Hutchinson A, Dean M, Lupski JR, Leppert M (1997) Mutation of the Stargardt disease gene (ABCR) in age-related macular degeneration. *Science (New York, NY)* 277: 1805-1807
3. Allikmets R, Singh N, Sun H, Shroyer NF, Hutchinson A, Chidambaram A, Gerrard B, Baird L, Stauffer D, Peiffer A, Rattner A, Smallwood P, Li Y, Anderson KL, Lewis RA, Nathans J, Leppert M, Dean M, Lupski JR (1997) A photoreceptor cell-specific ATP-binding transporter gene (ABCR) is mutated in recessive Stargardt macular dystrophy. *Nature genetics* 15: 236-246 DOI 10.1038/ng0397-236
4. Cornelis SS, Bax NM, Zernant J, Allikmets R, Fritsche LG, den Dunnen JT, Ajmal M, Hoyng CB, Cremers FP (2017) In Silico Functional Meta-Analysis of 5,962 ABCA4 Variants in 3,928 Retinal Dystrophy Cases. *Human mutation* 38: 400-408 DOI 10.1002/humu.23165
5. Lambertus S, van Huet RA, Bax NM, Hoefsloot LH, Cremers FP, Boon CJ, Klevering BJ, Hoyng CB (2015) Early-onset stargardt disease: phenotypic and genotypic characteristics. *Ophthalmology* 122: 335-344 DOI 10.1016/j.ophtha.2014.08.032
6. Westeneng-van Haften SC, Boon CJ, Cremers FP, Hoefsloot LH, den Hollander AI, Hoyng CB (2012) Clinical and genetic characteristics of late-onset Stargardt's disease. *Ophthalmology* 119: 1199-1210 DOI 10.1016/j.ophtha.2012.01.005
7. Fujinami K, Zernant J, Chana RK, Wright GA, Tsunoda K, Ozawa Y, Tsubota K, Robson AG, Holder GE, Allikmets R, Michaelides M, Moore AT (2015) Clinical and molecular characteristics of childhood-onset Stargardt disease. *Ophthalmology* 122: 326-334 DOI 10.1016/j.ophtha.2014.08.012
8. Klevering BJ, Blankenagel A, Mauerer A, Cremers FP, Hoyng CB, Rohrschneider K (2002) Phenotypic spectrum of autosomal recessive cone-rod dystrophies caused by mutations in the ABCA4 (ABCR) gene. *Investigative ophthalmology & visual science* 43: 1980-1985
9. Fishman GA, Stone EM, Grover S, Derlacki DJ, Haines HL, Hockey RR (1999) Variation of clinical expression in patients with Stargardt dystrophy and sequence variations in the ABCR gene. *Archives of ophthalmology* 117: 504-510
10. Armstrong JD, Meyer D, Xu S, Elfervig JL (1998) Long-term follow-up of Stargardt's disease and fundus flavimaculatus. *Ophthalmology* 105: 448-457; discussion 457-448 DOI 10.1016/S0161-6420(98)93026-3
11. Querques G, Leveziel N, Benhamou N, Voigt M, Soubrane G, Souied EH (2006) Analysis of retinal flecks in fundus flavimaculatus using optical coherence tomography. *The British journal of ophthalmology* 90: 1157-1162 DOI 10.1136/bjo.2006.094136
12. Klevering BJ, Blankenagel A, Mauerer A, Cremers FP, Hoyng CB, Rohrschneider K (2002) Phenotypic spectrum of autosomal recessive cone-rod dystrophies caused by mutations in the ABCA4 (ABCR) gene. *Investigative ophthalmology & visual science* 43: 1980-1985
13. Michaelides M, Chen LL, Brantley MA, Jr., Andorf JL, Isaak EM, Jenkins SA, Holder GE, Bird AC, Stone EM, Webster AR (2007) ABCA4 mutations and discordant ABCA4 alleles in patients and siblings with bull's-eye maculopathy. *Br J Ophthalmol* 91: 1650-1655 DOI 10.1136/bjo.2007.118356
14. Stargardt K (1909) Über familiäre, progressive Degeneration in der Maculagegend des Auges. *Graefe's archive for clinical and experimental ophthalmology = Albrecht von Graefes Archiv fur klinische und experimentelle Ophthalmologie*: 534-550
15. Franceschetti A (1965) A special form of tapetoretinal degeneration: fundus flavimaculatus. *Transactions - American Academy of Ophthalmology and Otolaryngology American Academy of Ophthalmology and Otolaryngology* 69: 1048-1053

16. van Huet RA, Bax NM, Westeneng-Van Haaften SC, Muhamad M, Zonneveld-Vrieling MN, Hoefsloot LH, Cremers FP, Boon CJ, Klevering BJ, Hoyng CB (2014) Foveal sparing in Stargardt disease. *Invest Ophthalmol Vis Sci* 55: 7467-7478 DOI 10.1167/iovs.13-13825
17. Fujinami K, Sergouniotis PI, Davidson AE, Wright G, Chana RK, Tsunoda K, Tsubota K, Egan CA, Robson AG, Moore AT, Holder GE, Michaelides M, Webster AR (2013) Clinical and molecular analysis of stargardt disease with preserved foveal structure and function. *Am J Ophthalmol* 156: 487-501 e481 DOI 10.1016/j.ajo.2013.05.003
18. Marmor MF, Fulton AB, Holder GE, Miyake Y, Brigell M, Bach M, International Society for Clinical Electrophysiology of V (2009) ISCEV Standard for full-field clinical electroretinography (2008 update). *Documenta ophthalmologica Advances in ophthalmology* 118: 69-77 DOI 10.1007/s10633-008-9155-4
19. Lois N, Holder GE, Bunce C, Fitzke FW, Bird AC (2001) Phenotypic subtypes of Stargardt macular dystrophy-fundus flavimaculatus. *Arch Ophthalmol* 119: 359-369
20. Khan KN, Kasilian M, Mahroo OAR, Tanna P, Kalitzeos A, Robson AG, Tsunoda K, Iwata T, Moore AT, Fujinami K, Michaelides M (2018) Early Patterns of Macular Degeneration in ABCA4-Associated Retinopathy. *Ophthalmology* 125: 735-746 DOI 10.1016/j.ophtha.2017.11.020
21. Fishman GA, Farber M, Patel BS, Derlacki DJ (1987) Visual acuity loss in patients with Stargardt's macular dystrophy. *Ophthalmology* 94: 809-814
22. Gelissen O, De Laey JJ (1985) A clinical review of Stargardt's disease and/or fundus flavimaculatus with follow-up. *International ophthalmology* 8: 225-235
23. Chun R, Fishman GA, Collison FT, Stone EM, Zernant J, Allikmets R (2014) The value of retinal imaging with infrared scanning laser ophthalmoscopy in patients with stargardt disease. *Retina* 34: 1391-1399 DOI 10.1097/IAE.000000000000070
24. Lee W, Noupou K, Oll M, Duncker T, Burke T, Zernant J, Bearely S, Tsang SH, Sparrow JR, Allikmets R (2014) The external limiting membrane in early-onset Stargardt disease. *Invest Ophthalmol Vis Sci* 55: 6139-6149 DOI 10.1167/iovs.14-15126
25. Vandenbroucke T, Buyl R, De Zaeytijd J, Bauwens M, Uvijls A, De Baere E, Leroy BP (2015) Colour Vision in Stargardt Disease. *Ophthalmic research* 54: 181-194 DOI 10.1159/000438906
26. Messias A, Reinhard J, Velasco e Cruz AA, Dietz K, MacKeben M, Trauzettel-Klosinski S (2007) Eccentric fixation in Stargardt's disease assessed by Tübingen perimetry. *Investigative ophthalmology & visual science* 48: 5815-5822 DOI 10.1167/iovs.06-0367





## CHAPTER 2.3

### Foveal sparing in Stargardt disease

*“Foveal sparing mainly occurs in patients with late-onset Stargardt and characterizes the mild end of the clinical variations in Stargardt disease. Long-term follow-up data provided insight in the natural course of foveal sparing. Although the etiology is unclear, we hypothesize on possible underlying factors. Knowledge on these fovea-protective factors can provide opportunities for future therapeutic strategies.”*

Ramon A.C. van Huet\*  
Nathalie M. Bax\*  
Sarah C. Westeneng-Van Haaften  
Muhamad Muhamad  
Marijke N. Zonneveld-Vrieling  
Lies H. Hoefsloot  
Frans P.M. Cremers  
Camiel J.F. Boon  
B. Jeroen Klevering  
Carel B. Hoyng  
\*Shared first author

*Investigative Ophthalmology & Visual Science. 2014 Oct 16;55(11):7467-78.*



**PURPOSE:** To provide a clinical and genetic description of a patient cohort with Stargardt disease (STGD1) with identifiable foveal sparing.

**METHODS:** Patients with retinal atrophy (defined as an absence of autofluorescence) that surrounds the fovea by at least 180° and does not include the fovea were defined as having foveal sparing; eyes with visual acuity (VA) worse than 20/200 were excluded. We reviewed the medical files and extracted data regarding medical history, VA, ophthalmoscopy, static perimetry, fundus photography, spectral-domain optical coherence tomography (SD-OCT), fluorescein angiography (FA), fundus autofluorescence (FAF), and electroretinography (ERG). We screened each patient's ABCA4 gene for mutations.

**RESULTS:** Seventeen eyes with foveal sparing were identified in 13 unrelated patients. In 4 eyes, the fovea gradually became atrophic after the initial foveal sparing. The mean age at onset was 51 years (range: 32-67 years). VA was 20/40 or better in all foveal sparing eyes, and 20/25 or better in 41%. FAF imaging revealed hyperautofluorescent flecks and parafoveal retinal atrophy, SD-OCT revealed sharply delineated atrophy, and perimetry revealed parafoveal scotomas with intact foveal sensitivity. Finally, genetic screening identified mutations in 19 of the 26 ABCA4 gene alleles.

**CONCLUSIONS:** Foveal sparing occurs mainly in patients with late-onset STGD1 and represents the milder end of the clinical spectrum in STGD1. The anatomy, metabolism, and biochemistry of the retina, as well as genetic variations in genes other than ABCA4, can influence the etiology of foveal sparing. Identifying these fovea-protecting factors will facilitate the future development of strategies designed to treat STGD1.

## Introduction

Within the retina, the macula provides the highest visual acuity and contains the highest density of cones.<sup>1,2</sup> Therefore, a loss of central vision is a hallmark feature of macular dystrophies. There are, however, exceptions to this rule. Foveal sparing is an intriguing phenomenon in which retinal atrophy surrounds a relatively preserved fovea, leaving central visual acuity largely unaffected. Although foveal sparing has been reported in a variety of conditions, including Stargardt disease (STGD1),<sup>3-5</sup> mitochondrial retinal dystrophy associated with the m.3243A>G mutation,<sup>6</sup> and geographic atrophy in age-related macular degeneration (AMD),<sup>7-11</sup> its etiology remains poorly understood.

STGD1 is an autosomal recessive retinal dystrophy that typically presents within the first two decades of life.<sup>12</sup> Although the clinical presentation of STGD1 varies widely, it is usually characterized by a progressive loss of central vision, irregular yellow-white fundus flecks, and the so-called “beaten bronze” atrophic macular lesions.<sup>13-15</sup> STGD1 has been linked to mutations in the *ABCA4* gene, which encodes an adenosine triphosphate (ATP)-binding cassette transporter (ABCR) expressed specifically in the cones and rods of the retina.<sup>16, 17</sup> Defects in ABCR function cause the accumulation of all-*trans*-retinal and its cytotoxic derivatives (e.g., diretinoid-pyridinium-ethanolamine) in photoreceptors and retinal pigment epithelial (RPE) cells, ultimately causing RPE cell death and the subsequent loss of photoreceptors.<sup>18</sup>

Mutations in *ABCA4* have been linked to a spectrum of phenotypes ranging from mild macular dystrophy to severe early-onset panretinal dystrophy.<sup>3, 19-22</sup> We previously postulated that disease severity may be correlated to the functional severity of the particular mutation in the resulting ABCR protein.<sup>19, 23-25</sup> The substantial clinical variability among patients with STGD1—including an age at onset of the symptoms that can range from 5-72 years of age, diverse fundoscopic features, diverse electrophysiological findings, and a variable time course of vision loss—suggests the presence of several strong modifying factors.<sup>3,13, 14</sup>

Recently, Fujinami et al. reported the clinical and molecular genetic findings of a cohort of STGD1 patients with relatively preserved foveal structure and function (based on seemingly normal autofluorescence at the fovea). Their study revealed the presence of two basic—yet distinct—STGD1 phenotypes, namely STGD1 patients with foveal sparing and STGD1 patients with early-onset foveal atrophy.<sup>26</sup> However, the onset of foveal involvement in STGD1 can vary substantially and can

occur in later disease stages, for example in late-onset STGD1.<sup>3</sup> This heterogeneity complicates the selection of homogeneous cohorts for clinical studies to investigate the subtype of STGD1 patients with foveal sparing.

Here, we report the clinical characteristics and the natural course of foveal sparing in a cohort of STGD1 patients with foveal sparing, and we explore the mechanisms that may underlie this phenomenon.

## Methods

### Patients and genetic analysis

The patient selection process is depicted in [Figure 1](#). The database of the Department of Ophthalmology at Radboud University Medical Center (Nijmegen, the Netherlands) contains 425 clinically suspected cases of STGD1. For 257 of these patients, an *ABCA4* genetic screen for known mutations was performed in the Department of Human Genetics at Radboud University Medical Center (Nijmegen, the Netherlands) using arrayed primer extension analysis (APEX) microarrays (Asper Biotech, Tartu, Estonia). Because STGD1 is autosomal recessive, if the Asper microarray screen revealed only one mutation in a given patient, we sequenced the exons and intron-exon boundaries in *ABCA4* to identify the mutation in the second allele. All mutations were confirmed using Sanger sequencing. The presence of one or two mutations in the *ABCA4* gene confirmed the diagnosis of STGD1 in 198 patients. For our study, we selected cases in which foveal sparing was documented using fundus photography and/or fundus autofluorescence (FAF) imaging. Patients with RPE atrophy (defined as an absence of autofluorescence surrounding the fovea by least 180°) that did not include the fovea were defined as having foveal sparing. Eyes with visual acuity of 20/200 or worse were presumed to have little or no foveal function and were therefore excluded. Twelve unrelated STGD1 patients with foveal sparing in at least one eye were included in this study. We also included one additional patient who initially presented with foveal sparing; in this patient, the fovea became atrophic as the disease progressed. To exclude pseudo-Stargardt pattern dystrophy,<sup>27</sup> the *PRPH2* gene was sequenced in all 13 patients.

This study was performed in accordance with the tenets of the Declaration of Helsinki, and all participating patients gave their informed consent prior to providing a blood sample and receiving additional ophthalmologic examinations.

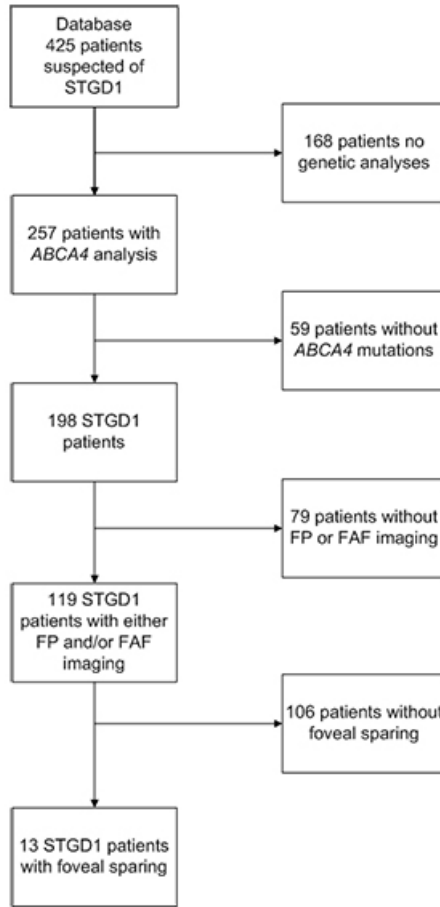


**Figure 1.** Flow-chart depicting the selection process of Stargardt patients with foveal sparing for inclusion in the study. FAF, fundus autofluorescence; FP, fundus photography; STGD1, Stargardt disease.

### Clinical examination

Clinical data were collected from the medical records of the 13 eligible patients. The data collected included the patient's age at onset, medical history, initial symptoms, and the overall course of the retinal disorder. Age at onset was defined as the age at which the initial symptoms were noted by the patient. We defined the duration of symptomatic disease as the time from the age at onset to the patient's current age. In the patients who were initially asymptomatic, the age at their first visit to the ophthalmologist was used to define disease duration.

The standard ophthalmic examination included a measurement of best-corrected visual acuity (BCVA) using Snellen visual acuity charts and ophthalmoscopy. The central visual field was assessed using a Humphrey perimeter (Carl Zeiss Meditec, Jena, Germany) using central 10-2, 24-2, or 30-2 threshold tests in

two, two, and four patients, respectively. Fundus photography (Topcon TRC50IX, Topcon Corporation, Tokyo, Japan) was performed in ten patients. Fluorescein angiography (FA) was performed in ten patients to screen for the presence of the dark choroid sign. Full-field electroretinography (ffERG; 8 patients) and multifocal ERG (mfERG; 7 patients) were performed using Dawson-Trick-Litzkow (DTL) electrodes and the RETI-port system (Roland Consults, Stasche & Finger GmbH, Brandenburg an der Havel, Germany). Both the ffERG and mfERG recordings were performed in accordance with the guidelines of the International Society for Clinical Electrophysiology of Vision (ISCEV).<sup>28</sup>

Cross-sectional images were obtained using spectral-domain optical coherence tomography (SD-OCT; Heidelberg Engineering, Heidelberg, Germany) in 12 patients; a 20°x15° 19-line scan covering the fovea was used. Total retinal thickness, outer nuclear layer (ONL) thickness, and photoreceptor-RPE (PR+RPE) complex thickness were measured at the foveal dip and at 0.25, 0.5, 1, 1.5, 2, and 2.5 mm eccentric distances using Heidelberg Eye Explorer software (Version 1.6.4.0, Heidelberg Engineering, Heidelberg, Germany). ONL thickness was measured from the outer plexiform layer to the external limiting membrane (ELM), PR+RPE thickness was measured from the ELM to Bruch membrane, and total retinal thickness was measured from the vitreous-retinal interface to RPE-Bruch membrane complex. Clinically normal values for total retinal thickness, ONL thickness, and PR+RPE thickness were obtained from 25 age-matched individuals (mean age: 46 years; range: 27-62 years) with no retinal or vitreoretinal disease; we performed a post-acquisition interpolation of the normal data using custom programs (MatLab R2011a, The MathWorks Inc., Natick, MA).

We acquired FAF images using a confocal scanning laser ophthalmoscope (cSLO, Spectralis, Heidelberg Engineering, Heidelberg, Germany). After the pupil was dilated, 30° and/or 55° field-of-view FAF images were obtained from all patients (except case 11) using an optically pumped solid-state laser with 488-nm excitation. Two independent observers (authors R.A.C.v.H. and N.M.B.) measured the size of the atrophic lesions (determined using the absence of autofluorescence) as described previously.<sup>29</sup>

## Results

### Clinical characteristics

Of the 198 patients with a confirmed diagnosis of STGD1, 13 unrelated patients (7%) had foveal sparing. The clinical characteristics of these 13 patients (including all 26 eyes) are summarized in [Table 1](#). This cohort included five women and eight men; all 13 patients were of Caucasian descent, with a mean age at onset of 52

years (range: 32-67 years). The mean disease duration was 9 years (range: 1-34 years). These patients were diagnosed between the age of 39 and 82 years (mean: 57 years). None of the patients were using hydroxychloroquine at the time of the study, nor had they used this drug in the past.

Foveal sparing was present in 17 of the 26 eyes (65%), and five of the 13 patients (38%) had bilateral foveal sparing. In seven of the patients with unilateral foveal sparing, five of the contralateral eyes had no signs of RPE atrophy or parafoveal atrophic RPE lesions that surrounded the fovea by less than 180°. In the remaining two eyes, and in both eyes in patient 12, the fovea degenerated after initial foveal sparing ([Table 1](#)).

Nine of the 13 patients (69%) initially experienced a decline in visual acuity. Other initial symptoms included paracentral scotoma in four patients (31%), metamorphopsia in two patients (15%), and nyctalopia in one patient (8%). Two patients (patients 2 and 13; 15%) initially experienced no visual complaints, but were referred to our department because of fundus abnormalities found during ophthalmologic screening for glaucoma or thyroid eye disease; after nine and six years, respectively, these two patients experienced a perceived decrease in visual acuity ([Table 1](#)). BCVA was 20/40 or better in all 17 eyes with foveal sparing; 7 of these 17 eyes (41%) had a BCVA of 20/25 or better. In the four eyes in which atrophy ultimately affected the fovea, BCVA had decreased to  $\leq 20/200$  from an initial acuity of 20/25 to 20/40 when the fovea was spared.

In 12 patients, a fundus examination revealed irregular flavimaculatus flecks scattered throughout the posterior pole and occasionally extending anterior to the vascular arcades ([Figures 2A-B and 3A](#)). One patient had small perifoveal yellow-white dots. Patient 12, who had bilateral foveal degeneration, developed extensive chorioretinal atrophy of the posterior pole and the midperiphery during the patient's 26 years of follow-up ([Figure 2C](#)). Masking of the choroidal background fluorescence (i.e., a so-called "dark choroid") was evident on FA imaging in seven patients, four of whom carried a single heterozygous *ABCA4* mutation ([Tables 1 and 2](#)). The flavimaculatus flecks were visible as an irregular pattern of hyperfluorescence and hypofluorescence on FA imaging ([Figure 3B](#)), and they appeared as hyperautofluorescent flecks on FAF imaging ([Figures 3C and 4](#)). The chorioretinal atrophy corresponded with sharply delineated areas that included both an absence of autofluorescence and structural thinning of the outer retinal layers on OCT ([Figure 3D](#)). Static perimetry revealed sharply delineated absolute parafoveal scotomas ([Figure 4](#)) with subnormal foveal sensitivity (median: 35 dB; range: 20-39 dB). Foveal sensitivity was not measurable (<0 dB) in patient 12, which is consistent with the anatomical findings and other functional results obtained from this patient.

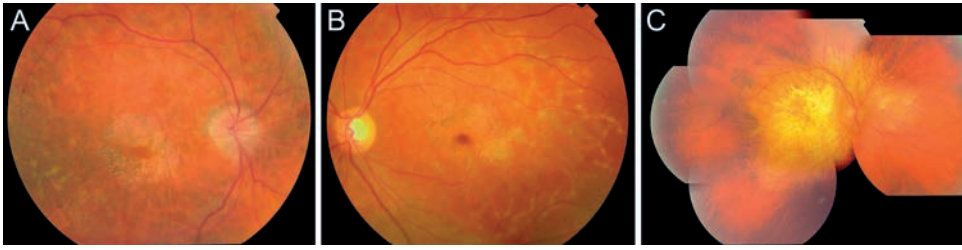


**Figure 2.** Fundus photographs of three patients with STGD1. **A**, Fundus photograph of the right eye of patient 4 (at age 60), showing fundus flavimaculatus flecks and parafoveal atrophy of the retinal pigment epithelium (RPE). **B**, Fundus photograph of the left eye of case 5 (at age 45), showing fundus flavimaculatus flecks and parafoveal atrophy of the RPE. **C**, Mosaic of fundus photographs of the right eye of case 12 (at age 73), showing profound central atrophy of the RPE; this patient previously had foveal sparing.

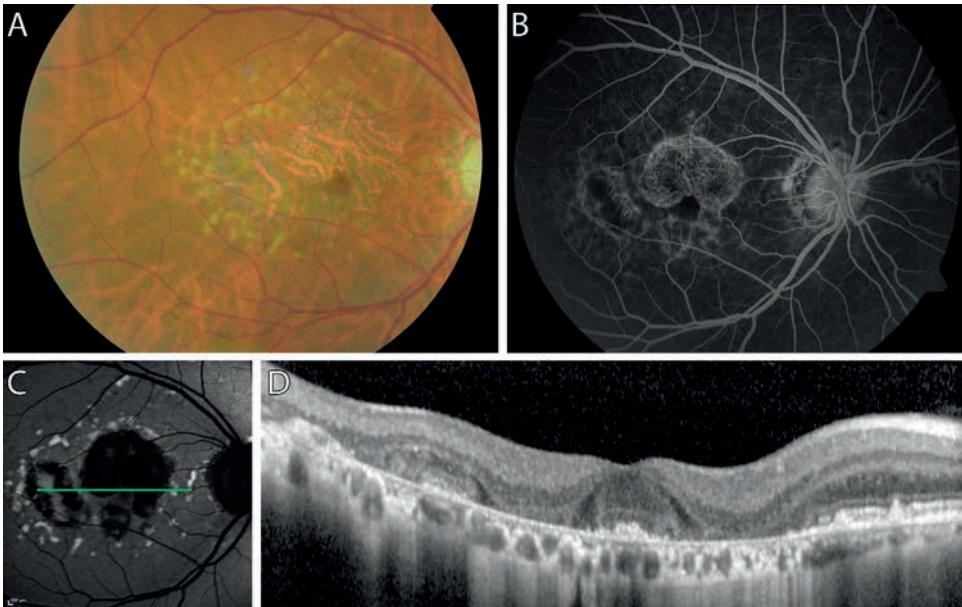


**Figure 3.** Multimodal imaging of the right fundus of patient 3 at age 62. **A**, Fundus photograph showing irregular flavimaculatus flecks and atrophy of the central retinal pigment epithelium (RPE); note that the fovea is spared. **B**, Fluorescein angiograph showing the “dark choroid” sign, hyperfluorescence, visible choroidal vessels due to window defects, and a normal-appearing fovea. **C**, Fundus autofluorescence image showing hyperautofluorescent flecks and RPE atrophy with foveal sparing. The green horizontal line indicates the scanning level of the optical coherence tomography (OCT) scan in panel D. **D**, An OCT scan through the fovea clearly shows the preserved cone photoreceptors in the fovea surrounded by atrophy of the outer retina and RPE.

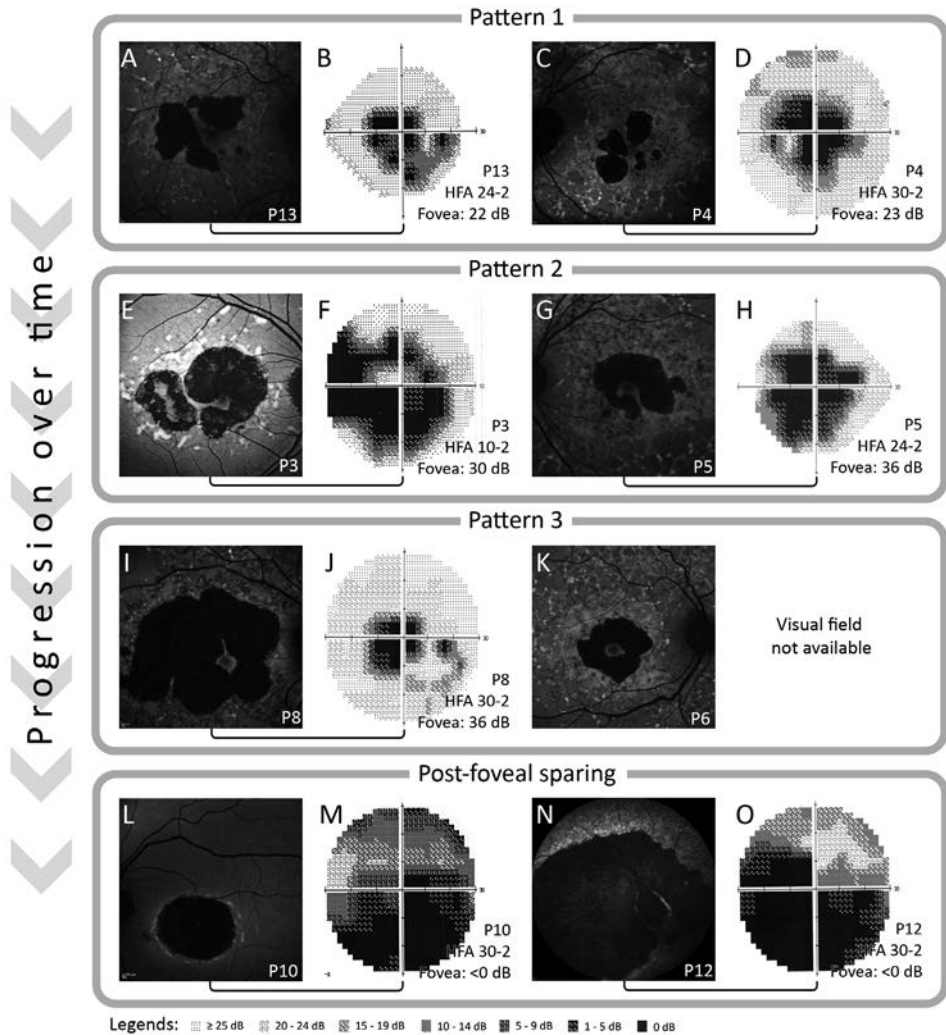


**Figure 4.** Natural course of fundus and perimetric changes in STGD1 with foveal sparing. FAF imaging can be used to identify the three stages that occur in foveal sparing. In stage 1, confluent parafoveal RPE lesions surround the macula, leaving several connections of intact RPE with the surrounding vital RPE (stage 1; A, C). Over time, the RPE atrophy progresses, and the lesions interconnect, leaving only one isthmus of RPE (stage 2; E, G). Further disease progression leads to an isolated fovea that is surrounded completely by RPE atrophy (stage 3; I, K). Eventually, RPE atrophy overcomes foveal resistance, leading to foveal degeneration (post-foveal sparing; L, N). Static perimetry examination reveals absolute perifoveal scotomas with intact foveal sensitivity in all eyes with foveal sparing (B, D, F, H, J). Large absolute scotomas with diminished foveal sensitivity were observed in the post-foveal sparing eyes (M, O). A/B, FAF (A) and 24-2 perimetry (B) in patient 13 at age 63. C/D FAF (C) and 30-2 perimetry (D) in patient 4 at age 60 and 61, respectively. E/F FAF (E) and 10-2 perimetry (F) in patient 3 at age 64 and 65, respectively. G/H, FAF (G) and 24-2 perimetry (H) in patient 5 at age 45. I/J, FAF (I) and 30-2 perimetry (J) in patient 8 at age 66 and 65, respectively. K, FAF in patient 6 at age 58. L/M, FAF (L) and 30-2 perimetry (M) in patient 10 at age 53. N/O, FAF (N) and 30-2 perimetry (O) in patient 12 at age 73.



ID/Sex/AO (Y)/Age (Y)	Foveal sparing	Initial symptoms	Visual acuity		Ophthalmoscopy	Perimetry	ffERG*		Dark Scotopic chorioid on FA
			RE	LE			RE/LE	RE/LE	
P8/F/32/66	RE	VA↓	20/30	20/20	RE: Macular RPE atrophy with small foveal residue, small macular intraretinal pigmentations, hypopigmented RPE in posterior pole LE: RPE atrophy lesions in posterior pole, hypopigmented RPE in posterior pole. Macular RPE atrophy lesions in the RE confluent surrounding the fovea, yellow-white flecks in posterior pole	Humphrey 30-2: (65y) RE: Pericentral absolute scotoma of ~15°, FS: 36 dB LE: Three paracentral spots of absolute visual field loss, FS: 34 dB	N/MR RE/LE (65y)	N/N RE/LE (65y)	Yes
P9/M/NA/63	RE	VA↓	20/40	20/15	Macular RPE atrophy lesions in the RE confluent surrounding the fovea, yellow-white flecks in posterior pole	NP	NP	NP	Yes
P10/F/39/53	RE (LE: post-foveal sparing)	Paracentral scotoma	20/25	20/20	Perifoveal RPE atrophy lesions in RE; macular RPE atrophy in LE; small yellow-white spots in perifoveal region in BE.	NP	N/N (47y)	N/N (47y)	No
P11/M/67/68	LE	VA↓	20/20	20/30	Confluent RPE spots in the posterior pole surrounding the fovea in LE; fovea already degenerated in RE; irregular yellow-white flecks surrounding the atrophic lesions	NP	NP	NP	Yes
P12/M/50/74	BE: post-foveal sparing)	Paracentral scotoma	CF	CF	Profound choriorretinal atrophy in posterior pole, small border of yellow-white surrounds atrophy	Humphrey 30-2: (low test reliability) BE mixed relative and absolute central scotoma, inferior worse than superior quadrants, FS: <0 dB	SR/SR	SR/SR	NP
P13/M/52/63	RE	Initially no symptoms, 6 years later VA↓, para-central scotoma	20/25	20/25	Confluent RPE spots in perifoveal region, yellow-white flecks reaching up to the midperiphery	Humphrey 30-2: (63y) BE: Pericentral absolute scotoma. FS: 35-37dB	N/SR (60y)	N/N (60y)	Yes

\*The abbreviations reflect the amplitude: N, normal (equal to or above the lower 5% of the range for a normal population: photopic  $\geq 78 \mu\text{V}$ , scotopic  $\geq 263 \mu\text{V}$ ); MR, moderately reduced (1-5% of normal range: photopic  $\geq 69 \mu\text{V}$  and  $< 78 \mu\text{V}$ , scotopic  $\geq 195 \mu\text{V}$  and  $< 263 \mu\text{V}$ ); SR, severely reduced ( $< 1\%$  of normal range: photopic  $< 69 \mu\text{V}$ , scotopic  $< 195 \mu\text{V}$ ).

AO, Age at onset; BE, both eyes; CF, counting fingers; F, female; FA, fluorescein angiography; ffERG, full-field electroretinography; FS, foveal sensitivity; LE, left eye; M, male; NP, not performed; RE, right eye; RPE, retinal pigment epithelium; VA↓, decrease in visual acuity.

Table 1 Clinical characteristics of the patients included in this study at most recent visit.

ID/Sex/AO (y)/Age (y)	Foveal sparing	Initial symptoms	Visual acuity		Ophthalmoscopy	Perimetry	fERG*		Dark choroid on FA
			RE	LE			Scotopic RE/LE	Photopic RE/LE	
P1/F/53/57	RE	Paracentral scotoma, metamorpho psia	20/40	20/25	RE: macular RPE atrophy surrounding the fovea, yellow-white fundus flecks in posterior pole LE: hypopigmentation and yellow-white flecks in posterior pole	Humphrey24-2: (56y) BE: Pericentral scotoma of ~10°, FS: 36- 34dB	N/N RE/LE	N/N RE/LE	Yes
P2/M/58/61	BE	Initially no symptoms, 9 years later	20/40	20/30	RPE atrophy with small foveal peninsula, yellow-white fundus flecks reaching up to the midperiphery	Humphrey 10-2: (59y) BE: Absolute pericentral scotoma (superior>inferior), FS: 24-28 dB	N/N (49y)	MR/MR (49y)	Yes
P3/M/60/63	BE	VA↓, nyctalopia	20/25	20/25	RPE atrophy surrounding the small foveal residue, yellow-white irregular flecks reaching as far as the vascular arcades	Humphrey 10-2: (65y) BE: Absolute pericentral scotoma, FS: 30- 34 dB	NP	NP	Yes
P4/M/57/60	BE	VA↓	20/30	20/30	RPE atrophy spots (confluent in RE) around the fovea, yellow-white irregular flecks reaching up to the midperiphery	Humphrey 30-2: BE: Absolute pericentral scotoma of ~20°, FS 20-23 dB	N/N	N/N	No
P5/F/43/45	BE	VA↓	20/30	20/30	RPE atrophy surrounding the fovea, fundus flavimaculatus flecks reaching up to vascular arcades	Humphrey 24-2: RE: mixed relative and absolute pericentral scotoma of ~20° with inferior-temporal absolute defect, FS: 39 dB. LE: absolute pericentral scotoma of ~20°, FS: 36 dB	MR/MR	N/MR	NP
P6/M/57/59	BE	VA↓	20/25	20/25	RPE atrophy surrounding the fovea completely in RE and incompletely (~270°) in LE, yellow-white irregular flecks in posterior pole as well as diffusely spread hypopigmented spots	NP FS: 36 dB	NP	NP	No
P7/F/NA/81	LE	Metamorpho psia	20/25	20/25	Yellow-white irregular flecks within the posterior pole. Parafoveal RPE atrophy lesions in LE.	NP	NP	NP	NP

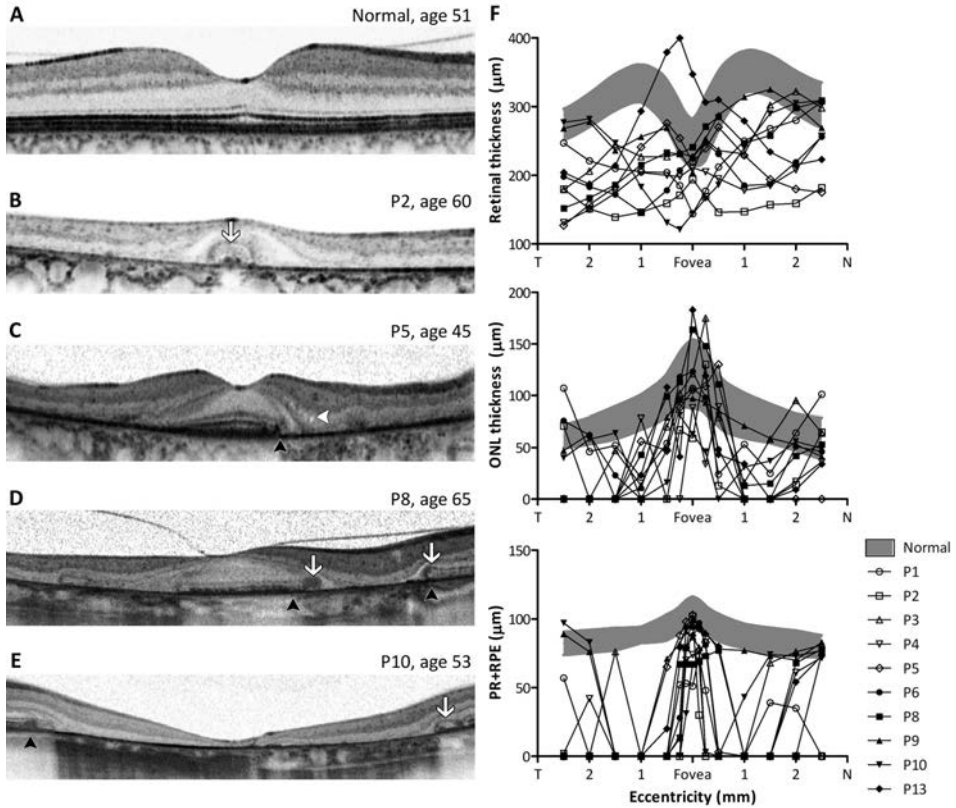


**Figure 5.** OCT analysis of Stargardt patients with foveal sparing. Panels A through E show the structural aspects of the macula in a healthy individual (A; age 51), case 2 (B; age 60), case 3 (C; age 45), case 8 (D; age 65), and case 10 (E; age 53). The white arrows in panel D indicate the locations of signs resembling outer retinal tubulation. The black arrowheads in panels C, D, and E indicate the locations of abrupt photoreceptor layer disturbances without gradual outer and/or inner segment loss. The white arrowhead in panel C indicates the presence of microcysts in the inner nuclear layer. F, Summary of thickness measurements of the total retina (top panel), ONL (middle panel), and PR+RPE (lower panel). The gray shaded areas show the distribution (mean  $\pm$  2SD) of the total retinal, ONL, and PR+RPE thickness in 25 age-matched healthy individuals (mean age: 46 years). ONL, outer nuclear layer; PR+RPE, photoreceptor-retinal pigment epithelium complex.

The results of the ffERG recordings in ten eyes with foveal sparing are summarized in Table 1. In these ten eyes, photopic amplitude was normal in seven eyes (70%) and moderately reduced in three eyes (30%), and scotopic amplitude was normal in eight eyes (80%) and moderately reduced in two eyes (20%). In the four eyes that developed an atrophic fovea after initial foveal sparing, the photopic and scotopic amplitudes were either normal or severely reduced (Table 1). In three patients (patient 5, right eye; patient 8, left eye; and patient 13, left eye), the scotopic amplitude was reduced more markedly than the amplitude of photopic

flash responses, although none of these patients had peripheral pigmentary retinopathy. No clear correlation was found between ffERG response and disease duration, visual acuity, or fundoscopic characteristics. We also measured mfERG in eight eyes with foveal sparing and found that the P1-response amplitudes in the central two rings (representing the foveal retina) were relatively intact compared to the outer three rings, which showed severely reduced responses.

### Retinal structure

SD-OCT imaging was performed in 12 patients and revealed highly localized damage to the lamellar architecture of the macula. We observed parafoveal atrophy of photoreceptors and RPE cells with sharp borders, represented by a loss of the bands associated with the ELM, the ellipsoid inner segments, and the RPE (Figure 5B-E).<sup>30</sup> These bands were present in the fovea, however, although many of the bands that corresponded to the ELM and ellipsoid inner segments were irregular. In addition, the longer outer segments—which are characteristic of cone photoreceptors in the foveal dip—were not observed in any of these 12 eyes (Figure 5A-D). In three eyes, we observed signs reminiscent of outer retinal tubulation at the border of the atrophic lesions (Figure 5D), although no rosette-like structures (as described by Zweifel and colleagues) were observed.<sup>31</sup> Microcystoid macular edema was present in three eyes (Figure 5C), and epiretinal gliosis with retinal wrinkling extending over the fovea was observed in one eye.

An analysis of the retinal lamellar architecture revealed that the overall retinal thickness in the foveal and parafoveal regions was generally decreased (Figure 5E). The thickness of both the ONL and PR+RPE layers was normal at the foveal center in most patients. However, in the parafoveal region, the PR+RPE was usually nearly absent, whereas the ONL was progressively thinner in this region (Figure 5F).

### Natural course of foveal sparing

An analysis of the longitudinal FAF data, which were available for six patients, enabled us to investigate the natural course of foveal sparing. In general, fundus flavimaculatus flecks were observed in the early stages, in some cases even before symptoms developed. Within one to two decades of diagnosis (range: 10-18 years), one or more sharply delineated parafoveal RPE atrophic areas appeared (Figure 4A). Over time, these lesions expanded and reached confluence around the fovea, thus producing the foveal sparing phenotype. We observed three distinct stages in the development of foveal sparing; these stages characterize the natural course of the phenomenon. In stage 1, parafoveal atrophic lesions emerge, with several intact RPE connections between the fovea and the surrounding vital RPE

(Figure 4A and 4C). In stage 2, the atrophic RPE lesions interconnect, leaving only a single isthmus of RPE, thus resulting in a “peninsula-like” appearance (Figure 4E and 4G). Stage 3 is characterized by an isolated fovea that is surrounded completely by RPE atrophy (Figure 4I and 4K). We measured the expansion rate of the atrophic lesions in four patients using the FAF follow-up data (Table 2). The rate of expansion ranged from 0.832 to 2.363 mm<sup>2</sup>/year in these patients, and the rate was positively correlated to the size of the atrophic lesions. Given this wide range of expansion rates, it is unclear how long foveal sparing is present before the foveal structure and function become significantly affected by the profound atrophy; however, we observed that the foveal structure and function were relatively preserved for up to six years in patients 8 and 12. Eventually, the remaining foveal tissue became progressively smaller, and atrophy of the central fovea was observed in four eyes (in patients 10, 11 and 12, Figures 4L, 4N and 5E); this was accompanied by a decline in central vision to 20/200 or worse.

**Table 2.** Results of progression analysis on fundus autofluorescence (FAF) imaging during follow-up in STGD1 patients with foveal sparing.

ID	Age at initial visit (years)	Duration follow-up		Eye	Atrophy at initial visit (mm <sup>2</sup> )*	Atrophy at follow-up (mm <sup>2</sup> )*	Expansion during follow-up (mm <sup>2</sup> )*	Progression rate (mm <sup>2</sup> /year)*
		Days	Years					
P1	57	597	1.6	Right	3.517	4.877	1.36	0.832
P2	59	842	2.3	Right	11.792	15.770	3.978	1.726
				Left	11.202	16.43	5.228	2.268
P8	63	1657	4.5	Right	16.308	27.027	10.719	2.363
P9	62	420	1.1	Right	3.570	4.601	1.031	0.897

\*Measurements were performed by two authors (RACvH and NMB), and the average of the two measurements are shown. Mean interobserver variance was 2.7% (range: 0.4%-9.8%).

### Genetic analysis and mutation screening

An examination of the pedigrees of the 13 unrelated patients with foveal sparing revealed a recessive inheritance pattern in five patients; the other eight patients appeared to be isolated cases. Mutations in the *ABCA4* gene were identified in 19 of the 26 alleles (73%, Table 3). We identified compound heterozygous mutations in six patients (46%) and single heterozygous mutations in the other seven patients (54%). In total, 13 different *ABCA4* variants were identified, including nine missense mutations, two splice site mutations, one nonsense mutation, and one synonymous variant that affects splicing.<sup>23</sup> Each of these variants has been described previously (Table 3).

The mutational effects of five of the identified mutations have been reported previously (Table 4). Although functional data regarding the effects of the other eight mutations is not available, we can speculate on the functional effect of the nonsense mutation (p.Gln1292\*). Assuming that the resulting mRNA is not

subject to nonsense-mediated decay, the resulting truncated protein will lack the second extracytoplasmic domain and the nucleotide-binding domain, which are involved in substrate and ATP binding, respectively.<sup>32</sup> [Table 5](#) summarizes the identified missense mutations in *ABCA4*, including allele frequencies in the exome variant server (EVS) and scores obtained from selected predictive tools. No differences in phenotype were observed between patients carrying severe mutations and patients carrying mild mutations. Finally, no pathogenic mutations in the *PRPH2* gene were identified in this cohort, thereby excluding the possibility of pseudo-Stargardt pattern dystrophy.<sup>27</sup>

**Table 3.** *ABCA4* mutations in STGD1 patients with foveal sparing

ID	Allele 1		Allele 2		References
	DNA variant	Effect	DNA variant	Effect	
P1	c.5461-10T→C	Unknown	NI	NA	35, 36
P2	c.3113C→T	p.Ala1038Val	c.3874C→T	p.Gln1292*	16, 37, 38, 58
P3	c.5461-10T→C	Unknown	c.5537T→C	p.Ile1846Thr	23, 35, 39, 58
P4	c.4363T→C	p.Cys1455Arg	NI	NA	40
P5	c.1822T→A	p.Phe608Ile	c.4685T→C	p.Ile1562Thr	23, 40, 41
P6	c.768G→T	Splice defect	c.3113C→T	p.Ala1038Val	16, 23, 37
P7	c.5196+1G→T	Splice defect	NI	NA	45, 58
P8	c.3874C→T	p.Gln1292*	NI	NA	38
P9	c.5461-10T→C	Unknown	NI	NA	35, 58
P10	c.1822T→A	p.Phe608Ile	NI	NA	23, 41
P11	c.286A→G	p.Asn96Asp	NI	NA	43
P12	c.1805G→A	p.Arg602Gln	c.4462T→C	p.Cys1488Arg	37, 39, 42-44
P13	c.3874C→T	p.Gln1292*	c.1928T→G	p.Val643Gly	38, 45

NI, not identified. \* = nonsense mutation. NA, not applicable

## Discussion

Here, we present the clinical characteristics of 13 STGD1 patients with foveal sparing in one or both eyes. The majority of these patients were diagnosed with late-onset STGD1; only three patients developed symptoms prior to the age of 45 ([Table 1](#)). In eyes with foveal sparing, visual acuity was relatively preserved; nevertheless, most of the patients experienced some loss of vision, which caused them to seek ophthalmologic care. In these instances, ophthalmoscopy readily revealed advanced retinal disease, with yellow-white irregular pisciform flecks and profound RPE atrophy adjacent to the fovea. Automated perimetry revealed perifoveal scotomas of various sizes with intact foveal sensibility. This combination of mild vision loss together with profound retinal abnormalities is typical among STGD1 patients with foveal sparing.

**Table 4.** Functional implications of *ABCA4* mutations

DNA variant (Effect)	Type of mutation	No. of Alleles	Predicted Effect on ABCR function	Classification of Mutations
c.768G→T (splice defect)	Splice site	1	No protein produced <sup>23</sup>	Severe
c.1805G→A (p.Arg602Gln)	Missense	1	No protein function due to mislocalization of the protein to the inner segment of the photoreceptor <sup>42</sup>	Severe
c.3113C→T (p.Ala1038Val)	Missense	2	Decreased ATP binding and ATPase activity <sup>37</sup>	Mild/Moderate
c.4462T→C (p.Cys1488Arg)	Missense	1	Decreased ATPase activity, reduced all- <i>trans</i> -retinal binding <sup>37, 44</sup>	Mild/Moderate
c.5461-10T→C (Unknown)	Splice site	3	Splice site intact, but presumed to be linked with an unidentified pathologic <i>ABCA4</i> mutation (linkage disequilibrium) <sup>59</sup>	Unknown

*ATP*, adenosine triphosphate; *ATPase*, adenosine triphosphatase.

Recently, Fujinami et al. reported the clinical and molecular findings of a cohort of Stargardt patients with a foveal sparing phenotype.<sup>26</sup> In their study, the authors included STGD1 patients with a functional fovea, irrespective of the presence of parafoveal RPE atrophy; thus, they studied a heterogeneous cohort of 40 patients. In contrast, in our cohort we defined foveal sparing as profound RPE atrophy that surrounded the fovea by at least 180 degrees and spared the fovea's structure and function. This clinical presentation is an rare finding among STGD1 patients, and our strict selection criterion resulted in a small but homogeneous cohort with a consistent phenotype and excluded STGD1 patients with late-onset disease that initiated with foveal atrophy. Moreover, our definition of foveal sparing is consistent with previously reported cases of foveal sparing in patients with other degenerative diseases.<sup>6, 8, 33, 34</sup> Despite the differences between our cohort and that the cohort described by Fujinami et al., the visual acuity and electrophysiology findings in their paper are similar to the findings in our study; nevertheless, none of our patients were carriers of the *ABCA4* p.Arg2030Gln missense mutation, which was suggested previously to be prevalent among STGD1 patients with foveal sparing.<sup>26</sup>

### The etiology of foveal sparing

In our study, screening the *ABCA4* gene identified 19 pathogenic mutations that were described previously in STGD1 and/or other *ABCA4*-associated retinopathies (Table 3),<sup>16, 23, 35-45</sup> interesting, however, foveal sparing was not described in any of the patients who were previously reported to carry these mutations. In a previously proposed model that links phenotype severity to the degree of residual ABCR function,<sup>23, 24</sup> late-onset STGD1 with foveal sparing was placed at the mild end of the spectrum of *ABCA4*-associated retinopathies.<sup>3</sup> Indeed, none of our

STGD1 patients with foveal sparing had two *ABCA4* variants that are associated with a severe loss of ABCR function. However, our knowledge regarding the functional consequences of *ABCA4* mutations identified to date is limited (Table 4). It can be extremely difficult to assess the effect of most missense variants using *in silico* predictions and allele frequencies in healthy individuals, for whom this information is often incomplete (Table 5); in addition, assessing the combined effect of carrying two *ABCA4* variants is particularly difficult. Functional assays are needed in order to form definitive conclusions regarding the effects of these mutations.

Because foveal sparing can be present in phenotypes that are independent of *ABCA4* mutations, including AMD and mitochondrial retinal dystrophy,<sup>6, 8-12, 17, 20, 25, 44, 45</sup> genetic factors other than *ABCA4* mutations are likely involved. These factors could include single-nucleotide polymorphisms (SNPs) and even mutations in retina-specific genes other than *ABCA4*, which suggests that a digenic or triallelic trait—in combination with the identified *ABCA4* mutations—may underlie the degenerative pattern observed in our patients. Moreover, anatomical, metabolic, and/or biochemical factors may underlie foveal sparing. For example, the average peak density of cones in the fovea is 199,000 cones/mm<sup>2</sup>, but can range from 98,200 to 324,100 cones/mm<sup>2</sup>.<sup>2</sup> The initial number of cones in the fovea may play a role in the development of foveal sparing; however, adaptive optics imaging techniques—which can provide the resolution needed to determine photoreceptor density *in vivo*—are not generally available in most ophthalmology practices. Another factor to consider is that S (“blue”) cone photoreceptors, which are absent in the foveal center, seem to be more vulnerable to retinal disease than M and L cones, although this selective vulnerability has not been reported in STGD1.<sup>46, 47</sup> Moreover, parafoveal rods appear to be more vulnerable than cones to the effects of aging and all-*trans*-retinal-mediated damage.<sup>48-50</sup> This difference may arise from the sole dependence of rods on the RPE for replenishing 11-*cis*-retinal; in contrast, cones are also supplied by Müller cells.<sup>51</sup> Furthermore, cone cells have a slower turnover rate of outer segments compared to rods,<sup>52</sup> although this does not necessarily result in higher all-*trans*-retinal levels in RPE cells, as regeneration is faster in cones than in rods.<sup>51</sup> Macular pigments, which can filter out high-energy light, may also serve a protective role, given that light exposure is crucial in the pathogenesis of STGD1.<sup>53, 54</sup> In addition, rod-derived cone viability factor (RdCVF), which is believed to prevent cone degeneration,<sup>55</sup> may also play a role. Importantly, the absolute levels of macular pigments and RdCVF may differ between STGD1 patients with foveal sparing and STGD1 patients without foveal sparing.



### Differential diagnosis and clinical significance of foveal sparing

When forming a diagnosis, foveal sparing–associated clinical entities other than late-onset STGD should be considered, including geographic atrophy in AMD, mitochondrial retinal dystrophy associated with the m.3243A→G mutation, central areolar choroidal dystrophy, and pseudo-Stargardt pattern dystrophy.<sup>6, 9, 10, 27, 29</sup> Importantly, misdiagnosing this condition can lead to inappropriate genetic counseling (these diseases display unique inheritance patterns) and/or an inaccurate estimate of the prognosis. Furthermore, in the event of an incorrect diagnosis of AMD, prescribing vitamin A–rich nutritional supplements can accelerate the accumulation of all-*trans*-retinal–derived toxins and increase the rate of disease progression, as shown in the retinas of homozygous *Abca4*-knockout mice.<sup>56</sup> STGD1 with foveal sparing can be diagnosed based on the presence of characteristic pisciform flecks together with RPE atrophy surrounding the fovea, a “dark choroid” sign on FA, and genetic analysis of the *ABCA4* gene. FAF imaging can clearly highlight the fundus flecks, which appear as hyperautofluorescent flecks, and RPE atrophy, which appears as an absence of autofluorescence. Retinal dystrophies that closely resemble STGD1 can follow other patterns of inheritance—for example, due to mutations in mitochondrial DNA—or can be autosomal dominant, with variable penetrance and expression. The fact that the “dark choroid” sign is present in approximately 85% of patients with STGD1<sup>57</sup> suggests a pivotal role for genetic analysis in the diagnosis of retinal dystrophies.

In conclusion, foveal sparing is a clinical phenomenon that occurs primarily in patients with late-onset STGD1 and is associated with the relative preservation of visual acuity, although visual acuity ultimately deteriorates by the end-stage of the disease. STGD1 patients with foveal sparing may be promising candidates for future therapeutic trials, as delayed degeneration of the fovea increases the time window for applying therapeutic interventions such as gene therapy. Although the mechanisms that underlie foveal sparing are currently unclear, expanding our knowledge of the metabolic and biochemical processes that lead to foveal sparing can facilitate the development of therapeutic strategies aimed at preserving foveal function.

**Table 5.** Characteristics of the missense mutations identified in ABCA4 in this study. Variants with unknown pathogenicity

DNA Variant	Effect	PhyloP <sup>1</sup>	Grantham <sup>2</sup>	Allele frequency in EVS <sup>3</sup>	SIFT (Class: score) <sup>4</sup>	PolyPhen-2 (Class: score) <sup>5</sup>	Align GVGDD <sup>6</sup>	Hypothetic effect
c.286A>G	p.Asn96Asp	3.27	23	1 in 8600	Deleterious (score: 0.00)	Possibly damaging: 0.852	Class C15	Unclear
c.1822T>A	p.Phe608Ile	3.27	21	1 in 8600	Deleterious (score: 0.00)	Possibly damaging: 0.937	Class C15	Unclear
c.1928T>G	p.Val643Gly	4.81	109	24 in 8600	Deleterious (score: 0.00)	Benign: 0.213	Class C65	Mild
c.4363T>C	p.Cys1455AArg	4.64	180	N/A	Deleterious (score: 0.00)	Probably damaging: 0.999	Class C65	Moderate/severe
c.4685T>C	p.Ile1562Thr	3.19	89	17 in 8600	Deleterious (score: 0.02)	Benign: 0.060	Class C25	Mild
c.5537T>C	p.Ile1846Thr	4.81	89	N/A	Deleterious (score: 0.00)	Probably damaging: 0.997	Class C65	Moderate/severe
Variants with known pathogenicity								
DNA Variant	Effect	PhyloP	Grantham	Allele frequency in EVS	SIFT (Class: score)	PolyPhen-2 (Class: score)	Align GVGDD	Effect
c.1305G>A	p.Arg602Gln	4.24	43	1 in 8600	Deleterious (score: 0.00)	Possibly damaging: 0.896	Class C35	Severe <sup>7</sup>
c.3113C>T	p.Ala1038Val	6.34	64	19 in 8600	Deleterious (score: 0.00)	Benign: 0.009	Class C65	Mild/moderate <sup>8</sup>
c.4462T>C	p.Cys1488AArg	4.89	180	N/A	Deleterious (score: 0.00)	Possibly damaging: 0.874	Class C65	Mild/moderate <sup>8,9</sup>

EVs, exome variant server; N/A, not available; PhyloP, phylogenetic profiling.

1. Siepel A, Pollard KS, Haussler D. Proceedings of the 10th International Conference on Research in Computational Molecular Biology (RECOMB 2006; April 2–5, 2006, Venice Lido, Italy) 2006. New methods for detecting lineage-specific selection; pp. 190–205.
2. Grantham R. Amino acid difference formula to help explain protein evolution. *Science*. 1974 Sep 6;185(4154):862–4.
3. Available at <http://evs.gs.washington.edu/EVS/>.
4. Available at <http://sift.jcvi.org>.
5. Available at <http://genetics.bwh.harvard.edu/pph2/>.
6. Tavtigian SV, Byrnes GB, Goldgar DE, Thomas A. Classification of rare missense substitutions, using risk surfaces, with genetic- and molecular-epidemiology applications. *Hum Mutat*. 2008 Nov;29(11):1342–54.
7. Wiszniewski W, Zaremba CM, Vatsenko AN, et al. ABCA4 mutations causing mislocalization are found frequently in patients with severe retinal dystrophies. *Hum Mol Genet* 2005;14:2769–2778.
8. Sun H, Smallwood PW, Nathans J. Biochemical defects in ABCR protein variants associated with human retinopathies. *Nat Genet* 2000;26:242–246.
9. Biswas-Fiss EE, Kurpad DS, Joshi K, Biswas SB. Interaction of extracellular domain 2 of the human retina-specific ATP-binding cassette transporter (ABCA4) with all-trans-retinol. *J Biol Chem* 2010;285:19372–19383.

## References

1. Curcio CA, Sloan KR, Jr., Packer O, Hendrickson AE, Kalina RE. Distribution of cones in human and monkey retina: individual variability and radial asymmetry. *Science* (80- ) 1987;236:579-582.
2. Curcio CA, Sloan KR, Kalina RE, Hendrickson AE. Human photoreceptor topography. *J Comp Neurol* 1990;292:497-523.
3. Westeneng-van Haften SC, Boon CJ, Cremers FP, Hoefsloot LH, den Hollander AI, Hoyng CB. Clinical and Genetic Characteristics of Late-onset Stargardt's Disease. *Ophthalmology* 2012;119:1199-1210.
4. Rotenstreich Y, Fishman GA, Anderson RJ. Visual acuity loss and clinical observations in a large series of patients with Stargardt disease. *Ophthalmology* 2003;110:1151-1158.
5. Nakao T, Tsujikawa M, Sawa M, Gomi F, Nishida K. Foveal sparing in patients with Japanese Stargardt's disease and good visual acuity. *Jpn J Ophthalmol* 2012;56:584-588.
6. de Laat P, Smeitink JA, Janssen MC, Keunen JE, Boon CJ. Mitochondrial Retinal Dystrophy Associated with the m.3243A>G Mutation. *Ophthalmology* 2013;120:2684-2696.
7. Baker CI, Dilks DD, Peli E, Kanwisher N. Reorganization of visual processing in macular degeneration: replication and clues about the role of foveal loss. *Vision Res* 2008;48:1910-1919.
8. Forte R, Querques G, Querques L, Leveziel N, Benhamou N, Souied EH. Multimodal evaluation of foveal sparing in patients with geographic atrophy due to age-related macular degeneration. *Retina* 2013;33:482-489.
9. Mones J, Biarnes M, Trindade F, Arias L, Alonso J. Optical coherence tomography assessment of apparent foveal swelling in patients with foveal sparing secondary to geographic atrophy. *Ophthalmology* 2013;120:829-836.
10. Schmitz-Valckenberg S, Fleckenstein M, Helb HM, Charbel Issa P, Scholl HP, Holz FG. In vivo imaging of foveal sparing in geographic atrophy secondary to age-related macular degeneration. *Invest Ophthalmol Vis Sci* 2009;50:3915-3921.
11. Sunness JS, Rubin GS, Zuckerbrod A, Applegate CA. Foveal-Sparing Scotomas in Advanced Dry Age-Related Macular Degeneration. *J Vis Impair Blind* 2008;102:600-610.
12. Stargardt K. Über familiäre, progressive Degeneration in der Maculagegend des Auges. *Graefes Arch Clin Exp Ophthalmol* 1909;534-550.
13. Fishman GA, Stone EM, Grover S, Derlacki DJ, Haines HL, Hockey RR. Variation of clinical expression in patients with Stargardt dystrophy and sequence variations in the ABCR gene. *Arch Ophthalmol* 1999;117:504-510.
14. Lois N, Holder GE, Bunce C, Fitzke FW, Bird AC. Phenotypic subtypes of Stargardt macular dystrophy-fundus flavimaculatus. *Arch Ophthalmol* 2001;119:359-369.
15. Lois N, Holder GE, Fitzke FW, Plant C, Bird AC. Intrafamilial variation of phenotype in Stargardt macular dystrophy-Fundus flavimaculatus. *Invest Ophthalmol Vis Sci* 1999;40:2668-2675.
16. Allikmets R, Singh N, Sun H, et al. A photoreceptor cell-specific ATP-binding transporter gene (ABCR) is mutated in recessive Stargardt macular dystrophy. *Nat Genet* 1997;15:236-246.
17. Molday LL, Rabin AR, Molday RS. ABCR expression in foveal cone photoreceptors and its role in Stargardt macular dystrophy. *Nat Genet* 2000;25:257-258.
18. Sparrow JR, Wu Y, Kim CY, Zhou J. Phospholipid meets all-trans-retinal: the making of RPE bis-retinoids. *J Lipid Res* 2010;51:247-261.
19. Cremers FP, van de Pol DJ, van Driel M, et al. Autosomal recessive retinitis pigmentosa and cone-rod dystrophy caused by splice site mutations in the Stargardt's disease gene ABCR. *Hum Mol Genet* 1998;7:355-362.
20. Birch DG, Peters AY, Locke KL, Spencer R, Megarity CF, Travis GH. Visual function in patients with cone-rod dystrophy (CRD) associated with mutations in the ABCA4(ABCR) gene. *Exp Eye Res* 2001;73:877-886.

21. Klevering BJ, Yzer S, Rohrschneider K, et al. Microarray-based mutation analysis of the ABCA4 (ABCR) gene in autosomal recessive cone-rod dystrophy and retinitis pigmentosa. *Eur J Hum Genet* 2004;12:1024-1032.
22. Klevering BJ, Maugeri A, Wagner A, et al. Three families displaying the combination of Stargardt's disease with cone-rod dystrophy or retinitis pigmentosa. *Ophthalmology* 2004;111:546-553.
23. Maugeri A, van Driel MA, van de Pol DJ, et al. The 2588G-->C mutation in the ABCR gene is a mild frequent founder mutation in the Western European population and allows the classification of ABCR mutations in patients with Stargardt disease. *Am J Hum Genet* 1999;64:1024-1035.
24. van Driel MA, Maugeri A, Klevering BJ, Hoyng CB, Cremers FP. ABCR unites what ophthalmologists divide(s). *Ophthalmic Genet* 1998;19:117-122.
25. Klevering BJ, Deutman AF, Maugeri A, Cremers FP, Hoyng CB. The spectrum of retinal phenotypes caused by mutations in the ABCA4 gene. *Graefes Arch Clin Exp Ophthalmol* 2005;243:90-100.
26. Fujinami K, Sergouniotis PI, Davidson AE, et al. Clinical and molecular analysis of stargardt disease with preserved foveal structure and function. *Am J Ophthalmol* 2013;156:487-501 e481.
27. Boon CJ, van Schooneveld MJ, den Hollander AI, et al. Mutations in the peripherin/RDS gene are an important cause of multifocal pattern dystrophy simulating STGD1/fundus flavimaculatus. *Br J Ophthalmol* 2007;91:1504-1511.
28. Marmor MF, Fulton AB, Holder GE, et al. ISCEV Standard for full-field clinical electroretinography (2008 update). *Doc Ophthalmol* 2009;118:69-77.
29. Boon CJ, Klevering BJ, Cremers FP, et al. Central areolar choroidal dystrophy. *Ophthalmology* 2009;116:771-782, 782 e771.
30. Spaide RF, Curcio CA. Anatomical correlates to the bands seen in the outer retina by optical coherence tomography: literature review and model. *Retina* 2011;31:1609-1619.
31. Zweifel SA, Engelbert M, Laud K, Margolis R, Spaide RF, Freund KB. Outer retinal tubulation: a novel optical coherence tomography finding. *Arch Ophthalmol* 2009;127:1596-1602.
32. Tsybovsky Y, Molday RS, Palczewski K. The ATP-binding cassette transporter ABCA4: structural and functional properties and role in retinal disease. *Adv Exp Med Biol* 2010;703:105-125.
33. Sunness JS, Bressler NM, Maguire MG. Scanning laser ophthalmoscopic analysis of the pattern of visual loss in age-related geographic atrophy of the macula. *Am J Ophthalmol* 1995;119:143-151.
34. Rath PP, Jenkins S, Michaelides M, et al. Characterisation of the macular dystrophy in patients with the A3243G mitochondrial DNA point mutation with fundus autofluorescence. *Br J Ophthalmol* 2008;92:623-629.
35. Maugeri A, Klevering BJ, Rohrschneider K, et al. Mutations in the ABCA4 (ABCR) gene are the major cause of autosomal recessive cone-rod dystrophy. *Am J Hum Genet* 2000;67:960-966.
36. Roberts LJ, Nossek CA, Greenberg LJ, Ramesar RS. Stargardt macular dystrophy: common ABCA4 mutations in South Africa--establishment of a rapid genetic test and relating risk to patients. *Mol Vis* 2012;18:280-289.
37. Sun H, Smallwood PM, Nathans J. Biochemical defects in ABCR protein variants associated with human retinopathies. *Nat Genet* 2000;26:242-246.
38. Ernest PJ, Boon CJ, Klevering BJ, Hoefsloot LH, Hoyng CB. Outcome of ABCA4 microarray screening in routine clinical practice. *Mol Vis* 2009;15:2841-2847.
39. Webster AR, Heon E, Lotery AJ, et al. An analysis of allelic variation in the ABCA4 gene. *Invest Ophthalmol Vis Sci* 2001;42:1179-1189.
40. Rosenberg T, Klie F, Garred P, Schwartz M. N965S is a common ABCA4 variant in Stargardt-related retinopathies in the Danish population. *Mol Vis* 2007;13:1962-1969.

41. Lewis RA, Shroyer NF, Singh N, et al. Genotype/Phenotype analysis of a photoreceptor-specific ATP-binding cassette transporter gene, ABCR, in Stargardt disease. *Am J Hum Genet* 1999;64:422-434.
42. Wiszniewski W, Zaremba CM, Yatsenko AN, et al. ABCA4 mutations causing mislocalization are found frequently in patients with severe retinal dystrophies. *Hum Mol Genet* 2005;14:2769-2778.
43. Papaioannou M, Ocaka L, Bessant D, et al. An analysis of ABCR mutations in British patients with recessive retinal dystrophies. *Invest Ophthalmol Vis Sci* 2000;41:16-19.
44. Biswas-Fiss EE, Kurpad DS, Joshi K, Biswas SB. Interaction of extracellular domain 2 of the human retina-specific ATP-binding cassette transporter (ABCA4) with all-trans-retinal. *J Biol Chem* 2010;285:19372-19383.
45. Allikmets R, Shroyer NF, Singh N, et al. Mutation of the Stargardt disease gene (ABCR) in age-related macular degeneration. *Science (80- )* 1997;277:1805-1807.
46. Pokorny J SV, Verriest G, Pinckers A. *Congenital and Acquired Color Vision Defects*. New York: Grune & Stratton; 1979.
47. Greenstein VC, Hood DC, Ritch R, Steinberger D, Carr RE. S (blue) cone pathway vulnerability in retinitis pigmentosa, diabetes and glaucoma. *Invest Ophthalmol Vis Sci* 1989;30:1732-1737.
48. Curcio CA. Photoreceptor topography in ageing and age-related maculopathy. *Eye (Lond)* 2001;15:376-383.
49. Curcio CA, Millican CL, Allen KA, Kalina RE. Aging of the human photoreceptor mosaic: evidence for selective vulnerability of rods in central retina. *Invest Ophthalmol Vis Sci* 1993;34:3278-3296.
50. Okano K, Maeda A, Chen Y, et al. Retinal cone and rod photoreceptor cells exhibit differential susceptibility to light-induced damage. *J Neurochem* 2012;121:146-156.
51. Wang JS, Kefalov VJ. The cone-specific visual cycle. *Prog Retin Eye Res* 2011;30:115-128.
52. Anderson DH, Fisher SK, Erickson PA, Tabor GA. Rod and cone disc shedding in the rhesus monkey retina: a quantitative study. *Exp Eye Res* 1980;30:559-574.
53. Weiter JJ, Delori F, Dorey CK. Central sparing in annular macular degeneration. *Am J Ophthalmol* 1988;106:286-292.
54. Aleman TS, Cideciyan AV, Windsor EA, et al. Macular pigment and lutein supplementation in ABCA4-associated retinal degenerations. *Invest Ophthalmol Vis Sci* 2007;48:1319-1329.
55. Leveillard T, Mohand-Said S, Lorentz O, et al. Identification and characterization of rod-derived cone viability factor. *Nat Genet* 2004;36:755-759.
56. Radu RA, Yuan Q, Hu J, et al. Accelerated accumulation of lipofuscin pigments in the RPE of a mouse model for ABCA4-mediated retinal dystrophies following Vitamin A supplementation. *Invest Ophthalmol Vis Sci* 2008;49:3821-3829.
57. Fishman GA, Farber M, Patel BS, Derlacki DJ. Visual acuity loss in patients with Stargardt's macular dystrophy. *Ophthalmology* 1987;94:809-814.
58. Kitiratschky VB, Grau T, Bernd A, et al. ABCA4 gene analysis in patients with autosomal recessive cone and cone rod dystrophies. *Eur J Hum Genet* 2008;16:812-819.
59. Rivera A, White K, Stohr H, et al. A comprehensive survey of sequence variation in the ABCA4 (ABCR) gene in Stargardt disease and age-related macular degeneration. *Am J Hum Genet* 2000;67:800-813.





## CHAPTER 2.4

### Foveal sparing in central retinal dystrophies

*“Foveal sparing occurs in patients with Stargardt disease, central areolar choroidal dystrophy, mitochondrial retinal dystrophy, and pseudo-Stargardt pattern dystrophy. The presence of foveal sparing in central retinal dystrophies with distinctly different underlying mechanisms suggests a disease-independent mechanism that prolongs the survival of the fovea. Long-term follow-up data provided insight in the natural course of foveal sparing. The associated preservation of visual acuity is important for the individual prognosis and has implications for the design of future therapeutic trials for inherited retinal disease.*

Nathalie M. Bax  
Dyon Valkenburg  
Stanley Lambertus  
B. Jeroen Klevering  
Camiel J.F. Boon  
Frank G. Holz  
Frans P.M. Cremers  
Monika Fleckenstein  
Moritz Lindner\*  
Carel B. Hoyng\*  
\*Shared last author

*Investigative Ophthalmology & Visual Science. In press.*



**PURPOSE:** To describe foveal sparing (FS) in central retinal dystrophies (RD).

**METHODS:** Participants for this retrospective study were identified from the retinal dystrophy database of the Department of Ophthalmology at Radboud University Medical Center. FS was defined as an intact foveal structure surrounded by at least 180° of chorioretinal atrophy, and a best-corrected visual acuity (BCVA) of <1.0 LogMAR (>20/200 Snellen). Eligible eyes were identified using fundus autofluorescence (FAF) images, and FS was confirmed using near infrared reflectance (NIR) imaging and spectral-domain optical coherence tomography when available. Clinical and demographic data were extracted from medical records. We performed quantification of FS and chorioretinal atrophic areas using semi-automated software on FAF and NIR images. We calculated the chronological change using eye-wise linear regression.

**RESULTS:** We identified 36 patients (56 eyes) with FS. RDs included: Stargardt disease (STGD1;20 patients), central areolar choroidal dystrophy (CACD;7 patients), mitochondrial retinal dystrophy (MRD;6 patients), pseudo-Stargardt pattern dystrophy (PSPD;3 patients). Median age at first presentation was 60 [inter-quartile range (IQR) 54–63] years. Median BCVA at first presentation ranged from 20/25 Snellen in STGD1, to 20/38 Snellen in MRD. Progression of the chorioretinal atrophic area ranged from 0.26 [0.25–0.28] mm/year in PSPD, to 0.14 (0.11–0.22) in CACD. Change in FS area over time was similar between the different dystrophies.

**CONCLUSIONS:** The presence of FS in different RDs suggests a disease-independent mechanism that prolongs the survival of the fovea. The associated preservation of BCVA is important for the individual prognosis and has implications for the design of therapeutic trials for RDs.

## Introduction

Retinal dystrophies (RDs) are among the leading causes for legal blindness in industrial countries.[1-3] Despite differences in underlying mechanisms, the common pathway in these disorders involves a selective atrophy of outer retinal layers, retinal pigment epithelium and associated choroidal layers, functionally paralleled by the development of absolute scotomas.[4]

Typically, patches of chorioretinal atrophy initially occur in the parafoveal retina. With spread over time, multifocal atrophic areas coalesce, and new atrophic areas may occur. On clinical examination, the fovea may remain uninvolved from chorioretinal atrophy until late in the course of the disease, when the fovea finally becomes atrophic. This phenomenon is referred to as “foveal sparing”, [5-9] and can be observed in several RDs, such as autosomal recessive Stargardt disease (STGD1), [8, 10-13] central areolar choroidal dystrophy (CACD), [14] and maternally inherited diabetes and deafness (MIDD). [15, 16] Geographic atrophy and reticular pseudo-drusen in age-related macular degeneration may also show a tendency to spare the fovea for a prolonged period of time. [7, 9, 17-20]

Although there is no consensus definition of the term “foveal sparing”, it could be distinguished from a perimacular ring scotoma, which is located more peripherally in the macula, resulting in a central visual island frequently observed in retinitis pigmentosa (RP). [21] Bull’s eye maculopathy is another separate entity, where an intact fovea is surrounded by a – usually oval shaped – area of outer retinal atrophy.

Historically, the term “foveal sparing” was coined by Hart et al. to describe the sparing of the fovea from hemifield defects. [22] In the context of macular disorders, Hart et al. were the first to describe a “sparing of foveal sensitivity in macular disease”, [22] while Sarks et al. specified an “enlargement and coalescence of atrophy into an almost complete ring around the fovea”. [7] These perimetric and funduscopy terms were brought together by Sunness et al. using the term “foveal sparing”, defined as an intact foveal structure surrounded by outer retinal and RPE atrophy. [20] The atrophy may either arrange as multiple independent spots, or in a ring or horseshoe-like fashion. [20]

The etiology of foveal sparing remains unclear, but it is highly remarkable that such a distinct preservation of the central macular tissue occurs in a variety of heterogenic retinal disorders. This suggests that the underlying mechanism of foveal sparing is, to a certain degree, disease-independent.

To date, the manifestations of foveal sparing in retinal dystrophies has not been analyzed systematically. Knowledge regarding the natural history of this peculiar phenomenon becomes even more important in the light of emerging therapeutic modalities aimed at prevention or slowing down of progressive chorioretinal atrophy in RDs (e.g. NCT01367444, NCT01736592, NCT01469832, and NCT02402660 on [www.clinicaltrials.gov](http://www.clinicaltrials.gov)).

A better understanding of the disease course of foveal sparing enables better stratification when including patients into a clinical trial and allows for a tailor-made prognosis. In addition, insight in the underlying mechanisms resulting in foveal sparing could open up new avenues for therapeutic approaches aimed at foveal preservation. In this study, we will provide a detailed description of foveal sparing in a large cohort of RD patients. We will analyze commonalities and discriminating features among the different RDs, and we will discuss the consequence for pathophysiological mechanisms regarding foveal sparing.

## Methods

### Patients selection

For this retrospective study, we employed the RD database of the Department of Ophthalmology at Radboud University Medical Center. The 1800 patients in this database have all been diagnosed with some form of inherited retinal disease, the large majority of which have been analyzed genetically. To readily identify patients with foveal sparing, we limited our search to patients with at least one fundus autofluorescence imaging (FAF) investigation. A genetically confirmed clinical diagnosis was also a requirement to be included in the search. In the context of this study, the foveal sparing had to fulfill two criteria. First, the fovea had to be surrounded by at least 180° of chorioretinal atrophy.[6, 8, 9] Second, a best-corrected visual acuity (BCVA) of  $\leq 1.0$  logMAR ( $\geq 20/200$  Snellen) had to be present.[8] Both eyes of a patient were included unless foveal sparing was only present in one of them.

The goal of the research is to study chorioretinal atrophy localized to the posterior pole, therefore we excluded generalized chorioretinal atrophy disorders like; retinitis pigmentosa, choroideremia, Bietti crystalline dystrophy, and gyrate atrophy. We excluded retinopathies with solely loss of photoreceptors encircling the fovea, like in Bull's eye maculopathy, because these entities do not fulfill the criteria of chorioretinal loss.

This retrospective study was approved by the Institutional Ethics Committee at Radboud University Medical Center (Nijmegen, The Netherlands), and was performed in accordance with the Tenets of the Declaration of Helsinki. All patients provided informed consent prior to additional ophthalmologic examinations to complete the clinical assessment and blood collection.

### Clinical data and image acquisition

A detailed medical and ophthalmologic history, including historical BCVA data, age at onset, age at diagnosis, and initial symptoms, was obtained from the medical records. Age at onset was defined as the age at which the patient first experienced visual complaints. In asymptomatic persons and patients where the age at onset could not be determined, the age at disease onset was considered equivalent to the age at diagnosis.

Standard imaging protocols were followed in the acquisition of retinal images. The FAF and NIR images were acquired using Spectralis HRA+OCT (Heidelberg Engineering, Heidelberg, Germany). The field of view was set to 30° x 30° or 55° x 55° with a minimum resolution of 768 x 768 pixels and centered on the macula. Single images were automatically aligned and averaged to maximize the signal-to-noise ratio using the manufacturer's software (automatic real-time [ART]-mode, Heidelberg Eye Explorer, Heidelberg Engineering). The SD-OCT scans were performed with the same device, and up to 100 single images were averaged to improve image quality. SD-OCT scans were 6.3 mm horizontal line scans through the fovea and follow-up mode was used for follow-up images. Furthermore, color fundus photographs (CFP) were obtained using a Topcon TRC50IX retinal camera (Topcon Corporation, Tokyo, Japan).

### Image grading

#### **Qualitative assessment**

Atrophy of retinal pigment epithelium and outer retina is typically associated by a sharply demarcated zone of dramatic reduction of autofluorescence (analogous to the previously employed definition of “definitely decreased autofluorescence”). [23] Where available, spectral-domain optical coherence tomography (SDOCT) was used to confirm foveal outer retinal integrity. If foveal sparing was lost during follow-up, all later visits were excluded from the analysis.

Qualitative assessment of the available FAF and SD-OCT images was performed to identify characteristic morphological features and atrophy patterns. In this explorative study, image analysis was performed by one trained reader (ML). As a

result of the retrospective nature of this dataset, some of the image grading tasks could not be performed in every eye or for every visit, because image availability varied per patient visit.

### **Quantitative assessment**

Measurements of atrophic area and foveal sparing area were performed as previously described,[9] [24] using the RegionFinder software (Heidelberg Engineering, version 2.5.5.0). In brief, the dramatic decrease of the FAF signal in GA areas compared with non-atrophic retinal areas is used by the Region-Finder for the segmentation of atrophy areas. The examiner/operator is required to define the center of each atrophic area. The software's so-called region-growing algorithm then identifies the borders of each atrophic area by the sharp change in signal intensity between atrophic and non-atrophic retina. This employed version of the RegionFinder includes a feature that automatically registers FAF to corresponding NIR images and allows the operator to easily switch from one modality to the other, thereby semi-automating the quantification of retinal pigment epithelium (RPE) atrophy and foveal sparing areas. In case no NIR images were available, measurements were only performed if the atrophy could be clearly discriminated from the physiologically decreased foveal autofluorescence due to the physiological attenuation of the autofluorescence signal in the foveal area by macular pigment. Atrophy measurements were performed in either 30° x 30° or 55° x 55° images within a single eye, as the software does not allow for quantitative comparison between images of different sizes. Only areas of sharply demarcated RPE atrophy, or "definitely decreased autofluorescence" (DDAF), were quantified, and quantification of foveal sparing required an area of DDAF surrounding the fovea by at least 270°.[9] Therefore, the foveal sparing area was not quantified in eyes with horseshoe-shaped atrophy surrounding the fovea by <270°. In case of incomplete foveal sparing, a constraint was placed by manually drawing a line at the most narrow place of the incomplete part of the residual foveal island.

Subfoveal retinal thickness (SRT) was assessed in SDOCT scans, transversing the foveola, as the distance between the internal limiting membrane (ILM) and the outer border of OCT band 4 (corresponding to the RPE/Bruch's membrane complex),[25] using the Heidelberg Eye Explorer "distance tool" (Heidelberg Engineering). A representative example is given in [supplementary Figure 1](#). Furthermore, the integrity of the retinal bands at the fovea was assessed.

As a result of the retrospective nature of this study, some of the image grading tasks could not be performed in every eye or for every visit, because image availability varied per patient visit.

### Genetic analysis

All samples were processed by the Department of Human Genetics of the Radboud University Medical Center in Nijmegen, the Netherlands. Genetic testing was targeted conform the clinical diagnosis.

Stargardt disease (STGD1): *ABCA4* analysis was performed using arrayed primer extension analysis (APEX) microarrays (Asper Biotech, Tartu, Estonia) and Sanger sequencing validation. The presence of two variants in the *ABCA4* gene confirmed the diagnosis STGD1. In cases where only one variant in *ABCA4* was identified, but the phenotype was characteristic for STGD1, this was deemed sufficient for the diagnosis. The following genetic variants were defined as severe: protein-truncating, canonical splice-site variants, as well as deletions spanning at least one exon. In case of missense variants, severity was predicted by bio-informatic means (SIFT, Polyphen, MutationTaster, and CADD). Cases with a clinical Stargardt-like phenotype and a mutation in the *PRPH2* gene, with or without an additional variant in a single *ABCA4* allele, were considered having pseudo-Stargardt pattern dystrophy (PSPD).[26]

Central areolar choroidal dystrophy (CACD): analysis of *PRPH2* was conducted using Sanger sequencing. One variant in the *PRPH2* gene, combined with the typical CACD phenotype, was considered sufficient to establish the diagnosis.

Mitochondrial retinal dystrophy (MRD): mitochondrial DNA was screened for mutations. The presence of the m.3243A>G mitochondrial mutation, combined with a characteristic clinical picture and visual symptoms, was required for the diagnosis of mitochondrial retinal dystrophy.

### Statistical analysis

R version 3.3.0 was used to perform statistical analysis. Decimal-scale visual acuity data were converted to LogMAR (Log(10) of the Minimal Angle of Resolution).

The rate of atrophy progression, and foveal sparing area loss over time, were calculated by eye wise linear regression from square-root transformed values, to reduce the dependency of enlargement rates on baseline lesion size, as previously suggested.[27] In this retrospective analysis, data for these parameters were not available for every single visit in every patient. To avoid exclusion of all data from a particular visit in case of a single missing parameter, subsets of visits were analyzed, when necessary. In these cases, cohort sizes and observation intervals were calculated separately. Unless stated differently, all data given represent medians and corresponding inter-quartile ranges. In this exploratory analysis, statistical tests for significance were not performed.

## Results

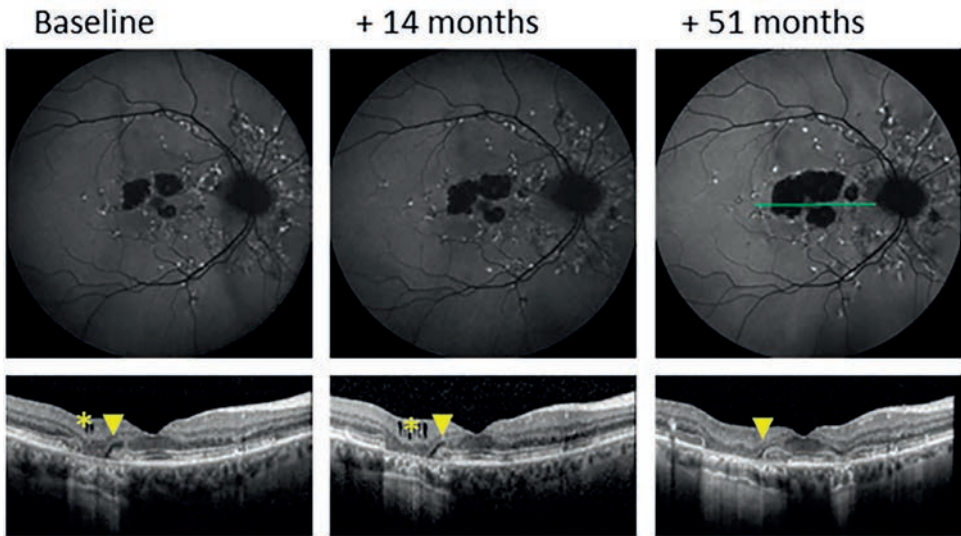
A total of 336 patients from the database of 1800 patients met the search criteria: FAF images and a genetically confirmed clinical diagnosis. In this cohort of 336 patients, we identified 36 individuals (56 eyes) with foveal sparing as previously defined. In 20 patients (56%), foveal sparing was present or developed in both eyes. Overall, this cohort included 20 of 176 (11.4%) STGD1 patients (31 eyes), 7 of 103 (6.8%) patients diagnosed with CACD (10 eyes), 6 of 21 (28.6%) MRD cases (10 eyes), 3 of 36 (8.3%) PSPD patients (5 eyes). A comprehensive overview of all patient characteristics is provided in [Table 1](#). Retinal images of foveal sparing in each of the conditions are depicted in [Figures 1-4](#).

**Table 1: Summary of patient characteristics**

	Stargardt Disease	Central areolar choroidal dystrophy	Mitochondrial retinal dystrophy	Pseudo-Stargardt
Patients in database (n)	176	103	21	36
Patients with foveal sparing (% / n)	11.4% / 20 Patients	6.8% / 7 Patients	28.6% / 6 Patients	8.3% / 3 Patients
Male:female ratio (n:n)	10:10	4:3	1:5	0:3
Median age at first presentation (y)	60.08 [54.72 - 62.12]	56.13 [52.74-59.36]	57.64 [53.4-64.21]	61.71 [61.65-64.40]
Median age at diagnosis (y)	57.31 [45.18 - 61.71]	55.98 [48.51-58.58]	58.21 [54.44-64.35]	61.72 [61.65-64.4]
Median time to diagnosis after symptoms onset (y)	1.60 [0.11 - 5.15]	0.76 [0.30-2.26] (data from 6 patients)	5.97[2.71-13.90]	14.91 [11.71-37.69]
Bilateral foveal sparing (%/n)	55% / 11 Patients	42.9% / 3 Patients	66.6% / 4 Patients	66.6% / 2 Patients
<i>Initial complaint (n):</i>				
Decreased VA	14	4	5	3
Diplopia	0	2	0	0
Metamorphopsia	4	3	0	0
Scotoma	0	1	0	0
None	1	0	0	0
Unknown	1	0	1	0

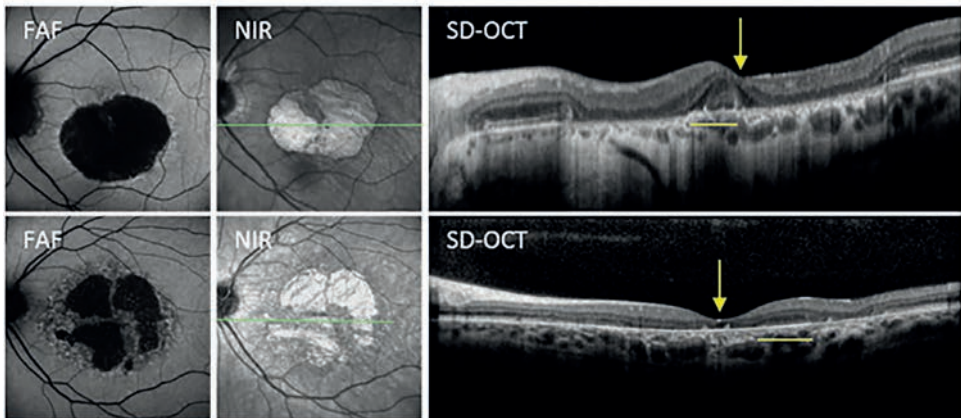
VA = visual acuity. Some patients mentioned two initial complaints. Y= years

**Figure 1:** Longitudinal retinal imaging of a representative eye with Stargardt disease (STGD1)



Serial fundus autofluorescence images (upper row), and spectral-domain optical coherence tomography (SD-OCT) scans centered on the fovea (lower row), of a representative right eye with foveal sparing in a patient with STGD1. Multiple atrophic lesions may be seen that coalesce over time. Cystoid lesions in the inner retina (asterisks) and elevation of the borders of outer retinal atrophy (arrowheads) may be seen. Location of the SD-OCT scan is indicated by the green line.

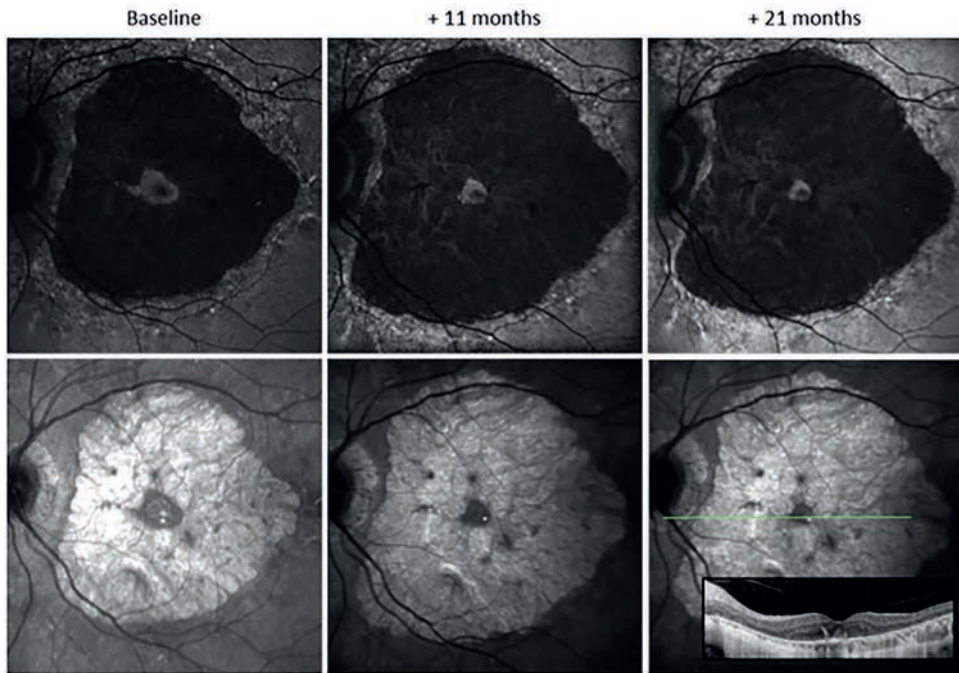
**Figure 2:** Retinal imaging of two representative central areolar choroidal dystrophy (CACD) cases



Fundus autofluorescence (FAF), near infrared reflectance and spectral domain optical coherence tomography (SD-OCT) scans of the left eyes of two patients with CACD. Foveal sparing may demarcate only poorly on FAF. Arrow: center of the foveal pit; Yellow bar: areas of intact retinal pigment epithelium in proximity to the foveal depression. Location of the SD-OCT scan is indicated by the green line.

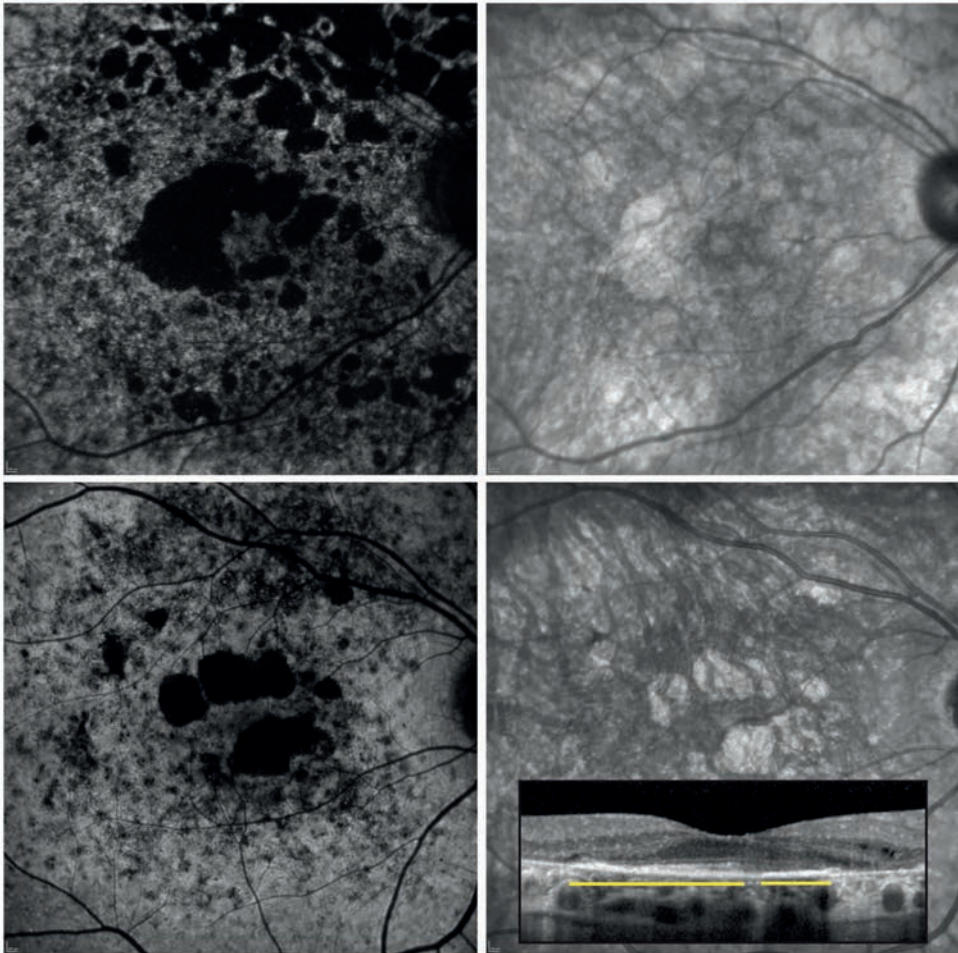


**Figure 3:** Longitudinal retinal imaging of a representative eye with mitochondrial retinal dystrophy (MRD)



*The left eye of a patient with MRD showing gradual contraction of the remaining foveal island in 21 months. Fundus autofluorescence (upper row) and near infrared reflectance (lower row) demonstrate retinal pigment epithelium atrophy encircling the fovea by 360°. The relatively spared fovea almost exactly centers on the foveal depression, as also shown by the spectral-domain optical coherence tomography scan (position is indicated by green line).*

**Figure 4:** Retinal imaging of two representative pseudo-Stargardt pattern dystrophy cases (PSPD)



*Fundus autofluorescence (left) and near-infrared reflectance image (right) of two right eyes of patients with PSPD. Multifocal areas of macular atrophy are usually observed in conjunction with more peripheral atrophic spots. Spectral-domain optical coherence tomography (inset, centered on the fovea) discloses outer retinal atrophy and disruption of retinal structure. The yellow bar indicates preservation of the retinal pigment epithelium.*

### Baseline

There was little variability in the age at first clinical presentation among the different RDs included. Median age at first presentation was 60 [54 – 63] years. Median values ranged from 56 years in CACD to 62 in PSPD ([Table 1](#)). Variability in the duration from experienced symptoms onset to the time where a dystrophy was diagnosed was more pronounced, with median values ranging from 0.8 [0.3 - 2.3] years in CACD to 15 [12 - 38] years in PSPD ([Table 1](#)).

At first presentation, median BCVA values were relatively high, ranging from 0.11 [0.09 – 0.26] LogMAR (20/25 [20/24 – 20/36] Snellen) in STGD1, to 0.28 [0.15 – 0.30] LogMAR (20/38 [20/28 – 20/39] Snellen) in MRD.

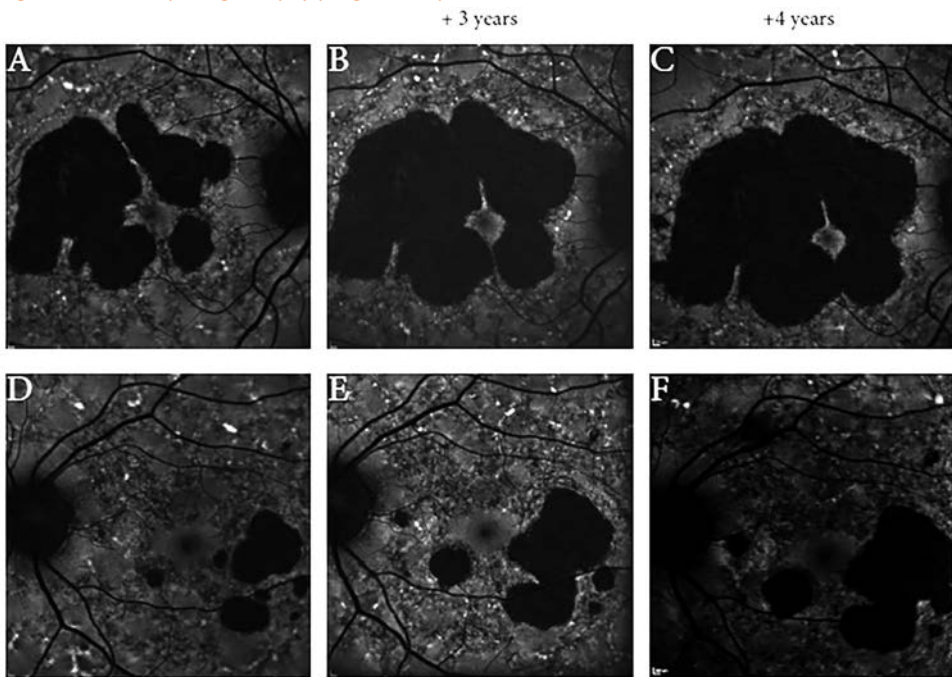
Qualitative assessment of the available FAF and SD-OCT images revealed characteristic features of foveal sparing morphology and atrophy progression. At baseline (first visit), foveal sparing was present in 52 eyes of 36 patients (bilateral in 15 patients). Thirty-two eyes (62%) presented with a multifocal atrophy pattern (e.g. [Figure 1](#)), 15 eyes (29%) presented with a horseshoe-type pattern (e.g. [Figure 1](#)), and we observed a solitary foveal island in 5 eyes (e.g. [Figure 3](#)). Sixteen eyes did not show sufficient atrophic changes to warrant the diagnosis and in six eyes there may have been foveal sparing, but at the time of investigation the foveal tissue was already lost. We compared both eyes in these 36 patients. We observed a high degree of symmetry between both eyes in individual patients: in MRD and PSPD, foveal sparing could be observed bilaterally in 66.6% of cases. Slightly lower values of 55% and 43% were found in STGD1 and CACD ([Table 1](#)).

### Follow-up

Over time, BCVA remained relatively stable when grouped according to underlying conditions. Decline of BCVA was most noticeable in STGD1 and PSPD, with a loss of 0.11 [0.01 – 0.13], and 0.13 [0.06 – 0.15] LogMAR, respectively.

Follow-up was available in 21 patients (58%). Of the 16 eyes without foveal sparing at baseline, five eyes developed foveal sparing over a median period of three years (range 1 - 4 years). We noticed this development only in STGD1 patients, and in none of the other conditions. Foveal sparing was lost during follow-up in five eyes over a median period of five years (range 3 – 8 years). In four of these eyes, a multifocal pattern was present at baseline, and foveal sparing was initially not present in one eye.

In all conditions, we noticed three distinct and consecutive patterns of atrophy, starting with multifocal atrophic lesions immediately adjacent to the fovea, to a horseshoe-type pattern into an isolated foveal island before the occurrence of central atrophy. [Figure 5](#) shows these four stages in the progression of foveal sparing in both eyes of a patient with STGD1.

**Figure 5: Foveal sparing atrophy progression pattern**

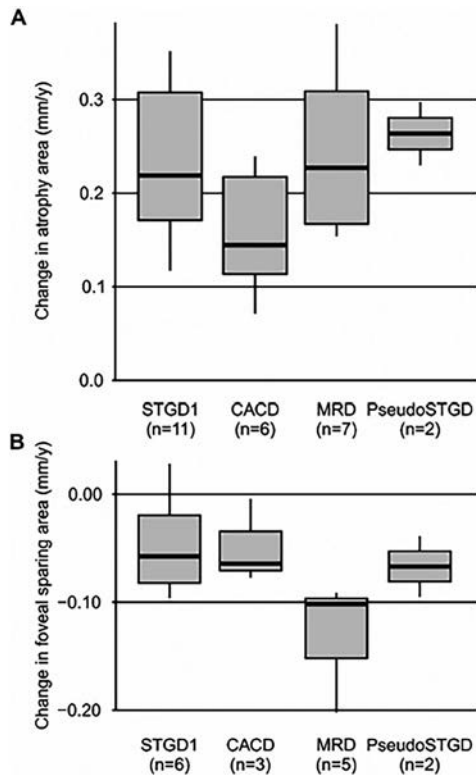
Fundus autofluorescence images of the right (A – C) and left (D – F) eye of a Stargardt patient with asymmetrical foveal sparing. Multifocal areas of retinal pigment epithelium (RPE) atrophy (A) develop and coalesce over time, forming a horseshoe-type atrophy pattern (B). In the last picture (C) the isthmus is severed leaving an isolated foveal island. The left eye reveals a similarly progressive atrophy pattern, albeit in an earlier stage.

5C has been published earlier in “Foveal sparing in Stargardt disease”, by Van Huet and Bax et al, IOVS, October 2014.

5E has been published earlier in “Clinical and genetic characteristics of late-onset Stargardt’s disease” by Westeneng- van Haften et al, Ophthalmology, June 2012.

Atrophy progression rates varied between 0.26 [0.25 – 0.28] mm/year in PSPD, to 0.14 [0.11 – 0.22] mm/year in CACD (Figure 6A). Loss of surface area of the spared fovea ranged from 0.06 [0.08 – 0.02] mm/year in STGD1 to 0.10 [0.15 – 0.10] mm/year in MRD (Figure 6B), and loss of SRT ranged from 13.84 [19.92 – 9.47]  $\mu\text{m}$ /year in MRD to 0.90 [5.13 – 1.50]  $\mu\text{m}$ /year in CACD.

A summary of all BCVA measurements and quantitative retinal image analyses can be found in [Table 2](#).

**Figure 6:** Change of atrophy area and foveal sparing area over time

Change of atrophy area (A) and foveal sparing area (B) over time as measured in registered fundus autofluorescence images in eyes with distinct retinal dystrophies and foveal sparing. STGD1: Stargardt disease, CACD: Central areolar choroidal dystrophy, MRD: Mitochondrial retinal dystrophy, PseudoSTGD: pseudo-Stargardt pattern dystrophy, mm/y = millimeter per year.

Please note progression rates were square root transformed to reduce the dependency of enlargement rates on baseline lesion size. The horizontal bar inside the boxes represents the median, the hinges correspond to the 25<sup>th</sup> and 27<sup>th</sup> percentiles. The upper and the lower whiskers extend to the largest (resp. smallest) value no further than  $1.5 * IQR$  from the hinges.

### Genetic analysis

An overview of all genetic variants is given in [Table 3](#). In only six of twenty STGD1 cases (30%) two *ABCA4* variants were detected. The most prevalent variant is c.5461-10T>C (5/26 = 19%). At least one severe *ABCA4* variant was detected in 19 cases (95%). In all CACD cases the same *PRPH2* missense variant (p.Arg142Trp) was identified. Likewise, in all MRD cases the same variant (m.3243A>G) was detected in the mitochondrial DNA.

Table 2: Summary of clinical and retinal imaging parameters

	Stargardt Disease		Central areolar choroidal dystrophy		Mitochondrial retinal dystrophy		Pseudo-Stargardt	
	n	Median [IQR]	n	Median [IQR]	n	Median [IQR]	n	Median [IQR]
Number of eyes with foveal sparing (total)	31		10		10		5	
Eyes with longitudinal data	19		10		7		2	
Follow-up time (y)	19	3.59 [1.87 - 4.48]	6	6.37[2.94 -7.15]	7	1.95 [1.55 - 5.51]	2	4.12[4.12-4.12]
<i>BCVA:</i>								
First visit (logMAR)		0.11 [0.09 - 0.26]		0.22 [0.13 - 0.28]		0.28 [0.15 - 0.30]		0.15 [0.11 - 0.14]
Loss to last follow-up (logMAR)	19	0.00 [-0.05 - 0.04]	6	0.01 [-0.05 - 0.03]	7	0.00 [-0.07 - 0.17]	2	0.15 [0.03 - 0.28]
Observation interval (y)		3.24 [1.87 - 4.61]		2.18 [1.29 - 4.14]		1.95 [1.55 - 5.03]		4.12 [4.12 - 4.12]
<i>Atrophy size:</i>								
First visit (mm <sup>2</sup> )		3.61 [1.64 - 7.96]		6.08 [3.29 - 8.42]		27.02 [22.24 - 29.27]		3.40 [3.06 - 3.75]
Change over time (√mm <sup>2</sup> /y)	11	0.22 [0.17 - 0.31]	6	0.14 [0.11 - 0.22]	5	0.23 [0.17 - 0.31]	2	0.26 [0.25 - 0.28]
Observation interval (y)		3.24 [2.41 - 3.96]		5.69 [2.64 - 6.40]		1.55 [1.55 - 5.96]		4.12 [4.12 - 4.12]
<i>Foveal Sparing size:</i>								
First visit (mm <sup>2</sup> )		0.42 [0.22 - 1.33]		1.16 [1.01 - 1.56]		2.19 [1.63-2.80]		1.27 [1.22 - 1.33]
Change over time (√mm <sup>2</sup> /y)	6	-0.06 [-0.08 - -0.02]	3	-0.06 [-0.07 - -0.03]	3	-0.10 [-0.15 - -0.10]	2	-0.07 [-0.08 - -0.05]
Observation interval (y)		1.87 [1.41 - 2.305]		3.65 [3.65 - 5.04]		3.967 [2.54 - 6.00]		3.06 [2.53 - 3.59]
<i>Subfoveal retinal thickness:</i>								
First visit (mm)		203 [187 - 223]		161 [138.2 - 182.5]		192 [189 - 210]		175 [160 - 190]
Change over time (mm/y)	15	-4.95 [-11.75 - -0.40]	4	-0.90 [-5.13 - 1.50]	5	-13.84 [-19.92 - -9.47]	2	-4.79 [-5.57 - -4.01]
Observation interval (y)		2.88 [2.31 - 3.61]		4.16 [2.90 - 4.77]		1.55 [1.55 - 2.07]		4.12 [4.115 - 4.12]

BCVA = best corrected visual acuity, FS = foveal sparing, logMAR = logarithm of the minimum angle of resolution, IQR = Inter-quartile range, y = years, mm = millimeter

21	PRPH2	c.658del	p.(Arg220Glyfs*36)	severe	ABCA4	**c.2588G>C	p.[Gly863Ala, Gly863del]	mild
22	PRPH2	c.441delT	p.(Gly148fs*5)	severe				
23	PRPH2	c.441delT	p.(Gly148fs*5)	severe				
24	m.	m.3243A>G		85				
25	m.	m.3243A>G	unknown					
26	m.	m.3243A>G	unknown					
27	m.	m.3243A>G		15				
28	m.	m.3243A>G		11				
29	m.	m.3243A>G		7	ABCA4	c.4771G>A	p.(Gly1591Arg)	unknown
30	PRPH2	c.424C>T	p.(Arg142Trp)	mild				
31	PRPH2	c.424C>T	p.(Arg142Trp)	mild				
32	PRPH2	c.424C>T	p.(Arg142Trp)	mild				
33	PRPH2	c.424C>T	p.(Arg142Trp)	mild				
34	PRPH2	c.424C>T	p.(Arg142Trp)	mild				
35	PRPH2	c.424C>T	p.(Arg142Trp)	mild				
36	PRPH2	c.424C>T	p.(Arg142Trp)	mild				

*\*c.5461-10T>C is found in cis with c.5603A>T, but the latter common coding variant does not contribute to the pathogenicity of this allele and thus omitted*  
*\*\*c.2588G>C is not analyzed for presence of c.5603A>T*

Table 3: An overview of all genetic variants in this study cohort

Patient	Gene	Variant 1	Protein / Heteroplasmy (ID24-29)	Effect	Gene	Variant 2	Protein	Effect
1	ABCA4	c.5196+1G>T	p.(?)	severe		+		
2	ABCA4	c.3734G>A	p.(Ser1245Asn)	mild		+		
3	ABCA4	*c.5461-10T>C	p.[Thr1821Valfs*13,Thr1821Aspfs*6]	severe		+		
4	ABCA4	c.4506C>A	p.(Cys1502*)	severe		+		
5	ABCA4	c.3874C>T	p.(Gln1292*)	severe	ABCA4	c.3113C>T	p.(Ala1038Val)	mild
6	ABCA4	c.5461-10T>C	p.[Thr1821Valfs*13,Thr1821Aspfs*6]	severe		+		
7	ABCA4	c.5461-10T>C	p.[Thr1821Valfs*13,Thr1821Aspfs*6]	severe		+		
8	ABCA4	c.3874C>T	p.(Gln1292*)	severe	ABCA4	c.5603A>T	p.(Asn1868Ile)	mild
9	ABCA4	c.3874C>T	p.(Gln1292*)	severe		+		
10	ABCA4	c.5461-10T>C	p.[Thr1821Valfs*13,Thr1821Aspfs*6]	severe		+		
11	ABCA4	c.5461-10T>C	p.[Thr1821Valfs*13,Thr1821Aspfs*6]	severe		+		
12	ABCA4	c.4363T>C	p.(Cys1455AArg)	severe	ABCA4	c.5603A>T	p.(Asn1868Ile)	mild
13	ABCA4	c.1822T>C	p.(Phe608Leu)	severe		+		
14	ABCA4	c.768G>T	p.(Leu257Valfs*17)	severe		+		
15	ABCA4	c.5813T>G	p.(Leu1938*)	severe	ABCA4	**c.2588G>C	p.[Gly863Ala,Gly863del]	mild
16	ABCA4	c.768G>T	p.(Leu257Valfs*17)	severe		+		
17	ABCA4	c.4773+1G>A	p.(?)	severe		+		
18	ABCA4	c.1822T>A	p.(Phe608Ile)	severe		+		
19	ABCA4	c.768G>T	p.(Leu257Valfs*17)	severe	ABCA4	c.3113C>T	p.(Ala1038Val)	mild
20	ABCA4	c.768G>T	p.(Leu257Valfs*17)	severe	ABCA4	c.5603A>T	p.(Asn1868Ile)	mild



## Discussion

Foveal sparing is a regularly encountered phenomenon in a variety of retinal disorders, including RDs like STGD1 and geographic atrophy in age-related macular degeneration. This study analyses the characteristics of foveal sparing in a wide range of retinal dystrophies, including STGD1, CACD, MRD, and PSPD. All the patients were in their 5<sup>th</sup> decade or older at first presentation, indicating that foveal sparing mainly manifests in RD patients with a relatively low rate of progression, where visual loss occurs later in life. The manifestation of foveal sparing in this heterogenic group of disorders is remarkably similar, in particular with regard to the kinetics of atrophy progression towards the fovea, which varies only slightly between disorder types. In general, RPE atrophy in foveal sparing progresses in a relatively fixed pattern, starting with small, multifocal areas of atrophy that surround the fovea. These, then gradually expand in all directions and coalesce, forming a horseshoe-type atrophy. The bridge of retinal tissue connecting the fovea to the non-atrophic part of the macula gradually narrows until this isthmus disappears, leaving a solitary foveal island. In the final stage this island is lost to atrophy. This sequence of steps is a common finding in these patients and can be of great prognostic help, although the rate of progression may differ. This pattern of RPE atrophy was symmetrical in 80% of the bilateral cases. This indicates, as already suggested by others,<sup>28</sup> that the fellow eye cannot automatically serve as control in therapeutic intervention trials for RDs in patients with foveal sparing.

Although the frequency of foveal sparing in our cohort was highest in the MRD group (29%), this was much lower than the previously reported number of 84% in a 2013 study by de Laat et al.[16] This may be an underestimation on our side due to inclusion bias since this study was not primarily designed to estimate the prevalence of foveal sparing in RDs, including MRD.

To date, the underlying mechanism of foveal sparing is incompletely understood. Disease independent factors are likely at play in view of the high heterogeneity of the underlying disorders. This notion is supported by the virtually identical kinetics of atrophy progression towards the fovea observed among most conditions (0.06 – 0.10 mm/year). The presence of multifocal areas of chorioretinal atrophy surrounding the fovea, and very similar square-root transformed atrophy progression rates of 0.116 mm/year were observed in age-related macular degeneration.[9] [28] The similarities between the phenomenon of foveal sparing in monogenic and multi-factorial disorders further supports the hypothesis of disease-independent mechanisms that shape the foveal sparing phenotype.

The general susceptibility to retinal degeneration may lie in metabolic differences between regions of the macula. Those differences may be associated with physical characteristics of foveal and peripheral cones; foveal cone outer segments physically resemble those of rods rather than peripheral cones. Furthermore, Müller cells are short and exist in a 1:1 ratio with foveolar cones, but are longer and have a lower ratio extrafoveally. [29]

A number of underlying mechanisms have been proposed involving the rod-derived cone viability factor (RdCVF), variations in macular pigment and peak distribution as well as cone density, increased vulnerability of certain parafoveal photoreceptors, and factors related to RPE and choroid. The RdCVF is secreted from rod photoreceptors and protects cones from degeneration.[30] An increased sensitivity of foveal cones to RdCVF, possibly complemented by higher secretion levels of RdCVF, may result in improved central cone survival.

A second hypothesis involves the macular pigments: lutein, zeaxanthin and meso-zeaxanthin. These carotenoids protect against macular damage through their antioxidant properties and by filtering potential harmful blue light. In eyes with foveal sparing, an uneven distribution of macular pigment might lead to protection of the most central photoreceptors, leaving the parafoveal photoreceptors relatively unprotected.[31, 32] Another explanation may lie in the highly variable peak cone density ranging from 98,200 to 324,100 cones/mm<sup>2</sup>. This remarkable inter-individual variability is much less pronounced in the area surrounding the fovea and may contribute to the phenomenon of foveal sparing. [33] *In vivo* determination of cone density with adaptive optics could solve the role of peak cone density in foveal sparing. Another factor that may be of influence is the increased vulnerability to age and degenerative disease of respectively rod photoreceptors and short wavelength (blue) S-cone photoreceptors.[34] [35] Both rods and S-cones are absent in the foveal center and the increased susceptibility to aging and/or disease may explain the relative preservation of the fovea in certain patient. An explanation may also lie in the unfavorably high ratio of rods per RPE cell in the parafoveal retina that could lead to an earlier decompensation of metabolic function promoting perifoveal atrophy.[16, 36] Finally, the unique choroidal blood supply to the fovea has been put forward as a factor leading to a local protective effect.[37, 38]

A common finding in these foveal sparing patients is late age at which the diagnosis is made. The well-preserved visual acuity leads to patient's delay and at the time of the first ophthalmologic consultation large areas of atrophy are already present. We know from this and other studies that the atrophy progression rate is relatively

slow,[39-41] disease-specific changes have therefore been present for years. In the 37 patients with foveal sparing in this study, only one patient experienced a scotoma as initial symptom. The large majority (N=26; 72%) patients present with loss of visual acuity. This late recognition of patients with foveal sparing RDs narrows the window of opportunity for therapeutic intervention, which is becoming increasingly important as novel therapeutic approaches emerge (NCT01367444, NCT01736592, NCT01469832, and NCT02402660 on [www.clinicaltrials.gov](http://www.clinicaltrials.gov)).

In the group of STGD1 patients, the high frequency of self-reported “decreased visual acuity” as initial symptom goes together with a high baseline visual acuity (0.11 [0.09 – 0.26]) LogMAR (approximately 20/25 Snellen). This is likely due to the fact that parafoveal scotomas affect high resolution visual tasks like face recognition and reading, whereas BCVA tests rely on the maximum resolution of the fovea.[7, 19, 20, 42] It is important to be aware that visual acuity tests are an imperfect measurement for macular function – in particular in patients with foveal sparing.

Preservation of the foveal tissue in the late stage of a RD is beneficial to the patient. The ProgSTAR study recently showed a stable BCVA in the STGD1 cohort with foveal sparing over the course of 3.24 years. In contrast, in the STGD1 cohort without foveal sparing and equivalent baseline visual acuity, an average loss of one line per year could be observed.[43]

Recently, it was shown that discrimination between foveal sparing and non-foveal sparing STGD1 phenotypes can be made as early as the time the first atrophic lesions become apparent, based on parameters like a late age-at-onset and thinning of the outer nuclear layer and ellipsoid zone.[8, 40] Yet, biomarkers that could predict foveal sparing at an even earlier stage are not available.

With regard to genetic predisposing factors, it has been suggested that the presence of relative mild genetic variants correlate with a less severe phenotype and a generally later age of onset.[11, 44] In 14 of the 20 (70%) STGD1 patients with foveal sparing, only one *ABCA4* variant could be detected. The percentage of unidentified second mutations is much lower (30%) in patients with a typical Stargardt phenotype with an age-at-onset in the second to third decade, a second mutation has not been identified. (In personal communication with Frans P.M. Cremers).

Deep-intronic variants were found in several mono-allelic cases.[45-48] Very recently, the hypomorphic intronic variant c.4253+43G>A was found to be associated with late-onset STGD1.[49] Zernant and colleagues determined that c.5603A>T (p.Asn1868Ile), previously suspected to be benign because of its high prevalence in the general population (minor allele frequency of 0.07), is disease-causing[50]. This variant was typically found in a compound heterozygous manner with a severe *ABCA4* variant in ~50% of mono-allelic cases and in ~80% of late-onset STGD1 cases.[50] Runhart et al. in addition found significant differences in age-at-onset between affected siblings and even non-penetrance in three families with asymptomatic bi-allelic siblings of affected persons.[51] The penetrance of this variant, when present together with a severe *ABCA4* variant in the other gene copy, was estimated to be less than 5%, suggesting a crucial role for genetic or environmental modifiers in STGD1. In the present study, the c.5603A>T variant was found in 3/20 (17%) of STGD1 cases with foveal sparing. In two other STGD1 cases where both alleles were identified, mild variants (p.(Ala1038Val) and p.[Gly863Ala, Gly863del]) were also found, corroborating the hypothesis that late-onset STGD1 can partially be explained by the combination of a severe with a mild *ABCA4* variant.

Therapeutic approaches for RDs are currently emerging. Recently, the Food and Drug Administration (FDA) approved gene therapy for *RPE65*-associated retinal dystrophy, a form of Leber congenital amaurosis. In addition, therapy trials for STGD1, choroideremia, Usher syndrome type 2A and several more are underway (NCT01367444, NCT01736592, NCT01469832, and NCT02402660 on [www.clinicaltrials.gov](http://www.clinicaltrials.gov)). To accurately assess efficacy of new therapeutic modalities in clinical trials, careful patient selection and well-thought out outcome measures are essential.[52] Eyes with foveal sparing could be candidates for inclusion into clinical trials, due to the clearly demarcated, well-measurable areas of progressive RPE atrophy and preserved BCVA, allowing for visual stabilization as one of the outcome measurement. In addition, in about half of the patients with foveal sparing, this phenomenon occurs in both eyes, which opens the opportunity of inter-eye comparison. Finally, these patients may benefit greatly from successful therapeutic intervention, as prolonged preservation of the fovea is paramount to daily functioning, and by extension to quality of life. The use of eyes with foveal sparing for clinical trials inevitably also comes with certain pitfalls. A long follow-up period would be necessary to accurately assess treatment effect if BCVA is used as parameter. And in our cohort, only 43% of the cases has a symmetrical disease progression. In such cases, an alternative outcome measure like atrophy progression, or change in the size of the spared fovea over time, is preferable.[41]

In summary, the phenomenon of foveal sparing was observed in several distinct retinal dystrophies. All patients presented with late-onset disease, and the pattern of perifoveal RPE atrophy progression was identical in all conditions. Remarkable similarities between foveal sparing pattern in RDs and age-related macular degeneration may suggest disease-independent mechanisms to shape the pattern of foveal sparing. Importantly, the observations made in this study will allow ophthalmologists to provide affected patients with a more accurate prognosis, and the characteristic aspects in terms of visual function loss and atrophy progression should be considered when including foveal-sparing and non-foveal sparing eyes in clinical trials.

Further research – including histopathology studies and detailed retinal imaging with adaptive optics – is necessary to elucidate the mechanisms involved in foveal sparing. The new insights gleaned from these studies might pave the way for new disease-independent (gene-)therapeutic approaches for prolonged preservation of foveal tissue in degenerative retinal disease.

## References

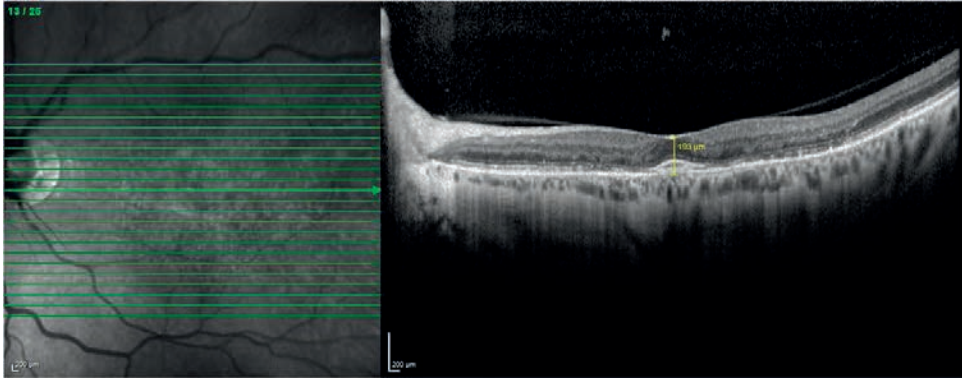
1. Congdon, N., et al., *Causes and prevalence of visual impairment among adults in the United States*. Arch Ophthalmol, 2004. **122**(4): p. 477-85.
2. Resnikoff, S., et al., *Global data on visual impairment in the year 2002*. Bull World Health Organ, 2004. **82**(11): p. 844-51.
3. Shintani, K., D.L. Shechtman, and A.S. Gurwood, *Review and update: current treatment trends for patients with retinitis pigmentosa*. Optometry, 2009. **80**(7): p. 384-401.
4. Agarwal, A., *Gass'atlas of macular disease*. 4th ed.
5. Sunness, J.S., *The natural history of geographic atrophy, the advanced atrophic form of age-related macular degeneration*. Mol Vis, 1999. **5**: p. 25.
6. Sunness, J.S., et al., *Enlargement of atrophy and visual acuity loss in the geographic atrophy form of age-related macular degeneration*. Ophthalmology, 1999. **106**(9): p. 1768-79.
7. Sarks, J.P., S.H. Sarks, and M.C. Killingsworth, *Evolution of geographic atrophy of the retinal pigment epithelium*. Eye (Lond), 1988. **2** ( Pt 5): p. 552-77.
8. van Huet, R.A., et al., *Foveal sparing in Stargardt disease*. Invest Ophthalmol Vis Sci, 2014. **55**(11): p. 7467-78.
9. Lindner, M., et al., *Directional Kinetics of Geographic Atrophy Progression in Age-Related Macular Degeneration with Foveal Sparing*. Ophthalmology, 2015. **122**(7): p. 1356-65.
10. Fujinami, K., et al., *A longitudinal study of Stargardt disease: quantitative assessment of fundus autofluorescence, progression, and genotype correlations*. Invest Ophthalmol Vis Sci, 2013. **54**(13): p. 8181-90.
11. Westeneng-van Haften, S.C., et al., *Clinical and genetic characteristics of late-onset Stargardt's disease*. Ophthalmology, 2012. **119**(6): p. 1199-210.
12. Rotenstreich, Y., G.A. Fishman, and R.J. Anderson, *Visual acuity loss and clinical observations in a large series of patients with Stargardt disease*. Ophthalmology, 2003. **110**(6): p. 1151-8.
13. Nakao, T., et al., *Foveal sparing in patients with Japanese Stargardt's disease and good visual acuity*. Jpn J Ophthalmol, 2012. **56**(6): p. 584-8.
14. Boon, C.J., et al., *Central areolar choroidal dystrophy*. Ophthalmology, 2009. **116**(4): p. 771-82, 782 e1.
15. Rath, P.P., et al., *Characterisation of the macular dystrophy in patients with the A3243G mitochondrial DNA point mutation with fundus autofluorescence*. Br J Ophthalmol, 2008. **92**(5): p. 623-9.
16. de Laat, P., et al., *Mitochondrial retinal dystrophy associated with the m.3243A>G mutation*. Ophthalmology, 2013. **120**(12): p. 2684-96.
17. Querques, G., et al., *Adaptive Optics Imaging of Foveal Sparing in Geographic Atrophy Secondary to Age-Related Macular Degeneration*. Retina, 2015.
18. Steinberg, J.S., et al., *Foveal Sparing of Reticular Drusen in Eyes With Early and Intermediate Age-Related Macular Degeneration*. Invest Ophthalmol Vis Sci, 2015. **56**(8): p. 4267-74.
19. Sunness, J.S., et al., *Visual function abnormalities and prognosis in eyes with age-related geographic atrophy of the macula and good visual acuity*. Ophthalmology, 1997. **104**(10): p. 1677-91.
20. Sunness, J.S., et al., *Foveal-Sparing Scotomas in Advanced Dry Age-Related Macular Degeneration*. J Vis Impair Blind, 2008. **102**(10): p. 600-610.
21. Stoll, M.R., *Pericentral ring scotoma*. Arch Ophthal, 1950. **43**(1): p. 66-91.
22. Hart, W.M., Jr. and R.M. Burde, *Three-dimensional topography of the central visual field. Sparing of foveal sensitivity in macular disease*. Ophthalmology, 1983. **90**(8): p. 1028-38.

23. Kuehlewein, L., et al., *Comparison of Manual and Semiautomated Fundus Autofluorescence Analysis of Macular Atrophy in Stargardt Disease Phenotype*. *Retina*, 2016. **36**(6): p. 1216-21.
24. Schmitz-Valckenberg, S., et al., *Semiautomated image processing method for identification and quantification of geographic atrophy in age-related macular degeneration*. *Invest Ophthalmol Vis Sci*, 2011. **52**(10): p. 7640-6.
25. Staurengi, G., et al., *Proposed lexicon for anatomic landmarks in normal posterior segment spectral-domain optical coherence tomography: the IN\*OCT consensus*. *Ophthalmology*, 2014. **121**(8): p. 1572-8.
26. Boon, C.J., et al., *Mutations in the peripherin/RDS gene are an important cause of multifocal pattern dystrophy simulating STGD1/fundus flavimaculatus*. *Br J Ophthalmol*, 2007. **91**(11): p. 1504-11.
27. Feuer, W.J., et al., *Square root transformation of geographic atrophy area measurements to eliminate dependence of growth rates on baseline lesion measurements: a reanalysis of age-related eye disease study report no. 26*. *JAMA Ophthalmol*, 2013. **131**(1): p. 110-1.
28. Mones, J., M. Biarnes, and F. Trindade, *Hyporeflective wedge-shaped band in geographic atrophy secondary to age-related macular degeneration: an underreported finding*. *Ophthalmology*, 2012. **119**(7): p. 1412-9.
29. Bird, A.C. and D. Bok, *Why the macula?* *Eye (Lond)*, 2018. **32**(5): p. 858-862.
30. Leveillard, T., et al., *Identification and characterization of rod-derived cone viability factor*. *Nat Genet*, 2004. **36**(7): p. 755-9.
31. Weiter, J.J., F. Delori, and C.K. Dorey, *Central sparing in annular macular degeneration*. *Am J Ophthalmol*, 1988. **106**(3): p. 286-92.
32. Aleman, T.S., et al., *Macular pigment and lutein supplementation in ABCA4-associated retinal degenerations*. *Invest Ophthalmol Vis Sci*, 2007. **48**(3): p. 1319-29.
33. Curcio, C.A., et al., *Human photoreceptor topography*. *J Comp Neurol*, 1990. **292**(4): p. 497-523.
34. Greenstein, V.C., et al., *S (blue) cone pathway vulnerability in retinitis pigmentosa, diabetes and glaucoma*. *Invest Ophthalmol Vis Sci*, 1989. **30**(8): p. 1732-7.
35. Curcio, C.A., et al., *Aging of the human photoreceptor mosaic: evidence for selective vulnerability of rods in central retina*. *Invest Ophthalmol Vis Sci*, 1993. **34**(12): p. 3278-96.
36. Snodderly, D.M., et al., *Retinal pigment epithelial cell distribution in central retina of rhesus monkeys*. *Invest Ophthalmol Vis Sci*, 2002. **43**(9): p. 2815-8.
37. Hayreh, S.S., *Physiological anatomy of the choroidal vascular bed*. *Int Ophthalmol*, 1983. **6**(2): p. 85-93.
38. Mauschitz, M.M., et al., *Topography of geographic atrophy in age-related macular degeneration*. *Invest Ophthalmol Vis Sci*, 2012. **53**(8): p. 4932-9.
39. Dreyhaupt, J., et al., *Modelling the natural history of geographic atrophy in patients with age-related macular degeneration*. *Ophthalmic Epidemiol*, 2005. **12**(6): p. 353-62.
40. Lambertus, S., et al., *Asymmetric Inter-Eye Progression in Stargardt Disease*. *Invest Ophthalmol Vis Sci*, 2016. **57**(15): p. 6824-6830.
41. Lindner, M., et al., *Differential Disease Progression in Atrophic Age-Related Macular Degeneration and Late-Onset Stargardt Disease*. *Invest Ophthalmol Vis Sci*, 2017. **58**(2): p. 1001-1007.
42. Lindner, M., et al., *Determinants of Reading Performance in Eyes with Foveal-Sparing Geographic Atrophy*. *Ophthalmol Retina*, 2019. **3**(3): p. 201-210.
43. Kong, X., et al., *Visual Acuity Loss and Associated Risk Factors in the Retrospective Progression of Stargardt Disease Study (ProgStar Report No. 2)*. *Ophthalmology*, 2016. **123**(9): p. 1887-97.

44. Maugeri, A., et al., *The 2588G-->C mutation in the ABCR gene is a mild frequent founder mutation in the Western European population and allows the classification of ABCR mutations in patients with Stargardt disease.* Am J Hum Genet, 1999. **64**(4): p. 1024-35.
45. Braun, T.A., et al., *Non-exonic and synonymous variants in ABCA4 are an important cause of Stargardt disease.* Hum Mol Genet, 2013. **22**(25): p. 5136-45.
46. Zernant, J., et al., *Analysis of the ABCA4 genomic locus in Stargardt disease.* Hum Mol Genet, 2014. **23**(25): p. 6797-806.
47. Bauwens, M., et al., *An augmented ABCA4 screen targeting noncoding regions reveals a deep intronic founder variant in Belgian Stargardt patients.* Hum Mutat, 2015. **36**(1): p. 39-42.
48. Bax, N.M., et al., *Heterozygous deep-intronic variants and deletions in ABCA4 in persons with retinal dystrophies and one exonic ABCA4 variant.* Hum Mutat, 2015. **36**(1): p. 43-7.
49. Zernant, J., et al., *Extremely hypomorphic and severe deep intronic variants in the ABCA4 locus result in varying Stargardt disease phenotypes.* Cold Spring Harb Mol Case Stud, 2018.
50. Zernant, J., et al., *Frequent hypomorphic alleles account for a significant fraction of ABCA4 disease and distinguish it from age-related macular degeneration.* J Med Genet, 2017. **54**(6): p. 404-412.
51. Runhart, E.H., et al., *The Common ABCA4 Variant p.Asn1868Ile Shows Nonpenetrance and Variable Expression of Stargardt Disease When Present in trans With Severe Variants.* Invest Ophthalmol Vis Sci, 2018. **59**(8): p. 3220-3231.
52. Holz, F.G., et al., *Imaging Protocols in Clinical Studies in Advanced Age-Related Macular Degeneration: Recommendations from Classification of Atrophy Consensus Meetings.* Ophthalmology, 2017. **124**(4): p. 464-478.



## Supplemental material



**Supplemental Figure 1:** Subfoveal retinal thickness (SRT) was assessed in SD-OCT scans. The fovea was identified by scrolling through the volumetric SD-OCT dataset. SRT was then measured as the distance between the internal limiting membrane (ILM) and the outer border of OCT band 4 (corresponding to the RPE/Bruch's membrane complex) using a Caliper tool (yellow) included into the software. This figure is from a patient with Central areolar choroidal dystrophy (left eye).





## CHAPTER 2.5

### Asymmetric inter-eye progression in Stargardt disease

*“Asymmetric inter-eye progression in Stargardt disease is most likely observed in patients with a later onset and patients carrying lower pathogenic ABCA4 combinations. This needs to be considered in novel therapeutic trials with a fellow-eye paired controlled design to optimize the power of a study.”*

Stanley Lambertus  
Nathalie M. Bax  
Joannes M.M. Groenewoud  
Frans P.M. Cremers  
Gert Jan van der Wilt  
B. Jeroen Klevering  
Thomas Theelen  
Carel B. Hoyng

Invest Ophthalmol Vis Sci. 2016 Dec 1;57(15):6824-6830.

The authors thank the Diagnostic Image Analysis Group, Department of Radiology and Nuclear Medicine, Radboud university medical center (Nijmegen, The Netherlands) for providing the image analysis algorithm.

**PURPOSE:** Asymmetry in disease progression between left and right eyes can occur in Stargardt disease (STGD1) and this needs to be considered in novel therapeutic trials with a fellow-eye paired controlled design. This study investigated the inter-eye discordance of best-corrected visual acuity (BCVA) and progression of retinal pigment epithelium (RPE) atrophy in STGD1.

**METHODS:** We performed a retrospective cohort study collecting 68 STGD1 patients (136 eyes) with  $\geq 1$  *ABCA4* variants and  $\geq 0.5$  year follow-up on BCVA and fundus autofluorescence. We compared inter-eye correlations of RPE atrophy progression between early-onset ( $\leq 10$  years), intermediate-onset (11 – 44), and late-onset ( $\geq 45$ ) STGD1 and *ABCA4* variant combinations by  $\chi^2$ -tests. We identified associations of discordant baseline BCVA and RPE atrophy with discordant RPE atrophy progression by odds ratios (OR). We defined discordance by differences  $> 1.5$  interquartile ranges  $\pm$  first/third interquartiles.

**RESULTS:** Progression of RPE atrophy correlated moderately between eyes ( $\rho = 0.766$ ), which decreased with later onset ( $P = 9.8 \times 10^{-7}$ ) and lower pathogenicity of *ABCA4* combinations ( $P = 0.007$ ). Twelve patients (17.6%) had discordant inter-eye RPE atrophy progression, associated with baseline discordance of RPE atrophy (OR, 6.50 [1.35 – 31.34]), but not BCVA (OR, 0.33 [0.04 – 2.85]).

**CONCLUSIONS:** Lower inter-eye correlations are more likely found in late-onset STGD1 and patients carrying low pathogenic *ABCA4* combinations. To achieve the highest power in a therapeutic trial, early-phase studies should minimize inter-eye discordance by selecting early-onset STGD1 patients carrying severe *ABCA4* variants without evidence of asymmetry at baseline.

## Introduction

Stargardt disease (STGD1) is one of the most common retinal dystrophies. Loss of macular function causes bilateral loss of visual acuity—usually at childhood.<sup>1,2</sup> The first manifestations of the disease may also occur in older patients, up to the seventh decade.<sup>3,4</sup> In general, the severity of the disease is associated with the age of onset: young patients tend to do worse.<sup>5</sup> The variation in age of onset and rate of progression is, for the most part, the result of combinations of over 900 variants in the *ABCA4* gene.<sup>6</sup>

*ABCA4* encodes the adenosine triphosphate (ATP)-binding cassette, subfamily A, member 4 transporter protein, which actively removes all-*trans*-retinal with its conjugate *N*-retinylidene-phosphatidylethanolamine from the photoreceptor outer segment disks.<sup>7</sup> Impaired removal results in condensation reactions, which lead to toxic levels of bisretinoids in the outer segment disks. Through phagocytosis of these outer segments, bisretinoids accumulate as lipofuscin deposits in the retinal pigment epithelium (RPE). These lipofuscin deposits are observed as yellowish-white flecks in the posterior pole.<sup>8</sup> The accumulation of toxic lipofuscin eventually leads to atrophy of the retinal pigment epithelium (RPE) and photoreceptors with subsequent loss of the neurosensory retina and choriocapillaris.<sup>9</sup>

Over time, RPE atrophy progresses, as uni- or multifocal areas enlarge and coalesce. However, there is considerable variability in these patterns of atrophy; they range from large central atrophic areas in early-onset STGD1 patients that can be seen at adolescence<sup>2</sup> to relatively small atrophic lesions encircling the fovea in older patients with late-onset STGD1.<sup>3</sup> The difference in atrophic lesion not only varies between patients<sup>10</sup>, but also the patterns of RPE loss may differ significantly between eyes of one patient. Even though the extent of abnormalities is often similar between left and right eyes,<sup>11,12</sup> some cases with remarkable differences have been described.<sup>13</sup>

Profound inter-eye differences in disease progression have impact on the statistical power in clinical trials; treated and untreated eyes must demonstrate a larger difference than do the inter-eye differences by their natural course. Otherwise, the required sample size will be unreasonably large. However, in early-phase clinical trials for novel treatments of STGD1<sup>14-16</sup> and other retinal dystrophies, small therapeutic effects have to be evaluated generally within two years with no more than a few dozen patients. Thus, better knowledge of inter-eye correlations is needed for fellow-eye paired controlled trials in which the untreated eyes of participants serve as a control.

In view of these upcoming interventional trials, we have studied the extent of asymmetric inter-eye progression of RPE atrophy in patients with STGD1. Fundus autofluorescence (FAF) imaging is a valuable tool to evaluate progression of RPE atrophy over time.<sup>17-20</sup> We therefore analyzed inter-eye discordance of RPE atrophy progression using FAF imaging along with visual acuity. We hypothesized that a later disease onset and less pathogenic combinations of *ABCA4* variants contribute to asymmetric inter-eye progression, and that the asymmetry will increase when asymmetry at baseline is already present.

## Methods

### Patient selection

We selected patients from the STGD1 database, containing 454 cases, of the Department of Ophthalmology at Radboud university medical center (Nijmegen, The Netherlands). We included patients in whom the clinical diagnosis of STGD1 was supported by the presence of  $\geq 1$  (likely) pathogenic *ABCA4* variants with a follow-up data of  $\geq 6$  months on FAF imaging. Ninety-three STGD1 patients met these inclusion criteria.

Ten cases were excluded because no RPE atrophy had developed during the entire follow-up time. Nine cases displayed RPE atrophy to such a degree that the lesions extended beyond the limits of the FAF image. One case was excluded because choroidal neovascularization occurred in one eye. Five cases were excluded because they participated in an interventional trial.<sup>21</sup> The remaining 68 cases were included in this study. The patient inclusion process is shown in [Supplemental Figure 1](#). This retrospective cohort study was approved by the Institutional Ethics Committee and was performed in accordance with the Declaration of Helsinki.

### Measurements

We documented sex, age at onset, age at baseline, and follow-up time. Age at onset was defined as either the age at which visual complaints were first noted, or, if unavailable, the age when the diagnosis was made. Disease onset groups were based on previously reported cut-off points: early-onset STGD1,  $\leq 10$  years<sup>2</sup> and late-onset STGD1,  $\geq 45$  years.<sup>3</sup> The remaining patients were grouped as intermediate-onset STGD1, 11 to 44 years. The age at baseline was the first visit with available imaging and visual acuity tests.

Best-corrected visual acuity (BCVA) was measured with a Snellen or Early Treatment Diabetic Retinopathy Study chart, then transformed into the logarithm of the minimum angle of resolution (logMAR) for analysis. Fundus autofluorescence ( $\lambda =$

488 nm, emission 500–700 nm) imaging was performed using a confocal scanning laser ophthalmoscope (Spectralis HRA+OCT; Heidelberg Engineering, Heidelberg, Germany). The field of view was set at 30° × 30° or 55° × 55° and was centered on the macula.<sup>22</sup>

### Image quantification

The total RPE atrophy area was automatically quantified in FAF images by an observer-independent image analysis algorithm. The algorithm automatically segmented the area starting from an arbitrarily selected seed point inside the atrophic area. This method was based on a combination of a region growing algorithm and a dynamic, user-independent threshold selection procedure using Otsu thresholding. Areas were square-root ( $\sqrt{\phantom{x}}$ ) transformed to correct for baseline RPE atrophy area.<sup>23</sup> A good agreement has previously been observed between manual area measurements and the automatically quantified values (Sanchez CI, et al. *IOVS* 2015;56:ARVO E-Abstract 5258), and was found to be consistent with the agreement within this cohort (intra-class correlation coefficient, 0.977; 95% confidence interval [CI], 0.951–0.987).

### Genetic analysis

All reported *ABCA4* variants ([Supplemental Table 1](#)) were classified as follows: 1) pathogenic: truncating alleles, significantly enriched in *ABCA4*-LOVD (<http://www.LOVD.nl/ABCA4>, in the public domain), which contains 6903 variants (861 unique variants) reported in 3987 persons with STGD1 or autosomal recessive cone-rod dystrophy (Cornelis SS, Cremers FPM, unpublished data, 2016); 2) likely pathogenic: nontruncating alleles, significantly enriched in *ABCA4*-LOVD; 3) likely benign: allele frequency (AF) *ABCA4*-LOVD/AF ExAC non-Finnish Caucasian < 1; 4) benign: ExAC AF > 0.006; 5) unknown pathogenicity: AF *ABCA4*-LOVD/AF ExAC non-Finnish Caucasian > 1, however not significantly enriched. Patients were then grouped by combinations of *ABCA4* pathogenicity: 1) Pathogenic/Pathogenic, 2) Pathogenic/Likely pathogenic, 3) Likely pathogenic/Likely pathogenic, 4) Pathogenic in combination with unknown pathogenicity, (likely) benign, or a variant that was not published until 31 December 2015, 5) Likely pathogenic in combination with unknown pathogenicity or (likely) benign (Cornelis SS, Cremers FPM, unpublished data, 2016).

### Statistical analysis

We analyzed BCVA and RPE atrophy measurements using SPSS version 22 (IBM Corp., IBM SPSS Statistics, Chicago, IL, USA) with parametric tests. Retinal pigment atrophy progression rates were calculated by the difference at the baseline and last follow-up visit divided by the follow-up time. Differences in disease duration



and follow-up time between disease onset groups were analyzed with the Kruskal-Wallis test.

We used Pearson's correlation coefficients ( $\rho$ ) to assess inter-eye correlations of baseline BCVA, baseline RPE atrophy, and RPE atrophy progression. We compared these correlations between disease-onset groups and *ABCA4* variant combination groups by first performing a Fisher transformation:  $z' = \frac{1}{2} \ln \frac{1+\rho}{1-\rho}$ . Then, these  $z'$ -scores were compared for homogeneity. The test for homogeneity employs the  $\chi^2$ -distribution for two and four degrees of freedom:  $\chi^2 = \sum (n_i - 3) (z'_i)^2 - \frac{[\sum (n_i - 3) (z'_i)]^2}{\sum (n_i - 3)}$  where the summation is over the three disease-onset groups and five *ABCA4* variant combination groups, respectively.<sup>24</sup>

Baseline BCVA and RPE atrophy differences between measurements and the average measurements of both eyes were calculated and plotted according to the method of Bland and Altman to assess the intra-individual agreement graphically.<sup>25</sup> Limits of agreement between eyes were plotted for each disease-onset group.

Lin's concordance correlation coefficient was calculated to evaluate the extent of inter-eye symmetry of baseline BCVA, baseline RPE atrophy, and RPE atrophy progression.<sup>26-28</sup> The consists of the product of a precision coefficient (Pearson's  $\rho$ ) and an accuracy coefficient. The accuracy coefficient indicates how far the best-fit line of all paired left- and right-eye measurements deviates from the 45° line on a square scatter plot, and is defined as  $\frac{2}{\omega + 1 / \omega + v^2}$ , where scale shift  $\omega = \frac{\sigma_{OD}}{\sigma_{OS}}$  and location shift relative to the scale  $v = \frac{\mu_{OD} - \mu_{OS}}{\sqrt{\sigma_{OD} \sigma_{OS}}}$  (OD, right eye; OS, left eye).<sup>29</sup> If all paired measurements exactly lie on the 45° line, a coefficient of 1 would be found, indicating perfect symmetry. Strength-of-agreement criteria were as follows: almost perfect, > 0.90; substantial, 0.80 – 0.90; moderate, 0.65 – 0.80; poor, < 0.65.<sup>30</sup>

As standard deviations can be affected by extreme differences and rely on distributional assumptions, box-and-whisker plots were used to identify outliers by differences >1.5 interquartile ranges (IQR) below the first ( $Q_1$ ) or above the third ( $Q_3$ ) interquartiles in baseline BCVA, baseline RPE atrophy, and RPE atrophy progression. Odds ratios were calculated to identify associations of discordant BCVA and RPE atrophy at baseline with RPE atrophy progression.

We performed sample size calculations and a sensitivity analysis for a theoretical intervention using nQuery Advisor 7.0 (Statistical Solutions, Boston, MA). We

used a two-sided paired t-test for differences in means of RPE atrophy progression with a test significance level ( $\alpha$ ) of 0.05 and a power of  $(1 - \beta)$  of 0.80. Standard deviations of differences between RPE atrophy progression of treated and nontreated eyes were obtained from the standard deviations and correlations of left and right eyes using the formula:  $\sigma_d = \sqrt{(\sigma_1^2 + \sigma_2^2 - 2\rho\sigma_1\sigma_2)}$ .

## Results I: Patient characteristics

A total of 68 patients (136 eyes) were included in this study (26 men, and 42 women). The median age at onset was 8.5 (range, 4 – 10), 20 (range, 11 – 42), and 50 (range, 45 – 69) years for 14 early-onset STGD1, 33 intermediate-onset STGD1, and 21 late-onset STGD1 patients, respectively. At baseline, the median disease duration was 5 years (range, 0 – 39). The distribution did not differ between the three disease-onset categories. Details of patient characteristics and inter-eye correlations at baseline and follow-up are depicted in [Table 1](#).

**Table 1.** Characteristics and Inter-Eye correlations at Baseline and at Follow-up in 68 Stargardt Patients

	Early-onset STGD1	Intermediate-onset STGD1	Late-onset STGD1	P-value
Patients	7 male 7 female	9 male 24 female	10 male 11 female	
Age at onset	8.5 (4 – 10)	20 (11 – 42)	50 (45 – 69)	
<b>Characteristics at baseline</b>				
Disease duration	7 (0 – 27)	4 (0 – 39)	5 (0 – 26)	0.768*
Age (years)	14.5 (9 – 31)	36 (13 – 56)	59 (45 – 81)	
BCVA (logMAR)	OD: 1.08 ( $\pm$ 0.41) OS: 1.09 ( $\pm$ 0.28) $\rho = 0.830$	OD: 0.67 (0.50) OS: 0.77 (0.49) $\rho = 0.723$	OD: 0.36 ( $\pm$ 0.39) OS: 0.40 ( $\pm$ 0.55) $\rho = 0.619$	0.419 <sup>†</sup>
$\sqrt{\text{RPE atrophy (mm)}}$	OD: 1.79 ( $\pm$ 1.29) OS: 1.76 ( $\pm$ 1.27) $\rho = 0.992$	OD: 1.31 ( $\pm$ 1.52) OS: 1.28 ( $\pm$ 1.58) $\rho = 0.931$	OD: 1.79 ( $\pm$ 1.10) OS: 1.51 ( $\pm$ 1.03) $\rho = 0.601$	$5.5 \times 10^{-8\ddagger}$
<b>Characteristics at follow-up</b>				
Follow-up time (years)	5.7 (1.1 – 9.7)	3.1 (.9 – 9.5)	3.8 (.5 – 7.6)	0.220*
Age (years)	21 (11 – 36)	33 (15 – 59)	64 (47 – 86)	
BCVA (logMAR)	OD: 1.23 ( $\pm$ 0.29) OS: 1.23 ( $\pm$ 0.29) $\rho = 0.897$	OD: 0.93 ( $\pm$ 0.44) OS: 0.88 ( $\pm$ 0.52) $\rho = 0.767$	OD: 0.63 ( $\pm$ 0.60) OS: 0.54 ( $\pm$ 0.60) $\rho = 0.527$	0.0497 <sup>†</sup>
$\sqrt{\text{RPE atrophy (mm)}}$	OD: 2.73 ( $\pm$ 1.23) OS: 2.77 ( $\pm$ 1.26) $\rho = 0.974$	OD: 1.89 ( $\pm$ 1.69) OS: 1.86 ( $\pm$ 1.62) $\rho = 0.938$	OD: 2.29 ( $\pm$ 1.55) OS: 2.17 ( $\pm$ 1.49) $\rho = 0.670$	$6.1 \times 10^{-4\ddagger}$

Median and ranges are shown for time variables. Mean and standard deviations are shown for all other variables. \*Kruskal Wallis for differences in disease duration and follow-up; <sup>†</sup> $\chi^2$  with 2 degrees of freedom for differences in inter-eye correlations.

### Baseline inter-eye correlations of Best-corrected visual acuity

At baseline, the mean ( $\pm$  standard deviation) BCVA in the right and left eyes was 0.66 ( $\pm$  0.51) logMAR and 0.72 ( $\pm$  0.53) logMAR, respectively. Twenty-four right eyes and 23 left eyes were identified as the better seeing eye; 21 pairs of eyes had equal BCVA. The overall inter-eye correlation ( $\rho$ ) in BCVA at baseline was 0.756 and did not differ between disease onset groups, although a trend of decreasing correlations at later disease onset was also observed at follow-up.

Next, we compared the average and differences of baseline BCVA between the left and right eyes by a Bland-Altman plot ([Supplemental figure 2A](#)), revealing discordance up to 1.70 logMAR. This discordance was most pronounced in 13 patients (two early-onset STGD1, seven intermediate-onset STGD1, and four late-onset STGD1), as defined by outlying differences below  $Q_1 - 1.5 \times IQR$  or above  $Q_3 + 1.5 \times IQR$  ([Supplemental figure 2B](#)). Overall, this resulted in an inter-eye agreement ( $\rho$ ) in baseline BCVA of 0.751 (95% confidence interval (CI), 0.626 – 0.838).

### Baseline inter-eye correlations of Retinal pigment epithelium atrophy

At baseline, the mean  $\sqrt$  RPE atrophy area in the right and left eyes was 1.56 mm ( $\pm$  1.36) and 1.45 mm ( $\pm$  1.36), respectively. Twenty-nine right eyes and 34 left eyes had the smallest RPE atrophy area; 5 pairs of eyes had no RPE atrophy. Although baseline RPE atrophy between the left and right eyes was highly correlated ( $\rho = 0.878$ ), the correlation was significantly decreased in late-onset STGD1 patients.

The Bland-Altman plot ([Supplemental figure 3A](#)) showed inter-eye differences up to 2.49 mm of baseline  $\sqrt$  RPE atrophy area. An inter-eye difference below  $Q_1 - 1.5 \times IQR$  or above  $Q_3 + 1.5 \times IQR$  ([Supplemental figure 3B](#)), that is, discordant RPE atrophy at baseline, was identified in eight patients (intermediate-onset STGD1, four patients; late-onset STGD1, four patients). The overall inter-eye agreement ( $\rho$ ) of baseline RPE atrophy was 0.876 (95% CI, 0.806 – 0.921).

## Results II: Discordance of RPE atrophy progression rates

### Inter-eye correlations of retinal pigment epithelium atrophy progression

The median follow-up time was 3.9 years (range, 0.5 – 9.7), of which the distribution did not differ between all disease-onset categories. The mean  $\sqrt$  RPE atrophy progression rates in the right and left eyes were 0.21 ( $\pm$  0.20) mm/y and 0.20 ( $\pm$  0.21) mm/y, respectively. Thirty-five right eyes and 31 left eyes were identified as the eye with the slowest progression rate. Two pairs of eyes showed no progression in 3.0 and 3.4 years, respectively. The progression rates of  $\sqrt$  RPE

atrophy correlated between the left and right eyes with  $\rho = 0.766$ , and increased with earlier disease-onset groups ( $P = 9.8 \times 10^{-7}$ ). Evaluating the inter-eye agreement in progression of RPE atrophy, the agreement between the eyes was  $= 0.765$  (95% CI, 0.645 – 0.847) ([Figure 1](#)).

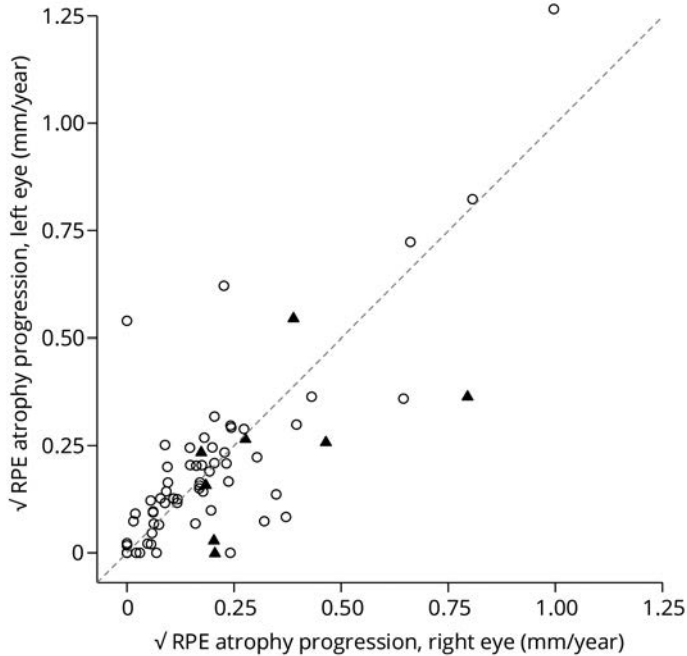


**Figure 1. A square scatter plot of inter-eye  $\sqrt{\text{RPE}}$  progression.** Circles are patients with differences in baseline  $\sqrt{\text{RPE}}$  atrophy between their eyes within  $Q_{1,3} \pm 1.5 \times \text{IQR}$ . Triangles are patients who fall outside the  $Q_{1,3} \pm 1.5 \times \text{IQR}$  for differences in baseline  $\sqrt{\text{RPE}}$  atrophy. Dashed line: 45° line of perfect agreement.  $Q_1$ , first interquartile;  $Q_3$ , third interquartile; IQR, interquartile range.

#### Discordant progression rates of RPE atrophy

Twelve out of 68 patients (early-onset STGD1, two patients (14%); intermediate-onset STGD1, four patients (12%); late-onset STGD1, six patients (29%)) had discordant RPE atrophy progression rates between their eyes by differences below  $Q_1 - 1.5 \times \text{IQR}$  or above  $Q_3 + 1.5 \times \text{IQR}$ . In four of these patients, the eye with the largest RPE atrophy area progressed faster than the other eye, thus increasing inter-eye discordance of RPE atrophy over time (mean difference,  $0.26 (\pm 0.10)$  mm/year; [Figure 2A](#)). In the other eight patients, the eye with the smallest RPE atrophy area progressed faster than the other eye, therefore reducing inter-eye discordance of RPE atrophy (mean difference,  $0.30 (\pm 0.12)$  mm/year; [Figure 2B](#)). The remaining 56 patients had similar progression rates between their eyes (mean difference,  $0.05 (\pm 0.04)$  mm/year, within  $Q_{1,3} \pm 1.5 \times \text{IQR}$ ; [Figure 2C](#)).

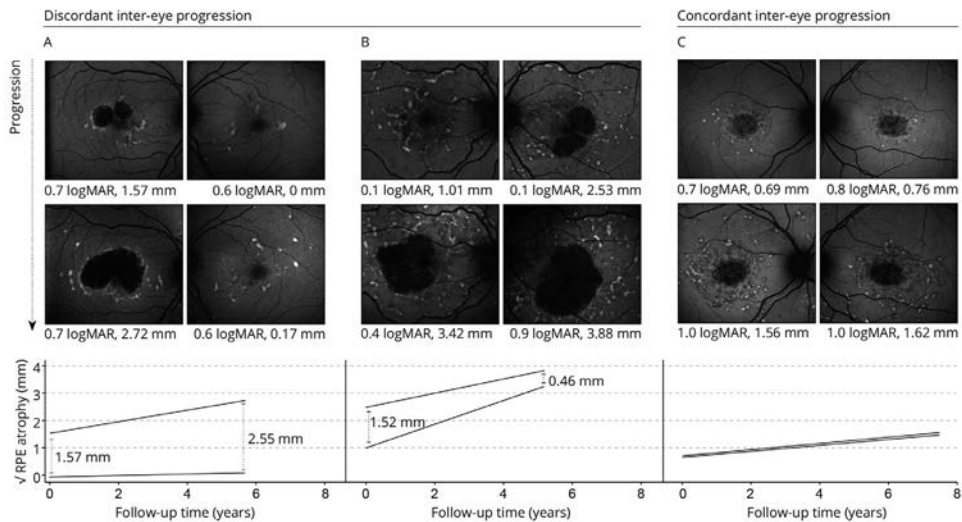


**Figure 2. Concordant and discordant inter-eye progression in Stargardt disease.** (A) 60-year old female with a disease duration of 1 year and increasing inter-eye differences. *ABCA4* variants: *c.5461-10T>C:p.[Thr1821Valfs\*13,Thr1821Aspfs\*6]/c.2757A>C:p.(Glu919Asp)*. (B) Eighty-one-year old female with a disease duration of 26 years and decreasing inter-eye differences. *ABCA4* variants: *c.5196+1G>T:p.(?)/+*. (C) Twenty-six-year old female with a disease duration of 6 years and similar progression rates between eyes. *ABCA4* variants: *c.1853G>A;4297G>A:p.(Gly618Glu;Val1433Ile)/c.2588G>C:p.[Gly863Ala;Gly863del]*.

### Baseline RPE atrophy and genetic associations with discordant RPE atrophy progression

Discordant RPE atrophy at baseline was associated with discordant RPE atrophy progression (odds ratio, 6.50; 95% CI, 1.35 – 31.34); this association was not found for discordant BCVA at baseline (odds ratio, 0.33 (95% CI, 0.04 – 2.85).

Furthermore, decreasing pathogenicity of *ABCA4* variant combinations were significantly associated with increasing discordant inter-eye progression ( $P = 0.007$ ). Proportions and correlations are depicted in [Table 2](#).

**Table 2. Proportions of Combinations of *ABCA4* Variants and Discordant RPE Atrophy Progression**

<i>ABCA4</i> Variant Combination	RPE Atrophy Progression		
	No Discordance	Discordant	Inter-Eye Correlation (Pearson's $\rho$ )
1. Pathogenic/pathogenic	3	1	0.995
2. Pathogenic/likely pathogenic	21	4	0.790
3. Likely pathogenic/likely pathogenic	9	0	0.597
4. Pathogenic/*	12	3	0.079
5. Likely pathogenic/*	11	4	0.346

The second *ABCA4* variant was likely benign, of unknown pathogenicity, or not found.

### Results III: Power calculations of a theoretical intervention trial

The power of a paired-control intervention trial will depend on the strength of correlations between pairs, that is, the left and right eye of each patient, and the expected treatment effect. For each two-fold increase in expected treatment effect, approximately a four-fold decrease in patient numbers is needed for a study at equal power. Stronger inter-eye correlations will have a linear beneficial effect on the number needed to include. The impact on these numbers is highest when a relatively modest treatment effect is expected. For instance, a correlation of  $\rho = 0.766$  would require 44 patients, whereas this number is reduced to 20 in the case of a correlation of  $\rho = 0.9$  (Figure 3). The specific inclusion criteria, for example, disease onset, *ABCA4* variant combinations, and baseline discordance can significantly affect the number needed to include.

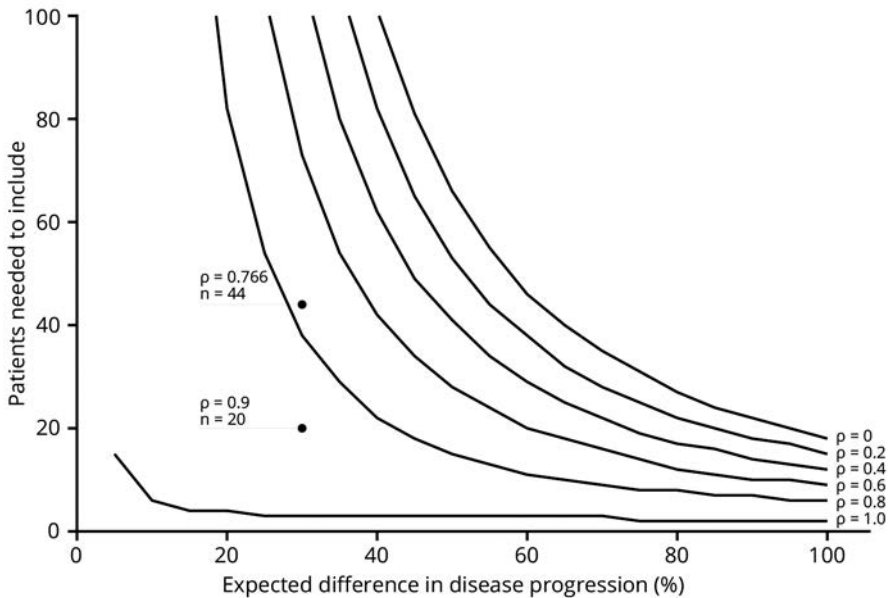


**Figure 3.** A sensitivity analysis for the power calculation of a theoretical intervention trial. Assuming a 30% reduction in disease progression (treatment effect), 44 patients are needed (inter-eye correlation  $\rho = 0.766$ ;  $\theta = 0.20$ ,  $\alpha = 0.05$ , two-sided paired samples t-test). The sample size will decrease to 20 in the case of an inter-eye correlation of 0.9. In the case of a correlation in disease progression of 1, 0.8, 0.6, 0.4, 0.2, and 0 between left and right eyes, 3, 38, 73, 108, 143, or 178 patients are needed, respectively.

## Discussion

Based on longitudinal FAF data in our current study, the overall agreement of inter-eye RPE atrophy progression in STGD1 was only moderate; it was highest in early-onset STGD1 and lowest in late-onset STGD1. Discordant progression rates were found in 12 out of 68 (17.6%) patients—which is surprisingly high—given that STGD1 is assumed to be a symmetrical inherited retinal disease. Discordant progression rates resulted in eyes either converging or diverging in atrophy size. Discrepancies of RPE atrophy progression rates were associated with discrepancies of RPE atrophy at baseline and less pathogenic *ABCA4* variant combinations.

Autosomal retinal dystrophies are expected to be symmetrical owing to the similar genetic and environmental background of both eyes. The majority of STGD1 patients exhibit bilateral symmetry in retinal features. Chen et al. illustrated this symmetry in left and right eyes of 24 STGD1 patients; they had highly correlated areas of RPE atrophy (Pearson's  $\rho = 0.998$ ).<sup>12</sup> McBain et al. studied the atrophy progression rates in 12 STGD1 patients, reporting a strong inter-eye correlation (Spearman's  $\rho = 0.846$ ).<sup>11</sup> In our cohort, these inter-eye correlations of RPE atrophy were substantially lower, but they can be explained by inclusion of late-onset STGD1 patients, which decreased the overall correlation. Inter-eye correlations of late-onset STGD1 were previously estimated to be moderate ( $\rho = 0.52$ ).<sup>20</sup> When late-onset STGD1 patients are excluded, our inter-eye correlations were similar to those reported by others.

Previous studies were limited by standard analyses of correlations, which cannot address the absolute symmetry within a patient. In contrast, we used Lin's concordance correlation coefficients and descriptive Bland-Altman plots, which are more appropriate and previously described in age-related macular degeneration.<sup>27</sup> In addition, there is an inherent increase in variability of inter-eye differences when the magnitude of atrophic areas increases. We corrected this by expressing the inter-eye differences as the square root, thus the differences were proportional to the magnitude of measurements. Moreover, square-root transformation corrected baseline dependence, which was reported previously with an average atrophy enlargement increase of  $0.016 \text{ mm}^2/\text{y}$  for each month of follow-up.<sup>10</sup>

Although we found that progression rates for atrophy are more likely to be discordant in eyes that differ more at baseline, progression rates are rather unpredictable between patients and between eyes within a patient. McBain et al. suggested that electroretinography could predict the rate of atrophy progression, but they did not account for baseline atrophy size. It would be interesting if

discordance in electroretinography between eyes of a patient would also predict inter-eye differences in progression, independent of their baseline atrophy size.<sup>10</sup> Burke et al. indicated that changes on optical coherence tomography would precede RPE atrophy and may thus predict the rates of atrophy progression.<sup>31</sup> These potential predictors for disease progression need to be addressed in future work.

The lower inter-eye correlations in older patients could be explained by the increased time within which stochastic factors, for example, small initial differences leading to significant differences later, can influence phenotypic expression. Differences in *ABCA4* variant expression may alter disease severity between eyes with mild variants, which can have a slightly different pathogenicity. In contrast, differences in expression would not influence progression speed much in severe *ABCA4* combinations as both variants would cause an equally severe phenotype.

The statistical power of a randomized controlled trial increases when differences are measured between correlated left and right eyes. To this extent, we recommend a fellow-eye paired trial design for retinal dystrophies, for example, as applied in a phase II gene therapy trial for choroideremia with 30 patients enrolled (ClinicalTrials.gov, [NCT02407678](https://clinicaltrials.gov/ct2/show/study/NCT02407678)). To achieve 80% statistical power in this trial, an effect size of at least 0.53 is required.<sup>32</sup> For the same expected effect size, a patient-controlled trial would need 58 patients in each arm.<sup>33</sup> Even in multicenter trials, such high sample sizes are difficult to obtain in rare retinal dystrophies. However, it is important to bear in mind that a fellow-eye paired control is impossible for pharmaceutical strategies in which both eyes of a patient are being treated (ClinicalTrials.gov, [NCT02402660](https://clinicaltrials.gov/ct2/show/study/NCT02402660)). Furthermore, it is preferred that an effect on relatively slow retinal degeneration is detected to identify a potential long-term benefit rather than a temporary gain of visual function.<sup>34</sup>

A therapeutic trial will gain a major advantage from a fellow-eye control in early-onset STGD1 because of their high inter-eye correlations. However, discordance was also present in some of these younger patients. As the progression can be better predicted in similar rather than in discordant eyes, retinal asymmetry needs to be considered as an exclusion criterion for small early-phase trials. Such stringent criteria will increase the chance of detecting efficacy with fewer patients. Criteria would include early-onset STGD1 patients with concordant retinal abnormalities between their eyes carrying severe *ABCA4* variants; not only do these patients have the highest inter-eye symmetry in disease progression, but they are also expected to have the most severe disease course.<sup>1, 2</sup> In these patients, therapy will potentially provide the most benefit, and in these patients, its effect has the highest chance to be detected.



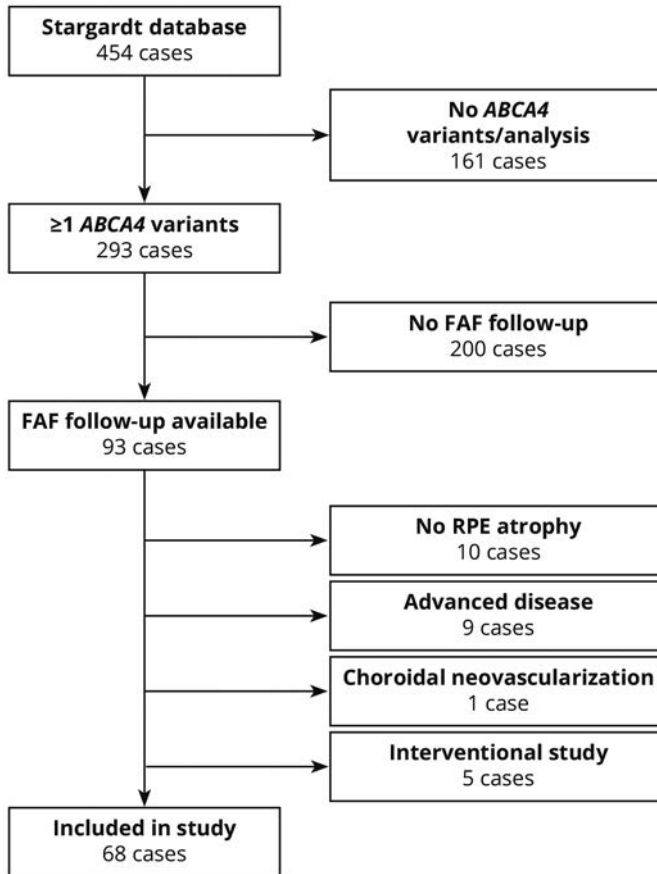
## References

1. Fujinami K, Zernant J, Chana RK, et al. Clinical and molecular characteristics of childhood-onset Stargardt disease. *Ophthalmology* 2015;122(2):326-34.
2. Lambertus S, van Huet RA, Bax NM, et al. Early-onset stargardt disease: phenotypic and genotypic characteristics. *Ophthalmology* 2015;122(2):335-44.
3. Westeneng-van Haaften SC, Boon CJ, Cremers FP, et al. Clinical and genetic characteristics of late-onset Stargardt's disease. *Ophthalmology* 2012;119(6):1199-210.
4. Yatsenko AN, Shroyer NF, Lewis RA, Lupski JR. Late-onset Stargardt disease is associated with missense mutations that map outside known functional regions of ABCR (ABCA4). *Hum Genet* 2001;108(4):346-55.
5. Rotenstreich Y, Fishman GA, Anderson RJ. Visual acuity loss and clinical observations in a large series of patients with Stargardt disease. *Ophthalmology* 2003;110(6):1151-8.
6. Allikmets R, Singh N, Sun H, et al. A photoreceptor cell-specific ATP-binding transporter gene (ABCR) is mutated in recessive Stargardt macular dystrophy. *Nat Genet* 1997;15(3):236-46.
7. Weng J, Mata NL, Azarian SM, et al. Insights into the function of Rim protein in photoreceptors and etiology of Stargardt's disease from the phenotype in abcr knockout mice. *Cell* 1999;98(1):13-23.
8. Stargardt K. Über familiäre, progressive degeneration in der makulagegend des auges. *Graefes Arch Clin Exp Ophthalmol* 1909;71:534-50.
9. Armstrong JD, Meyer D, Xu S, Elfervig JL. Long-term follow-up of Stargardt's disease and fundus flavimaculatus. *Ophthalmology* 1998;105(3):448-57; discussion 57-8.
10. Fishman GA, Stone EM, Grover S, et al. Variation of clinical expression in patients with Stargardt dystrophy and sequence variations in the ABCR gene. *Arch Ophthalmol* 1999;117(4):504-10.
11. McBain VA, Townend J, Lois N. Progression of retinal pigment epithelial atrophy in stargardt disease. *Am J Ophthalmol* 2012;154(1):146-54.
12. Chen B, Tosha C, Gorin MB, Nusinowitz S. Analysis of autofluorescent retinal images and measurement of atrophic lesion growth in Stargardt disease. *Exp Eye Res* 2010;91(2):143-52.
13. Fujinami K, Sergouniotis PI, Davidson AE, et al. Clinical and molecular analysis of Stargardt disease with preserved foveal structure and function. *Am J Ophthalmol* 2013;156(3):487-501. e1.
14. Han Z, Conley SM, Naash MI. Gene therapy for Stargardt disease associated with ABCA4 gene. *Adv Exp Med Biol* 2014;801:719-24.
15. Schwartz SD, Hubschman JP, Heilwell G, et al. Embryonic stem cell trials for macular degeneration: a preliminary report. *Lancet* 2012;379(9817):713-20.
16. Charbel Issa P, Barnard AR, Herrmann P, et al. Rescue of the Stargardt phenotype in Abca4 knockout mice through inhibition of vitamin A dimerization. *Proc Natl Acad Sci U S A* 2015;112(27):8415-20.
17. Cukras CA, Wong WT, Caruso R, et al. Centrifugal expansion of fundus autofluorescence patterns in Stargardt disease over time. *Arch Ophthalmol* 2012;130(2):171-9.
18. Fujinami K, Lois N, Mukherjee R, et al. A longitudinal study of Stargardt disease: quantitative assessment of fundus autofluorescence, progression, and genotype correlations. *Invest Ophthalmol Vis Sci* 2013;54(13):8181-90.
19. Lois N, Halfyard AS, Bird AC, et al. Fundus autofluorescence in Stargardt macular dystrophy-fundus flavimaculatus. *Am J Ophthalmol* 2004;138(1):55-63.
20. Lambertus S, Lindner M, Bax NM, et al. Progression of Late-Onset Stargardt Disease. *Invest Ophthalmol Vis Sci* 2016;57(13):5186-91.
21. Teussink MM, Lee MD, Smith RT, et al. The effect of light deprivation in patients with Stargardt disease. *Am J Ophthalmol* 2015;159(5):964-72. e2.

22. Boon CJ, Jeroen Klevering B, Keunen JE, et al. Fundus autofluorescence imaging of retinal dystrophies. *Vision Res* 2008;48(26):2569-77.
23. Feuer WJ, Yehoshua Z, Gregori G, et al. Square root transformation of geographic atrophy area measurements to eliminate dependence of growth rates on baseline lesion measurements: a reanalysis of age-related eye disease study report no. 26. *JAMA Ophthalmol* 2013;131(1):110-1.
24. Cohen J, & Cohen, P. Chapter: 2.8.3 Fisher's z' Transformation and Comparisons between independent rs. *Applied multiple regression/correlation analysis for the behavioral sciences*, Second edition ed. Hillsdale, NJ: Erlbaum 1983.
25. Bland JM, Altman DG. Statistical Methods for Assessing Agreement between Two Methods of Clinical Measurement. *Lancet* 1986;1(8476):307-10.
26. Lin LI. A Concordance Correlation-Coefficient to Evaluate Reproducibility. *Biometrics* 1989;45(1):255-68.
27. Fleckenstein M, Adrion C, Schmitz-Valckenberg S, et al. Concordance of disease progression in bilateral geographic atrophy due to AMD. *Invest Ophthalmol Vis Sci* 2010;51(2):637-42.
28. Lin L, Hedayat AS, Sinha B, Yang M. Statistical methods in assessing agreement: Models, issues, and tools. *Journal of the American Statistical Association* 2002;97(457):257-70.
29. Lin LI. A note on the concordance correlation coefficient. *Biometrics* 2000;56:324-5.
30. McBride GB. A proposal for strength-of-agreement criteria for Lin's Concordance Correlation Coefficient. NIWA Client Report: HAM2005-06. 2005.
31. Burke TR, Rhee DW, Smith RT, et al. Quantification of peripapillary sparing and macular involvement in Stargardt disease (STGD1). *Invest Ophthalmol Vis Sci* 2011;52(11):8006-15.
32. O'Brien RG, Muller KE. Unified Power Analysis for t-Tests Through Multivariate Hypotheses. In: Edwards LK, ed. *Applied Analysis of Variance in Behavioral Science*. New York: Marcel Dekker, 1993.
33. Dixon WJ, Massey FJJ. *Introduction to Statistical Analysis*, Fourth Edition ed. New York: McGraw Hill, 1983.
34. Cideciyan AV, Jacobson SG, Beltran WA, et al. Human retinal gene therapy for Leber congenital amaurosis shows advancing retinal degeneration despite enduring visual improvement. *Proc Natl Acad Sci U S A* 2013;110(6):E517-25.

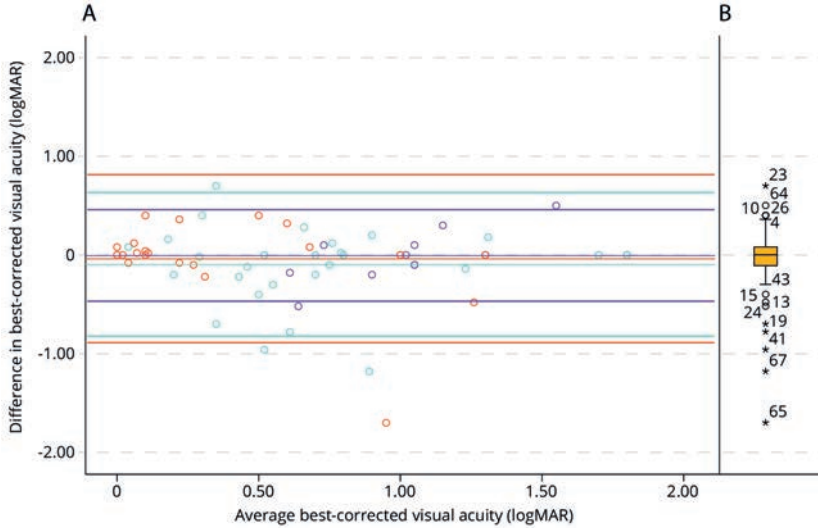
## Supplementary material

*Supplementary Figure 1. Flow chart depicting the selection process for patient inclusion in this study.*

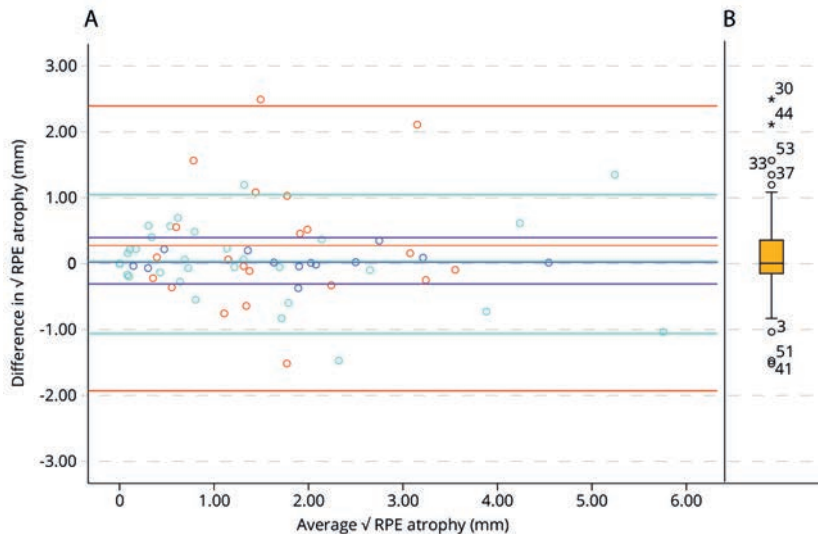


*FAF = fundus autofluorescence, RPE = retinal pigment epithelium.*

**Supplementary Figure 2. (A)** Bland-Altman plot of best-corrected visual acuity (BCVA). The average BCVA of all paired eyes (right minus left eye) were compared with the differences in BCVA between the eyes. The mean differences and limits of agreement are shown for (Purple) early-onset Stargardt disease (STGD1), (Turquoise) intermediate-onset STGD1, and (Red) late-onset STGD1. **(B)** Box-and-whisker plot of the differences in BCVA: dots are outlying differences below  $Q1 - 1.5 \times IQR$  or above  $Q3 + 1.5 \times IQR$ , and asterisks are extreme differences below  $Q1 - 3 \times IQR$  or above  $Q3 + 3 \times IQR$ .  $Q1$  = first interquartile,  $Q3$  = third interquartile,  $IQR$  = interquartile range.



**Supplementary Figure 3. (A)** Bland-Altman plot of  $\sqrt{RPE}$  atrophy area. The average area of all paired eyes (right minus left eye) were compared with the differences in measurements between the eyes. The mean differences and limits of agreement are shown for (Purple) early-onset Stargardt disease (STGD1), (Turquoise) intermediate-onset STGD1, and (Red) late-onset STGD1. **(B)** Box-and-whisker plot of the differences in  $\sqrt{RPE}$  atrophy area: dots are outlying differences below  $Q1 - 1.5 \times IQR$  or above  $Q3 + 1.5 \times IQR$ , and asterisks are extreme values below  $Q1 - 3 \times IQR$  or above  $Q3 + 3 \times IQR$ .  $Q1$  = first interquartile,  $Q3$  = third interquartile,  $IQR$  = interquartile range.



Supplementary Table 1. ABCA4 variants identified in this cohort.

Patient	Variant 1	Effect		Variant 2	Effect	
1 <sup>a</sup>	c.2588G>C	p.[Gly863Ala, Gly863del]	Likely pathogenic	c.656G>C	p.(Arg219Thr)	Likely pathogenic
2 <sup>c,d</sup>	c.5461-10T>C	p.(Thr1821Valfs*13, Thr1821Aspfs*6)	Pathogenic	c.5461-10T>C	p.(Thr1821Valfs*13, Thr1821Aspfs*6)	Pathogenic
3	c.2409_2410del	p.(Phe804Trpfs*3)	Pathogenic <sup>†</sup>	c.2588G>C	p.[Gly863Ala, Gly863del]	Likely pathogenic
4 <sup>b,e</sup>	c.5461-10T>C	p.(Thr1821Valfs*13, Thr1821Aspfs*6)	Pathogenic	+		
5 <sup>ab</sup>	c.5461-10T>C	p.(Thr1821Valfs*13, Thr1821Aspfs*6)	Pathogenic	c.5537T>C	p.(Ile1846Thr)	Likely pathogenic
6 <sup>c</sup>	c.5461-10T>C	p.(Thr1821Valfs*13, Thr1821Aspfs*6)	Pathogenic	c.214G>A	p.(Gly72Arg)	Likely pathogenic
7 <sup>c</sup>	c.5461-10T>C	p.(Thr1821Valfs*13, Thr1821Aspfs*6)	Pathogenic	c.5537T>C	p.(Ile1846Thr)	Likely pathogenic
8 <sup>c</sup>	c.1822T>A	p.(Phe608Ile)	Likely pathogenic	c.5882G>A	p.(Gly1961Glu)	Likely pathogenic
9 <sup>c</sup>	c.768G>T	p.(?)	Pathogenic	c.1822T>A	p.(Phe608Ile)	Likely pathogenic
10 <sup>a,e</sup>	c.164A>G	p.(His55Arg)	Likely pathogenic	c.6119G>A	p.(Arg2040Gln)	Unknown pathogenicity
11	c.3033-?_3364+?del	p.(?)	Pathogenic <sup>†</sup>	c.5714+5G>A	p.[=, ?]	Likely pathogenic
12	c.768G>T	p.(?)	Pathogenic	c.2588G>C	p.[Gly863Ala, Gly863del]	Likely pathogenic
13	c.768G>T	p.(?)	Pathogenic	c.2588G>C	p.[Gly863Ala, Gly863del]	Likely pathogenic
14 <sup>a,e</sup>	c.4462T>C	p.(Cys1488Arg)	Likely pathogenic	+		
15 <sup>c</sup>	c.5882G>A	p.(Gly1961Glu)	Likely pathogenic	+		
16	c.2409_2410del	p.(Phe804Trpfs*3)	Pathogenic <sup>†</sup>	c.2588G>C	p.[Gly863Ala, Gly863del]	Likely pathogenic
17 <sup>a</sup>	c.3364G>A	p.(Glu1122Lys)	Likely pathogenic	c.6089G>A	p.(Arg2030Gln)	Likely pathogenic
18	c.1853G>A;4297G>A	p.(Gly618Glu;Val1433Ile)	Likely pathogenic	c.2588G>C	p.[Gly863Ala, Gly863del]	Likely pathogenic
19	c.1822T>A	p.(Phe608Ile)	Likely pathogenic	c.2588G>C	p.[Gly863Ala, Gly863del]	Likely pathogenic
20	c.4506C>A	p.(Cys1502*)	Pathogenic	+		
21	c.3233G>A	p.(Gly1078Glu)	Likely pathogenic	+		
22	c.5337C>A	p.(Tyr1779*)	Pathogenic	c.5461-10T>C	p.(Thr1821Valfs*13, Thr1821Aspfs*6)	Pathogenic
23	c.5762_5763dup	p.(Ala1922Trpfs*18)	Pathogenic	c.2588G>C	p.[Gly863Ala, Gly863del]	Likely pathogenic
24	c.5882G>A	p.(Gly1961Glu)	Likely pathogenic	c.2906A>G	p.(Lys969Arg)	Likely pathogenic
25 <sup>a,e</sup>	c.768G>T	p.(?)	Pathogenic	+		
26	c.5461-10T>C	p.(Thr1821Valfs*13, Thr1821Aspfs*6)	Pathogenic	c.2588G>C	p.[Gly863Ala, Gly863del]	Likely pathogenic
27 <sup>a,e</sup>	c.768G>T	p.(?)	Pathogenic	+		
28	c.5461-10T>C	p.(Thr1821Valfs*13, Thr1821Aspfs*6)	Pathogenic	c.4685T>C	p.(Ile1562Thr)	Likely benign
29 <sup>c</sup>	c.286A>G	p.(Asn96Asp)	Likely pathogenic	c.286A>G	p.(Asn96Asp)	Likely pathogenic
30 <sup>c</sup>	c.4363T>C	p.(Cys1455Arg)	Likely pathogenic	+		
31	c.5882G>A	p.(Gly1961Glu)	Likely pathogenic	+		
32	c.6088C>T	p.(Arg2030*)	Pathogenic	c.2588G>C	p.[Gly863Ala, Gly863del]	Likely pathogenic
33	c.2409_2410del	p.(Phe804Trpfs*3)	Pathogenic <sup>†</sup>	c.2588G>C	p.[Gly863Ala, Gly863del]	Likely pathogenic
34	c.5882G>A	p.(Gly1961Glu)	Likely pathogenic	c.5537T>C	p.(Ile1846Thr)	Likely pathogenic
35	c.768G>T	p.(?)	Pathogenic	c.5882G>A	p.(Gly1961Glu)	Likely pathogenic
36 <sup>c</sup>	c.4773+1G>A	p.(?)	Pathogenic	c.5461-10T>C	p.(Thr1821Valfs*13, Thr1821Aspfs*6)	Pathogenic
37	c.768G>T	p.(?)	Pathogenic	c.5882G>A	p.(Gly1961Glu)	Likely pathogenic
38	c.5882G>A	p.(Gly1961Glu)	Likely pathogenic	c.6285T>C	p.(Asp2095Asp)	Benign <sup>†</sup>
39 <sup>e</sup>	c.3335C>A	p.(Thr112Asn)	Likely pathogenic	+		
40 <sup>a,b,e</sup>	c.3874C>T	p.(Gln1292*)	Pathogenic	c.1928T>G	p.(Val643Gly)	Likely benign
41 <sup>b</sup>	c.1822T>C	p.(Phe608Leu)	Likely pathogenic	+		
42 <sup>a,b,e</sup>	c.3874C>T	p.(Gln1292*)	Pathogenic	c.3113C>T	p.(Ala1038Val)	Likely pathogenic
43 <sup>a,e</sup>	c.768G>T	p.(?)	Pathogenic	+		
44 <sup>a,b,e</sup>	c.3874C>T	p.(Gln1292*)	Pathogenic	+		
45	c.4773+1G>A	p.(?)	Pathogenic	c.2588G>C	p.[Gly863Ala, Gly863del]	Likely pathogenic
46	c.1622T>C;3113C>T	p.[Leu541Pro; Ala1038Val]	Likely pathogenic	c.6316C>T	p.(Arg2106Cys)	Likely pathogenic
47	c.6428T>G	p.(Met2143Arg)	Likely pathogenic <sup>‡</sup>	+		
48	c.5461-10T>C	p.(Thr1821Valfs*13, Thr1821Aspfs*6)	Pathogenic	+		
49	c.3874C>T	p.(Gln1292*)	Pathogenic	c.6320G>A	p.(Arg2107His)	Likely pathogenic
50	c.5196+1137G>A	p.(?)	Likely pathogenic	+		
51 <sup>a,b,e</sup>	c.5196+1G>T	p.(?)	Pathogenic	+		
52 <sup>a,b,e</sup>	c.5461-10T>C	p.(Thr1821Valfs*13, Thr1821Aspfs*6)	Pathogenic	+		
53 <sup>a</sup>	c.5461-10T>C	p.(Thr1821Valfs*13, Thr1821Aspfs*6)	Pathogenic	c.2757A>C	p.(Glu919Asp)	Likely benign <sup>§</sup>
54 <sup>a</sup>	c.5461-10T>C	p.(Thr1821Valfs*13, Thr1821Aspfs*6)	Pathogenic	+		
55 <sup>d</sup>	c.1822T>A	p.(Phe608Ile)	Likely pathogenic	+		
56	c.768G>T	p.(?)	Pathogenic	c.768G>T	p.(?)	Pathogenic
57	c.1822T>A	p.(Phe608Ile)	Likely pathogenic	+		
58	c.3033-?_3364+?del	p.(?)	Pathogenic <sup>†</sup>	c.5714+5G>A	p.[=, ?]	Likely pathogenic
59 <sup>a,e</sup>	c.6238del	p.(Ser2080Profs*35)	Pathogenic <sup>†</sup>	c.2588G>C	p.[Gly863Ala, Gly863del]	Likely pathogenic
60 <sup>a</sup>	c.5813T>G	p.Leu1938*	Pathogenic <sup>†</sup>	c.2588G>C	p.[Gly863Ala, Gly863del]	Likely pathogenic
61	c.4773+1G>A	p.(?)	Pathogenic	+		
62	c.4128+1G>A	p.(?)	Pathogenic <sup>  </sup>	c.3259G>A	p.(Glu1087Lys)	Likely pathogenic
63	c.4128+1G>A	p.(?)	Pathogenic <sup>  </sup>	c.3259G>A	p.(Glu1087Lys)	Likely pathogenic
64	c.2160+1G>T	p.(?)	Pathogenic	c.4139C>T	p.(Pro1380Leu)	Likely pathogenic
65 <sup>e</sup>	c.1822T>A	p.(Phe608Ile)	Likely pathogenic	+		
66	c.4540-2A>G	p.(?)	Pathogenic	c.5882G>A	p.(Gly1961Glu)	Likely pathogenic
67	c.3259G>A	p.(Glu1087Lys)	Likely pathogenic	+		
68	c.5762_5763dup	p.(Ala1922Trpfs*18)	Pathogenic	+		

“Pathogenic” = Truncating alleles, significantly enriched in ABCA4-LOVD; “Likely pathogenic” = Non-truncating alleles, significantly enriched in ABCA4-LOVD; “Unknown pathogenicity” = (AF ABCA4-LOVD/AF ExAC non-Finnish Caucasian) > 1, however not significantly enriched; “Likely benign” = (AF ABCA4-LOVD/AF ExAC non-Finnish Caucasian) < 1; “Benign” = ExAC AF >0.006. AF = allele frequency.

† These unreported variants either result in a premature stop codon or a frame shift ending in a stop codon. The mRNA produced might be targeted for nonsense mediated decay.  
‡ The unreported variant c.6285T>C does not alter the protein sequence.  
§ The unreported variants c.6428T>G (phyloP: 9.18 and Grantham: 91) and c.2757A>C (phyloP: 0.44 and Grantham: 45) are expected to be likely pathogenic and likely benign, respectively.  
|| This unreported variant very likely results in a skip of exon 27 resulting in a frameshift.

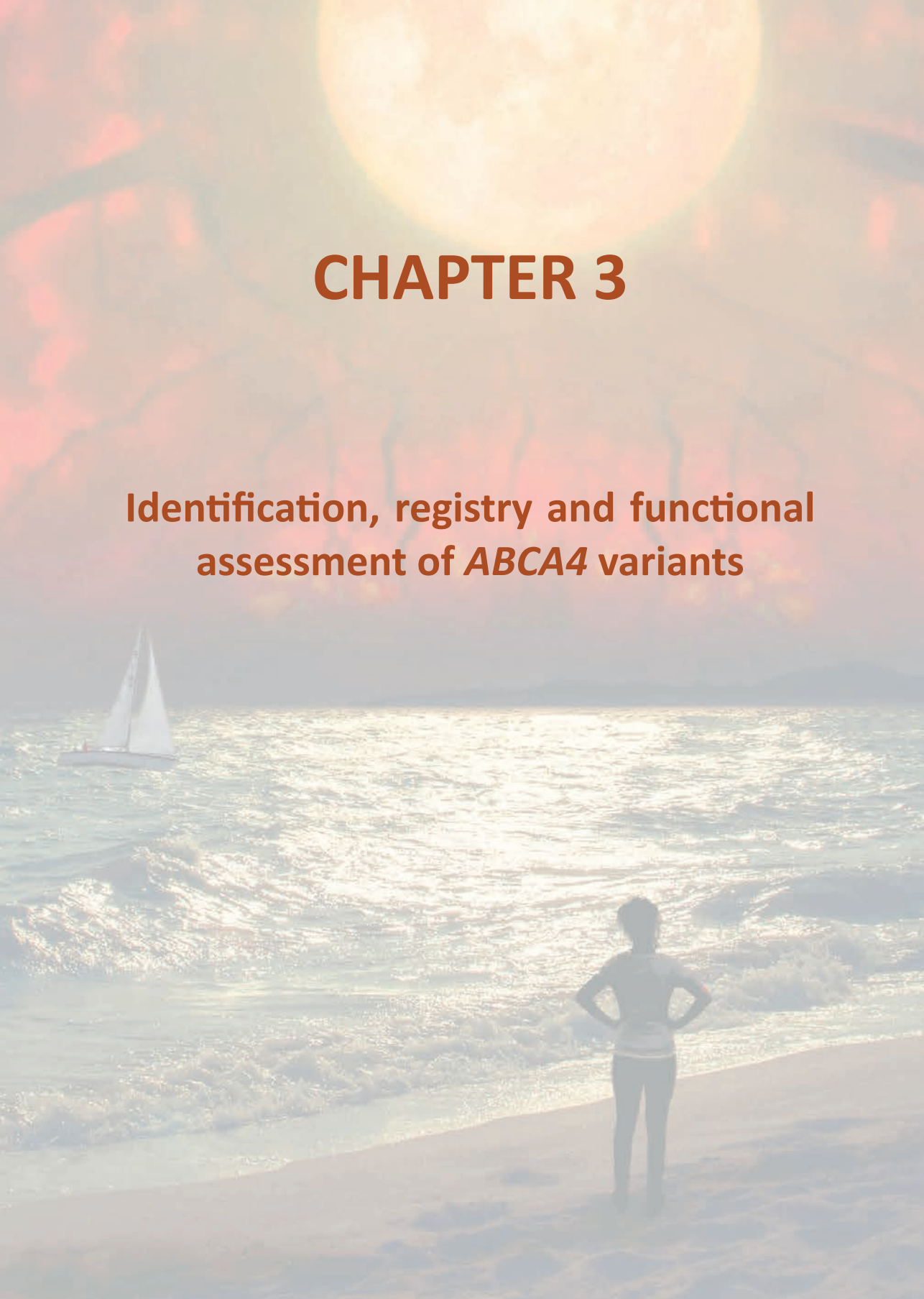
Several cases were mentioned earlier:

- a) Westeneng-van Haafte SC, Boon CJ, Cremers FP, Hoefsloot LH, den Hollander AI, Hoyng CB. Clinical and genetic characteristics of late-onset Stargardt’s disease. *Ophthalmology* 2012;119:1199-1210.
- b) van Huet RA, Bax NM, Westeneng-Van Haafte SC, et al. Foveal sparing in Stargardt disease. *Invest Ophthalmol Vis Sci* 2014;55:7467-7478.
- c) Lambertus S, van Huet RA, Bax NM, et al. Lambertus S, van Huet RA, Bax NM, et al. Early-onset Stargardt disease: phenotypic and genotypic characteristics. *Ophthalmology* 2015;122:335-344.
- d) Sangermano R, Bax NM, Bauwens M, et al. Photoreceptor Progenitor mRNA Analysis Reveals Exon Skipping Resulting from the ABCA4 c.5461-10T-->C Mutation in Stargardt Disease. *Ophthalmology* 2016;123:1375-1385
- e) Lambertus S, Lindner M, Bax NM, et al. Progression of Late-Onset Stargardt Disease. *Invest Ophthalmol Vis Sci* 2016;57:5186-5191.



# CHAPTER 3

Identification, registry and functional  
assessment of *ABCA4* variants







## CHAPTER 3.1

### In silico functional meta-analysis of 5,962 ABCA4 variants in 3,928 retinal dystrophy cases.

*“The clinical outcome in STGD1 depends on the severity of two ABCA4 variants. To provide an accurate prognosis and to select patients for novel treatments, it is important to assess the functional significance of non-truncating ABCA4 variants. All published ABCA4 variants were collected in a Leiden Open (source) Variant Database (LOVD) in this study. In silico meta-analysis of 5,962 variants in 3,928 ABCA4-associated retinal dystrophy cases was performed, which allowed us to predict the functional effects. These studies will facilitate the pathogenicity assessment of variants with unknown significance found in diagnostics.”*

Stéphanie S. Cornelis  
Nathalie M. Bax  
Jana Zernant  
Rando Allikmets  
Lars G. Fritsche  
Johan T. den Dunnen  
M. Ajmal  
Carel B. Hoyng  
Frans P.M. Cremers

*Human Mutation 2017;38(4):400-408*

We thank Christian Gilissen and Riccardo de Bin for their advice on statistical analyses.

Variants in the *ABCA4* gene are associated with a spectrum of inherited retinal diseases (IRDs), most prominently with autosomal recessive (ar) Stargardt disease (STGD1) and ar cone-rod dystrophy. The clinical outcome to a large degree depends on the severity of the variants. To provide an accurate prognosis and to select patients for novel treatments, functional significance assessment of nontruncating *ABCA4* variants is important. We collected all published *ABCA4* variants from 3,928 retinal dystrophy cases in a Leiden Open Variation Database, and compared their frequency in 3,270 Caucasian IRD cases with 33,370 non-Finnish European control individuals. Next to the presence of 270 protein-truncating variants, 191 nontruncating variants were significantly enriched in the patient cohort. Furthermore, 30 variants were deemed benign. Assessing the homozygous occurrence of frequent variants in IRD cases based on the allele frequencies in control individuals confirmed the mild nature of the p.[Gly863Ala, Gly863del] variant and identified three additional mild variants (p.(Ala1038Val), c.5714+5G>A, and p.(Arg2030Gln)). The p.(Gly1961Glu) variant was predicted to act as a mild variant in most cases. Based on these data, *in silico* analyses, and American College of Medical Genetics and Genomics guidelines, we provide pathogenicity classifications on a five-tier scale from benign to pathogenic for all variants in the *ABCA4*-LOVD database.

## Introduction

Variants in *ABCA4* (MIM# 601691) are associated with a wide variety of inherited retinal diseases (IRDs) [Allikmets et al., 1997b; Cremers et al., 1998; Rozet et al., 1998; Maugeri et al., 2000]. Homozygous or compound heterozygous variants in *ABCA4* can cause autosomal recessive (ar) Stargardt disease (STGD1) and a more severe phenotype, ar cone-rod dystrophy (CRD).

Mostly, STGD1 patients present with yellow-white fundus flecks, hence the term “fundus flavimaculatus” [Stargardt, 1909]. Furthermore, the disease is characterized by retinal pigment epithelium changes and extensive chorioretinal atrophy [Fishman et al., 1999]. *ABCA4*-associated IRDs have a broad phenotypic variation, ranging from an early age at onset that mostly results in panretinal atrophy [Martinez-Mir et al., 1998; Klevering et al., 2005; Fujinami et al., 2015; Lambertus et al., 2015] to a milder foveal sparing phenotype in patients with a late age at onset [Westeneng-van Haaften et al., 2012; van Huet et al., 2014].

The exact molecular effect of most variants underlying the variety in phenotypes is still unknown. *ABCA4* encodes the protein ABCA4 (ATP-binding cassette transporter, subfamily A, member 4), which is located in the outer segment disk membranes of cone and rod photoreceptor cells. ABCA4 is a 2,273 amino acid glycoprotein with two tandem halves. Each half contains a single transmembrane segment followed by a large exocyttoplasmic domain, iterating transmembrane segments, and an ATP binding domain [Molday et al., 2009].

Previously, a genotype–phenotype model was proposed. According to this model, the severity of the functional consequences of the combination of *ABCA4* variants correlates with the severity of the clinical phenotype [van Driel et al., 1998; Maugeri et al., 1999]. Persons with a severe and a mild variant or two moderately severe variants are expected to present with STGD1, persons with a severe and a moderately severe variant with CRD, and individuals with two severe variants with a severe form of CRD. The latter phenotype has been associated with an early age at onset ( $\leq 10$  years) [Simonelli et al., 2005; Lambertus et al., 2015] and in a later stage often resembles retinitis pigmentosa (RP) [Cremers et al., 1998; van Driel et al., 1998; Maugeri et al., 1999]. Furthermore, studies from this century confirmed that the disease phenotype correlates with the presence of severe variants [Simonelli et al., 2005; Fujinami et al., 2013; Kjellstrom, 2014]. In contrast, two “mild” or “hypomorphic” variants are expected not to give rise to a disease phenotype [Maugeri et al., 1999]. This model explains that there is an unusual high carrier frequency of these mild variants in the general population,

which can be as high as 5.5% (c.2588G>C; p.[Gly863Ala, Gly863del] in Sweden [Maugeri et al., 2002]) and 11.3% (c.5882G>A; p.(Gly1961Glu) in Somalia [Guymer et al., 2001]).

Sequence analysis of the protein coding exons reveals biallelic variants in approximately 75% of the STGD1 cases [Allikmets et al., 1997b; Lewis et al., 1999; Maugeri et al., 1999; Rivera et al., 2000; Webster et al., 2001]. The identification of one variant only was found more often in patients with a late age at onset than in patients with an early onset STGD1 [Utz et al., 2014]. Monoallelic *ABCA4* variants have also been reported in patients with a typical fine granular pattern with peripheral punctuate spots and in patients with age-related macular degeneration [Allikmets et al., 1997a; Fritsche et al., 2012]. However, it is possible that a subset of this latter patient group contains misdiagnosed late-onset STGD1 patients [Dryja et al., 1998; Souied et al., 2000]. In a subset of STGD1 and arCRD cases with initially only one variant, deep-intronic variants were identified later that in some instances were shown to result in the insertion of pseudo-exons into the mRNA [Braun et al., 2013; Zernant et al., 2014; Bauwens et al., 2015; Bax et al., 2015].

The *ABCA4* gene carries a conspicuously high number of noncanonical splice site variants, many of which with an unknown functional effect, such as the c.5461-10T>C variant was. By analyzing patient-derived photoreceptor progenitor cells, it was recently shown that this apparently benign variant results in the skipping of exon 39 or of exons 39 and 40 [Sangermano et al., 2016].

Categorizing *ABCA4* variants as either benign or pathogenic is important for patients to qualify for several therapies. The effect of deep-intronic variants potentially can be treated using antisense oligonucleotides [Collin et al., 2012; Garanto et al., 2016; Gerard et al., 2016]. STGD1 patients are eligible for therapy trials, like gene augmentation (trial number NCT01367444, NCT01736592), stem cell therapy (trial number NCT01469832), and small molecule drugs (trial number NCT02402660) [Dalkara et al., 2016] (<https://clinicaltrials.gov/ct2/show/NCT01367444>), if biallelic disease-causing *ABCA4* variants have been identified. Additionally, it is important for genetic counseling to know which variants give rise to which grade of pathogenicity in the disease phenotype.

In this study, we therefore gathered all *ABCA4* variants published before 2016 that were associated with STGD1, arCRD and arRP. We uploaded all the published variants into the *ABCA4* Leiden Open source Variant Database (LOVD) and assessed the pathogenicity of all nonprotein-truncating variants based on

their prevalence in the *ABCA4* patient dataset (below abbreviated as “*ABCA4*-LOVD”) versus controls. In addition, we performed *in silico* predictions, analyzed the homozygous occurrence of variants combined with the age of onset of the IRD, their presence in patients with an early onset, and their occurrence with a frequent mild variant. Based on this information and the American College of Medical Genetics and Genomics (ACMG) guidelines, all variants in the *ABCA4*-LOVD database were classified according to their pathogenicity.

## Methods

### Literature search

All peer-reviewed publications from before 2016 which reported *ABCA4* variants (NM\_000350.2) in associated retinal dystrophies, such as STGD1, arCRD, and arRP patients, were collected by a Pubmed search. We did not collect *ABCA4* variants reported in patients with age-related macular degeneration. Among others, the variant combinations, disease phenotype, and the age of onset were annotated. Clear duplicates, for example, persons with the same variants, the same identification number, and/or age of onset, were removed. Familial cases with the exact same variant combination from the same authors were also removed from the dataset, but have been uploaded to the LOVD.

### Variant data analysis

For cDNA numbering, we used +1 as the A of the ATG translation initiation codon in the reference sequence, with the initiation codon as codon 1. The frequency of the variants in the IRD group was compared to the frequency of the variants in the Exome Aggregation Consortium (ExAC) database Version 0.3.1, which contains exome data from over 60,000 individuals worldwide (<http://exac.broadinstitute.org/>). Individuals with severe pediatric diseases are excluded from the ExAC database. Therefore, this control dataset does not contain variants of individuals with severe early onset IRD, but might contain variants of individuals with a later onset or a milder phenotype of IRD. The majority of the published *ABCA4* variants in patients were identified in non-Finnish Caucasian individuals. To have reasonable power in the statistical comparisons, we therefore chose to use the Caucasian population as a control group and had to exclude non-Caucasian patients for statistical comparisons. Fisher’s exact tests were used to analyze whether variants were significantly enriched in the Caucasian *ABCA4*-LOVD (*ABCA4*-LOVD\_Cauc) patient group compared to the non-Finnish European (nFE) population in ExAC consisting of 33,370 individuals. After this, a correction by the false discovery rate (FDR) of Benjamini–Hochberg, classical one stage method [Benjamini and Hochberg, 1995] was performed to increase the number of true

significant findings allowing an error margin of 5% on the total of the data. These tests were performed three times: (1) for all *ABCA4*-LOVD\_Cauc patients, (2) for biallelic cases only, and (3) for monoallelic cases only. The latter two tests were performed in order to assess if biallelic variants show different significance or trends compared to the monoallelic variants. A clear difference could indicate that monoallelic patients show a different form of disease or carry *ABCA4* variants by chance, while the cause of their similar phenotype resides elsewhere.

When an exonic variant location was absent in ExAC, the allele count of ExAC was assumed to be 66,598 for that location as 95% of the known variant locations have an allele count of 66,598 or higher. Furthermore, the coverage plots available in ExAC were checked for drops in coverage. For those variants that were located in a region with low coverage, the coverage of the closest variant in ExAC was taken for statistical analysis. Finally, the number of singletons in ExAC was compared to the number of singletons in the patient group by using a chi-square test. In this way, we investigated if the number of recent *de novo* variants is found more frequent in the patient group, as these are often a cause of disease [Veltman and Brunner, 2012].

According to the genotype–phenotype model described above, all the variants that were found in a homozygous manner in STGD1 cases of any ethnicity were annotated to have at least a moderate effect. Variants that were found in a homozygous manner in persons with an average age at onset  $\leq 10$  years of age were annotated to have a severe effect. For all the variants that were present in a compound heterozygous manner, the ones that occurred together with the mild variant p.[Gly863Ala, Gly863del] or the p.(Gly1961Glu) variant, which in the majority of cases was deemed mild (see below), were annotated to be likely severe, according to a generally accepted model [Maugeri et al., 1999].

### *In silico* analyses

SMART domains and their locations were obtained from <http://smart.embl-heidelberg.de/>. Furthermore, 12 transmembrane segments were obtained from the Uniprot Web site <http://www.uniprot.org/>. The number of missense variants per domain was compared to the expected amount of missense variants per domain with a chi-square test and Bonferroni correction. The expected number of missense variants per domain was calculated by dividing the number of missense variants per domain in the ExAC database by the total amount of missense variants in the protein in the ExAC database, multiplied by the total number of variants enriched in the *ABCA4*-LOVD\_Cauc. PhyloP scores, which are based on the conservation of nucleotides among multiple organisms, were

obtained from the UCSC genome browser tool “Table browser” using the Cons 46-Way track and the Vertebrate PhyloP conservation table for the February 2009 genome release GRCh37/hg19 <http://genome.ucsc.edu/> (Clade: Mammal, Genome: Human, assembly: February 2009 (GRCh37/hg19), Group: Comparative Genomics, Track: Conservation) [Karolchik et al., 2004]. Grantham scores were obtained from the original paper [Grantham, 1974]. Combined Annotation Dependent Depletion (CADD) scores were obtained from the Web site <http://cadd.gs.washington.edu/home> [Kircher et al., 2014] and the odds ratios (ORs) were calculated for each variant  $x$  by the formula:

$$\frac{AF(x) \text{ in } ABCA4LOVD\_Cauc / (1 - AF(x) \text{ in } ABCA4LOVD\_Cauc)}{AF(x) \text{ in } nFE\_ExAC / (1 - AF(x) \text{ in } nFE\_ExAC)}$$

In which  $AF(x)$  is the allele frequency of variant  $x$ . ORs and their 95% confidence intervals were calculated using the Fisher’s exact test for count data as implemented in R (<http://www.R-project.org>). Reported confidence intervals were not adjusted for multiple testing.

Patients in which one allele contained a missense variant and the second allele contained a truncating variant, were studied further on the assumption that the effect of the truncating allele is always the same. In this way, the type of missense variant likely plays a big role in the range of the ages at onset among different patients, in which a severe missense variant is likely to lead to an earlier age at onset than a mild missense variant. PhyloP, Grantham and CADD scores as well as the ORs of these missense variants were plotted against the age of IRD onset of corresponding patients to support this hypothesis. Furthermore, Spearman correlation tests with Bonferroni correction were performed to assess which of the prediction programs and the OR were significantly correlating with the age of onset and therefore deemed to be good predictors of the pathogenic nature of all the variants.

To assess the splicing scores, we employed the following programmes via the Alamut Visual version 2.7.1 (Interactive Biosoftware): SpliceSiteFinder-like, Alamut Visual software version 2.7.1: SpliceSiteFinder-like, MaxEntScan, NNSPLICE, GeneSplicer, and Human Splicing Finder [Reese, et al., 1997; Pertea, et al., 2001; Cartegni, et al., 2003; Yeo and Burge, 2004; Desmet, et al., 2009].

### Pathogenicity classifications

All the variants in the ABCA4-LOVD dataset were classified into five pathogenicity categories: (1) pathogenic, when the variant is truncating; (2) likely pathogenic, when the variant is nontruncating and enriched in the ABCA4-LOVD dataset



compared to the nFE ExAC control group; (3) uncertain significance, when the variant is nontruncating, more frequent in the *ABCA4*-LOVD dataset than in the nFE ExAC control group, but not significantly enriched; (4) likely benign, when the variant has a higher frequency in the nFE ExAC population than in the *ABCA4*-LOVD dataset; (5) benign, when the variant has a frequency  $>0.005$  in the nFE ExAC population and is not one of the known mild variants p.[Gly863Ala, Gly863del] or p.(Gly1961Glu). In addition, all the variants in the *ABCA4*-LOVD dataset were classified according to the ACMG guidelines [Richards et al., 2015]. In this classification, the types of evidence for a mutation to be pathogenic are put in different categories:

- pathogenic, very strong criterion (PVS), for example, “this variant is truncating”,
- pathogenic, strong criterion (PS), for example, “another variant leading to the same amino acid change has been associated with disease before”,
- pathogenic, moderate criterion (PM), for example, “the variant is located in a well-established functional domain”,
- pathogenic, supporting criterion (PP), for example, “all *in silico* prediction programs predict pathogenicity.”

After categorizing the different criteria, the ACMG gives a scoring method of how to sum the criteria to come to a final pathogenicity class. For example, a variant can be classified as pathogenic if it meets 1 PS, 2 PM, and at least 2 PP criteria.

## Results

### All variants

In total, variants of 4,137 patients were gathered from 148 papers, in which 6,284 variants were reported. Duplicate removal as well as excluding family members led to a total amount of 3,928 patients and 5,962 alleles ([Supp. Table S1](#)). The total *ABCA4*-LOVD comprised 303 patients with homozygous variants, 1,869 patients with compound heterozygous variants, and 1,015 patients carrying one variant. Remaining variants most likely occurred in compound heterozygous state, although this is unknown because the variants were described per cohort instead of per patient. The number of monoallelic cases could be an overestimation because in some follow-up studies a second allele was identified and published, without mentioning that the patient was already published before. The 5,962 variants consisted of 913 unique variants, including 64 complex alleles—alleles with multiple variants in *cis*- and 10 deep-intronic variants ([Table 1](#)).

**Table 1:** Distribution of all variants in the ABCA4- LOVD patient dataset

Variant types	Total	Number of unique variants
Missense	3,842	471
Protein truncating <sup>α</sup>	1,423	314
Noncanonical splice site	310	49
Of which missense	77	13
Of which synonymous	7	3
Nontruncating indels	42	16
Synonymous	9	5
Complex alleles	357	64
Deep intronic variants	63	10
Total	5,962	913

<sup>α</sup> Including big deletions and missense variants at the first codon.

After removal of the variants that had a lower frequency in the ABCA4-LOVD patient dataset versus the ExAC database, and exclusion of the complex and deep-intronic alleles, which are not represented in ExAC, 4,683 alleles and 807 different variants remained. Of these variants, 316 (3,645 in total; Table 2; Supp. Table S2) were significantly enriched in the ABCA4-LOVD\_Cauc dataset (Fisher's exact test,  $P < 0.05$ , FDR of 5%) compared to the nFE population in ExAC. These were composed of 169 truncating variants, which were therefore annotated as category 1 (pathogenic) in the LOVD database, and 250 other variants that were classified as category 2 (likely pathogenic). Furthermore, there were 347 singleton variants unique in the patient group, which usually indicate recent *de novo* events. This is a significantly higher proportion than the occurrence of singletons in the ExAC control group (chi-square test,  $P = 2.3 \times 10^{-189}$ ) and therefore most likely a significant amount of these singletons are disease causing. Comparing the frequency of the subgroup of biallelic variants only with their frequency in the ExAC control group, revealed 229 significantly enriched variants (Fisher's exact test,  $P < 0.05$ , FDR of 5%). As, strictly speaking, Stargardt patients should have two pathogenic variants, these 229 variants might be most informative. Comparing the subgroup of monoallelic variants only, which was more than twice as small as the biallelic variants subgroup, to the ExAC control group showed 80 significantly

enriched variants (Fisher's exact test,  $P < 0.05$ , FDR of 5%). Interestingly, six variants were enriched in the monoallelic subgroup, which were not enriched in the biallelic subgroup. This could indicate that these variants are mere chance findings. However, three out of these six variants were truncating variants, c.2099G>A; p.(Trp700<sup>α</sup>), c.4956T>G; p.(Tyr1652<sup>\*</sup>), c.5898+1G>T; p.(?), making it unlikely that they are benign. Of note, the three nontruncating variants, c.4610C>T; p.(Thr1537Met), c.5914G>A; p.(Gly1972Arg), c.6446G>T; p.(Arg2149Leu), were present in the biallelic group as well.

**Table 2.** Distribution of enriched variants in the ABCA4-LOVD Cauc patient dataset

Variant types	Total	Number of unique variants
Missense	2,566	169
Protein truncating <sup>α</sup>	875	125
Noncanonical splice site	230	18
Of which missense	49	2
Of which synonymous	2	1
Nontruncating indels	19	5
Synonymous	6	2
Total	3,645	316

*α* Including big deletions and missense variants at the first codon.

Complex alleles and deep intronic variants were not tested due to the absence of these variants in ExAC. The total frequency of significantly enriched variants per allele is 0.56 in the patient dataset compared to 0.021 in the ExAC database. Therefore, in the ExAC database about one in every 24 persons is a carrier of a presumed pathogenic ABCA4 variant.

### Frequent ABCA4 variants

The p.(Gly1961Glu) variant is the most frequent variant in the ABCA4-LOVD (536/6,670 alleles), followed by p.[Gly863Ala, Gly863del], present in 261 of 6,670 alleles. In the ExAC nFE population, the p.[Gly863Ala, Gly863del] variant is more frequent than p.(Gly1961Glu) (allele frequency 0.0081 for p.[Gly863Ala, Gly863del] vs. 0.0047 for p.(Gly1961Glu)) in ExAC. The third most frequent variant is c.5461-10T>C (p.[Thr1821Valfs, Thr1821Aspfs]), a noncanonical splice

variant that recently was shown to result in the skipping of exon 39 or exon 39/40 [Sangermano et al., 2016] and is present in 156 of 6,670 alleles in the ABCA4-LOVD\_Cauc vs. 26/66,486 alleles of nFE in ExAC ([Supp. Table S1](#)).

### Missense variants

For all the missense variants, Grantham, PhyloP, and CADD scores were obtained. Furthermore, the OR was determined by comparing the allele count in the ABCA4-LOVD\_Cauc patient dataset with the nFE ExAC control dataset ([Supp. Table S3](#)). When the *in silico* scores were compared to the age of onset of cases carrying missense variants on one allele as well as a truncating variant on the other allele, a significant negative correlation was found for the OR ( $\rho = -0.34$ ,  $P < 0.04$ ; [Supp. Fig. S1](#)) but not for the Grantham ([Supp. Fig. S2](#)), CADD ([Supp. Fig. S3](#)), and PhyloP ([Supp. Fig. S4](#)) scores. Of note, Grantham scores  $>90$  were not observed for missense variants observed in patients with an onset of disease above 25 years of age, indicating that high Grantham scores might be related to an earlier age of onset, while variants with a low Grantham score can be found in patients with all ages of onset.

### Protein-truncating variants

About a quarter of all variants that were associated with disease according to the enrichment analysis of the total Caucasian dataset were protein truncating ([Supp. Table S4](#)), among which is composed of about one-third stop mutations, one-third frameshift mutations, and one-third canonical splice site mutations. Only 26 of the 313 truncating variants were listed in ExAC, illustrating that most of these variants are very rare.

### Homozygosity analysis

According to the widely accepted genotype–phenotype correlation model mentioned above, patients with a severe variant in a homozygous state are expected to present with an early-onset form of STGD1 or arCRD. Furthermore, all homozygous variants that cause STGD1 with an onset between 10 and 45 years of age are expected to have at least a moderate effect. Finally, homozygous mild variants are not expected to give rise to a monogenic IRD. Therefore, in this analysis, variants were annotated accordingly. In total, 58 nontruncating variants were found in a homozygous state ([Supp. Table S5](#)).

The two presumed mild variants, p.[Gly863Ala, Gly863del] and p.(Gly1961Glu), were found in a homozygous state in 2 and 16 cases, respectively. This is significantly less than expected based on their ExAC frequencies and an STGD1 prevalence of one in 10,000 individuals ( $P < 3.3 \times 10^{-306}$  and  $P = 1.8 \times 10^{-172}$ , chi-square

test, Bonferroni adjusted) (Table 3). These results confirm that both variants in the far majority of IRD cases can be considered as mild alleles. Regarding the p.(Gly1961Glu) variant, the Hardy–Weinberg equilibrium was maintained in the disease population even though we might expect less homozygous cases due to the absence of disease in case of a mild effect on protein function in homozygous state. However, if we consider its allele frequency in ExAC (0.005), it is expected to occur in a homozygous state in  $\sim 1/40,000$  persons in the general population, and it thereby would represent  $\sim 25\%$  of STGD1 cases. In the ABCA4-LOVD\_Cauc, it is only found in a homozygous state in 16/3,335 (0.48%) of cases with one or two likely causal ABCA4 variants. From this analysis, we can confer that  $>95\%$  of p.(Gly1961Glu) alleles can be considered to be mild. Furthermore, the three variants c.3113C>T (p.(Ala1038Val)), c.5714+5G>A (p.(?)), and c.6089G>A (p.(Arg2030Gln)) were deemed mild alleles as they were not found homozygously in patients even though this was expected based on their frequency in ExAC (Table 2).

**Table 3.** Variants Occurring Significantly Less in a Homozygous State in the Caucasian ABCA4-LOVD than Expected Based on the Frequency in the ExAC Non-Finnish European Population (Chi-Square Test, Corrected by FDR).

DNA variant	Protein variant	No. of observed homozygous cases	No. of expected homozygous cases	Bonferroni corrected P-value
c.2588G>C	p.[Gly863Ala, Gly863del]	2	2143	$<<3.3 \times 10^{-306}$
c.5882G>A	p.(Gly1961Glu)	16	730	$1.8 \times 10^{-172}$
c.3113C>T	p.(Ala1038Val)	0	126	$1.2 \times 10^{-29}$
c.5714+5G>A	p.(?)	0	12	0.0019
c.6089G>A	p.(Arg2030Gln)	0	10	0.0070

*The number of expected homozygous cases is based on the frequency of the variant in the control nFE population and a disease prevalence of one ABCA4-associated macular dystrophy patient in 10,000 individuals. This means that the ABCA4-LOVD\_Cauc cohort represents 32,700,000 individuals of a normal population.*

In 37 IRD cases carrying homozygous nontruncating variants, the age of disease onset was reported (Fig. 1). Thirteen variants led to an early average age of onset, which indicates severe pathogenicity of these variants. These included seven missense variants, four complex alleles, and two noncanonical splice site changes.

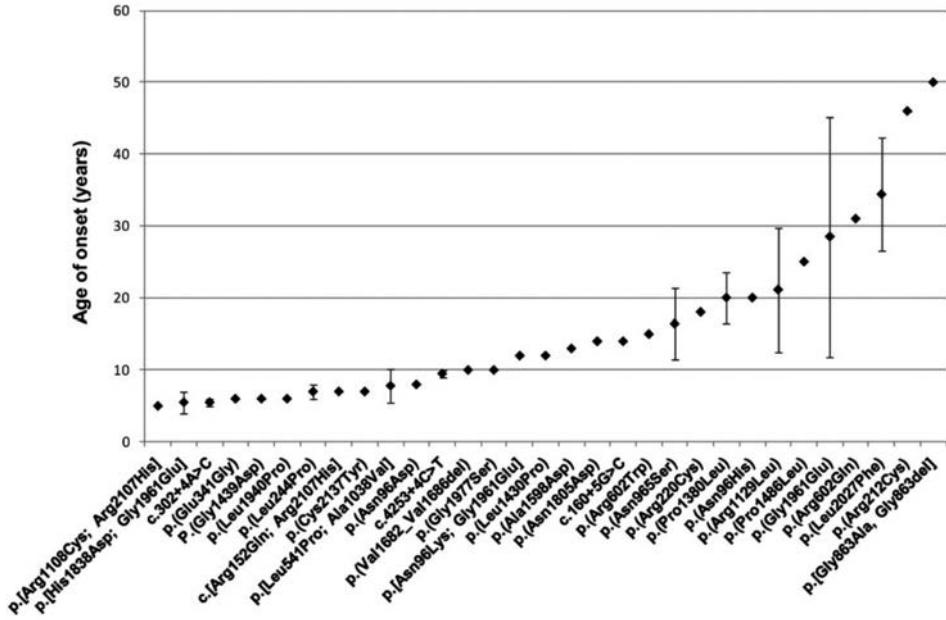


**Figure 1:** Age of disease onset analysis for STGD1 cases carrying homozygous ABCA4 variants. Standard deviations are shown for variants that occurred homozygously more than once.

### Compound heterozygosity analysis of mild ABCA4 variants

The variants that were deemed mild by the homozygosity analysis are expected to be accompanied by a severe allele when they are found on one allele of STGD1 or arCRD patients. In ABCA4-LOVD\_Cauc, a second variant was reported in 160 cases with p.[Gly863Ala, Gly863del], in 34 cases with p.(Ala1038Val), in 73 cases with c.5714+5G>A, in 323 cases with p.(Gly1961Glu), and in 24 cases with p.(Arg2030Gln) cases. As expected, all of these alleles occurred more often with known truncating alleles compared to other nontruncating variants, but this was only significant for the p.(Gly1961Glu) variant ( $P = 0.0076$ , chi-square test, Bonferroni corrected) (Supp. Tables S6 and S7). For the nontruncating variants that were found to accompany mild deemed variants in patients, the reported age of onset was depicted per variant (Supp. Figs. S5–S9). Of note, in eight cases combinations of mild alleles were present in the ABCA4-LOVD dataset with reported ages of onset <20 years, indicating that these data should be interpreted with caution.

### Early onset analysis

Patients that presented with *ABCA4*-associated IRD in the first decade of their life were expected to harbor two severe mutations. For patients with an early age of disease onset mentioned, 20 different missense variants, complex alleles with only missense variants, or noncanonical splice site variants were identified, which thereby are indicated to be severe alleles (Supp. Table S8). This included the p.(Gly1961Glu) variant and interestingly also the complex allele including this same variant, namely p.[His1838Asp; Gly1961Glu]. This could indicate that in the p.(Gly1961Glu) case the presence of the histidine to aspartic acid change may have been missed.

### Complex allele p.[Leu541Pro; Ala1038Val]

Among the 285 complex alleles (Supp. Table S8) that have been reported in the *ABCA4*-LOVD, 195 consisted of the p.[Leu541Pro; Ala1038Val] variant. These were reported in a homozygous state in 18 patients, indicating that this complex allele has a moderate to severe effect on the protein function. Interestingly, both variants alone are also enriched in the *ABCA4*-LOVD\_Cauc dataset. Individually, the p.(Leu541Pro) and p.(Ala1038Val) variants have allele frequencies of 0.000180 and 0.00196, respectively, in the nFE ExAC. As mentioned above, the single p.(Ala1038Val) variant was defined as a mild variant based on its frequency. The p.(Leu541Pro) variant does occur in a homozygous manner in the *ABCA4*-LOVD dataset and is therefore expected to have a moderate to severe effect on its own.

### Protein domain variant analysis

To assess the variant distribution over the different protein domains, SMART domains and their locations were obtained from <http://smart.embl-heidelberg.de/>. Two ATPase domains were present at amino acid positions 955–1145 and 1964–2148 (Fig. 2). The number of missense variants per ATPase domain and the number of missense variants for all transmembrane regions combined were compared to the expected amount of variants per domain based on the fraction of variants per each domain in the ExAC database. Interestingly, the amount of variants in the ATPase domains was significantly higher than expected ( $P = 1.2^{-07}$  for the first domain,  $P = 4.7^{-05}$  for the second domain, chi-square test, Bonferroni corrected), whereas the amount of variants in the transmembrane regions was not significantly higher ( $P = 0.26$ , chi-square test).

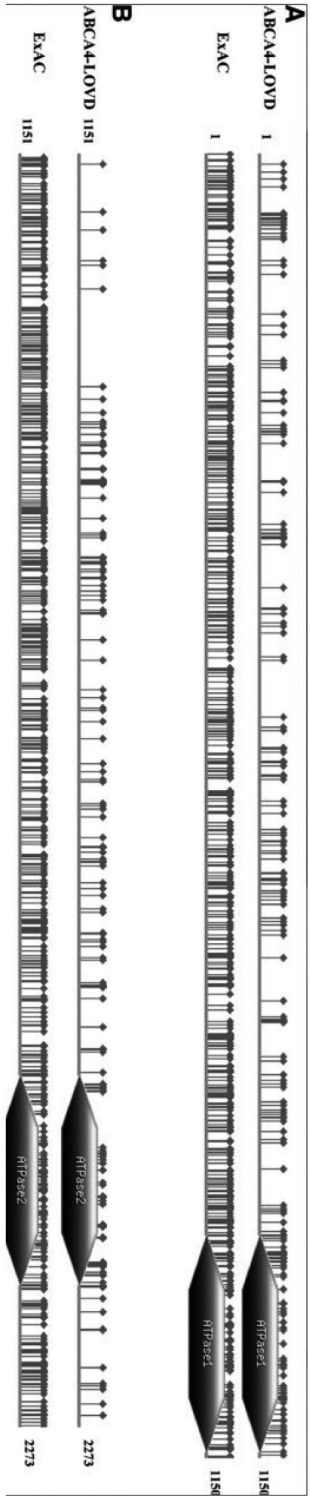


**Figure 2:** Schematic distribution of missense variants in ABCA4. **(A)** Missense variants enriched in the first 1,150 amino acids of the ABCA4 protein in the ABCA4-LOVD\_Cauc group (top) compared to the missense variants specific for ExAC (bottom). **(B)** Missense variants enriched in the last 1,123 amino acids of the ABCA4 protein in the ABCA4-LOVD\_Cauc group (top) compared to the missense variants specific for ExAC (bottom). Each flag represents a missense



### Benign variants

Thirty variants were published to be disease causing while their frequency in the *ABCA4*-LOVD dataset was lower than in the ExAC database. This makes their pathogenicity unlikely, and therefore, these variants were classified as category 4 (likely benign) in the LOVD database ([Supp. Table S9](#)). However, the low frequency ratio of some of these variants may result from a reporting bias, if they were identified but not published as causative because of their relatively high frequency. Ten of these variants have an allele frequency in the nFE population that is higher than 0.005. Based on Hardy–Weinberg equations, these variants cannot be disease causing in view of the prevalence of the disease and are therefore classified as category 5 (benign) ([Supp. Table S9](#)).

Furthermore, five variants that were significantly enriched in the *ABCA4*-LOVD dataset had allele frequencies of  $>0.005$  in a population other than the nFE population, which could indicate a mild pathogenic nature of these variants or a benign nature. In the latter case, the patients carrying these variants most likely descend from a person of a non-nFE ethnicity (comments in [Supp. Table S2](#)). Finally, 269 variants were found not to be enriched significantly, although their frequency was higher in the cohort than it was in the control population. These variants were classified as having an uncertain significance ([Supp. Table S10](#)).

### Splice site predictions

Among the noncanonical splice site changes (i.e., splice acceptor site variants at intronic positions  $-3$  to  $-14$ , splice donor site variants at intronic positions  $+3$  to  $+8$ , or the first or last nucleotide of the exon), 30 variants were found to be enriched in *ABCA4*-LOVD\_Cauc. Additionally, 10 deep intronic variants and 15 other noncanonical splice site variants were present in the total *ABCA4*-LOVD dataset. For 34 of the variants close to the exon borders, at least three of five splice site prediction programs predicted that the splice site had a reduced splice prediction score of at least 10%. Furthermore, seven deep intronic variants were predicted to create new splice sites ([Supp. Table S11](#)). Splice predictions for missense variants led to the identification of 13 missense variants that show a decrease in canonical splice site prediction scores of  $>10\%$  ([Supp. Table S12](#)).

Synonymous variants in the *ABCA4*-LOVD\_Cauc, including polymorphisms, were collected and *in silico* assessed ([Supp. Table S13](#)). The c.6342G>A variant has a high ratio of *ABCA4*-LOVD\_Cauc frequency/ExAC frequency ( $>40$ ) and showed mild to high predictions for the introduction of a new splice site by all five splice site prediction programs (an increase in a predicted splice site ranging between 1.2 and 72% of the total possible scores). Furthermore, for four additional

synonymous variants (i.e., c.618C>T, c.873G>A, c.4128G>A, and c.4773G>C), a decrease or increase of >10% of the total possible splice prediction score was predicted by at least three out of five programs, indicating a possible pathogenic nature of these variants.

### ACMG variant classification

Finally, all the variants from the ABCA4-LOVD dataset were classified according to the new guidelines of the ACMG (November, 2015). By the classification mentioned in the Methods section, 195 variants were classified as pathogenic, 274 as likely pathogenic, 260 as uncertain significance, and 10 as benign. Interestingly, there was one variant, c.2948C>T, which was not present in the ABCA4-LOVD\_Cauc, but was still classified as likely pathogenic due to its location in domain 1, the fact that other variants in this codon have been reported to cause disease as well, and its high *in silico* scores (PhyloP 6.41, CADD 25.8, and Grantham 89). Finally, 21 missense variants had a moderate to high OR and Grantham score, predicting them to be of a moderate to severe pathogenicity. Of note, 18 frameshift, stop, and canonical splice site variants were classified as “uncertain significance” due to the lack of supporting information to classify them as pathogenic.

### Leiden Open Source Variant Database

All the recorded published variants with the description of the phenotype, including age of onset, phenotype of onset, segregation information, and disease definitions, when given, were uploaded to the LOVD ([www.LOVD.nl/ABCA4](http://www.LOVD.nl/ABCA4)). Their references can be found in the Suppl. Materials. Furthermore, all the variants were categorized as either (1) pathogenic, (2) likely pathogenic, (3) uncertain significance, (4) likely benign or (5) benign based on the frequency data, enrichment in the ABCA4-LOVD dataset, and whether or not the variant was truncating as mentioned above.

## Discussion

We collected *ABCA4* variants from 4,137 patients with *ABCA4*-associated phenotypes. Of the 913 different reported variants, the majority comprised missense variants (51.6%), followed by protein-truncating variants (34.4%) (Table 1).

### Severity classification

In this study, 316 variants have been found to be significantly enriched in the *ABCA4* gene of likely Caucasian IRD patients. These include 125 truncating variants, 169 missense variants, 18 noncanonical variants, and four small insertion/deletions (Table 2). We predicted 81 variants to have a moderately severe to severe pathogenic nature based on allele combinations, early onset disease analysis, and *in silico* assessments.

Furthermore, five variants (p.[Gly863Ala, Gly863del], p.(Gly1961Glu), p.(Ala1038Val), c.5714+5G>A, p.(Arg2030Gln)) were identified to have a mild pathogenic effect in most cases based on their low or absent homozygous occurrence, while having a relatively high allele frequency. One interesting finding was the homozygous occurrence of p.(Gly1961Glu) in 16 different cases, including two cases with an early age at onset. Even though this is still significantly less than expected based on the frequency in ExAC (chi-square test,  $P = 3.5 \times 10^{-173}$ ), it indicates that in a small percentage of cases the p.(Gly1961Glu) allele can act as a moderate to severe variant. In the *ABCA4*-LOVD dataset, eleven complex alleles containing p.(Gly1961Glu) were reported. This could indicate that the p.(Gly1961Glu) variant is an old variant next to which multiple other variants have arisen over time *in cis* due to recombination or *de novo* mutation events, such as in the case of p.[His1838Asp; Gly1961Glu]. Alternatively, although deletions are very rare in *ABCA4* [Yatsenko et al., 2003; Zernant et al., 2014], a small fraction of these homozygous cases might be explained by sizeable heterozygous deletions overlapping these variants [Maugeri et al., 1999; Rozet et al., 1999].

Interestingly, the p.(Asp2177Asn) variant was clearly not enriched in the *ABCA4*-LOVD\_Cauc dataset, whereas this variant has been associated with age-related macular degeneration in a previous study [Zhang et al., 2015]. Furthermore, five variants were significantly enriched in the *ABCA4*-LOVD patient dataset, while their frequency in another population was  $>0.005$ . This could either indicate a mild pathogenic nature of the variants or false positives due to descent from a non-Caucasian ancestor.

Finally, we note that polymorphisms present in more than 25% of persons in the general population were frequently reported as causative. Medical doctors should, therefore, assess an *ABCA4* variant in their patient with caution when it has been reported in STGD1/CRD patients, as it might still be a benign variant. This paper provides a list of variants that can be used to check if a variant is likely pathogenic based on data in a Caucasian population.

### Additional findings

For a genotype–phenotype assessment, we looked at age of onset and variant relationships. We identified cases with an unexpected early age of onset based on the mild pathogenicity of the variants that were identified. Therefore, the assessment of the variants solely based on the age of onset or the occurrence with a mild allele is not trustworthy on its own. Similarly, we have found mild mutations in a homozygous state, which raises questions about the other variants that have been found in a homozygous state. However, due to the low frequency of those variants, the chances are very small that their homozygous state occurred by chance in a patient with a STGD1/CRD phenotype, without additional variants having been identified. Other phenotypic data were not taken up in the analysis, because there is too much variation in criteria used for diagnoses of the patients. Additionally, we found a significant correlation between ORs of *ABCA4* missense variants and the age of onset in STGD1 and arCRD patients that presented with one of these missense variants on one allele and a truncating variant on the other allele, whereas Grantham, PhyloP, and CADD scores did not correlate significantly with the age of onset of these patients.

In the protein domain analysis, we tested if the number of mutations in the *ABCA4* protein domains was enriched in the *ABCA4*-LOVD\_Cauc dataset to investigate whether certain domains are more crucial for normal protein function. In the *ABCA4*-LOVD\_Cauc dataset, the number of missense variants in the first ATPase domain of the protein is significantly higher compared to what would be expected based on the missense variant density in that domain in the nFE population ( $P = 1.2^{-07}$ , chi-square test, Bonferroni corrected). The same is true for the second ATPase domain of the protein, although this is less significant ( $P = 4.7^{-05}$ , chi-square test, Bonferroni corrected). This could be in line with the findings of Ahn et al. [2003], which indicated that the first ATPase domain binds ATP better and has more ATPase activity than the second. The same paper shows that the combination of both domains has increased ATPase binding and activity compared to each of the domains on their own [Ahn et al., 2003].

## Confounders

In this study, we used all the published variants in *ABCA4* that have been found in Stargardt disease and CRD patients. However, the use of different techniques to identify variants in *ABCA4* may have caused a bias in the data because each of the mutation scanning techniques is imperfect. This should be taken into account when interpreting the identified enrichment of certain variants in this dataset.

We deemed five variants to have a mild pathogenicity effect due to their high relative frequency and the low or absent amount of patients that are homozygous for these mutations. Perhaps not all studies have reported these variants due to the possibility that their high frequency has been interpreted as belonging to a benign variant. This might especially be the case for the p.(Ala1038Val) variant, which often occurs together with the p.(Leu541Pro) variant in *cis* and could therefore have been omitted from publications. Therefore, replication of this result in a dataset of patients in which it is known that all the p.(Ala1038Val) variants found in the dataset have been taken along in the analysis will be needed to confirm this result.

Low *ABCA4* expression levels due to variants in *cis*- or *trans*-acting elements could explain the high amount of monoallelic cases. Ensembl reports ~20 enhancer regions near *ABCA4* [Flicek et al., 2014]. Furthermore, Scheetz et al. found an eQTL, a c-Rel binding site, 6.6 kb upstream of the transcription start site in the SHRSP rat that correlated with increased *Abca4* expression, and which was absent in SR/JrHsd rats [Scheetz et al., 2006]. The region 10 kb upstream of the human *ABCA4* gene contains more than six elements that meet the c-Rel binding site motif according to Chen and Ghosh [1999] that might have a similar function.

In 9.5% of the identified alleles, complex alleles were identified. Our variant analyses in persons carrying homozygous or compound heterozygous variants did not take into account that additional unknown noncoding variants could similarly be in linkage disequilibrium with the studied variants. Furthermore, in particular in monoallelic cases, we cannot exclude the possibility that the actual cause of disease is situated in other genes [Littink et al., 2010; Zaneveld et al., 2015].

One limitation of this study is that the ExAC dataset containing control individuals does not match the population of published patients perfectly. Even though both datasets contain non-Finnish Caucasian individuals, the *ABCA4*-LOVD\_Cauc dataset is obtained from different locations, creating a bias toward benign variants that are frequent in *ABCA4*-LOVD\_Cauc. Furthermore, the ExAC database can contain STGD1 patients, which were genotyped as healthy controls before presenting with

symptoms. However, in view of the prevalence of *ABCA4*-associated STGD1 and arCRD (~1 in 8,000 individuals) and the large allelic heterogeneity, our assessment of individual variants can only be slightly affected by the presence of a few STGD1 or arCRD cases in ExAC. Another limitation is the fact that the patients present in this study over time were diagnosed by different ophthalmologists using different criteria and that their genotypes have been revealed by different techniques. Therefore, there is no consistency in how many regions of the gene have not been tested (accurately) causing an underestimation of the total number of variants present in the *ABCA4*-LOVD group.

### Splice site prediction programs

In our scoring procedure, we gave the results of each prediction program the same weight, even though Tang et al. reported that splice prediction programs differ in their prediction strength, depending on the variant location affecting splicing [Tang et al., 2016]. Of note, when we assessed all the possible noncanonical splice site variants, we encountered a small deficiency in the assessment of the Human Splicing Finder prediction tool. In some cases, the reference score changed when we looked at different variants that were situated close the same splice site (e.g., the reference splice site at c.4773 was 86.0 when assessing c.4773+3A>G and was 84.6 when assessing c.4773+5G>A). Although no extreme differences were encountered, it does decrease the reliability of this version of the tool.

### Leiden Open Source Variant Database

All the data that were collected in this study have been merged with a small set of previously registered variants and uploaded in the publicly available *ABCA4* LOVD. By combining as many data as possible, we were able to identify many variants to be associated with IRDs. We consider our efforts as a first significant step toward a comprehensive *ABCA4* LOVD as thousands of *ABCA4* variants have likely been identified in academic and nonacademic diagnostic centers, but have not been published. Sharing genetic data of additional patients will increase statistical power and can lead to the classification of additional pathogenic and benign variants. If scientific journals would make uploading of IRD-associated variants in publicly available databases compulsory for the acceptance of papers, a growing body of variant data would become available to systematically assess the functionalities of IRD-associated variants.

### Future research

At the moment, mainly Caucasian patients have been genotyped and often the ethnicity of patients is not well annotated. Collecting more accurate data of patients of all ethnicities will give a better overview of *ABCA4* variants in STGD1

patients worldwide. Furthermore, in order to use phenotypic data to investigate the direct effect of a variant on the phenotype, it would be very useful if more standardized criteria will be used worldwide, such as the Fishman criteria for diagnosing different stages of STGD1 [Fishman et al., 1999]. *In vivo* analysis of variants in retinal organoids can finally be used to confirm pathogenicity as well as to assess haplotype effects on expression levels.

## References

- Ahn J, Beharry S, Molday LL, Molday RS. 2003. Functional Interaction between the Two Halves of the Photoreceptor-specific ATP Binding Cassette Protein ABCR (ABCA4) EVIDENCE FOR A NON-EXCHANGEABLE ADP IN THE FIRST NUCLEOTIDE BINDING DOMAIN. *Journal of Biological Chemistry* 278(41):39600-39608.
- Allikmets R, Shroyer NF, Singh N, Seddon JM, Lewis RA, Bernstein PS, Peiffer A, Zabriskie NA, Li Y, Hutchinson A. 1997. Mutation of the Stargardt disease gene (ABCR) in age-related macular degeneration. *Science* 277(5333):1805-1807.
- Allikmets, R, Singh, N, Sun, H, Shroyer, NF, Hutchinson, A, Chidambaram, A, Gerrard, B, Baird, L, Stauffer, D, Peiffer, A, Rattner, A, Smallwood, P, et al. 1997b. A photoreceptor cell-specific ATP-binding transporter gene (ABCR) is mutated in recessive Stargardt macular dystrophy. *Nat Genet* 15: 236–246.
- Bauwens M, De Zaeytijd J, Weisschuh N, Kohl S, Meire F, Dahan K, Depasse F, De Jaegere S, De Ravel T, De Rademaeker M. 2015. An augmented ABCA4 screen targeting noncoding regions reveals a deep intronic founder variant in Belgian Stargardt patients. *Human mutation* 36(1):39-42.
- Bax NM, Sangermano R, Roosing S, Thiadens AA, Hoefsloot LH, den Born LI, Phan M, Klevering BJ, Westeneng-van Haaften C, Braun TA. 2015. Heterozygous Deep-Intronic Variants and Deletions in ABCA4 in Persons with Retinal Dystrophies and One Exonic ABCA4 Variant. *Human mutation* 36(1):43-47.
- Benjamini Y, Hochberg Y. 1995. Controlling the false discovery rate: a practical and powerful approach to multiple testing. *Journal of the Royal Statistical Society. Series B (Methodological)*:289-300.
- Braun TA, Mullins RF, Wagner AH, Andorf JL, Johnston RM, Bakall BB, Deluca AP, Fishman GA, Lam BL, Weleber RG. 2013. Non-exonic and synonymous variants in ABCA4 are an important cause of Stargardt disease. *Human molecular genetics* 22(25):5136-5145.
- Cartegni L, Wang J, Zhu Z, Zhang MQ, Krainer AR. 2003. ESEfinder: a web resource to identify exonic splicing enhancers. *Nucleic acids research* 31(13):3568-3571.
- Chen FE, Ghosh G. 1999. Regulation of DNA binding by Rel/NF- $\kappa$ B transcription factors: structural views. *Oncogene* 18(49).
- Collin, RW, den Hollander, AI, der Velde-Visser, SD, Benniselli, J, Bennett, J, Cremers, FP. 2012. Antisense oligonucleotide (AON)-based therapy for leber congenital amaurosis caused by a frequent mutation in CEP290. *Mol Ther Nucleic Acids* 1: e14.
- Cremers FP, van de Pol DJ, van Driel M, den Hollander AI, van Haren FJ, Knoers NV, Tijmes N, Bergen AA, Rohrschneider K, Blankenagel A. 1998. Autosomal recessive retinitis pigmentosa and cone-rod dystrophy caused by splice site mutations in the Stargardt's disease gene ABCR. *Human molecular genetics* 7(3):355-362.
- Dalkara D, Goureau O, Marazova K, Sahel JA. 2016. Let there be light: gene and cell therapy for blindness. *Human gene therapy(ja)*.
- Desmet F-O, Hamroun D, Lalonde M, Collod-Bérout G, Claustres M, Bérout C. 2009. Human Splicing Finder: an online bioinformatics tool to predict splicing signals. *Nucleic acids research* 37(9):e67-e67.
- Dryja TP, Briggs CE, Berson EL, Rosenfeld PJ, Abitbol M. 1998. ABCR gene and age-related macular degeneration. *Science* 279(5354):1107-1107.
- Fishman, GA, Stone, EM, Grover, S, Derlacki, DJ, Haines, HL, Hockey, RR. 1999. Variation of clinical expression in patients with Stargardt dystrophy and sequence variations in the ABCR gene. *Arch Ophthalmol* 117: 504–510.
- Flicek P, Amode MR, Barrell D, Beal K, Billis K, Brent S, Carvalho-Silva D, Clapham P, Coates G, Fitzgerald S. 2014. Ensembl 2014. *Nucleic acids research* 42(D1):D749-D755.



- Fritsche LG, Fleckenstein M, Fiebig BS, Schmitz-Valckenberg S, Bindewald-Wittich A, Keilhauer CN, Renner AB, Mackensen F, Mößner A, Pauleikhoff D. 2012. A Subgroup of Age-Related Macular Degeneration is Associated With Mono-Allelic Sequence Variants in the ABCA4 Gene. *Age-Related Macular Degeneration. Investigative ophthalmology & visual science* 53(4):2112-2118.
- Fujinami, K, Lois, N, Mukherjee, R, McBain, VA, Tsunoda, K, Tsubota, K, Stone, EM, Fitzke, FW, Bunce, C, Moore, AT, Webster, AR, Michaelides, M. 2013. A longitudinal study of Stargardt disease: quantitative assessment of fundus autofluorescence, progression, and genotype correlations. *Invest Ophthalmol Vis Sci* 54: 8181– 8190.
- Fujinami, K, Zernant, J, Chana, RK, Wright, GA, Tsunoda, K, Ozawa, Y, Tsubota, K, Robson, AG, Holder, GE, Allikmets, R. 2015. Clinical and molecular characteristics of childhood-onset Stargardt disease. *Ophthalmology* 122: 326– 334.
- Garanto, A, Chung, DC, Duijkers, L, Corral-Serrano, JC, Messchaert, M, Xiao, R, Bennett, J, Vandenberghe, LH, Collin, RW. 2016. In vitro and in vivo rescue of aberrant splicing in CEP290-associated LCA by antisense oligonucleotide delivery. *Hum Mol Genet* 25: 2552– 2563.
- Gerard X, Garanto A, Rozet J-M, Collin RW. 2016. Antisense Oligonucleotide Therapy for Inherited Retinal Dystrophies. *Retinal Degenerative Diseases: Springer*. p 517-524.
- Grantham R. 1974. Amino acid difference formula to help explain protein evolution. *Science* 185(4154):862-864.
- Guymer RH, Héon E, Lotery AJ, Munier FL, Schorderet DF, Baird PN, McNeil RJ, Haines H, Sheffield VC, Stone EM. 2001. Variation of codons 1961 and 2177 of the Stargardt disease gene is not associated with age-related macular degeneration. *Archives of ophthalmology* 119(5):745-751.
- Karolchik D, Hinrichs AS, Furey TS, Roskin KM, Sugnet CW, Haussler D, Kent WJ. 2004. The UCSC Table Browser data retrieval tool. *Nucleic acids research* 32(suppl 1):D493-D496.
- Kircher M, Witten DM, Jain P, O’Roak BJ, Cooper GM, Shendure J. 2014. A general framework for estimating the relative pathogenicity of human genetic variants. *Nature genetics* 46(3):310.
- Kjellstrom, U. 2014. Association between genotype and phenotype in families with mutations in the ABCA4 gene. *Mol Vis* 20: 89– 104.
- Klevering, BJ, Deutman, AF, Maugeri, A, Cremers, FP, Hoyng, CB. 2005. The spectrum of retinal phenotypes caused by mutations in the ABCA4 gene. *Graefes Arch Clin Exp Ophthalmol* 243: 90– 100.
- Lambertus S, van Huet RA, Bax NM, Hoefsloot LH, Cremers FP, Boon CJ, Klevering BJ, Hoyng CB. 2015. Early-onset Stargardt disease: phenotypic and genotypic characteristics. *Ophthalmology* 122(2):335-344.
- Lewis, RA, Shroyer, NF, Singh, N, Allikmets, R, Hutchinson, A, Li, Y, Lupski, JR, Leppert, M, Dean, M. 1999. Genotype/phenotype analysis of a photoreceptor-specific ATP-binding cassette transporter gene, ABCR, in Stargardt disease. *Am J Hum Genet* 64: 422– 434.
- Littink KW, Koenekoop RK, van den Born LI, Collin RW, Moruz L, Veltman JA, Roosing S, Zonneveld MN, Omar A, Darvish M and others. 2010. Homozygosity mapping in patients with cone-rod dystrophy: novel mutations and clinical characterizations. *Invest Ophthalmol Vis Sci* 51(11):5943-51.
- Martinez-Mir, A, Paloma, E, Allikmets, R, Ayuso, C, del Rio, T, Dean, M, Vilageliu, L, Gonzalez-Duarte, R, Balcells, S. 1998. Retinitis pigmentosa caused by a homozygous mutation in the Stargardt disease gene ABCR. *Nat Genet* 18: 11– 12.
- Maugeri, A, Klevering, BJ, Rohrschneider, K, Blankenagel, A, Brunner, HG, Deutman, AF, Hoyng, CB, Cremers, FP. 2000. Mutations in the ABCA4 (ABCR) gene are the major cause of autosomal recessive cone-rod dystrophy. *Am J Hum Genet* 67: 960– 966.

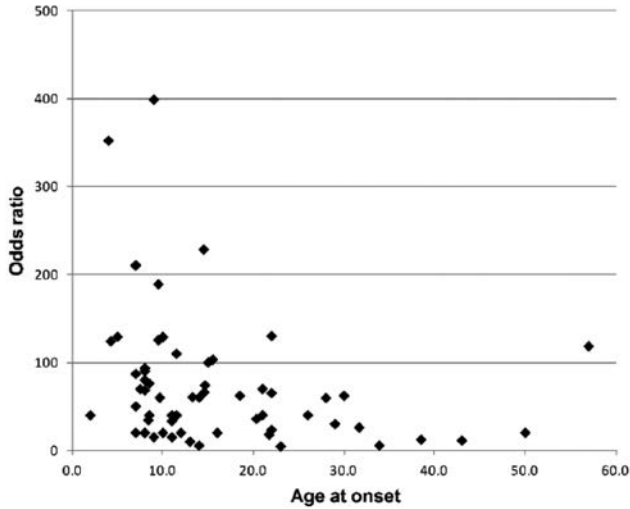
- Maugeri A, van Driel MA, van de Pol DJ, Klevering BJ, van Haren FJ, Tijmes N, Bergen AA, Rohrschneider K, Blankenagel A, Pinckers AJ and others. 1999b. The 2588G-->C mutation in the ABCR gene is a mild frequent founder mutation in the Western European population and allows the classification of ABCR mutations in patients with Stargardt disease. *Am J Hum Genet* 64(4):1024-35.
- Molday, RS, Zhong, M, Quazi, F. 2009. The role of the photoreceptor ABC transporter ABCA4 in lipid transport and Stargardt macular degeneration. *BBA-Mol Cell Biol* L1791: 573– 583.
- Pertea M, Lin X, Salzberg SL. 2001. GeneSplicer: a new computational method for splice site prediction. *Nucleic acids research* 29(5):1185-1190.
- Reese MG, Eeckman FH, Kulp D, Haussler D. 1997. Improved splice site detection in Genie. *Journal of computational biology* 4(3):311-323.
- Richards, S, Aziz, N, Bale, S, Bick, D, Das, S, Gastier-Foster, J, Grody, WW, Hegde, M, Lyon, E, Spector, E. 2015. Standards and guidelines for the interpretation of sequence variants: a joint consensus recommendation of the American College of Medical Genetics and Genomics and the association for molecular pathology. *Genet Med* 17: 405– 423.
- Rivera, A, White, K, Stohr, H, Steiner, K, Hemmrich, N, Grimm, T, Jurklies, B, Lorenz, B, Scholl, HP, Apfelstedt-Sylla, E, Weber, BH. 2000. A comprehensive survey of sequence variation in the ABCA4 (abcr) gene in Stargardt disease and age-related macular degeneration. *Am J Hum Genet* 67: 800– 813.
- Rozet, JM, Gerber, S, Ghazi, I, Perrault, I, Ducroq, D, Souied, E, Cabot, A, Dufier, JL, Munnich, A, Kaplan, J. 1999. Mutations of the retinal specific ATP binding transporter gene (abcr) in a single family segregating both autosomal recessive retinitis pigmentosa rp19 and Stargardt disease: evidence of clinical heterogeneity at this locus. *J Med Genet* 36: 447– 451.
- Rozet, JM, Gerber, S, Souied, E, Perrault, I, Chatelin, S, Ghazi, I, Leowski, C, Dufier, JL, Munnich, A, Kaplan, J. 1998. Spectrum of ABCR gene mutations in autosomal recessive macular dystrophies. *Eur J Hum Genet* 6: 291– 295.
- Sangermano, R, Bax, NM, Bauwens, M, den Born, LI, Baere, E, Garanto, A, Collin, RW, Goercharn-Ramlal, AS, den Engelsman-van Dijk, AH, Rohrschneider, K. 2016. Photoreceptor progenitor mRNA analysis reveals exon skipping resulting from the ABCA4 c. 5461-10t→ C mutation in Stargardt disease. *Ophthalmology* 123: 1375– 1385.
- Scheetz TE, Kim K-YA, Swiderski RE, Philp AR, Braun TA, Knudtson KL, Dorrance AM, DiBona GF, Huang J, Casavant TL. 2006. Regulation of gene expression in the mammalian eye and its relevance to eye disease. *Proceedings of the National Academy of Sciences* 103(39):14429-14434.
- Simonelli, F, Testa, F, Zernant, J, Nesti, A, Rossi, S, Allikmets, R, Rinaldi, E. 2005. Genotype-phenotype correlation in Italian families with Stargardt disease. *Ophthalmic Res* 37: 159– 167.
- Souied EH, Ducroq D, Rozet JM, Gerber S, Perrault I, Munnich A, Coscas G, Soubrane G, Kaplan J. 2000. ABCR gene analysis in familial exudative age-related macular degeneration. *Investigative ophthalmology & visual science* 41(1):244-247.
- Stargardt, K. 1909. Über familiäre, progressive degeneration in der maculagegend des auges. *Graefes Arch Clin Exp Ophthalmol* 71: 534– 550.
- Tang, R, Prosser, DO, Love, DR. 2016. Evaluation of bioinformatic programmes for the analysis of variants within splice site consensus regions. *Adv Bioinformatics* 2016: 5614058.
- Utz VM, Coussa RG, Marino MJ, Chappelov AV, Pauer GJ, Hagstrom SA, Traboulsi EI. 2014. Predictors of visual acuity and genotype-phenotype correlates in a cohort of patients with Stargardt disease. *British Journal of Ophthalmology*:bjophthalmol-2013-304270.
- van Driel MA, Maugeri A, Klevering BJ, Hoyng CB, Cremers FP. 1998. ABCR unites what ophthalmologists divide (s). *Ophthalmic genetics* 19(3):117-122.
- Huet, RA, Bax, NM, Westeneng-Van Haaften, SC, Muhamad, M, Zonneveld-Vrieling, MN, Hoefsloot, LH, Cremers, FP, Boon, CJ, Klevering, BJ, Hoyng, CB. 2014. Foveal sparing in Stargardt disease. *Invest Ophthalmol Vis Sci* 55: 7467– 7478.

- Veltman, JA, Brunner, HG. 2012. De novo mutations in human genetic disease. *Nat Rev Genet* 13: 565– 575.
- Webster, AR, Heon, E, Lotery, AJ, Vandenburg, K, Casavant, TL, Oh, KT, Beck, G, Fishman, GA, Lam, BL, Levin, A, Heckenlively, JR, Jacobson, SG, et al. 2001. An analysis of allelic variation in the ABCA4 gene. *Invest Ophthalmol Vis Sci* 42: 1179– 1189.
- Westeneng-van Haaften SC, Boon CJ, Cremers FP, Hoefsloot LH, den Hollander AI, Hoyng CB. 2012. Clinical and genetic characteristics of late-onset Stargardt’s disease. *Ophthalmology* 119(6):1199-1210.
- Yatsenko, AN, Shroyer, NF, Lewis, RA, Lupski, JR. 2003. An ABCA4 genomic deletion in patients with Stargardt disease. *Hum Mutat* 21: 636– 644.
- Yeo G, Burge CB. 2004. Maximum entropy modeling of short sequence motifs with applications to RNA splicing signals. *Journal of Computational Biology* 11(2-3):377-394.
- Zaneveld J, Siddiqui S, Li H, Wang X, Wang H, Wang K, Li H, Ren H, Lopez I, Dorfman A and others. 2015. Comprehensive analysis of patients with Stargardt macular dystrophy reveals new genotype-phenotype correlations and unexpected diagnostic revisions. *Genet Med* 17(4):262-70.
- Zernant J, Xie YA, Ayuso C, Riveiro-Alvarez R, Lopez-Martinez M-A, Simonelli F, Testa F, Gorin MB, Strom SP, Bertelsen M. 2014b. Analysis of the ABCA4 genomic locus in Stargardt disease. *Human molecular genetics*:ddu396.
- Zhang R, Wang L-Y, Wang Y-F, Wu C-R, Lei C-L, Wang M-X, Ma L. 2015. Associations of the G1961E and D2177N variants in ABCA4 and the risk of age-related macular degeneration. *Gene* 567(1):51-57.

## Supplementary material

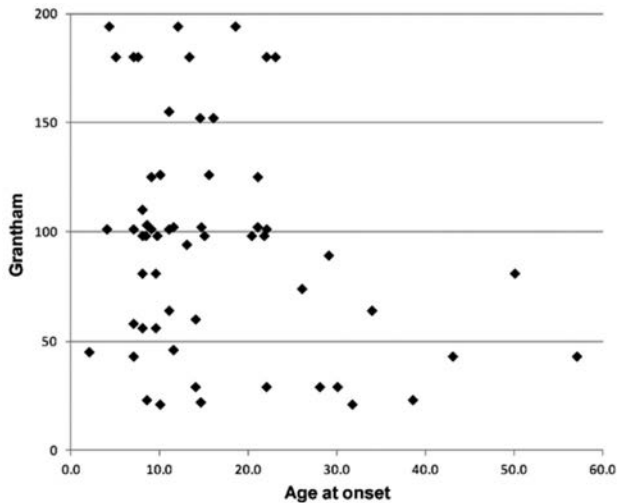
Figures, legends to supplementary tables (Excel file) by references of publications 1997-2015 listing ABCA4 variants.

**Supplementary Figure 1:**



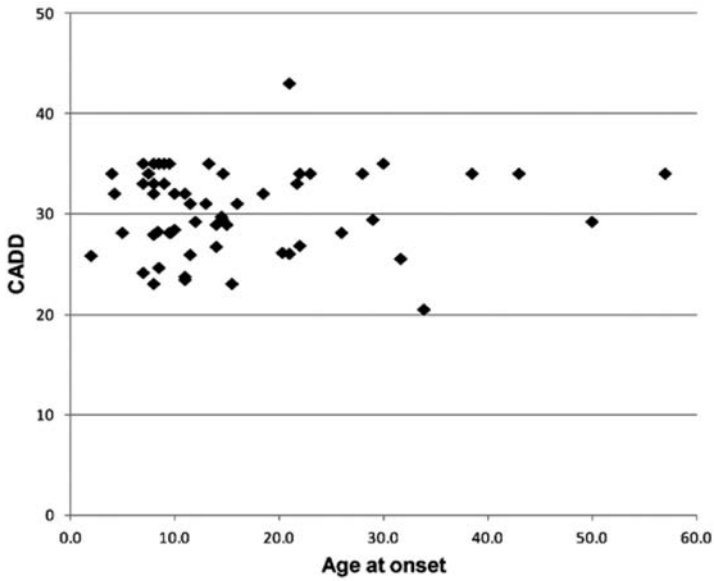
Age of onset of patients with one null allele and one missense variant plotted against the odds ratio of the missense variant. The age of onset correlates with the odds ratio ( $\rho = -0.34$ ,  $p < 0.03$ , Bonferroni corrected).

**Supplementary Figure 2:**



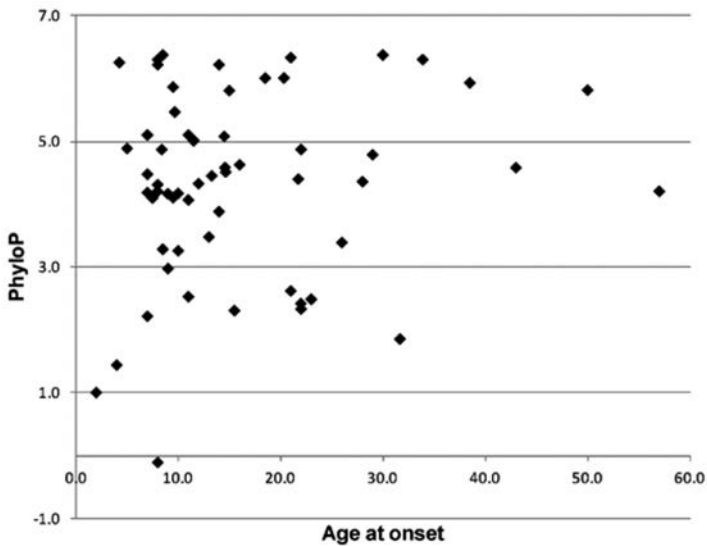
Age of onset of patients with one null allele and one missense variant plotted against the Grantham score of the missense variant. The age of onset does not correlate significantly with the Grantham score ( $\rho = -0.21$ ,  $p < 0.20$ ).

**Supplementary Figure 3:**



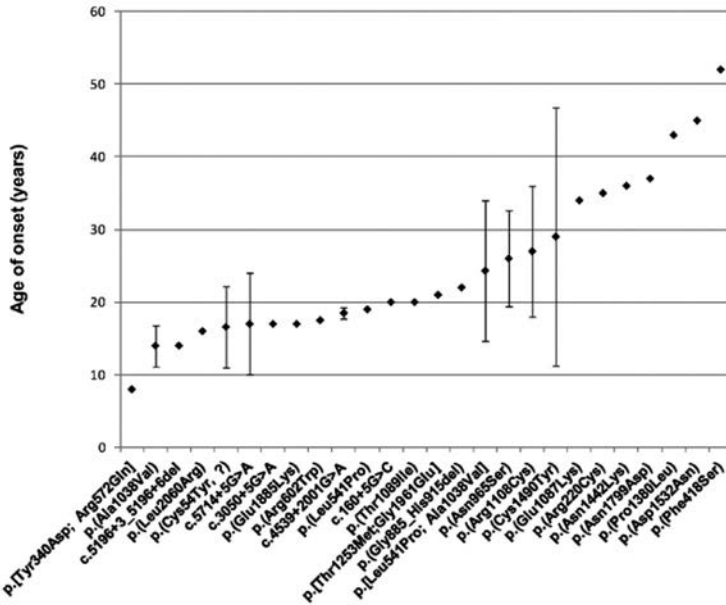
Age of onset of patients with one null allele and one missense variant plotted against the CADD score of the missense variant. The number of patients in this analysis seemed too small to perform statistics.

**Supplementary Figure 4:**



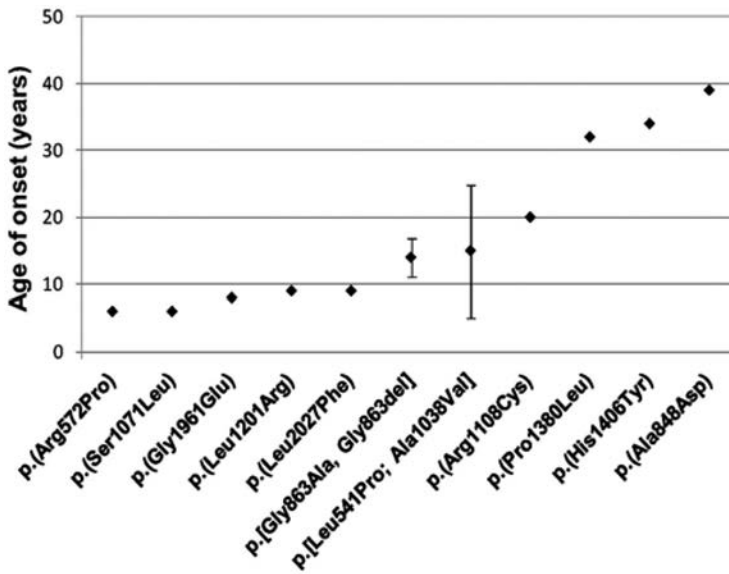
Age of onset of patients with one null allele and one missense variant plotted against the PhyloP score of the missense variant. The age of onset does not significantly correlate with the PhyloP score ( $p = 0.13$ ,  $p > 0.25$ , Bonferroni corrected).

Supplementary Figure 5:



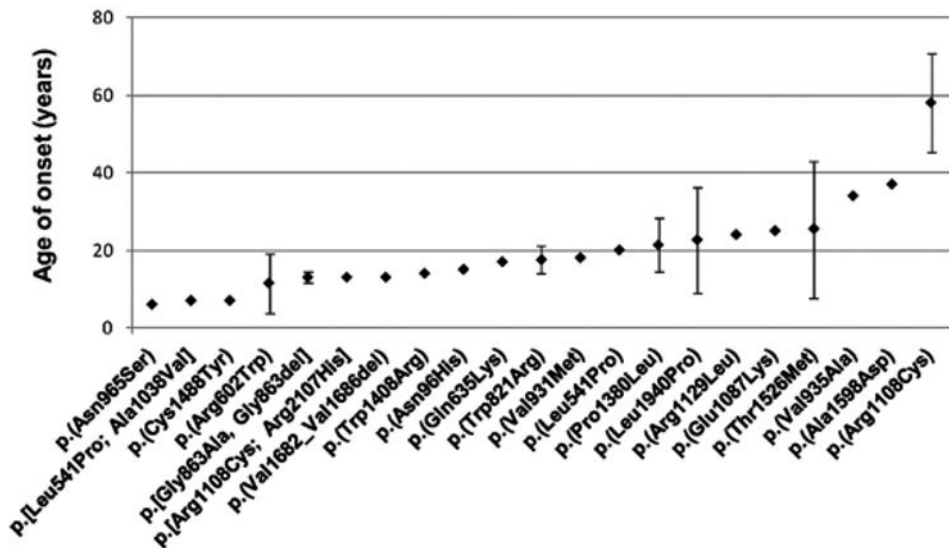
Age of onset analysis for compound heterozygotes carrying one mild c.2588G>C variant. Standard deviations are shown for variants that were reported with an age of onset more than once.

Supplementary Figure 6:



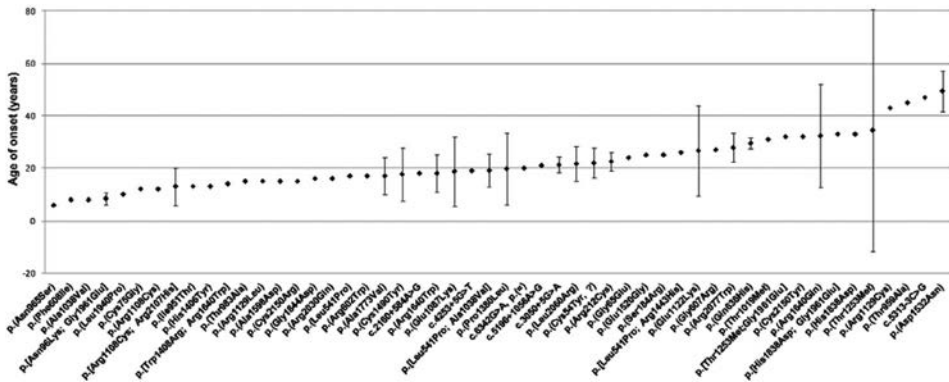
Age of onset analysis for compound heterozygotes carrying one mild c.3113C>T variant. Standard deviations are shown for variants that were reported with an age of onset more than once.

Supplementary Figure 7

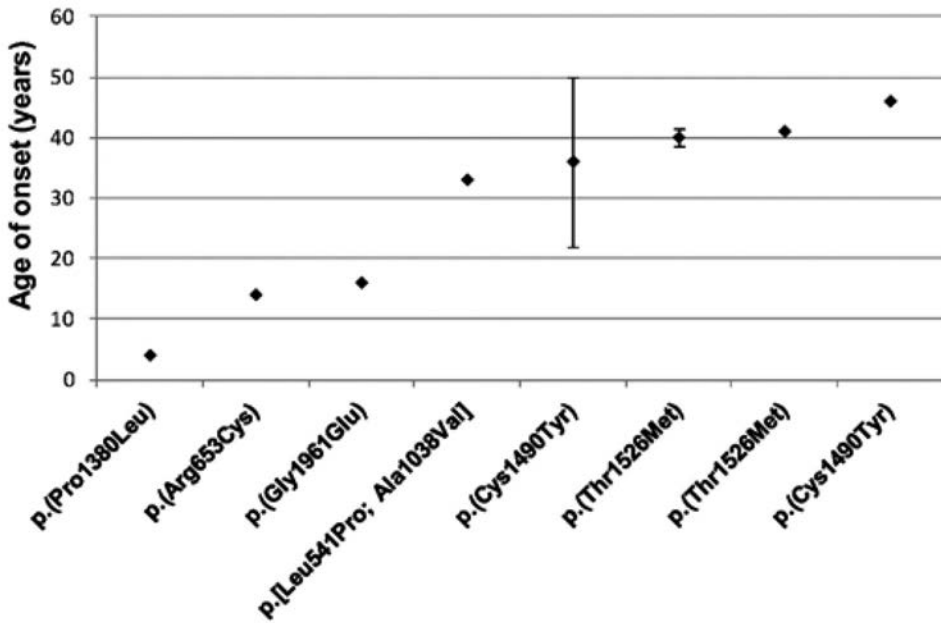


Age of onset analysis for compound heterozygotes carrying one mild c.5714+5G>A variant. Standard deviations are shown for variants that were reported with an age of onset more than once.

Supplementary Figure 8:



Age of onset analysis for compound heterozygotes carrying one mild c.5882G>A variant. Standard deviations are shown for variants that were reported with an age of onset more than once.

**Supplementary Figure 9:**

Age of onset analysis for compound heterozygotes carrying one mild c.6089G>A variant. Standard deviations are shown for variants that were reported with an age of onset more than once

**Legends of supplementary tables**

The Excel file of supplementary tables is available at <https://onlinelibrary.wiley.com/doi/full/10.1002/humu.23165>; section “supporting information” (humu23165-superior-0002-tableS1-S13.xlsx).

**Table S1.** Overview of *ABCA4* variants in 3,928 patients with retinal dystrophy. References to each variant can be found online at [www.LOVD.nl/ABCA4](http://www.LOVD.nl/ABCA4). Genomic location, DNA variant, protein variant, *ABCA4*-LOVD allele count (AC), *ABCA4*-LOVD allele frequency (AF), ExAC allele frequency, the study variant severity classification and the ACMG variant severity classification (Richards, et al., 2015) are given for each non-complex and non-deep intronic variant. Complex and deep-intronic variants are given at the bottom. For the classification of this study the following criteria were used. Benign: ExAC allele frequency >0.006; Likely benign: (*ABCA4*-LOVD AF/ExAC non-Finnish Caucasian AF) <1; Unknown pathogenicity: (*ABCA4*-LOVD AF/ExAC non-Finnish Caucasian AF) >1, however not significantly enriched; Likely pathogenic: Non-truncating alleles, significantly enriched in *ABCA4*-LOVD or truncating alleles, not significantly enriched in *ABCA4*-LOVD; Pathogenic: Truncating alleles significantly enriched in *ABCA4*-LOVD; Not applicable: variants were identified in patients of a



non- Caucasian ethnicity only. Due to low numbers of reported patients of this ethnicity, variants could not be statistically compared to a matching control group. \*Truncating alleles that were not tested in the Fisher Exact test due to absence in the Caucasian patient cohort. \*\*Truncating alleles that were not significantly enriched in the Caucasian patient cohort.

**Table S2.** Variants significantly enriched in Caucasian retinal dystrophy patients. Variant information, including allele count (AC), allele frequency (AF) and total allele number (AN) are given per variant, as well as statistical information, including odds ratio, odds ratio confidence intervals (CI) (Clower; Clupper) and a false detection rate corrected p-value (Fisher-exact test).

**Table S3.** Missense variants identified in patients with retinal dystrophy. Variant information is given together with *in silico* scores and pathogenicity verdict based on homozygosity, occurrence with the c.2588G>C variant, occurrence with the c.5882G>A variant and occurrence in patients with an early onset.

**Table S4.** Truncating variants identified in patients with retinal dystrophy. Variant information is given together with the odds ratio. \*The *ABCA4*-LOVD allele frequency/ExAC allele frequency as well as the odds ratio are based on a hypothetical occurrence of one allele in the ExAC database, to estimate a minimum.

**Table S5.** Non-truncating alleles identified in a homozygous state in patients with retinal dystrophy. The number of cases with an early age of onset were mentioned for each variant.

**Table S6.** Non-truncating alleles together with the c.2588G>C variant identified in patients with retinal dystrophy.

**Table S7.** Non-truncating alleles together with the c.5882G>A variant identified in patients with retinal dystrophy.

**Table S8.** Complex *ABCA4* alleles identified in retinal dystrophy patients. Allele count and allele frequency of all reported complex alleles in the *ABCA4* gene.

**Table S9.** (Likely) benign variants. Variants with an equal or lower allele frequency in the LOVD-*ABCA4* cohort compared to ExAC. Variants with an allele frequency >0.005 are annotated as benign, the remaining variants are annotated as likely benign.

**Table S10** Variants of uncertain pathogenicity. Both the variants that were not significantly enriched in the ABCA4-LOVD group as well as the variants that were found in patients of ethnicities other than Caucasian are given with their frequency, odds ratios, odds ratio confidence intervals (CI) (Clower; Clupper) as well as *in silico* prediction information.

**Table S11.** Splice site prediction effects of non-canonical splice site variants. Splice site prediction effects are given from SpliceSiteFinder like, MaxEntScan, NNSPLICE, Gene Splicer and Human Splicing Finder, which were obtained by Alamut Visual, version 2.7. Predictions that differ from the original by >10% are marked red.

**Table S12. Splice site prediction effects of missense variants.** Splice site prediction effects are given from SpliceSiteFinder like, MaxEntScan, NNSPLICE, Gene Splicer and Human Splicing Finder, which were obtained by Alamut Visual, version 2.7. Predictions that differ from the original by >10% are marked red. Only the missense variants that showed >10% change by >2 splice prediction programs are mentioned. Variants that are substitutions at the first or last nucleotide of the exon, are in bold.

**Table S13. Splice site prediction effects of synonymous variants.** Splice site prediction effects are given from SpliceSiteFinder like, MaxEntScan, NNSPLICE, Gene Splicer and Human Splicing Finder, which were obtained by Alamut Visual, version 2.7, for variants that decrease the canonical splice site predictions and variants that increase alternative splice sites. Predictions that differ from the original canonical splice site by >10% are marked red. Predictions that occur at a non-canonical position are marked in yellow.

## References of publications 1997-2015 listing ABCA4 variants in patients with retinal dystrophy.

Abu-Safieh L, Alrashed M, Anazi S, Alkuraya H, Khan AO, Al-Owain M, Al-Zahrani J, Al-Abdi L, Hashem M, Al-Tarimi S, Sebai MA, Shamia A et al. 2013. Autozygome-guided exome sequencing in retinal dystrophy patients reveals pathogenetic mutations and novel candidate disease genes. *Genome Res* 23:236-247.

Aguirre-Lamban J, Riveiro-Alvarez R, Garcia-Hoyos M, Cantalapiedra D, Avila-Fernandez A, Villaverde-Montero C, Trujillo-Tiebas MJ, Ramos C, Ayuso C. 2010. Comparison of high-resolution melting analysis with denaturing high-performance liquid chromatography for mutation scanning in the *abca4* gene. *Invest Ophthalmol Vis Sci* 51:2615-2619.

Alapati A, Goetz K, Suk J, Navani M, Al-Tarouti A, Jayasundera T, Tumminia SJ, Lee P, Ayyagari R. 2014. Molecular diagnostic testing by eyeGene: Analysis of patients with hereditary retinal dystrophy phenotypes involving central vision loss. *Invest Ophthalmol Vis Sci* 55:5510-5521.

Allikmets R, Shroyer NF, Singh N, Seddon JM, Lewis RA, Bernstein PS, Peiffer A, Zabriskie NA, Li Y, Hutchinson A, Dean M, Lupski JR et al. 1997a. Mutation of the stargardt disease gene (*abcr*) in age-related macular degeneration. *Science* 277:1805-1807.

Allikmets R, Singh N, Sun H, Shroyer NF, Hutchinson A, Chidambaram A, Gerrard B, Baird L, Stauffer D, Peiffer A, Rattner A, Smallwood P et al. 1997b. A photoreceptor cell-specific atp-binding transporter gene (*abcr*) is mutated in recessive stargardt macular dystrophy. *Nat Genet* 15:236-246.

Allikmets R, Wasserman WW, Hutchinson A, Smallwood P, Nathans J, Rogan PK, Schneider TD, Dean M. 1998. Organization of the *abcr* gene: Analysis of promoter and splice junction sequences. *Gene* 215:111-122.

Audere M, Rutka K, Sepetiene S, Lacey B. 2015. Presentation of complex homozygous allele in *abca4* gene in a patient with retinitis pigmentosa. *Case Rep Ophthalmol Med* 2015:452068.

Battu R, Verma A, Hariharan R, Krishna S, Kiran R, Jacob J, Ganapathy A, Ramprasad VL, Kumaramanickavel G, Jeyabalan N, Ghosh A. 2015. Identification of novel mutations in *abca4* gene: Clinical and genetic analysis of Indian patients with stargardt disease. *Biomed Res Int* 2015:940864.

Baum L, Chan WM, Li WY, Lam DS, Wang PB, Pang CP. 2003. *Abca4* sequence variants in Chinese patients with age-related macular degeneration or stargardt's disease. *Ophthalmologica* 217:111-114.

Bauwens M, De Zaeytijd J, Weisschuh N, Kohl S, Meire F, Dahan K, Depasse F, De Jaegere S, De Ravel T, De Rademaeker M, Loeys B, Coppieters F et al. 2015. An augmented *abca4* screen targeting noncoding regions reveals a deep intronic founder variant in Belgian stargardt patients. *Hum Mutat* 36:39-42.

Bax NM, Sangermano R, Roosing S, Thiadens AA, Hoefsloot LH, van den Born LI, Phan M, Klevering BJ, Westeneng-van Haaften C, Brauns TA, Zonneveld-Vrieling MN, de Wijs I et al. 2015. Heterozygous deep-intronic variants and deletions in *abca4* in persons with retinal dystrophies and one exonic *abca4* variant. *Hum Mutat* 36:43-47.

Beheshtian M, Saeed Rad S, Babanejad M, Mohseni M, Hashemi H, Eshghabadi A, Hajizadeh F, Akbari MR, Kahrizi K, Riazi Esfahani M, Najmabadi H. 2015. Impact of whole exome sequencing among Iranian patients with autosomal recessive retinitis pigmentosa. *Arch Iran Med* 18:776-785.

Beit-Ya'acov A, Mizrahi-Meissonnier L, Obolensky A, Landau C, Blumenfeld A, Rosenmann A, Banin E, Sharon D. 2007. Homozygosity for a novel *abca4* founder splicing mutation is associated with progressive and severe stargardt-like disease. *Invest Ophthalmol Vis Sci* 48:4308-4314.

Birch DG, Peters AY, Locke KL, Spencer R, Megarity CF, Travis GH. 2001. Visual function in patients with cone-rod dystrophy (crd) associated with mutations in the *abca4(abcr)* gene. *Exp Eye Res* 73:877-886.

Booij JC, Bakker A, Kulumbetova J, Moutaoukil Y, Smeets B, Verheij J, Kroes HY, Klaver CC, van Schooneveld M, Bergen AA, Florijn RJ. 2011. Simultaneous mutation detection in 90 retinal disease genes in multiple patients using a custom-designed 300-kb retinal resequencing chip. *Ophthalmology* 118:160-167 e161-163.

Boulanger-Scemama E, El Shamieh S, Demontant V, Condroyer C, Antonio A, Michiels C, Boyard F, Saraiva JP, Letexier M, Souied E, Mohand-Saïd S, Sahel JA et al. 2015. Next-generation sequencing applied to a large French cone and cone-rod dystrophy cohort: Mutation spectrum and new genotype-phenotype correlation. *Orphanet J Rare Dis* 10:85.

Braun TA, Mullins RF, Wagner AH, Andorf JL, Johnston RM, Bakall BB, Deluca AP, Fishman GA, Lam BL, Weleber RG, Cideciyan AV, Jacobson SG et al. 2013. Non-exonic and synonymous variants in *abca4* are an important cause of stargardt disease. *Hum Mol Genet* 22:5136-5145.

Briggs CE, Rucinski D, Rosenfeld PJ, Hirose T, Berson EL, Dryja TP. 2001. Mutations in *abcr (abca4)* in patients with stargardt macular degeneration or cone-rod degeneration. *Invest Ophthalmol Vis Sci* 42:2229-2236.

Burke TR, Allikmets R, Smith RT, Gouras P, Tsang SH. 2010. Loss of peripapillary sparing in non-group I stargardt disease. *Exp Eye Res* 91:592-600.

Burke TR, Duncker T, Woods RL, Greenberg JP, Zernant J, Tsang SH, Smith RT, Allikmets R, Sparrow JR, Delori FC. 2014. Quantitative fundus autofluorescence in recessive stargardt disease. *Invest Ophthalmol Vis Sci* 55:2841-2852.

Burke TR, Fishman GA, Zernant J, Schubert C, Tsang SH, Smith RT, Ayyagari R, Koenekoop RK, Umfress A, Ciccarelli ML, Baldi A, Iannaccone A et al. 2012a. Retinal phenotypes in patients homozygous for the G1961E mutation in the *abca4* gene. *Invest Ophthalmol Vis Sci* 53:4458-4467.

Burke TR, Tsang SH, Zernant J, Smith RT, Allikmets R. 2012b. Familial discordance in stargardt disease. *Mol Vis* 18:227-233.

Cella W, Greenstein VC, Zernant-Rajang J, Smith TR, Barile G, Allikmets R, Tsang SH. 2009. G1961E mutant allele in the stargardt disease gene *abca4* causes bull's eye maculopathy. *Exp Eye Res* 89:16-24.

Chacon-Camacho OF, Granillo-Alvarez M, Ayala-Ramirez R, Zenteno JC. 2013. *Abca4* mutational spectrum in Mexican patients with stargardt disease: Identification of 12 novel mutations and evidence of a founder effect for the common p.A1773V mutation. *Exp Eye Res* 109:77-82.

Chen X, Zhao K, Sheng X, Li Y, Gao X, Zhang X, Kang X, Pan X, Liu Y, Jiang C, Shi H, Chen X et al. 2013. Targeted sequencing of 179 genes associated with hereditary retinal dystrophies and 10 candidate genes identifies novel and known mutations in patients with various retinal diseases. *Invest Ophthalmol Vis Sci* 54:2186-2197.

Chen Y, Ratnam K, Sundquist SM, Lujan B, Ayyagari R, Gudiseva VH, Roorda A, Duncan JL. 2011. Cone photoreceptor abnormalities correlate with vision loss in patients with stargardt disease. *Invest Ophthalmol Vis Sci* 52:3281-3292.

Cideciyan AV, Swider M, Aleman TS, Tsybovsky Y, Schwartz SB, Windsor EA, Roman AJ, Sumaroka A, Steinberg JD, Jacobson SG, Stone EM, Palczewski K. 2009. Abca4 disease progression and a proposed strategy for gene therapy. *Hum Mol Genet* 18:931-941.

Corton M, Nishiguchi KM, Avila-Fernandez A, Nikopoulos K, Riveiro-Alvarez R, Tatu SD, Ayuso C, Rivolta C. 2013. Exome sequencing of index patients with retinal dystrophies as a tool for molecular diagnosis. *PLoS One* 8:e65574.

Cremers FP, van de Pol DJ, van Driel M, den Hollander AI, van Haren FJ, Knoers NV, Tijmes N, Bergen AA, Rohrschneider K, Blankenagel A, Pinckers AJ, Deutman AF et al. 1998. Autosomal recessive retinitis pigmentosa and cone-rod dystrophy caused by splice site mutations in the stargardt's disease gene *abcr*. *Hum Mol Genet* 7:355-362.

Downes SM, Packham E, Cranston T, Clouston P, Seller A, Nemeth AH. 2012. Detection rate of pathogenic mutations in *abca4* using direct sequencing: Clinical and research implications. *Arch Ophthalmol* 130:1486-1490.

Ducroq D, Rozet JM, Gerber S, Perrault I, Barbet D, Hanein S, Hakiki S, Dufier JL, Munnich A, Hamel C, Kaplan J. 2002. The *abca4* gene in autosomal recessive cone-rod dystrophies. *Am J Hum Genet* 71:1480-1482.

Duncker T, Stein GE, Lee W, Tsang SH, Zernant J, Bearelyly S, Hood DC, Greenstein VC, Delori FC, Allikmets R, Sparrow JR. 2015a. Quantitative fundus autofluorescence and optical coherence tomography in *abca4* carriers. *Invest Ophthalmol Vis Sci* 56:7274-7285.

Duncker T, Tsang SH, Lee W, Zernant J, Allikmets R, Delori FC, Sparrow JR. 2015b. Quantitative fundus autofluorescence distinguishes *abca4*-associated and non-*abca4*-associated bull's-eye maculopathy. *Ophthalmology* 122:345-355.

Duncker T, Tsang SH, Woods RL, Lee W, Zernant J, Allikmets R, Delori FC, Sparrow JR. 2015c. Quantitative fundus autofluorescence and optical coherence tomography in *prph2/rds*- and *abca4*-associated disease exhibiting phenotypic overlap. *Invest Ophthalmol Vis Sci* 56:3159-3170.

Duno M, Schwartz M, Larsen PL, Rosenberg T. 2012. Phenotypic and genetic spectrum of danish patients with *abca4*-related retinopathy. *Ophthalmic Genet* 33:225-231.

Eandi CM, Grignolo FM, Passerini I, Marchese C. 2014. Homozygous c.1937+1g>a splice-site variant of the *abca4* gene is associated with stargardt disease. *Eur J Ophthalmol* 24:814-817.

Eisenberger T, Neuhaus C, Khan AO, Decker C, Preising MN, Friedburg C, Bieg A, Gliem M, Charbel Issa P, Holz FG, Baig SM, Hellenbroich Y et al. 2013. Increasing the yield in targeted next-generation sequencing by implicating cnv analysis, non-coding exons and the overall variant load: The example of retinal dystrophies. *PLoS One* 8:e78496.

Ernest PJ, Boon CJ, Klevering BJ, Hoefsloot LH, Hoyng CB. 2009. Outcome of abca4 microarray screening in routine clinical practice. *Mol Vis* 15:2841-2847.

Fernandez-San Jose P, Corton M, Blanco-Kelly F, Avila-Fernandez A, Lopez-Martinez MA, Sanchez-Navarro I, Sanchez-Alcudia R, Perez-Carro R, Zurita O, Sanchez-Bolivar N, Lopez-Molina MI, Garcia-Sandoval B et al. 2015. Targeted next-generation sequencing improves the diagnosis of autosomal dominant retinitis pigmentosa in spanish patients. *Invest Ophthalmol Vis Sci* 56:2173-2182.

Fishman GA, Stone EM, Eliason DA, Taylor CM, Lindeman M, Derlacki DJ. 2003. Abca4 gene sequence variations in patients with autosomal recessive cone-rod dystrophy. *Arch Ophthalmol* 121:851-855.

Fishman GA, Stone EM, Grover S, Derlacki DJ, Haines HL, Hockey RR. 1999. Variation of clinical expression in patients with stargardt dystrophy and sequence variations in the abcr gene. *Arch Ophthalmol* 117:504-510.

Fujinami K, Lois N, Davidson AE, Mackay DS, Hogg CR, Stone EM, Tsunoda K, Tsubota K, Bunce C, Robson AG, Moore AT, Webster AR et al. 2013a. A longitudinal study of stargardt disease: Clinical and electrophysiologic assessment, progression, and genotype correlations. *Am J Ophthalmol* 155:1075-1088 e1013.

Fujinami K, Lois N, Mukherjee R, McBain VA, Tsunoda K, Tsubota K, Stone EM, Fitzke FW, Bunce C, Moore AT, Webster AR, Michaelides M. 2013b. A longitudinal study of stargardt disease: Quantitative assessment of fundus autofluorescence, progression, and genotype correlations. *Invest Ophthalmol Vis Sci* 54:8181-8190.

Fujinami K, Sergouniotis PI, Davidson AE, Mackay DS, Tsunoda K, Tsubota K, Robson AG, Holder GE, Moore AT, Michaelides M, Webster AR. 2013c. The clinical effect of homozygous abca4 alleles in 18 patients. *Ophthalmology* 120:2324-2331.

Fujinami K, Sergouniotis PI, Davidson AE, Wright G, Chana RK, Tsunoda K, Tsubota K, Egan CA, Robson AG, Moore AT, Holder GE, Michaelides M et al. 2013d. Clinical and molecular analysis of stargardt disease with preserved foveal structure and function. *Am J Ophthalmol* 156:487-501 e481.

Fujinami K, Zernant J, Chana RK, Wright GA, Tsunoda K, Ozawa Y, Tsubota K, Webster AR, Moore AT, Allikmets R, Michaelides M. 2013e. Abca4 gene screening by next-generation sequencing in a british cohort. *Invest Ophthalmol Vis Sci* 54:6662-6674.

Fukui T, Fujikado T, Tsujikawa M, Okada M, Yamamoto S, Tano Y. 2006. Null abca4 gene mutations found in japanese patients with panretinal degeneration. *Jpn J Ophthalmol* 50:179-181.

Fukui T, Yamamoto S, Nakano K, Tsujikawa M, Morimura H, Nishida K, Ohguro N, Fujikado T, Irifune M, Kuniyoshi K, Okada AA, Hirakata A et al. 2002. Abca4 gene mutations in japanese patients with stargardt disease and retinitis pigmentosa. *Invest Ophthalmol Vis Sci* 43:2819-2824.

Fumagalli A, Ferrari M, Soriani N, Gessi A, Foglieni B, Martina E, Manitto MP, Brancato R, Dean M, Allikmets R, Cremonesi L. 2001. Mutational scanning of the abcr gene with double-gradient denaturing-gradient gel electrophoresis (dg-dgge) in italian stargardt disease patients. *Hum Genet* 109:326-338.

Gemenetzi M, Lotery AJ. 2013. Phenotype/genotype correlation in a case series of stargardt's patients identifies novel mutations in the abca4 gene. *Eye (Lond)* 27:1316-1319.

Genead MA, Fishman GA, Stone EM, Allikmets R. 2009. The natural history of stargardt disease with specific sequence mutation in the *abca4* gene. *Invest Ophthalmol Vis Sci* 50:5867-5871.

Gerber S, Rozet JM, van de Pol TJ, Hoyng CB, Munnich A, Blankenagel A, Kaplan J, Cremers FP. 1998. Complete exon-intron structure of the retina-specific atp binding transporter gene (*abcr*) allows the identification of novel mutations underlying stargardt disease. *Genomics* 48:139-142.

Gerth C, Andrassi-Darida M, Bock M, Preising MN, Weber BH, Lorenz B. 2002. Phenotypes of 16 stargardt macular dystrophy/fundus flavimaculatus patients with known *abca4* mutations and evaluation of genotype-phenotype correlation. *Graefes Arch Clin Exp Ophthalmol* 40:628-638.

Glockle N, Kohl S, Mohr J, Scheurenbrand T, Sprecher A, Weisschuh N, Bernd A, Rudolph G, Schubach M, Poloschek C, Zrenner E, Biskup S et al. 2014. Panel-based next generation sequencing as a reliable and efficient technique to detect mutations in unselected patients with retinal dystrophies. *Eur J Hum Genet* 22:99-104.

Gonzalez-del Pozo M, Mendez-Vidal C, Bravo-Gil N, Vela-Boza A, Dopazo J, Borrego S, Antinolo G. 2014. Exome sequencing reveals novel and recurrent mutations with clinical significance in inherited retinal dystrophies. *PLoS One* 9:e116176.

Heathfield L, Lacerda M, Nossek C, Roberts L, Ramesar RS. 2013. Stargardt disease: Towards developing a model to predict phenotype. *Eur J Hum Genet* 21:1173-1176.

Horn P, Harder J, Lohmann CP, Lanzl I. 2010. [bilateral loss of vision in an 11-year-old]. *Ophthalmologe* 107:848-851.

Huang L, Zhang Q, Li S, Guan L, Xiao X, Zhang J, Jia X, Sun W, Zhu Z, Gao Y, Yin Y, Wang P et al. 2013. Exome sequencing of 47 chinese families with cone-rod dystrophy: Mutations in 25 known causative genes. *PLoS One* 8:e65546.

Huang XF, Huang F, Wu KC, Wu J, Chen J, Pang CP, Lu F, Qu J, Jin ZB. 2015. Genotype-phenotype correlation and mutation spectrum in a large cohort of patients with inherited retinal dystrophy revealed by next-generation sequencing. *Genet Med* 17:271-278.

Hwang JC, Zernant J, Allikmets R, Barile GR, Chang S, Smith RT. 2009. Peripapillary atrophy in stargardt disease. *Retina* 29:181-186.

Jaakson K, Zernant J, Kulm M, Hutchinson A, Tonisson N, Glavac D, Ravnik-Glavac M, Hawlina M, Meltzer MR, Caruso RC, Testa F, Maugeri A et al. 2003. Genotyping microarray (gene chip) for the *abcr* (*abca4*) gene. *Hum Mutat* 22:395-403.

Jin X, Qu LH, Meng XH, Xu HW, Yin ZQ. 2014. Detecting genetic variations in hereditary retinal dystrophies with next-generation sequencing technology. *Mol Vis* 20:553-560.

Jinda W, Taylor TD, Suzuki Y, Thongnoppakhun W, Limwongse C, Lertrit P, Suriyaphol P, Trinavarat A, Atchaneeyasakul LO. 2014. Whole exome sequencing in thai patients with retinitis pigmentosa reveals novel mutations in six genes. *Invest Ophthalmol Vis Sci* 55:2259-2268.

Jonsson F, Burstedt MS, Sandgren O, Norberg A, Golovleva I. 2013. Novel mutations in *crb1* and *abca4* genes cause leber congenital amaurosis and stargardt disease in a swedish family. *Eur J Hum Genet* 21:1266-1271.

Kang Derwent JJ, Derlacki DJ, Hetling JR, Fishman GA, Birch DG, Grover S, Stone EM, Pepperberg DR. 2004. Dark adaptation of rod photoreceptors in normal subjects, and in patients with stargardt disease and an abca4 mutation. *Invest Ophthalmol Vis Sci* 45:2447-2456.

Kitiratschky VB, Grau T, Bernd A, Zrenner E, Jagle H, Renner AB, Kellner U, Rudolph G, Jacobson SG, Cideciyan AV, Schaich S, Kohl S et al. 2008. Abca4 gene analysis in patients with autosomal recessive cone and cone rod dystrophies. *Eur J Hum Genet* 16:812-819.

Kjellstrom U. 2014. Association between genotype and phenotype in families with mutations in the abca4 gene. *Mol Vis* 20:89-104. Kjellstrom U. 2015. Reduced macular function in abca4 carriers. *Mol Vis* 21:767-782.

Klevering BJ, Blankenagel A, Maugeri A, Cremers FP, Hoyng CB, Rohrschneider K. 2002. Phenotypic spectrum of autosomal recessive cone-rod dystrophies caused by mutations in the abca4 (abcr) gene. *Invest Ophthalmol Vis Sci* 43:1980-1985.

Klevering BJ, Deutman AF, Maugeri A, Cremers FP, Hoyng CB. 2005. The spectrum of retinal phenotypes caused by mutations in the abca4 gene. *Graefes Arch Clin Exp Ophthalmol* 243:90-100.

Klevering BJ, Maugeri A, Wagner A, Go SL, Vink C, Cremers FP, Hoyng CB. 2004a. Three families displaying the combination of stargardt's disease with cone-rod dystrophy or retinitis pigmentosa. *Ophthalmology* 111:546-553.

Klevering BJ, van Driel M, van de Pol DJ, Pinckers AJ, Cremers FP, Hoyng CB. 1999. Phenotypic variations in a family with retinal dystrophy as result of different mutations in the abcr gene. *Br J Ophthalmol* 83:914-918.

Klevering BJ, Yzer S, Rohrschneider K, Zonneveld M, Allikmets R, van den Born LI, Maugeri A, Hoyng CB, Cremers FP. 2004b.

Microarray-based mutation analysis of the abca4 (abcr) gene in autosomal recessive cone-rod dystrophy and retinitis pigmentosa. *Eur J Hum Genet* 12:1024-1032.

Kousal B, Zahlava J, Vejvalkova S, Hejtmankova M, Liskova P. 2014. [the molecular genetic and clinical findings in two probands with stargardt disease]. *Cesk Slov Oftalmol* 70:228-233.

Lambertus S, van Huet RA, Bax NM, Hoefsloot LH, Cremers FP, Boon CJ, Klevering BJ, Hoyng CB. 2015. Early-onset stargardt disease: Phenotypic and genotypic characteristics. *Ophthalmology* 122:335-344.

Lee W, Xie Y, Zernant J, Yuan B, Bearely S, Tsang SH, Lupski JR, Allikmets R. 2016. Complex inheritance of abca4 disease: Four mutations in a family with multiple macular phenotypes. *Hum Genet* 135:9-19.

Lewis RA, Shroyer NF, Singh N, Allikmets R, Hutchinson A, Li Y, Lupski JR, Leppert M, Dean M. 1999. Genotype/phenotype analysis of a photoreceptor-specific atp-binding cassette transporter gene, abcr, in stargardt disease. *Am J Hum Genet* 64:422-434.

Littink KW, Koenekoop RK, van den Born LI, Collin RW, Moruz L, Veltman JA, Roosing S, Zonneveld MN, Omar A, Darvish M, Lopez I, Kroes HY et al. 2010. Homozygosity mapping in patients with cone-rod dystrophy: Novel mutations and clinical characterizations. *Invest Ophthalmol Vis Sci* 51:5943-5951.



Maia-Lopes S, Aguirre-Lamban J, Castelo-Branco M, Riveiro-Alvarez R, Ayuso C, Silva ED. 2009. Abca4 mutations in portuguese stargardt patients: Identification of new mutations and their phenotypic analysis. *Mol Vis* 15:584-591.

Maia-Lopes S, Silva ED, Silva MF, Reis A, Faria P, Castelo-Branco M. 2008. Evidence of widespread retinal dysfunction in patients with stargardt disease and morphologically unaffected carrier relatives. *Invest Ophthalmol Vis Sci* 49:1191-1199.

Martinez-Mir A, Paloma E, Allikmets R, Ayuso C, del Rio T, Dean M, Vilageliu L, Gonzalez-Duarte R, Balcells S. 1998. Retinitis pigmentosa caused by a homozygous mutation in the stargardt disease gene abcr. *Nat Genet* 18:11-12.

Maugeri A, Klevering BJ, Rohrschneider K, Blankenagel A, Brunner HG, Deutman AF, Hoyng CB, Cremers FP. 2000. Mutations in the abca4 (abcr) gene are the major cause of autosomal recessive cone-rod dystrophy. *Am J Hum Genet* 67:960-966.

Maugeri A, van Driel MA, van de Pol DJ, Klevering BJ, van Haren FJ, Tijmes N, Bergen AA, Rohrschneider K, Blankenagel A, Pinckers AJ, Dahl N, Brunner HG et al. 1999. The 2588g->c mutation in the abcr gene is a mild frequent founder mutation in the western european population and allows the classification of abcr mutations in patients with stargardt disease. *Am J Hum Genet* 64:1024-1035.

Michaelides M, Chen LL, Brantley MA, Jr., Andorf JL, Isaak EM, Jenkins SA, Holder GE, Bird AC, Stone EM, Webster AR. 2007. Abca4 mutations and discordant abca4 alleles in patients and siblings with bull's-eye maculopathy. *Br J Ophthalmol* 91:1650-1655.

Miraldi Utz V, Coussa RG, Marino MJ, Chappelov AV, Pauer GJ, Hagstrom SA, Traboulsi EI. 2014. Predictors of visual acuity and genotype-phenotype correlates in a cohort of patients with stargardt disease. *Br J Ophthalmol* 98:513-518.

Muller PL, Gliem M, Mangold E, Bolz HJ, Finger RP, McGuinness M, Betz C, Jiang Z, Weber BH, MacLaren RE, Holz FG, Radu RA et al. 2015. Monoallelic abca4 mutations appear insufficient to cause retinopathy: A quantitative autofluorescence study. *Invest Ophthalmol Vis Sci* 56:8179-8186.

Mullins RF, Kuehn MH, Radu RA, Enriquez GS, East JS, Schindler EI, Travis GH, Stone EM. 2012. Autosomal recessive retinitis pigmentosa due to abca4 mutations: Clinical, pathologic, and molecular characterization. *Invest Ophthalmol Vis Sci* 53:1883-1894.

Nasonkin I, Illing M, Koehler MR, Schmid M, Molday RS, Weber BH. 1998. Mapping of the rod photoreceptor abc transporter (abcr) to 1p21-p22.1 and identification of novel mutations in stargardt's disease. *Hum Genet* 102:21-26.

Noupuu K, Lee W, Zernant J, Greenstein VC, Tsang S, Allikmets R. 2016. Recessive stargardt disease phenocopying hydroxychloroquine retinopathy. *Graefes Arch Clin Exp Ophthalmol* 254:865-872.

Noupuu K, Lee W, Zernant J, Tsang SH, Allikmets R. 2014. Structural and genetic assessment of the abca4-associated optical gap phenotype. *Invest Ophthalmol Vis Sci* 55:7217-7226.

Oishi M, Oishi A, Gotoh N, Ogino K, Higasa K, Iida K, Makiyama Y, Morooka S, Matsuda F, Yoshimura N. 2014. Comprehensive molecular diagnosis of a large cohort of japanese retinitis pigmentosa and usher syndrome patients by next-generation sequencing. *Invest Ophthalmol Vis Sci* 55:7369-7375.

Oldani M, Marchi S, Giani A, Cecchin S, Rigoni E, Persi A, Podavini D, Guerrini A, Nervegna A, Staurengi G, Bertelli M. 2012. Clinical and molecular genetic study of 12 italian families with autosomal recessive stargardt disease. *Genet Mol Res* 11:4342-4350.

Ozgul RK, Durukan H, Turan A, Oner C, Ogus A, Farber DB. 2004. Molecular analysis of the abca4 gene in turkish patients with stargardt disease and retinitis pigmentosa. *Hum Mutat* 23:523.

Paloma E, Coco R, Martinez-Mir A, Vilageliu L, Balcells S, Gonzalez-Duarte R. 2002. Analysis of abca4 in mixed spanish families segregating different retinal dystrophies. *Hum Mutat* 20:476.

Paloma E, Martinez-Mir A, Vilageliu L, Gonzalez-Duarte R, Balcells S. 2001. Spectrum of abca4 (abcr) gene mutations in spanish patients with autosomal recessive macular dystrophies. *Hum Mutat* 17:504-510.

Papaioannou M, Ocaka L, Bessant D, Lois N, Bird A, Payne A, Bhattacharya S. 2000. An analysis of abcr mutations in british patients with recessive retinal dystrophies. *Invest Ophthalmol Vis Sci* 41:16-19.

Passerini I, Sodi A, Giambene B, Mariottini A, Menchini U, Torricelli F. 2010. Novel mutations in of the abcr gene in italian patients with stargardt disease. *Eye (Lond)* 24:158-164.

Ritter M, Zotter S, Schmidt WM, Bittner RE, Deak GG, Pircher M, Sacu S, Hitzenberger CK, Schmidt-Erfurth UM, Macula Study Group V. 2013. Characterization of stargardt disease using polarization-sensitive optical coherence tomography and fundus autofluorescence imaging. *Invest Ophthalmol Vis Sci* 54:6416-6425.

Riveiro-Alvarez R, Lopez-Martinez MA, Zernant J, Aguirre-Lamban J, Cantalapiedra D, Avila-Fernandez A, Gimenez A, Lopez-Molina MI, Garcia-Sandoval B, Blanco-Kelly F, Corton M, Tatu S et al. 2013. Outcome of abca4 disease-associated alleles in autosomal recessive retinal dystrophies: Retrospective analysis in 420 spanish families. *Ophthalmology* 120:2332-2337.

Riveiro-Alvarez R, Vallespin E, Wilke R, Garcia-Sandoval B, Cantalapiedra D, Aguirre-Lamban J, Avila-Fernandez A, Gimenez A, Trujillo-Tiebas MJ, Ayuso C. 2008. Molecular analysis of abca4 and crb1 genes in a spanish family segregating both stargardt disease and autosomal recessive retinitis pigmentosa. *Mol Vis* 14:262-267.

Riveiro-Alvarez R, Valverde D, Lorda-Sanchez I, Trujillo-Tiebas MJ, Cantalapiedra D, Vallespin E, Aguirre-Lamban J, Ramos C, Ayuso C. 2007. Partial paternal uniparental disomy (upd) of chromosome 1 in a patient with stargardt disease. *Mol Vis* 13:96-101.

Rivera A, White K, Stohr H, Steiner K, Hemmrich N, Grimm T, Jurklies B, Lorenz B, Scholl HP, Apfelstedt-Sylla E, Weber BH. 2000. A comprehensive survey of sequence variation in the abca4 (abcr) gene in stargardt disease and age-related macular degeneration. *Am J Hum Genet* 67:800-813.

Roberts LJ, Nossek CA, Greenberg LJ, Ramesar RS. 2012. Stargardt macular dystrophy: Common abca4 mutations in south africa-- establishment of a rapid genetic test and relating risk to patients. *Mol Vis* 18:280-289.

Rosenberg T, Klie F, Garred P, Schwartz M. 2007. N965s is a common abca4 variant in stargardt-related retinopathies in the danish population. *Mol Vis* 13:1962-1969.

Rossi S, Testa F, Attanasio M, Orrico A, de Benedictis A, Corte MD, Simonelli F. 2012. Subretinal fibrosis in stargardt's disease with fundus flavimaculatus and *abca4* gene mutation. *Case Rep Ophthalmol* 3:410-417.

Rozet JM, Gerber S, Ghazi I, Perrault I, Ducrocq D, Souied E, Cabot A, Dufier JL, Munnich A, Kaplan J. 1999. Mutations of the retinal specific atp binding transporter gene (*abcr*) in a single family segregating both autosomal recessive retinitis pigmentosa *rp19* and stargardt disease: Evidence of clinical heterogeneity at this locus. *J Med Genet* 36:447-451.

Rozet JM, Gerber S, Souied E, Perrault I, Chatelin S, Ghazi I, Leowski C, Dufier JL, Munnich A, Kaplan J. 1998. Spectrum of *abcr* gene mutations in autosomal recessive macular dystrophies. *Eur J Hum Genet* 6:291-295.

Rudolph G, Kalpadakis P, Haritoglou C, Rivera A, Weber BH. 2002. [Mutations in the *abca4* gene in a family with stargardt's disease and retinitis pigmentosa (*stgd1/rp19*)]. *Klin Monbl Augenheilkd* 219:590-596.

Sanchez-Alcudia R, Corton M, Avila-Fernandez A, Zurita O, Tatu SD, Perez-Carro R, Fernandez-San Jose P, Lopez-Martinez MA, del Castillo FJ, Millan JM, Blanco-Kelly F, Garcia-Sandoval B et al. 2014. Contribution of mutation load to the intrafamilial genetic heterogeneity in a large cohort of spanish retinal dystrophies families. *Invest Ophthalmol Vis Sci* 55:7562-7571.

Schindler EI, Nylén EL, Ko AC, Affatigato LM, Heggen AC, Wang K, Sheffield VC, Stone EM. 2010. Deducing the pathogenic contribution of recessive *abca4* alleles in an outbred population. *Hum Mol Genet* 19:3693-3701.

Sciezynska A, Ozieblo D, Ambroziak AM, Korwin M, Szulborski K, Krawczynski M, Stawinski P, Szaflik J, Szaflik JP, Ploski R, Oldak M. 2016. Next-generation sequencing of *abca4*: High frequency of complex alleles and novel mutations in patients with retinal dystrophies from central europe. *Exp Eye Res* 145:93-99.

September AV, Vorster AA, Ramesar RS, Greenberg LJ. 2004. Mutation spectrum and founder chromosomes for the *abca4* gene in south african patients with stargardt disease. *Invest Ophthalmol Vis Sci* 45:1705-1711.

Shroyer NF, Lewis RA, Lupski JR. 2000. Complex inheritance of *abcr* mutations in stargardt disease: Linkage disequilibrium, complex alleles, and pseudodominance. *Hum Genet* 106:244-248.

Shroyer NF, Lewis RA, Yatsenko AN, Lupski JR. 2001a. Null missense *abcr* (*abca4*) mutations in a family with stargardt disease and retinitis pigmentosa. *Invest Ophthalmol Vis Sci* 42:2757-2761.

Shroyer NF, Lewis RA, Yatsenko AN, Wensel TG, Lupski JR. 2001b. Cosegregation and functional analysis of mutant *abcr* (*abca4*) alleles in families that manifest both stargardt disease and age-related macular degeneration. *Hum Mol Genet* 10:2671-2678.

Siemiatkowska AM, Arimadyo K, Moruz LM, Astuti GD, de Castro-Miro M, Zonneveld MN, Strom TM, de Wijs IJ, Hoefsloot LH, Faradz SM, Cremers FP, den Hollander AI et al. 2011. Molecular genetic analysis of retinitis pigmentosa in indonesia using genome-wide homozygosity mapping. *Mol Vis* 17:3013-3024.

Simonelli F, Testa F, de Crecchio G, Rinaldi E, Hutchinson A, Atkinson A, Dean M, D'Urso M, Allikmets R. 2000. New abcr mutations and clinical phenotype in italian patients with stargardt disease. *Invest Ophthalmol Vis Sci* 41:892-897.

Simonelli F, Testa F, Zernant J, Nesti A, Rossi S, Allikmets R, Rinaldi E. 2005. Genotype-phenotype correlation in italian families with stargardt disease. *Ophthalmic Res* 37:159-167.

Simonelli F, Testa F, Zernant J, Nesti A, Rossi S, Rinaldi E, Allikmets R. 2004. Association of a homozygous nonsense mutation in the abca4 (abcr) gene with cone-rod dystrophy phenotype in an italian family. *Ophthalmic Res* 36:82-88.

Singh HP, Jalali S, Hejtmancik JF, Kannabiran C. 2006. Homozygous null mutations in the abca4 gene in two families with autosomal recessive retinal dystrophy. *Am J Ophthalmol* 141:906-913.

Singh HP, Jalali S, Narayanan R, Kannabiran C. 2009. Genetic analysis of indian families with autosomal recessive retinitis pigmentosa by homozygosity screening. *Invest Ophthalmol Vis Sci* 50:4065-4071.

Sodi A, Bini A, Passerini I, Forconi S, Menchini U, Torricelli F. 2010. Different patterns of fundus autofluorescence related to abca4 gene mutations in stargardt disease. *Ophthalmic Surg Lasers Imaging* 41:48-53.

Song H, Rossi EA, Latchney L, Bessette A, Stone E, Hunter JJ, Williams DR, Chung M. 2015. Cone and rod loss in stargardt disease revealed by adaptive optics scanning light ophthalmoscopy. *JAMA Ophthalmol* 133:1198-1203.

Souied EH, Ducroq D, Rozet JM, Gerber S, Perrault I, Sterkers M, Benhamou N, Munnich A, Coscas G, Soubrane G, Kaplan J. 1999. A novel abcr nonsense mutation responsible for late-onset fundus flavimaculatus. *Invest Ophthalmol Vis Sci* 40:2740-2744.

Stenirri S, Alaimo G, Manitto MP, Brancato R, Ferrari M, Cremonesi L. 2008. Are microarrays useful in the screening of abca4 mutations in italian patients affected by macular degenerations? *Clin Chem Lab Med* 46:1250-1255.

Stenirri S, Battistella S, Fermo I, Manitto MP, Martina E, Brancato R, Ferrari M, Cremonesi L. 2006. De novo deletion removes a conserved motif in the c-terminus of abca4 and results in cone-rod dystrophy. *Clin Chem Lab Med* 44:533-537.

Stenirri S, Fermo I, Battistella S, Galbiati S, Soriani N, Paroni R, Manitto MP, Martina E, Brancato R, Allikmets R, Ferrari M, Cremonesi L. 2004. Denaturing hplc profiling of the abca4 gene for reliable detection of allelic variations. *Clin Chem* 50:1336-1343.

Strom SP, Gao YQ, Martinez A, Ortube C, Chen Z, Nelson SF, Nusinowitz S, Farber DB, Gorin MB. 2012. Molecular diagnosis of putative stargardt disease probands by exome sequencing. *BMC Med Genet* 13:67.

Testa F, Rossi S, Sodi A, Passerini I, Di Iorio V, Della Corte M, Banfi S, Surace EM, Menchini U, Auricchio A, Simonelli F. 2012. Correlation between photoreceptor layer integrity and visual function in patients with stargardt disease: Implications for gene therapy. *Invest Ophthalmol Vis Sci* 53:4409-4415.

Valverde D, Riveiro-Alvarez R, Aguirre-Lamban J, Baiget M, Carballo M, Antinolo G, Millan JM, Garcia Sandoval B, Ayuso C. 2007. Spectrum of the *abca4* gene mutations implicated in severe retinopathies in spanish patients. *Invest Ophthalmol Vis Sci* 48:985-990.

Valverde D, Riveiro-Alvarez R, Bernal S, Jaakson K, Baiget M, Navarro R, Ayuso C. 2006. Microarray-based mutation analysis of the *abca4* gene in spanish patients with stargardt disease: Evidence of a prevalent mutated allele. *Mol Vis* 12:902-908.

van Huet RA, Bax NM, Westeneng-Van Haaften SC, Muhamad M, Zonneveld-Vrieling MN, Hoefsloot LH, Cremers FP, Boon CJ, Klevering BJ, Hoyng CB. 2014. Foveal sparing in stargardt disease. *Invest Ophthalmol Vis Sci* 55:7467-7478.

Wang F, Wang H, Tuan HF, Nguyen DH, Sun V, Keser V, Bowne SJ, Sullivan LS, Luo H, Zhao L, Wang X, Zaneveld JE et al. 2014. Next generation sequencing-based molecular diagnosis of retinitis pigmentosa: Identification of a novel genotype-phenotype correlation and clinical refinements. *Hum Genet* 133:331-345.

Webster AR, Heon E, Lotery AJ, Vandenberg K, Casavant TL, Oh KT, Beck G, Fishman GA, Lam BL, Levin A, Heckenlively JR, Jacobson SG et al. 2001. An analysis of allelic variation in the *abca4* gene. *Invest Ophthalmol Vis Sci* 42:1179-1189.

Westeneng-van Haaften SC, Boon CJ, Cremers FP, Hoefsloot LH, den Hollander AI, Hoyng CB. 2012. Clinical and genetic characteristics of late-onset stargardt's disease. *Ophthalmology* 119:1199-1210.

Xi Q, Li L, Traboulsi EI, Wang QK. 2009. Novel *abca4* compound heterozygous mutations cause severe progressive autosomal recessive cone-rod dystrophy presenting as stargardt disease. *Mol Vis* 15:638-645.

Xin W, Xiao X, Li S, Jia X, Guo X, Zhang Q. 2015. Identification of genetic defects in 33 probands with stargardt disease by wes-based bioinformatics gene panel analysis. *PLoS One* 10:e0132635.

Yatsenko AN, Shroyer NF, Lewis RA, Lupski JR. 2001. Late-onset stargardt disease is associated with missense mutations that map outside known functional regions of *abcr* (*abca4*). *Hum Genet* 108:346-355.

Yatsenko AN, Shroyer NF, Lewis RA, Lupski JR. 2003. An *abca4* genomic deletion in patients with stargardt disease. *Hum Mutat* 21:636-644.

Yzer S, van den Born LJ, Zonneveld MN, Lopez I, Ayyagari R, Teye-Botchway L, Mota-Vieira L, Cremers FP, Koenekoop RK. 2007. Molecular and phenotypic analysis of a family with autosomal recessive cone-rod dystrophy and stargardt disease. *Mol Vis* 13:1568-1572.

Zaneveld J, Siddiqui S, Li H, Wang X, Wang H, Wang K, Li H, Ren H, Lopez I, Dorfman A, Khan A, Wang F et al. 2015. Comprehensive analysis of patients with stargardt macular dystrophy reveals new genotype-phenotype correlations and unexpected diagnostic revisions. *Genet Med* 17:262-270.

Zernant J, Collison FT, Lee W, Fishman GA, Noupou K, Yuan B, Cai C, Lupski JR, Yannuzzi LA, Tsang SH, Allikmets R. 2014a. Genetic and clinical analysis of *abca4*-associated disease in african american patients. *Hum Mutat* 35:1187-1194.

Zernant J, Schubert C, Im KM, Burke T, Brown CM, Fishman GA, Tsang SH, Gouras P, Dean M, Allikmets R. 2011. Analysis of the *abca4* gene by next-generation sequencing. *Invest Ophthalmol Vis Sci* 52:8479-8487.

Zernant J, Xie YA, Ayuso C, Riveiro-Alvarez R, Lopez-Martinez MA, Simonelli F, Testa F, Gorin MB, Strom SP, Bertelsen M, Rosenberg T, Boone PM et al. 2014b. Analysis of the *abca4* genomic locus in stargardt disease. *Hum Mol Genet* 23:6797-6806.

Zhang K, Garibaldi DC, Kniazeva M, Albini T, Chiang MF, Kerrigan M, Sunness JS, Han M, Allikmets R. 1999a. A novel mutation in the *abcr* gene in four patients with autosomal recessive stargardt disease. *Am J Ophthalmol* 128:720-724.

Zhang K, Kniazeva M, Hutchinson A, Han M, Dean M, Allikmets R. 1999b. The *abcr* gene in recessive and dominant stargardt diseases: A genetic pathway in macular degeneration. *Genomics* 60:234-237.

Zhao L, Wang F, Wang H, Li Y, Alexander S, Wang K, Willoughby CE, Zaneveld JE, Jiang L, Soens ZT, Earle P, Simpson D et al. 2015. Next-generation sequencing-based molecular diagnosis of 82 retinitis pigmentosa probands from northern ireland. *Hum Genet* 134:217-230.

Zhou Y, Tao S, Chen H, Huang L, Zhu X, Li Y, Wang Z, Lin H, Hao F, Yang Z, Wang L, Zhu X. 2014. Exome sequencing analysis identifies compound heterozygous mutation in *abca4* in a chinese family with stargardt disease. *PLoS One* 9:e9196



## CHAPTER 3.2

### Heterozygous deep-intronic variants and deletions in *ABCA4* in persons with retinal dystrophies and one exonic *ABCA4* variant.

*“The most frequently mutated inherited retinal dystrophy gene, ABCA4, shows an unusual phenomenon, i.e. in a very high proportion of patients with STGD1, one or no ABCA4 variants were found. Braun et al. (2013) identified 5 deep-intronic variants in a cohort of STGD1 cases with one ABCA4 variant. We analyzed 45 retinal dystrophy patients with one ABCA4 variant for the presence of these and other deep-intronic variants, and in addition tested these patients for the presence of heterozygous deletions. In this way we found six probands with heterozygous deep-intronic mutations, two probands with heterozygous deletions, and one proband with a heterozygous deep-intronic mutation and an intragenic deletion. As antisense oligonucleotide-based therapies are being development, these patients are eligible for this novel treatment.”*

Nathalie M. Bax\*, Riccardo Sangermano\*, Susanne Roosing\*  
Alberta A. Thiadens, Lies H. Hoefsloot  
L. Ingeborgh van den Born, Milan Phan  
B. Jeroen Klevering, S. Carla Westeneng- van Haaften  
Terry A. Braun, Marijke N. Zonneveld- Vrieling  
Ilse J. de Wijs, Merve Mutlu  
Ed M. Stone, Anneke I. den Hollander  
Caroline C.W. Klaver, Carel B. Hoyng  
Frans P.M. Cremers

\*Shared first author

*Human Mutation. 2015;36(1):43-7*



Variants in *ABCA4* are responsible for autosomal recessive Stargardt disease and cone-rod dystrophy. Sequence analysis of *ABCA4* exons previously revealed one causative variant in each of 45 probands. To identify the 'missing' variants in these cases we performed multiplex ligation-dependent probe amplification-based deletion scanning of *ABCA4*. In addition, we sequenced the promoter region, fragments containing five deep-intronic splice variants and 15 deep-intronic regions containing weak splice sites. Heterozygous deletions spanning *ABCA4* exon 5 or exons 20-22 were found in two probands, heterozygous deep-intronic variants were identified in six probands, and a deep-intronic variant was found together with an exon 20-22 deletion in one proband. Based on ophthalmologic findings and characteristics of the identified exonic variants present in *trans*, the deep intronic variants V1 and V4 were predicted to be relatively mild and severe, respectively. These findings are important for proper genetic counseling and for the development of variant-specific therapies.

The ATP-binding cassette, subfamily A, member 4 (ABCA4) protein is located at the rim of the outer segment discs in rods and in the cell membrane of cones. Variants in *ABCA4* (MIM #601691) were associated with autosomal-recessive Stargardt disease (STGD1) [Allikmets et al., 1997b]. Subsequently, different combinations of *ABCA4* variants have been linked to a spectrum of phenotypes ranging from mild macular dystrophy to severe early-onset panretinal dystrophy [Allikmets et al., 1997a; Cremers et al., 1998; Maugeri et al., 1999; Klevering et al., 2004]. In the proposed genotype–phenotype correlation model, a combination of a mild and a severe *ABCA4* variant causes STGD1 [Maugeri et al., 1999], the most frequent associated disease, whereas a moderate and a severe variant gives rise to a more severe phenotype, cone-rod dystrophy (CRD) [Cremers et al., 1998]. Two severe variants in *ABCA4* result in a panretinal CRD [Cremers et al., 1998; Klevering et al., 2004].

A significant subset of individuals with classic STGD1 however carries only one or no *ABCA4* variant [Maugeri et al., 1999]. A proportion of these cases may be explained by the identification of variants in genes that are associated with retinal dystrophies resembling STGD1. *ELOVL4* [Edwards et al., 2001] and *PRPH2* [Poloschek et al., 2010] contain variants that are responsible for autosomal-dominant STGD. Furthermore, the “missing” variants in STGD1 patients may be the result of the limitations of the employed molecular genetic analysis. Homozygous *ABCA4* deletions disrupting the open reading frame are not expected to account for the “missing” variants in STGD1 as they would result in a panretinal dystrophy. Heterozygous deletions, however, can have been missed as PCR-based mutation scanning and Sanger sequencing of *ABCA4* exons would not detect small heterozygous deletions. Southern blot analysis revealed heterozygous deletions of exon 18 [Yatsenko et al., 2003] and exons 20–22 [Maugeri et al., 1999].

Deep sequencing of the *ABCA4* mRNA of healthy retinal tissues revealed several low-expressed alternative transcripts of *ABCA4* [Braun et al., 2013]. Sequence analysis of rarely used deep-intronic splice sites in STGD1 individuals identified variants at five splice junctions (i.e., V1 through V5), causing intron retention or premature termination of an exon [Braun et al., 2013]. The variants V6 and V7 reported in the same study are not deep-intronic and can be identified using regular exon analysis.

Previously, we employed a palette of genotyping methods to scan for exonic *ABCA4* variants and deletions [Maugeri et al., 1999; Jaakson et al., 2003]. In this study, we have expanded our genotyping studies to identify the second variant in maculopathy cases with one *ABCA4* allele. Forty-five probands with one heterozygous *ABCA4* variant (33 STGD1, four STGD1/CRD, five arCRD, three ar cone dystrophy [CD]; Supp. Table S1), a cohort of 81 STGD1 probands with two

*ABCA4* variants and nine additional STGD1 probands without *ABCA4* variants, were ascertained in The Netherlands, the majority of which originates from the Southeast. One hundred and sixty-seven ethnically matched healthy control samples were collected in The Netherlands.

Clinical data were collected from the medical records. From the patients with an intronic variant, data were collected focused on the age at diagnosis, best corrected visual acuity (BCVA) using Snellen visual acuity, ophthalmoscopy, and full-field electroretinography (ffERG). FfERG was performed using Dawson–Trick–Litzkow electrodes and the RETI-port system (Roland Consults, Stasche & Finger GmbH, Brandenburg an der Havel, Germany), and the recordings were performed in accordance with the guidelines of the International Society for Clinical Electrophysiology of Vision (ISCEV) [Marmor et al., 2009]. The inclusion criteria for STGD1 were the presence of progressive retinal dystrophy with beaten-metal appearance and/or yellow-white pisciform flecks and/or autofluorescent depositions under the RPE. Inclusion criteria for CRD were a progressive decline of visual acuity, and on ERG a reduction of both cone and rod responses, with cone responses equally or more severely reduced. Exclusion criteria were an onset >40 years, extinguished scotopic or photopic responses on ERG, and congenital nystagmus. This study was approved by the local medical ethics committees and adhered to the tenets of the Declaration of Helsinki. All participants provided signed, informed consent for participation in the study, retrieval of medical records, and use of blood and DNA for research.

Blood samples were obtained of probands, their parents, and when possible, affected and unaffected siblings. DNA was isolated from peripheral blood lymphocytes by standard procedures. Multiplex ligation-dependent probe amplification (MLPA) reagents were obtained according to the manufacturer's instructions (SALSA MLPA kit P151-P152 *ABCA4*; MRC-Holland, Amsterdam, The Netherlands). Primers used to perform Sanger sequencing of all coding regions including the intron–exon boundaries and the putative promoter region (hg19 chr1:94,587,564–94,586,601; c.-963>c.1) of *ABCA4* are described in Supp. Table S2. Supp. Table S3 lists the primers employed to perform Sanger sequencing of the deep-intronic variants (V1–V5). Sanger sequencing of the 15 regions encompassing rarely used splice sites was performed using previously described primers [Braun et al., 2013]. The variants reported in this study were submitted to the locus-specific database for *ABCA4* at <http://www.lovd.nl/ABCA4>.

An overview of the genetic analyses performed previously and in this study is provided in [Supp. Table S1](#). Sequence analysis of the promoter region did not yield any variants. An in-frame deletion of exons 20–22 (c.2919-?\_3328+?del; p.S974Qfs\*64) was identified previously by Southern blotting [Maugeri et al.,

1999]. As part of a diagnostic deletion scanning protocol, DNAs of 27 patients with retinal dystrophies and one heterozygous *ABCA4* variant were fully analyzed for heterozygous *ABCA4* deletions using MLPA, which yielded two probands carrying the exon 20–22 deletion in a heterozygous state (A-IV:2 and F-II:1; Fig. 1; Table 1). A-IV:2 is a member of a previously described multiplex family segregating several monogenic and multifactorial retinal dystrophies [Klevering et al., 2004]. She was diagnosed with STGD1/CRD and carried the c.768G>T variant on the other allele, which is a frequent causative *ABCA4* variant [Maugeri et al., 1999]. The exon 20–22 deletion was also found in a second cousin (A-IV:1) who carried the c.5461–10T>C variant in a heterozygous state. Finally, another family member with STGD1 (A-III:3) carried this deletion, but no second *ABCA4* variant was detected. As described previously, III:1 and III:3 also carry the same maternal haplotype containing *ABCA4* [Klevering et al., 2004]. Ophthalmological investigations were not carried out for III:1. In Family F, this deletion was found together with a heterozygous missense variant (p.C1488R) and a heterozygous deep-intronic splice variant (see below).

**Table 1:** Retinal dystrophies-associated variants identified in *ABCA4*

Family	Diagnosis	<i>ABCA4</i> allele 1 (DNA)	<i>ABCA4</i> allele 1 (protein)	<i>ABCA4</i> allele 2 (DNA)	<i>ABCA4</i> allele 2 (protein)
A	STGD1/CRD	c.768G>T	p.(?)	c.2919-?_3328+?del	p.(S974Qfs*64)
B	STGD1	c.768G>T	p.(?)	c.443-?_570+?del	p.(G148Vfs*89)
C	STGD1	c.5584+6T>C	p.(?)	c.4539+2001G>A (V4)	p.(?)
D	CRD	c.5461–10T>C	p.(?)	c.4539+2001G>A (V4)	p.(?)
E	STGD1/CRD	c.5381C>A	p.(A1794D)	c.4539+2001G>A (V4)	p.(?)
F	STGD1/CRD	c.2919-?_3328+? del/c.4462T>C	p.(S974Qfs*64)/ (p.C1488R)	c.5196+1137G>T (V1)	p.(?)
G	STGD1/CRD	c.4892T>C	p.(L1631P)	c.4539+2001G>A (V4)	p.(?)
H	STGD1	c.3874C>T	p.(Q1292*)	c.5196+1137G>T (V1)	p.(?)
I	CD	c.5882G>A	p.(G1961E)	c.4539+2001G>A (V4)	p.(?)

*Nucleotide numbering uses +1 as the A of the ATG translation initiation codon in NM\_000350.2, with the initiation codon as codon 1. To determine the correct mutation nomenclature, <http://www.LOVD.nl/mutalyzer>, Alamut Visual version 2.4 (Interactive Biosoftware, Rouen, France), and <http://www.hgvs.org/mutnomen/> were employed.*

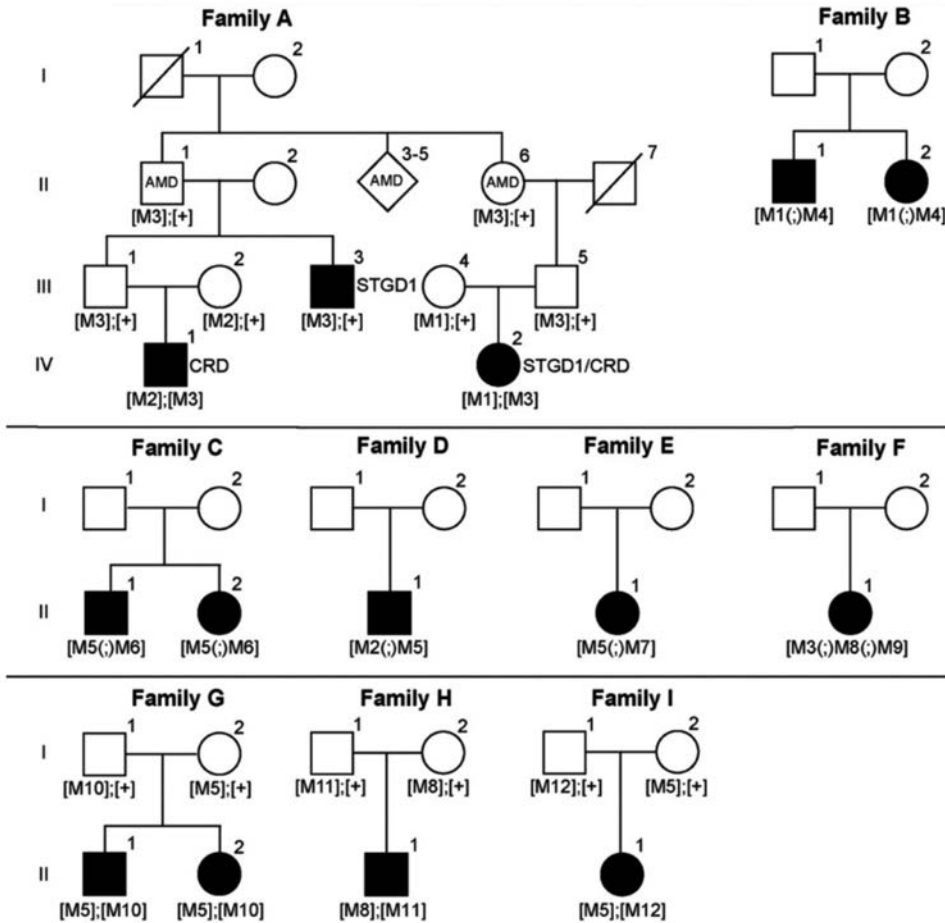


**Figure 1:** Pedigrees with retinal dystrophies and ABCA4 variants. **A–B:** Families with retinal dystrophies due to compound heterozygous exonic ABCA4 variants and intragenic deletions. Family A is adapted from Klevering et al. (2004), and contains several monogenic and multifactorial retinal dystrophies. A heterozygous deletion of exons 20–22 was found in A-IV:1, A-IV:2, and A-III:3. The latter patient does not carry a second ABCA4 variant. In Family B, a heterozygous deletion spanning exon 5 was identified. **C–I:** Families with retinal dystrophies due to combinations of exonic ABCA4 variants and deep-intronic variants. The exception is proband F-II:1, who carried a deletion spanning exon 20–22, together with a missense mutation, and a deep-intronic variant V1. Segregation analysis was not possible for Families B–F. ABCA4 variants: M1: c.768G>T; M2: c.5461–10T>C; M3: p.(S974Qfs\*64); M4: p.(G148Vfs\*89); M5: c.4539+2001G>A (V4); M6: c.5584+6T>C; M7: p.(A1794D); M8: c.5196+1137G>A (V1); M9: p.(C1488R); M10: p.(L1631P); M11: p.(Q1292\*); M12: p.(G1961E).

Using MLPA probes spanning exon 5, a novel heterozygous deletion with unknown boundaries (c.443-?\_570+?del), resulting in a predicted truncated protein (p.G148Vfs\*89), was detected in a STGD1 proband and an affected sibling of Family B (Fig. 1). Both also carried the c.768G>T variant in a heterozygous state. The identification of heterozygous *ABCA4* deletions of exon 5 and exons 20–22 explained six cases of three families (Fig. 1).

The 45 probands with one heterozygous *ABCA4* allele, as well as a group of nine STGD individuals without any pathogenic *ABCA4* variant, were analyzed for the presence of five deep-intronic variants (V1 through V5) and analyzed for sequence variants at the splice sites of 15 additional cryptic exons [Braun et al., 2013]. The deep-intronic variant c.5196+1137G>A (V1) was detected in isolated cases of two families (Families F and H; Fig. 1; Table 1). In Family F, the proband also carried a heterozygous missense variant (p.C1488R) and a heterozygous deletion of exons 20–22, but segregation analysis was not possible due to unavailability of parental DNAs. The second deep-intronic variant identified in our cohort was c.4539+2001G>A (V4), which was found in a heterozygous state in five probands (Families C–E, G, and I; Fig. 1; Table 1). In two STGD1 siblings of family C, V4 was found together with the heterozygous splice site variant c.5584+6T>C. The CRD phenotype in the sporadic patient in Family D is very likely caused by heterozygous variant V4 together with a heterozygous variant that is in linkage disequilibrium with the splice-site variant c.5461–10T>C. Individual II:1 of Family E carries the severe heterozygous missense variant p.A1794D and V4, together causing STGD1/CRD. Two siblings of Family G with STGD1/CRD carry the heterozygous missense variant p.L1631P, together with the heterozygous variant V4. The bull’s eye phenotype in a sporadic case of Family I is caused by the heterozygous variant V4 and the heterozygous missense variant p.G1961E. The analysis of the remainder of the variants or alternatively spliced exons did not yield additional variants in our cohort. None of the deep-intronic variants were identified in the nine STGD cases without exonic *ABCA4* variants.

Using Sanger sequencing, we did not identify variants V1 and V4 in 167 ethnically matched controls. In the 45 retinal disease probands with one heterozygous exonic *ABCA4* allele and in nine STGD cases with no *ABCA4* variant, we did not find the deep-intronic variants V2, V3, and V5, nor any variants in the 15 regions encompassing weak splice sites [Braun et al., 2013]. For STGD cases with no *ABCA4* variant, we should bear in mind that the genetic defects can very well reside in other genes.

The clinical characteristics of five unrelated patients with intronic variants from Families E through I are shown in [Supp. Table S4](#). They are all of Caucasian descent. These patients were diagnosed between the age of 12 and 23 years (mean: 18.4 years). The mean follow-up of disease was 25 years (range: 12–49 years). Patients from Families F and H showed the intronic variant V1. The proband from Family F carried an exon 20–22 deletion in *trans*, a protein-truncating (severe) allele [Maugeri et al., 1999]. She shows a STGD1 phenotype with a CRD pattern and a BCVA at last visit (age 35 years) of 20/600. The patient from Family H carried a nonsense variant in *trans*, and showed a typical STGD1 phenotype. His BCVA at last visit was 20/400 (age 32 years). Based on these results, V1 is deemed to have a mild effect on the function of ABCA4. Employing RNA extracted from keratinocytes derived from a STGD1 proband carrying V1 and p.T1526M (E.M.S., personal communication), Braun et al. (2013) identified intronic RNA insertions due to V1 in a significant fraction of RNA. Assuming that the ABCA4 RNA splicing in keratinocytes is similar to that in the retina, this argues for a severe effect of V1, which is in contradiction with our assessment. V1 was very recently found as the most frequent deep-intronic variant (10/233) in STGD1 probands with one ABCA4 variant [Zernant et al., 2014] and not present in 368 European controls. It was deemed nonpathogenic as it was present in 8/200 (4%) African-American controls and only found in 1/46 (2%) African-American STGD1 cases with one ABCA4 variant. However, the c.2588G>C variant in ABCA4, previously shown to be a mild allele, was found in a heterozygous state in 3% and 6% of Dutch and Swedish STGD1 cases, respectively [Maugeri et al., 1999; Maugeri et al., 2002]. The V1 variant c.5196+1137G>A is present at an orthologous position in *Macaca mulatta* as the major allele, and shown not to affect exon 36/exon 37 splicing [Zernant et al., 2014]. This result does not rule out pathogenicity of V1 in humans, however, as differences in RNA splicing have been reported between, for example, human patients and a “humanized” knock-in mouse that carries the same segment of human CEP290 with a deep-intronic variant [Garanto et al., 2013].

Patients from Families E, G, and I showed the intronic variant V4. Patients from Families E and I carried the p.A1794D and p.G1961E variants in *trans*, respectively, both of which were deemed to be mild variants in previous studies as they were identified in typical STGD1 cases that carried protein-truncating variants on the other allele [Maugeri et al., 1999; Burke et al., 2012]. The proband from Family E at her last visit had a BCVA of 20/1200 (age 67 years) and showed a STGD1/CRD picture. The proband from Family I showed a CD phenotype. Based on these data, it is proposed that V4 has a severe effect on ABCA4 function.

As reverse-transcription polymerase chain reaction analysis using lymphoblast RNA from patients carrying V4 did not yield consistent results (data not shown), there is no experimental proof for this assumption. In the absence of detailed RNA analysis, we cannot be sure that V4 is disease-causing, and it is still possible that the causative variant is in linkage disequilibrium with V4. Although we did not perform haplotype analysis for V4, it is plausible that all probands carrying this variant share a common haplotype. Our findings, together with the frequent occurrence of V4 in *trans* with exonic *ABCA4* variants in a Belgian STGD1 cohort (E. de Baere, personal communication), strongly suggest that V4 is a founder mutation.

In contrast to the cohort from Iowa, the remaining deep-intronic splice variants V2, V3, and V5 were not identified in our cohort. We also did not identify variants in the 15 additional regions containing infrequently used deep-intronic splice sites as described elsewhere [Braun et al., 2013]. From the initial cohort of 127 probands with STGD or STGD/CRD, 88 cases (69%) are currently solved with two *ABCA4* alleles, which is a remarkable difference to the Iowa cohort in which 91.8% of the cases were explained.

Identification of a second *ABCA4* variant is of high significance for the relevant patients as this clearly implicates *ABCA4* as the underlying gene, and thereby autosomal-recessive inheritance of the gene defects. In view of the high frequency of heterozygous *ABCA4* variants in healthy individuals, that is, up to 1/20 individuals [Maugeri et al., 1999], the presence of one allele can be coincidental and the genetic cause situated in another gene. Affected persons with two *ABCA4* variants are also eligible for experimental treatments based on gene augmentation. Moreover, the nine persons from families C through I carrying heterozygous deep-intronic variants V1 or V4 in principle are eligible for a novel type of treatment based on correcting erroneously spliced RNAs, using antisense oligonucleotides. In fibroblasts and immortalized lymphocytes of patients with Leber congenital amaurosis, the potential of this approach was shown by reversing the effect of a deep-intronic splice defect in *CEP290* [Collin et al., 2012]. The “correction” of one of two alleles may be beneficial and the added advantage of this approach versus *ABCA4* gene augmentation is that overexpression of the *ABCA4* gene is not possible.

In conclusion, in this study we identified previously “hidden” *ABCA4* alleles in nine of 45 (20%) families with retinal dystrophies, leaving 36 of the 45 (80%) probands with one heterozygous exonic *ABCA4* allele unexplained. To identify additional putative intronic *ABCA4* variants in the remaining monoallelic cases, intronic DNA sequencing can be combined with mRNA analysis of differentiated retinal-like cells derived from patient’s somatic cells.



## References

- Allikmets, R, Shroyer, NF, Singh, N, Seddon, JM, Lewis, RA, Bernstein, PS, Peiffer, A, Zabriskie, NA, Li, Y, Hutchinson, A, Dean, M, Lupski, JR, et al. 1997a. Mutation of the Stargardt disease gene (ABCR) in age-related macular degeneration. *Science* 277: 1805– 1807.
- Allikmets, R, Singh, N, Sun, H, Shroyer, NF, Hutchinson, A, Chidambaram, A, Gerrard, B, Baird, L, Stauffer, D, Peiffer, A, Rattner, A, Smallwood, P, et al. 1997b. A photoreceptor cell-specific ATP-binding transporter gene (ABCR) is mutated in recessive Stargardt macular dystrophy. *Nat Genet* 15: 236– 246.
- Braun, TA, Mullins, RF, Wagner, AH, Andorf, JL, Johnston, RM, Bakall, BB, Deluca, AP, Fishman, GA, Lam, BL, Weleber, RG, Cideciyan, AV, Jacobson, SG, et al. 2013. Non-exonic and synonymous variants in ABCA4 are an important cause of Stargardt disease. *Hum Mol Genet* 22: 5136– 5145.
- Burke, TR, Fishman, GA, Zernant, J, Schubert, C, Tsang, SH, Smith, RT, Ayyagari, R, Koenekoop, RK, Umfress, A, Ciccarelli, ML, Baldi, A, Iannaccone, A, et al. 2012. Retinal phenotypes in patients homozygous for the G1961E mutation in the ABCA4 gene. *Invest Ophthalmol Vis Sci* 53: 4458– 4467.
- Collin, RW, den Hollander, AI, Velde-Visser, SD, Benniselli, J, Bennett, J, Cremers, FP. 2012. Antisense oligonucleotide (AON)-based therapy for Leber congenital amaurosis caused by a frequent mutation in CEP290. *Mol Ther Nucleic Acids* 1: e14.
- Cremers, FP, de Pol, DJ, Driël, M, den Hollander, AI, Haren, FJ, Knoers, NV, Tijmes, N, Bergen, AA, Rohrschneider, K, Blankenagel, A, Pinckers, AJ, Deutman, AF, et al. 1998. Autosomal recessive retinitis pigmentosa and cone-rod dystrophy caused by splice site mutations in the Stargardt's disease gene ABCR. *Hum Mol Genet* 7: 355– 362.
- Edwards, AO, Donoso, LA, Ritter, R. 2001. A novel gene for autosomal dominant Stargardt-like macular dystrophy with homology to the SUR4 protein family. *Invest Ophthalmol Vis Sci* 42: 2652– 2663.
- Garanto, A, Beersum, SE, Peters, TA, Roepman, R, Cremers, FP, Collin, RW. 2013. Unexpected CEP290 mRNA splicing in a humanized knock-in mouse model for Leber congenital amaurosis. *PLoS One* 8: e79369.
- Jaakson, K, Zernant, J, Kulm, M, Hutchinson, A, Tonisson, N, Glavac, D, Ravnik-Glavac, M, Hawlina, M, Meltzer, MR, Caruso, RC, Testa, F, Maugeri, A, et al. 2003. Genotyping microarray (gene chip) for the ABCR (ABCA4) gene. *Hum Mutat* 22: 395– 403.
- Klevering, BJ, Maugeri, A, Wagner, A, Go, SL, Vink, C, Cremers, FPM, Hoyng, CB. 2004. Three families displaying the combination of Stargardt's disease with cone-rod dystrophy or retinitis pigmentosa. *Ophthalmology* 111: 546– 553.
- Marmor, MF, Fulton, AB, Holder, GE, Miyake, Y, Brigell, M, Back, M; International Society for Clinical Electrophysiology of Vision. 2009. ISCEV standard for full-field clinical electroretinography (2008 update). *Doc Ophthalmol* 118: 69– 77.
- Maugeri, A, Flothmann, K, Hemmrich, N, Ingvast, S, Jorge, P, Paloma, E, Patel, R, Rozet, JM, Tammur, J, Testa, F, Balcells, S, Bird, AC, et al. 2002. The ABCA4 2588G>C Stargardt mutation: single origin and increasing frequency from South-West to North-East Europe. *Eur J Hum Genet* 10: 197– 203.
- Maugeri, A, Driël, MA, de Pol, DJ, Klevering, BJ, Haren, FJ, Tijmes, N, Bergen, AA, Rohrschneider, K, Blankenagel, A, Pinckers, AJ, Dahl, N, Brunner, HG, et al. 1999. The 2588G→C mutation in the ABCR gene is a mild frequent founder mutation in the Western European population and allows the classification of ABCR mutations in patients with Stargardt disease. *Am J Hum Genet* 64: 1024– 1035.
- Poloschek, CM, Bach, M, Lagreze, WA, Glaus, E, Lemke, JR, Berger, W, Neidhardt, J. 2010. ABCA4 and ROM1: implications for modification of the PRPH2-associated macular dystrophy phenotype. *Invest Ophthalmol Vis Sci* 51: 4253– 4265.

- Yatsenko, AN, Shroyer, NF, Lewis, RA, Lupski, JR. 2003. An ABCA4 genomic deletion in patients with Stargardt disease. *Hum Mutat* 21: 636–644.
- Zernant, J, Xie, YA, Ayuso, C, Riveiro-Alvarez, R, Lopez-Martinez, MA, Simonelli, F, Testa, F, Gorin, MB, Strom, SP, Bertelsen, M, Rosenberg, T, Boone, PM, et al. 2014. Analysis of the ABCA4 genomic locus in Stargardt disease. *Hum Mol Genet* 23: 6797–6806.

## Supplemental material

**Supplemental Table S1.** Genotyping studies in retinal dystrophy patients with one *ABCA4* variant

Proband/ Family	Pheno- type	MA2002/ SSCP/ DGGE	Sanger sequencing	<i>ABCA4</i> MLPA	NGS	<i>PRPH2</i> sequencing	Analysis del exon 20-22	Promoter analysis	Analysis V1-5; V8-V21
1	STGD1	yes			yes	yes	yes	yes	yes
2	STGD1	yes			yes	yes	yes	yes	yes
3	STGD1	yes			yes	yes	yes	yes	yes
4	STGD1	yes			yes	yes	yes	yes	yes
5/A	STGD1/CRD		yes			yes	yes	yes	yes
6	STGD1		yes			yes	yes	yes	yes
7	CRD	yes	yes			yes	yes	yes	yes
8	STGD1	yes			yes	yes	yes	yes	yes
9	CRD	yes			yes	yes	yes	yes	yes
10	CRD	yes			yes	yes	yes	yes	yes
11	CD		yes			yes	yes	yes	yes
12	STGD1		yes	yes		yes	yes	yes	yes
13	STGD1		yes	yes		yes	yes	yes	yes
14	STGD1		yes	yes		yes	yes	yes	yes
15	STGD1		yes	yes		yes	yes	yes	yes
16	STGD1		yes	yes		yes	yes	yes	yes
17	STGD1		yes	yes		yes	yes	yes	yes
18	CRD	yes			yes	yes	yes	yes	yes
19	CD		yes	yes		yes	yes	yes	yes
20	STGD1		yes	yes		yes	yes	yes	yes
21	STGD1		yes	yes		yes	yes	yes	yes
22	STGD1		yes	yes		yes	yes	yes	yes
23	STGD1		yes	yes		yes	yes	yes	yes
24	STGD1	yes			yes	yes	yes	yes	yes
25	STGD1	yes	yes	yes	yes	yes	yes	yes	yes
26	STGD1		yes	yes		yes	yes	yes	yes
27	STGD1		yes	yes		yes	yes	yes	yes
28	STGD1		yes	yes		yes	yes	yes	yes
29	STGD1		yes	yes		yes	yes	yes	yes
30	STGD1	yes				yes	yes	yes	yes
31	STGD1		yes	yes		yes	yes	yes	yes
32	STGD1		yes	yes		yes	yes	yes	yes
33	STGD1		yes	yes		yes	yes	yes	yes
34	STGD1		yes	yes		yes	yes	yes	yes
35	STGD1		yes	yes		yes	yes	yes	yes
36	STGD1	yes				yes	yes	yes	yes
37	STGD1		yes	yes		yes	yes	yes	yes
38/B	STGD1	yes	yes	yes	yes	yes	yes	yes	yes
39/C	STGD1	yes			yes	yes	yes	yes	yes
40/D	CRD	yes			yes	yes	yes	yes	yes
41/E	STGD1/CRD	yes			yes	yes	yes	yes	yes
42/F	STGD1/CRD		yes	yes		yes	yes	yes	yes
43/G	STGD1/CRD		yes	yes		yes	yes	yes	yes
44/H	STGD1		yes	yes		yes	yes	yes	yes
45/I	CD		yes	yes		yes	yes	yes	yes
<b>Total</b>		<b>17</b>	<b>31</b>	<b>27</b>	<b>14</b>	<b>45</b>	<b>44</b>	<b>45</b>	<b>45</b>

DGGE, denaturing gradient gel electrophoresis; MLPA, multiplex ligation-dependent probe amplification; NGS, fluidigm-based next generation sequencing; SSCP, single strand conformation polymorphism.

**Supplemental Table S2. Primers for Sanger sequencing of ABCA4**

<i>ABCA4</i>	Forward (5'- 3')	Reverse (5'- 3')	Product size (bp)	T(a) (°C)
promoter region 1.1	CGCAAACCTCTATGAAGTCAGCA	GGCCCATTACTGTCATTCCA	249	58
promoter region 1.2	TGTCCCTTGGGATCACAGAT	CGGCAGATCTGAAGTGATCC	352	58
promoter region 1.3	AGCACCAAGCAGCCACTACT	GCACCAGGAAATTGAGGT	388	58
promoter region 1.4	AAGACATCCCCCTCAGGAAC	GGTCCAGTTCTTCCAGAGCA	389	58
Exon 1	GACCAATCTGGTCTTCGTG	GTTTATTTGCTCCACACCTC	145	56
Exon 2	TAGCACCCTGAACCTTCTCT	AAGGCCAGACCAAAGTCTC	191	58
Exon 3	CCTGCTTGGTCTCCATGAC	ACGTGAAGGGGTGTGCAAC	249	58
Exon 4	GCTATTTCTTATTAATGAGGC	CCAACCTCTCCCTGTTCTTTC	259	58
Exon 5	GACCCATTTCCCCTTCAAC	AGGCTGGGTGCTTCCCTC	230	56
Exon 6	CTTCTCTACCACAGGGCAG	AGGAATCACCTTGCAATTGG	289	58
Exon 7	TGCCTATGTGTATATACC	TAAGTGGGGTAAATGGTGG	220	58
Exon 8	GAGCATTGGCCTCACAGCAG	TTAACCAACATGAGAGGCC	356	56
Exon 9	AAGCAATGGGGAGTTTCTGT	GAGATGTGATACCAGGAAG	289	58
Exon 10	GACACACAAAAGTTCTCTCT	TCCCCTCCCCTCCCCATC	222	58
Exon 11	CTAAGCAGAGCAGTACTG	ACTTGACTTGCTAAGGGAG	314	58
Exon 12	GGTCTCTCACACTCTCT	ATTTCCCACTGACTTTGGAG	286	58
Exon 13	GAGGTGTGAGTGAGCTATCC	CCCATTAGCGTGTATGG	282	58
Exon 14	CCTCTACCAGGTACAGAGC	GGGAAAGGAACCAAAGTATTC	330	58
Exon 15	AGGCTGGTGGGAGAGAGC	AGTGGACCCCCTCAGAGG	407	58
Exon 16	CTGTTGCATTGGATAAAAGGC	GATGAATGGAGAGGGCTGG	330	58
Exon 17	CTGCGGTAAGGTAGGATAGGG	CACACCGTTTACATAGAGGGC	232	58
Exon 18	CCTCTCCCCTCCTTCTCTG	GTCAGTTTCCGTAGGCTTC	279	58
Exon 19	TGGGGCCATGTAATTAGGC	TGGGAAAGAGTAGACAGCCG	322	58
Exon 20	ACTGAACCTGGTGTGGGG	TATCTCTGCCTGTGCCAG	325	60
Exon 21	GTAAGATCAGCTGCTGGAAG	GAAGCTCTCCTGTCCAAGC	301	58
Exon 22	CACCCTCCACAGCCCCTTAAC	TCGTTGTGGTTCTGTACTCAG	291	58
Exon 23	TTTTTGCAACTATATAGCCAGG	AGCCTGTGTGAGTAGCCATG	384	58
Exon 24	GCATCAGGGAGAGGCTGTC	CCCAGCAATATTGGGAGATG	212	54
Exon 25	GGTAACCTCACAGTCTTCC	GGGAACGATGGCTTTTTGC	379	58
Exon 26	CAAAAACAGAGCTGGGTTAG	ACTTTCGAGATGGAACTTGG	191	58
Exon 27	GCTACCAGCCTGGTATTTCAATTG	GTTATAACCCATGCCTGAAG	493	56
Exon 28	CCACCAGGGGCTGATTAG	CCCAAACCCACACAGAGGAG	289	58
Exon 29	GTTGCATGATGTTGGCAGC	TCTTAGGACAGGGGCGCG	185	58
Exon 30	GTCAGCAACTTTGAGGCTG	ACTCAGGAGATACCAGGGAC	314	58
Exon 31	TAAGTCTCAAGTTCCAAGG	TCTTCTACAGGGCAGCCAG	193	58
Exon 32	GAAAGTTAACGGCCTGCT	CATGGATGTGAGGTGTGC	185	58
Exon 33	TTCATGTTCCCTACAAAACCC	CATGAGAGTTTCTCATTCTATGG	265	58
Exon 34	GCTTAACTACCATGAATGAG	ATTCCTTGCTAGATTTACAGC	286	56
Exon 35	GCAGCGTCTCCAATGTCCTC	AAGAGTGGAGAAGGTGACAAG	255	58
Exon 36	GTATCTTCTCTCTTGTGC	ACACACAAGCTCCACCTTG	304	58
Exon 37	TTGAGAGCTGGCAGCAG	CCACCAGGCTTCTTTCAG	226	58

<i>ABCA4</i>	Forward (5'-3')	Reverse (5'-3')	Product size (bp)	T(a) (°C)
Exon 38	GGAATGGAATGTGGA ACTCC	CACATACTCTACTATCCTAC	253	58
Exon 39	TGCTGTCTGTGAGAGCATC	TCCCAGCTTTGGACCCAG	268	58
Exon 40	CCAGGTCTGTGGGGTGAG	AGTTCTGGATGCCCTGAG	241	60
Exon 41	GGACACTGTACAGCCAGC	GACGAGTTATAACACAGGG	319	58
Exon 42	CTCCTAAACCATCCTTTGCTC	AGGCAGGCACAAGAGCTG	214	58
Exon 43	CTTACCCTGGGGCCTGAC	CTCAGAGCCACCCTACTATAG	277	58
Exon 44	GAAGCTTCTCCAGCCCTAGC	TGCACTCTCATGAAACAGGC	287	58
Exon 45	GTTTGGGGTGTTTGCTTGTC	ACCTATTTCCCAACCCAAGAG	257	58
Exon 46	GAAGCAGTAATCAGAAGGGC	GCCTCACATTCTTCCATGCTG	256	58
Exon 47	TCACATCCCACAGGCAAGAG	AGGTGGATCCACAGAAGGC	256	58
Exon 48	GATTACCTTAGGCCCAACC	ACACTGGGTGTTCTGGACC	228	60
Exon 49	GTGTAGGGTGGTGTTTTCC	AAGCCCAGTGAACCAGCTGG	365	58
Exon 50	GGAGAGAAAGATGGCCCATATA	GTGTGTTTGTTTCTGCTGC	305	58

**Supplemental Table S3.** Primers for Sanger sequencing of deep intronic variants (V1-V5) in

Deep intronic variant	Forward (5'-3')	Reverse (5'-3')	Product size (bp)	T(a) (°C)
V1/V2/V3	GACCAACATGAGCCTCCATT	GGTGGGCCTAGCTCCTTTTA	349	58
V4/V5	AGGGATCCAAAAGAAGGAC	GGGACCAAGGACCAACACTA	293	58

**Supplemental Table S4.** Clinical characteristics of the patients included in this study at findings at first diagnosis and most recent visit

Patient	Gender	Age (y)	BCVA	Fundus	fERG*	Diagnosis	AIV (y)	BCVA	Fundus	fERG*	Diagnosis
E-II-1	F	18	20/200	Macular pigment changes, yellow flecks reaching up to vascular arcades	Photopic: N Scotopic: RE: MR, LE: N	STGD1	67	20/1200	Large RPE atrophic regions	Photopic: ND Scotopic: RE: SR, LE: ND	STGD1 with CRD pattern
F-II-1	F	23	20/50	Paravoveal hypopigmentation and yellow-white flecks in posterior pole	Photopic and scotopic: N	STGD1	35	20/600	Profound chorioretinal atrophy macula and midperiphery. Intraretinal pigmentations in the macula	Photopic: N, Scotopic: RE: MR, LE: SR	STGD1 with CRD pattern
G-II-2	F	12	NP	NP	NP	STGD1	48	20/400	Large RPE atrophic regions	Photopic: SR, Scotopic: N	STGD1 with CRD pattern
H-II-1	M	18	20/100	Subtle flecks perimacular	Photopic and scotopic: N	STGD1	32	20/400	Macular RPE atrophy, midperiphery flecks	NP	STGD1
I-II-1	F	21	20/100	Bull's eye, no flecks	Photopic and scotopic: N	Bull's eye maculopathy	35	20/400	Bull's eye, no flecks	Photopic: RE: MR, LE: SR Scotopic: N	CD

**AAD, Age at diagnosis; AIV, age at last visit; BCVA, best corrected visual acuity (Snellen); CD, cone dystrophy; CRD, cone-rod dystrophy; STGD1, Stargardt disease type 1; fERG, full-field electroretinogram; F, female; M, male; LE, left eye; RE, right eye. \*The abbreviations reflect the amplitude: N, normal (equal to or above the lower 5% of the range for a normal population: photopic  $\geq 78\mu\text{V}$ , scotopic  $\geq 263\mu\text{V}$ ); MR, moderately reduced (1-5% of normal range: photopic  $\geq 69\mu\text{V}$  and  $<78\mu\text{V}$ , scotopic  $\geq 195\mu\text{V}$  and  $<263\mu\text{V}$ ); SR, severely reduced ( $<1\%$  of normal range: photopic  $<69\mu\text{V}$ , scotopic  $<195\mu\text{V}$ ); ND, not detectable; NP, not perform**



## CHAPTER 3.3

### Photoreceptor progenitor mRNA analysis reveals exon skipping resulting from the *ABCA4* c.5461-10T → C mutation in Stargardt disease

*“We investigated the effect of the c.5461-10T>C variant on splicing by analyzing mRNA from photoreceptor progenitor cells (PPCs) derived from persons with STGD1 who carry this variant in a homozygous or heterozygous state. In addition, we performed in vitro minigene splicing studies to show that this variant results in truncation of the predicted ABCA4 protein.”*

Riccardo Sangermano  
Nathalie M. Bax  
Miriam Bauwens  
L. Ingeborgh van den Born  
Elfride de Baere  
Alex Garanto  
Rob W. Collin  
Angelique S. Goerharn- Ramlal  
Anke H. den Engelsman- van Dijk  
Karl Rohrschneider  
Carel B. Hoyng  
Frans P.M. Cremers  
Silvia Albert

*Ophthalmology* 2016;123(6):1375-85.

The authors thank Erwin van Wijk for providing the Gateway-adapted minigene vector.



**PURPOSE:** To elucidate the functional effect of the *ABCA4* variant c.5461-10T→C, one of the most frequent variants associated with Stargardt disease (STGD1).

**DESIGN:** Case series.

**PARTICIPANTS:** Seventeen persons with STGD1 carrying *ABCA4* variants and 1 control participant.

**METHODS:** Haplotype analysis of 4 homozygotes and 11 heterozygotes for c.5461-10T→C and sequence analysis of the *ABCA4* gene for a homozygous proband. Fibroblasts were reprogrammed from 3 persons with STGD1 into induced pluripotent stem cells, which were differentiated into photoreceptor progenitor cells (PPCs). The effect of the c.5461-10T→C variant on RNA splicing by reverse-transcription polymerase chain reaction was analyzed using PPC mRNA. In vitro assays were performed with minigene constructs containing *ABCA4* exon 39. We analyzed the natural history and ophthalmologic characteristics of 4 persons homozygous for c.5461-10T→C.

**MAIN OUTCOME MEASURES:** Haplotype and rare variant data for *ABCA4*, RNA splice defects, age at diagnosis, visual acuity, fundus appearance, visual field, electroretinography (ERG) results, fluorescein angiography results, and fundus autofluorescence findings.

**RESULTS:** The frequent *ABCA4* variant c.5461-10T→C has a subtle effect on splicing based on prediction programs. A founder haplotype containing c.5461-10T→C was found to span approximately 96 kb of *ABCA4* and did not contain other rare sequence variants. Patient-derived PPCs showed skipping of exon 39 or exons 39 and 40 in the mRNA. HEK293T cell transduction with minigenes carrying exon 39 showed that the splice defects were the result of the c.5461-10T→C variant. All 4 subjects carrying the c.5461-10T→C variant in a homozygous state showed a young age of STGD1 onset, with low visual acuity at presentation and abnormal cone ERG results. All 4 demonstrated severe cone–rod dystrophy before 20 years of age and were legally blind by 25 years of age.

**CONCLUSIONS:** The *ABCA4* variant c.5461-10T→C is located on a founder haplotype lacking other disease-causing rare sequence variants. In vitro studies revealed that it leads to mRNA exon skipping and *ABCA4* protein truncation. Given the severe phenotype in persons homozygous for this variant, we conclude that this variant results in the absence of *ABCA4* activity.

## Introduction

Biallelic variants in the gene encoding the ATP-binding cassette transporter type A4 (*ABCA4*) have been identified in approximately 75% of cases with autosomal recessive Stargardt disease (STGD1)<sup>1, 2, 3, 4, 5</sup> and in approximately 30% of patients with autosomal recessive cone-rod dystrophy (CRD).<sup>6</sup> In severe CRD cases, the phenotype can resemble retinitis pigmentosa. More recently, late-onset STGD1<sup>7</sup> and STGD1 cases with a fine granular pattern with peripheral spots on autofluorescence examination<sup>8</sup> have been associated with the presence of 1 or 2 *ABCA4* variants. The clinical variability observed in *ABCA4*-associated cases can be explained by a genotype-phenotype correlation model in which the residual activity of the mutant *ABCA4* protein determines the clinical phenotype.<sup>2, 9</sup> Persons with severe CRD carry 2 *ABCA4* null alleles, whereas persons with STGD1 carry 2 moderately severe variants or a combination of a mild and a severe variant.<sup>2, 9</sup> The *ABCA4* protein has been proposed to act as a flippase for 11-*cis* and *all-trans* isomers of *N*-retinylidene-phosphatidylethanolamine across disc membranes, thereby facilitating the removal of retinal products from the disc membranes and preventing the accumulation of potentially toxic bisretinoid compounds (e.g., A2E) in photoreceptor and retinal pigment epithelial cells.<sup>10, 11</sup>

To provide an accurate prognosis for persons with *ABCA4* variants, it is important to assess the functional consequences of the approximately 1000 *ABCA4* variants that have been reported to date. This is straightforward for protein-truncating variants (i.e., stop mutations, frameshift mutations, canonical splice-site mutations), but much more difficult for rare missense mutations (i.e., amino acid substitutions) and noncanonical splice variants (i.e., RNA splice variants outside the conserved intronic dinucleotides at the ends of introns) with an unclear functional effect. The pathogenicity of selected amino acid substitutions has been studied by assessing mutant *ABCA4* protein stability, ATP-binding properties, ATPase activity, and mislocalization.<sup>12, 13, 14, 15</sup>

An unusually high proportion of STGD1 cases from northern Europe and the United States (approximately 30%) shows only 1 *ABCA4* variant, despite comprehensive Sanger sequencing and deletion analysis of the 50 protein coding exons.<sup>1, 2, 3, 4, 16, 17</sup> Very recently, deep-intronic variants (i.e., variants not located near the coding exons) have been identified that can explain a proportion of these so-called missing mutations.<sup>16, 17, 18, 19</sup> The identification of both *ABCA4* alleles and experimental proof that they have an effect on *ABCA4* function also are crucial for the selection of persons with STGD1 for upcoming gene-specific trials, such as gene augmentation

(i.e., <https://clinicaltrials.gov/ct2/show/NCT01367444?term=ABCA4&rank=8> and <https://clinicaltrials.gov/ct2/show/NCT01736592?term=ABCA4&rank=12>) or other types of treatment.

The identification of mRNA abnormalities is hampered by the photoreceptor-specific expression of *ABCA4*.<sup>5</sup> This is particularly important for noncanonical splice variants with unknown effects on splicing. The third most frequent *ABCA4* variant, c.5461-10T→C (previously denoted as IVS38-10T→C; Cornelis S, Cremers FPM, unpublished data, 2015), on the basis of prediction programs has a very small effect on splicing efficiency. In our classical STGD1 patients, it is found very often together with the mild c.2588G→C (p.Gly863Ala)/(p.Gly863del) variant, suggesting that c.5461-10T→C represents a severe *ABCA4* variant.

In this study, we investigated the effect of the c.5461-10T→C variant on splicing by analyzing mRNA from photoreceptor progenitor cells (PPCs) derived from persons with STGD1 who carry this variant in a homozygous or heterozygous state. In addition, we performed in vitro minigene splicing studies to show that this variant results in truncation of the predicted *ABCA4* protein.

## Methods

### Subjects and Clinical Evaluation

We ascertained 15 persons with STGD1 carrying the c.5461-10T→C variant in a homozygous state (patients 1–4) or compound heterozygous state (patients 5–15) from the Netherlands and Germany. In addition, we studied 2 individuals with STGD1 with a single *ABCA4* allele (patients 16 and 17) and a control. Genotype data for patients 1 through 17 can be found in [Supplemental Table 1](#). This study was approved by the institutional review board and adhered to the tenets of the Declaration of Helsinki. We studied all recent and available retrospective data of patients 1 through 4. This included history on initial symptoms, age at diagnosis, regression of Snellen best-corrected visual acuity (converted in [Fig 1](#) to equivalent logarithm of the minimum angle of resolution visual acuity), and description of the fundus abnormalities. Thereafter, we also examined available color vision testing results, visual fields (Goldmann), fundus photography, fluorescein angiography, fundus autofluorescence imaging (confocal scanning laser ophthalmoscope [Spectralis; Heidelberg Engineering, Heidelberg, Germany]), spectral-domain optical coherence tomography (Spectralis), and full-field electroretinography (ffERG).

## Molecular Genetic Analysis

### *In silico* analysis of the ABCA4 c.5461-10T→C variant on splicing

The possible effect of the noncanonical splice variant c.5461-10T→C in ABCA4 on splicing was assessed by the use of 5 algorithms (SpliceSiteFinder, MaxEntScan, NNSPLICE, GeneSplicer, and Human Splicing Finder) via Alamut Visual software version 2.7 (Interactive Biosoftware, Rouen, France; [www.interactive-biosoftware.com](http://www.interactive-biosoftware.com)).

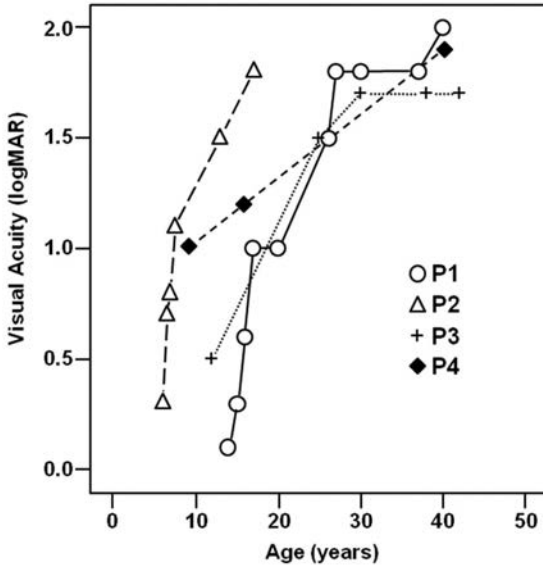


**Figure 1:** Graph showing visual acuity in 4 persons with Stargardt disease with the homozygous c.5461-10T→C ABCA4 mutation. Snellen best-corrected visual acuity (BCVA) was converted to equivalent logarithm of the minimum angle of resolution (logMAR) visual acuity: logMAR 0.5 = 20/60 Snellen; logMAR 1.0 = 20/200 Snellen; logMAR 1.4 = 20/500 Snellen = blindness (World Health Organization criteria). Age at diagnosis for these persons was between 6 and 14 years; legal blindness was observed in all 4 patients before the age of 25 years. P = patient.

### Haplotype analysis

Eighteen single nucleotide polymorphisms (SNPs) were selected from within the ABCA4 gene and flanking sequences on the basis of their high degree of heterozygosity in the Dutch population (average minor allele frequency, 0.39; Genome of the Netherlands; <http://www.nlgenome.nl/>). Polymerase chain reaction (PCR) primers were designed to analyze amplicons of approximately 270 bp containing these SNPs. Reaction mixtures (25 µl) contained Taq DNA polymerase, 1 U/µl (catalog no., 11647679001; Roche, Basel, Switzerland), 10X PCR buffer containing MgCl<sub>2</sub>, 25 mM MgCl<sub>2</sub>, 10 mM dNTPs (deoxynucleotide triphosphates), and 10 µM of each primer pair and of 50 ng genomic DNA. Polymerase chain reaction analyses were performed by using the Veriti Thermal Cycler (Thermo Fisher Scientific, Waltham, MA), and PCR conditions were a first denaturation step of 95° C for 5 minutes followed by 35 cycles of melting (95° C for 30 seconds), annealing (58° C for 30 seconds), and extension (72° C for 45 seconds) steps, with a final elongation of 72° C for 5 minutes. Polymerase chain reaction products were Sanger sequenced in a 3100 or 3730 DNA Analyzer (Thermo Fisher Scientific). Primer details are given in Supplemental Table 2 .

### ***Haloplex targeted ABCA4 enrichment and sequence analysis***

For patient 1, the *ABCA4* locus was enriched by using a custom Haloplex Target Enrichment kit (Agilent, Santa Clara, CA). Probes were designed with SureDesign (Agilent) to target a 365-kb region (chr1:94337885–94703604, GRCh37/hg19 assembly) encompassing the entire *ABCA4* gene and flanking regulatory elements that have been conserved in different species.<sup>20</sup> This study used multispecies comparison to map cis-regulatory domains of genes assuming they are located in regions of synteny. The 365-kb region corresponds to a region of synteny. The probes covered more than 98% of the targeted regions, and gaps in coverage corresponded to repeat-rich regions. Subsequently, samples were sequenced by using Illumina sequencing technology (MiSeq; Illumina, San Diego, CA) to obtain 2×250-bp reads. Data analysis was performed with CLC Bio Software (CLC Bio Genomics Workbench; Qiagen, Hilden, Germany). Reads were aligned against a reference genome (GRCh37/hg 19 assembly), and variants were identified and annotated by a custom-designed workflow. Variants were considered for further filtering only if they were present in at least 1 forward and 1 reverse read, in a minimum of 20% of all reads, and with a minimum coverage of 5 reads. The variants were annotated further by Alamut Batch (Interactive Biosoftware) and RegulomeDB (<http://www.regulomedb.org>). Variants were filtered on the basis of population frequency, as determined by Genome of the Netherlands, a database containing genomic sequences from approximately 500 control individuals from the Netherlands,<sup>21</sup> and Exome Aggregation Consortium (Cambridge, MA), a dataset of 60706 unrelated individuals sequenced as part of various disease-specific and population genetic studies (available at: <http://exac.broadinstitute.org>; accessed November 10, 2015).

### ***Patient-derived fibroblast reprogramming***

Skin biopsy samples from 3 persons with STGD1 and from 1 control were collected, washed in phosphate-buffered saline (catalog no., P5493; Sigma Aldrich, St. Louis, MO), dissected, and processed as described in the Supplemental Materials (available at [www.aaajournal.org](http://www.aaajournal.org)). After approximately 1 month, a pure culture of fibroblasts was reprogrammed by following the protocol described in the Supplemental Materials (available at [www.aaajournal.org](http://www.aaajournal.org)). Briefly, fibroblasts were transduced with 4 lentiviral vectors containing the stemness-related genes *OCT3/4*, *NANOG*, *KLF4*, and *c-MYC* and cultured in stem cell-specific medium for 1 month. Subsequently, induced pluripotent stem cell (iPSC) colonies were picked and expanded on Vitronectin-coated plates (catalog no., A14700; Thermo Fisher Scientific) in Essential E8 medium (catalog no., A1517001; Thermo Fisher Scientific).

### ***Induced pluripotent stem cell differentiation into photoreceptor progenitor cells***

Induced pluripotent stem cell clumps were cut with the StemPro Ez-passage disposable stem cell passaging tool (catalog no., 23181-010; Thermo Fisher Scientific) and cultured in ultralow-attachment 24-well plates (catalog no., corn3473; VWR, Amsterdam, the Netherlands) to form embryoid bodies for 4 days. Embryoid body medium consisted of DMEM/F-12 (Dulbecco's Modified Eagle Medium: Nutrient Mixture F-12) containing 10% (volume/volume), knockout serum replacement (catalog no., 10828-028; Thermo Fisher Scientific) supplemented with nonessential amino acids (catalog no., M7145; Sigma Aldrich), L-glutamine (catalog no., G8541; Sigma Aldrich), B27 supplements (catalog no., 12587010; Thermo Fisher Scientific), N2 supplements (catalog no., 17502048; Thermo Fisher Scientific), 5 ng/ml insulin-like growth factor-1 (catalog no., I3769; Sigma Aldrich), 1 ng/ml Dickkopf-related protein-1 (catalog no., SRP3258; Sigma Aldrich), and 1 ng/ml Noggin (catalog no., SRP3227; Sigma Aldrich). Embryoid bodies then were transferred to attachment culture conditions on Matrigel (catalog no., corn354230; VWR)-coated plates and cultivated for 2 weeks in PPC intermediate medium consisting of DMEM/F-12 containing L-glutamine, nonessential amino acids, B27 supplements, N2 supplements, 10 ng/ml insulin-like growth factor-1, 5 ng/ml recombinant fibroblast growth factor basic (catalog no., F0291; Sigma Aldrich), 10 ng/ml Dickkopf-related protein-1, and 10 ng/ml Noggin. Two weeks after the start of the differentiation, the PPC final medium, consisting of PPC intermediate medium, with 40 ng/ml 3,3',5-Triiodo-L-thyronine sodium salt (catalog no., T6397; Sigma Aldrich), 20 mM Taurine (catalog no., T0625; Sigma Aldrich), 2 ng/ml recombinant FGF acidic (catalog no., 231-BC-025; R&D Systems, McKinley Place, MN), and 10  $\mu$ M DAPT (catalog no., D5942; Sigma Aldrich) was added.

### ***RNA isolation and cDNA synthesis***

All RNA isolations and cDNA synthesis were performed as follows. Total RNA was isolated by using the NucleoSpin RNA Clean-up Kit (catalog no., 740955-50; Macherey-Nagel, Düren, Germany) according to the manufacturer's protocol. RNA was quantified and cDNA was synthesized from 1  $\mu$ g RNA by using the iScript cDNA synthesis kit (catalog no., 1708891; Bio-Rad, Hercules, CA) following the manufacturer's instructions.

### ***Induced pluripotent stem cell and photoreceptor progenitor cells characterization by quantitative polymerase chain reaction and immunofluorescence***

RNA isolation and cDNA synthesis were performed as described above. Primers for the quantitative PCR analysis are listed in [Supplemental Table 3](#) (available at [www.aaojournal.org](http://www.aaojournal.org)). Quantitative PCR was performed with the GoTaq Real-Time

qPCR Master Kit (catalog no., A6002; Promega, Madison, WI). Samples were processed in an Applied Biosystem 7900HT fast real-time PCR system (Thermo Fisher Scientific). Each sample was assayed in triplicate and normalized against the expression of the housekeeping gene *GUSB*. Relative quantification was based on the  $2^{-(\Delta\Delta Ct)}$  method, with fibroblasts and undifferentiated iPSCs as calibrators for the characterization of iPSCs and PPCs, respectively.

For immunofluorescence, cells cultivated in slide flasks (catalog no., 10439672; Thermo Fisher Scientific) were fixed for 20 minutes in 4% (weight/volume) paraformaldehyde at room temperature. Antigen retrieval was required for all experiments, and donkey serum (6% [volume/volume] in Tris-buffered saline and 0.5% [volume/volume] Triton X-100) was used during the blocking and for the dilution of the antibodies. Primary and secondary antibodies used for both iPSC and PPC characterization are listed in [Supplemental Table 4](#) (available at [www.aaojournal.org](http://www.aaojournal.org)). The slides were incubated with the primary antibody overnight at 4° C. The sections were washed 3 times for 5 minutes with Tris-buffered saline and incubated for 2 hours at 37° C with the secondary antibody. This was followed by 3 further washes of 5 minutes in Tris-buffered saline, and then the slides were mounted with Vectashield-containing DAPI (4',6-diamidino-2-phenylindole) mounting medium (catalog no., H-1200; Vector Laboratories, Inc, Burlingame, CA) and observed in a Zeiss Imager Z2 microscope (Zeiss, Oberkochen, Germany). Images were captured with the software Zen Pro 2012 (Carl Zeiss, Sliedrecht, the Netherlands).

### ***ABCA4* transcript analysis**

Photoreceptor progenitor cells were harvested from patients 1, 16, and 17 and 1 healthy control after 45 days of differentiation. Reverse-transcription (RT) PCR was performed by using a forward primer located in *ABCA4* exon 36 (5'-CCACCTACTGGGTGACCAAC-3') and a reverse primer located in *ABCA4* exon 41 (5'-AACAAATGGGCTCCTTAGTGG-3'). All reaction mixtures (50  $\mu$ l) contained 10  $\mu$ M of each primer pair, *Taq* DNA polymerase, 1 U/ $\mu$ l (catalog no., 11647679001; Roche), 10X PCR buffer without MgCl<sub>2</sub>, 25 mM MgCl<sub>2</sub>, 10 mM dNTPs, and 50 ng cDNA. Polymerase chain reaction analysis was performed by using the Veriti Thermal Cycler (Thermo Fisher Scientific), and PCR conditions were a first denaturation step of 94° C for 5 minutes followed by 35 cycles of melting (94° C for 30 seconds), annealing (58° C for 30 seconds), and extension (72° C for 1 minute) steps, with a final elongation step of 72° C for 5 minutes. The RT-PCR products were run on a 1.5% (weight/volume) agarose gel, and the resulting bands were excised and

purified with the NucleoSpin Gel & PCR cleanup kit (catalog no., 740609.250; Macherey-Nagel) according to the manufacturer's protocol. Finally, 100 ng of the purified nucleic acid was analyzed by Sanger sequencing in a 3100 or 3730 DNA Analyzer (Thermo Fisher Scientific).

### **Generation of minigenes and in vitro splice assays**

To amplify 2 segments of the genomic region encompassing exon 39 of the *ABCA4* gene, we designed PCR primers located in introns 38 (forward) and 40 (reverse), as described in [Supplemental Table 5](#) (available at [www.aaojournal.org](http://www.aaojournal.org)). The primers were designed with Primer3 software (available at: <http://bioinfo.ut.ee/primer3-0.4.0>). The PCR reaction mixtures (50  $\mu$ l) contained 10  $\mu$ M of each primer pair, a high-fidelity *Taq* polymerase AccuPrime *Taq* DNA Polymerase System (catalog no., 12339-016; Invitrogen, Carlsbad, CA), 10X AccuPrime PCR buffer II, and 200 ng genomic DNA from patient 1 and 1 healthy control. The resulting PCR products were run on a 1% (weight/volume) agarose gel, their bands were excised, and the nucleic acid was purified with the NucleoSpin Gel and PCR cleanup kit (catalog no., 740609.250; Macherey-Nagel), according to the manufacturer's protocol. One hundred fifty nanograms of each purified insert were cloned into the pDONR201 vector by using the Gateway BP Clonase Enzyme Mix (catalog no., 11789021; Thermo Fisher Scientific).

A plasmid containing the genomic region encompassing exons 3 through 5 of *RHO* inserted at the *EcoRI/SalI* sites in the pCI-NEO vector<sup>23</sup> was adapted to the Gateway cloning system and used for in vivo splicing assays. The plasmid was digested with *EcoNI* and *PflMI* (catalog no., R0521S; New England Biolabs, Ipswich, MA), resulting in the removal of exon 4 and part of the flanking intronic sequences, and was blunted using large (Klenow) fragment DNA polymerase I (catalog no., M0210S; New England Biolabs) according to manufacturer's instructions. Subsequently, a blunt-end Gateway cloning cassette containing attR1 and attR2 sites and the pCI-neo vector was ligated by using the Rapid DNA Ligation Kit (catalog no., 11635379001; Roche) to generate pCI-NEO-*RHO* exon3,5/DEST. The different pDONR cloned constructs were validated by Sanger sequencing, and 150 ng of each were cloned into the destination vector pCI-NEO-*RHO* exon3,5/DEST by using the Gateway LR Clonase enzyme mix (catalog no., 11791043; Thermo Fisher Scientific). Four minigene constructs were generated, 2 with the wild-type and 2 with the c.5461-10T $\rightarrow$ C variant.



HEK293T cells (ATCC CRL-3216; American Type Culture Collection [ATCC], Wesel, Germany) were grown in DMEM supplemented with 10% (volume/volume) fetal calf serum (catalog no., F7524; Sigma Aldrich), 1% (volume/volume) Na pyruvate (catalog no., S8636; Sigma Aldrich), and penicillin/streptomycin (catalog no., P4333; Sigma Aldrich). Cells were seeded in 12-well plates at a density of  $2.5 \times 10^5$  cells/well and transfected the day after with 1  $\mu\text{g}$  of each minigene plus FuGENE HD Transfection Reagent (catalog no., E2311; Promega) with a DNA-to-liposome ratio of 1  $\mu\text{g}$ :3  $\mu\text{l}$ , according to the manufacturer's instructions. Medium was replaced after 24 hours, and cells were harvested 48 hours after transfection. Total RNA isolation and cDNA production was performed as described before. All RT-PCR reactions were performed as described above, and PCR conditions were an initial denaturation step of 94° C for 5 minutes followed by 35 cycles of melting (94° C for 30 seconds), annealing (58° C for 30 seconds), and extension (72° C for 1 minute) steps, with a final elongation step of 72° C for 5 minutes. The splicing efficiency of exons of interest was determined by RT-PCR with forward and reverse primers residing in exons 3 and 5 of *RHO* (Supplemental Table 5, available at [www.aaojournal.org](http://www.aaojournal.org)). The RT-PCR products were resolved on a 2% (weight/volume) agarose gel, the resulting bands were excised, and the nucleic acid was purified by using NucleoSpin Gel & PCR cleanup (Macherey-Nagel), and Sanger sequencing was performed on 100 ng of each purified band by using the same primers used in the PCR reaction.

## Results

### Clinical characteristics of patients carrying the homozygous c.5461-10 T→C ABCA4 mutation

Clinical characteristics of patients with the homozygous c.5461-10T→C variant are shown in [Table 1](#). All patients had loss of central vision early in life and were diagnosed with STGD1 between 6 and 14 years of age. On follow-up, visual acuity showed a sharp decline to severe visual impairment within 2 or 3 years from first symptoms ([Fig 1](#)), leading to legal blindness (visual acuity, 20/500 or lower) in early adulthood. [Figure 2](#) depicts fundus, fundus angiography, fundus autofluorescence, and optical coherence tomography images in several disease stages of patient 2, as well fundus photographs of patients 3 and 4 after 30 years of follow-up. Funduscopy at diagnosis revealed a maculopathy in all 4 patients with perimacular lipofuscin deposits extending toward the midperiphery (fundus flavimaculatus; especially in patients 1 and 3, data not shown). Through the years, the central lesions evolved into atrophy of the retinal layers, retinal pigment epithelium, and choriocapillaries ([Fig 2G-I](#)). In the mid periphery, retinal pigment epithelium mottling occurred followed by atrophy in all 4 patients, with hyperpigmentation in patient 1 (data not shown) and patient 3 ([Fig 2H](#)). We could retrieve the BCVA at the first ophthalmic visit in 21 out of 31 patients; the median BCVA at that time was 20/32 Snellen (20/20 - 20/400). The median interval and 95% confidence interval (CI) between the age at onset and decline in BCVA to mild, moderate, severe visual impairment and blindness was 1 year (95% CI, 0.0 - 2.25), 4 years (95% CI, 3.1 - 4.9) and 12 years (CI 95% 7.8 – 16.2). One patient reached blindness 34 years after the first symptoms of onset at age 9. In many patients, the visual acuity findings were quite variable early in the course of the disease as shown in [Figure 1](#).

At presentation, ERG cone responses were reduced in all 4 patients, suggesting early generalized cone disease. On follow-up, cone dysfunction developed into progressive loss of cone and rod responses, leading to a nondetectable ERG response in patients 1, 2, and 3. Color vision defects varied from normal to defects in the red–green or blue–yellow axis at the first visit. Later color vision disturbances became more diffuse. Goldmann perimetry performed in patients 1 and 3 revealed large central scotomas.

**Table 1:** Clinical characteristics of patients homozygous for c.5461-10 T→C

Patient No.	Gender	Age (yrs)	Age at Diagnosis (yrs)	Initial Symptoms	Age at Diagnostic Examination (yrs)	Best-Corrected Visual Acuity (Snellen)	Fundus Findings	Color Vision	Visual Field Findings	Fluorescein Angiography Findings	Fundus Autofluorescence Findings	Full-Field Electroretinography Results	
												Red Function	Cone Function
1	M	52	14	Decreased visual acuity	17 and 40	20/200	Fundus flavimaculatus, peripapillary atrophy Central and peripheral choroidal atrophy with bone spicules	Red-green deficiency	Relative central scotoma	Dark choroid	NP	N	Reduced
2	M	20	6	Decreased visual acuity	6 and 17	20/100	No (fishtail) flecks, hypopigmented juxtafoveal Central to midperipheral atrophy	NP	NP	Dark choroid	NP	N	Reduced
3	F	43	12	Decreased visual acuity	12 and 42	20/60	Ball's-eye maculopathy with fundus flavimaculatus	Panel D15: saturated version, normal; desaturated, B-Y defect	Absolute central scotoma, with intact periphery (30 yrs)	NP	NP	12 yrs, mildly reduced; 25 yrs, mildly significantly reduced	12 yrs, near normal; 25 yrs, significantly reduced
4	M	46	9	Decreased visual acuity	9 and 40	20/200	Large atrophic RPE lesions with hyperpigmentations in the posterior pole, hypopigmentations and hyperpigmentations in the periphery Maculopathy	Panel D15: saturated version, normal; desaturated version, diffusely abnormal; HRR mildly abnormal	Absolute central scotoma with intact periphery	NP	NP	N	Significantly reduced
						CF (-10 D)	Pronounced atrophy posterior pole, atrophic lesions periphery with RPE alterations	Panel D15: saturated version, diffusely abnormal	NP	NP	NP	Severely reduced	NR

B-Y = blue-yellow color defect; CF = counting fingers; D = diopter; F = female; HRR = Hardy-Rand and Rittler; M = male; N = normal; NP = not performed; NR = nonrecordable; RPE = retinal pigment epithelium.

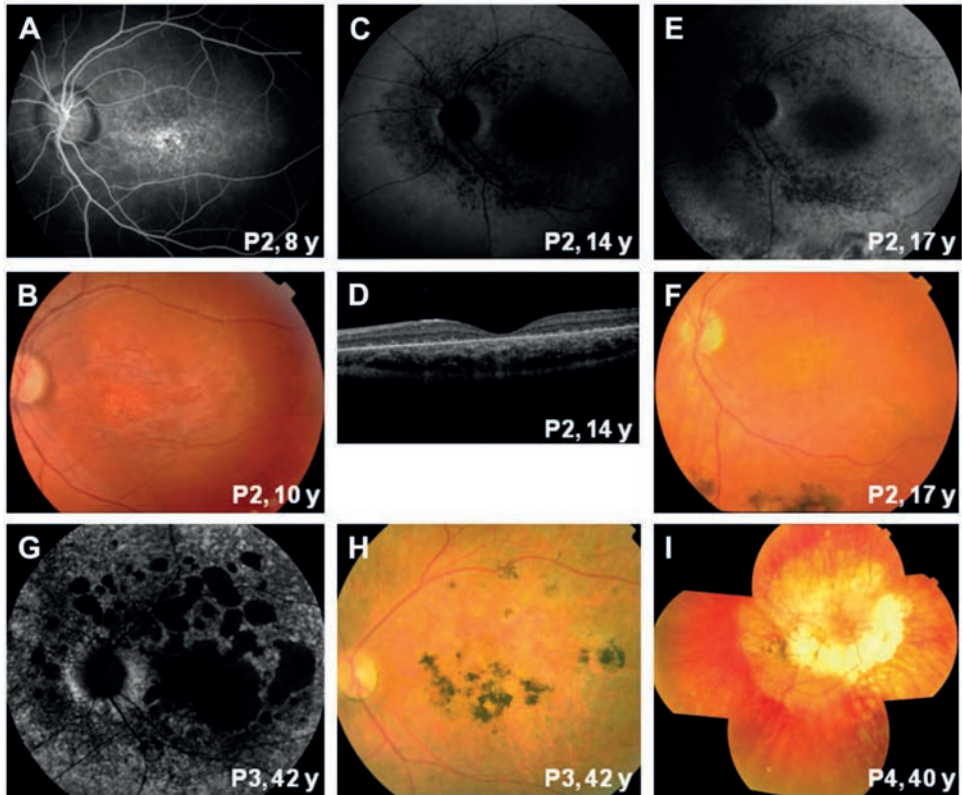


**Figure 2.** Chorioretinal images for 3 Stargardt patients with the homozygous *c.5461-10T→C* ABCA4 mutation: (A–F) patient 2 (P2), (G,H) patient 3 (P3), and (I) patient 4 (P4). A, Fluorescein angiogram of the left eye at 8 years of age showing a dark choroid sign. B, Fundus photograph of the left eye obtained at 10 years of age showing a hypopigmented macula and no flecks. C, Autofluorescence image of the left eye obtained at 14 years of age showing an atrophic macula and hypofluorescence up to the arcades and peripapillary. D, Optical coherence tomography scan of the left eye obtained at 14 years of age showing loss of the retinal pigment epithelium (RPE) layer. E, Autofluorescence image of the left eye obtained at 17 years of age showing an atrophic macula and hypofluorescence up to the periphery. F, Fundus photograph of the left eye obtained at 17 years of age showing central to mid-peripheral atrophy. G, Autofluorescence image of the left eye obtained at 42 years of age showing central and peripheral large atrophic lesions. H, Fundus photograph of the left eye obtained at 42 years of age showing large atrophic lesions with hyperpigmentation. I, Fundus photograph mosaic obtained at 40 years of age showing pronounced atrophy posterior pole, atrophic lesions, and RPE alterations in the periphery. y = years.

### Haplotype and sequence analysis

To investigate whether 4 persons with c.5461-10T→C homozygous STGD1 and 11 heterozygous persons with STGD1 shared an identical genomic segment, we performed haplotype analysis by using 18 SNPs located in and outside the *ABCA4* gene (Supplemental Fig 1, available at [www.aaojournal.org](http://www.aaojournal.org)). Eight SNPs were present in a homozygous state in the 4 c.5461-10T→C homozygotes, and the corresponding haplotype also was found in a heterozygous state in the 11 patients carrying c.5461-10T→C. Therefore, we defined the minimal shared haplotype between rs548122 (g.94,565,430) and rs35270729 (g.94,469,543) of chromosome 1, spanning 95.9 kb. These data suggest that the c.5461-10C→T variant resides on a so-called founder haplotype spanning exons 6 to 44 of the *ABCA4* gene. To investigate further if c.5461-10T→C was the only rare variant present in the shared haplotype, we performed targeted next-generation sequencing of the entire *ABCA4* genomic locus for patient 1 at an average depth of coverage of 62X, which did not identify additional rare variants. None of these variants, except c.5461-10T→C, was present at an allele frequency of less than 0.01 in Genome of the Netherlands and Exome Aggregation Consortium data, strongly suggesting that the c.5461-10T→C variant is the only rare variant in the shared haplotype.

### Generation of induced pluripotent stem cells and photoreceptor progenitor cells

Control and patient fibroblast lines were reprogrammed successfully into iPSCs. Quantitative PCR analysis on all cell lines confirmed the expression of the pluripotency markers *LIN28*, *NANOG*, *OCT3/4*, and *SOX2* normalized against *GUSB* expression (Supplemental Fig 2, available at [www.aaojournal.org](http://www.aaojournal.org)), which was comparable between control and patient cell lines. *ABCA4* was used as negative control. To corroborate the gene expression results, we performed immunofluorescence staining that showed expression of *OCT3/4*, *NANOG*, *SSEA4*, and *TRA-1-81* (Supplemental Fig 3, available at [www.aaojournal.org](http://www.aaojournal.org)).

Control and patient iPSC lines were differentiated successfully into photoreceptor-like cells by a 60-day protocol in which cells cultured on Matrigel-coated dishes were kept in PPC-specific medium until the end of the experiment. Samples for quantitative PCR were obtained before the differentiation (iPSCs) and at 1 and 2 months of differentiation. Adult neural retina cDNA was used for comparison of gene expression. The expression of neural (*PAX6*) and photoreceptor progenitor (*CRX* and *CHX10*) markers in the cell line derived from patient 1 increased after 1 month of differentiation and remained constant up to 2 months of the differentiation (Fig 3B). In the control line, the expression of the same genes was much lower than in the patient, and after 2 months, their

expression decreased (Fig 3A, B). In both cell lines, the expression of the blue and red–green cone markers (OPN1SW and OPN1M/LW, respectively) and rod markers (RHO, NRL, and RCV1) increased after 1 and 2 months, except for OPN1SW, which in the control decreased in the second month (Fig 3A, B). *ABCA4* expression was very low in fibroblasts and iPSCs and increased considerably on differentiation into PPCs, where it remained constant until the second month (Supplemental Fig 4, available at [www.aaajournal.org](http://www.aaajournal.org)). The expression of *ABCA4* increased consistently in both patient-derived cell lines after 1 month of differentiation. In patient 1, the moderately high *ABCA4* expression was comparable with the high *CRX*, *CHX10*, and *OPN1SW* expression (Fig 3B). *OPN1M/LW* and *RCV1* expression also was confirmed by immunofluorescence staining (Fig 3C, D). Fig 3E clearly shows the different densities of progenitor (PAX6 positive, in green) and photoreceptor (*ABCA4* positive, in red) cells in the culture after 2 months of differentiation.

### *ABCA4* transcript analysis

The 5 algorithms used to assess the effect of c.5461-10T→C on splicing consistently predicted a very subtle weakening of the splice acceptor site of *ABCA4* exon 39 (Supplemental Fig 5A, available at [www.aaajournal.org](http://www.aaajournal.org)). To investigate the role of the c.5461-10T→C variant on RNA splicing, we analyzed total RNA derived from 30-day differentiated PPCs of persons with STGD1 who carried this variant in a homozygous or heterozygous state. Because the variant is located in *ABCA4* intron 38, we performed RT-PCR analysis of *ABCA4* exons 36 to 41. We found the expected wild-type 584-bp fragment in a control PPC line, adult human neural retina, a PPC generated from patient 16, who carried the c.5461-10T→C variant and an unknown second *ABCA4* variant, and a PPC established from patient 17, who carried the c.1822T→A (p.Phe608Ile) allele and an unknown second *ABCA4* allele (Fig 4A). Patients 1 and 16 showed bands of 460 bp and 330 bp, which on Sanger sequence analysis revealed deletions of exon 39 and of exons 39 and 40 (Fig 4B). *ABCA4* exons 39 and 40 consist of 124 and 130 nucleotides, respectively, and therefore the loss of exon 39 and the loss of exons 39 and 40 are predicted to result in shifts of the open reading frame and premature stop codons, that is, p.Thr1821Valfs\*13 and p.Thr1821Aspfs\*6, respectively.

Figure 3.

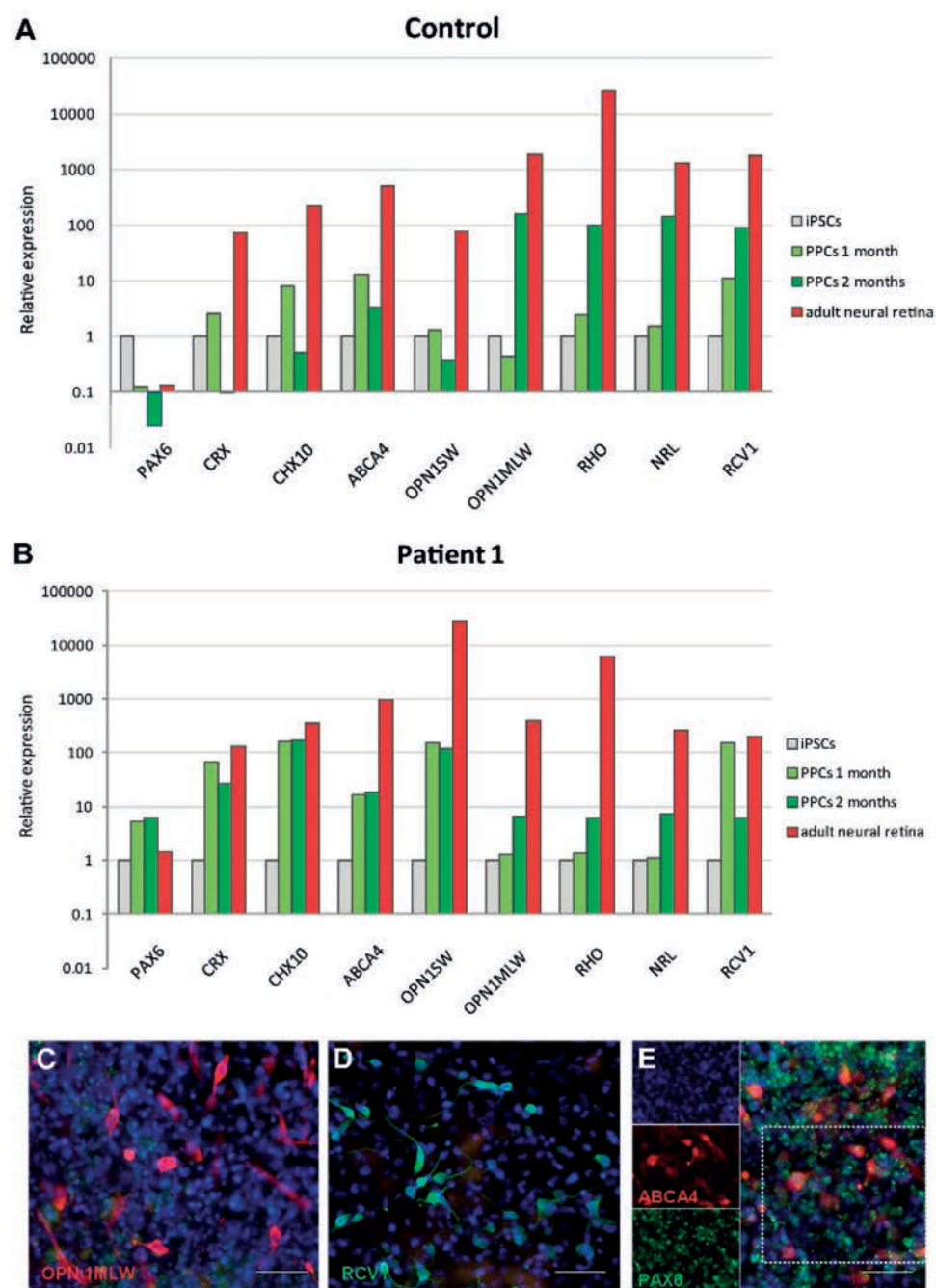


**Figure 3.** Retinal gene expression profiles and immunofluorescence of patient-derived photoreceptor progenitor cells (PPCs). Gene expression profile of (A) control-derived and (B) patient-derived PPCs after 1 and 2 months of differentiation compared with induced pluripotent stem cells (iPSCs) and adult neural retina. The appearance of PPCs can be deduced by the increase in expression of PAX6, CRX, and CHX10. The differentiation into photoreceptor-like cells is shown by the increased expression of ABCA4, NRL, OPN1SW, OPN1M/LW, RCV1, and RHO after 1 month of differentiation. In the control, the expression of the genes CRX, CHX10, ABCA4, and OPN1SW increased after 1 month, but it decreased in the second month of differentiation. However, expression of genes for green-red cones (OPN1M/LW) and rods (RCV1, NRL, and RHO) consistently increased in the second month. In the patient sample, the expression remained constant during the differentiation, with the exception of CRX and RCV1, for which the expression decreased, and NRL, OPN1M/LW, and RHO for which expression increased. Immunofluorescence staining of patient cells showed (C) cone cells expressing OPN1M/LW and (D) rods expressing RCV1. E, Coexpression of PAX6 and ABCA4 showed the different density of PPCs (PAX6 positive) and photoreceptor-like cells (ABCA4 positive). The dotted box represents the magnified area of the figures on the left side. DAPI was used to nuclear staining (blue). Scale bars = 50  $\mu$ m.

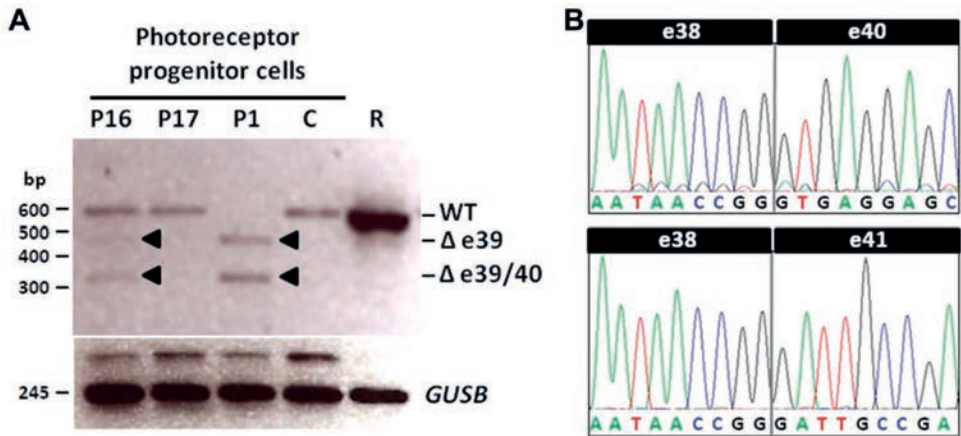


**Figure 4.** The c.5461-10T→C variant results in skipping of exons 39 or of exons 39 and 40 in mRNA of photoreceptor progenitor cells (PPCs). **A**, Reverse-transcription polymerase chain reaction (PCR) results of ABCA4 exons (e) 36 to 41 showing a single expected 584-bp fragment in a control PPC (C), adult neural retina (R), patient 16 (P16), who was heterozygous for c.5461-10T→C and an unknown second allele, and patient 17 (P17), who carried c.1822T→A (p.Phe608Ile) and an unknown second allele. Patients 1 (P1) and 16, who carried the variant in homozygous and heterozygous states, respectively, show fragments of 460 bp and 330 bp, suggesting deletions of exon 39 or of exon 39 and 40 (black arrowheads). Reverse-transcription PCR analysis of GUSB was performed as a control. **B**, Sanger sequence analysis of the mutant fragments showing the exon 39 (upper panel) or exons 39 and 40 (lower panel) skipping events. bp = base pairs; WT = wild-type.



### In vitro splice assays using *ABCA4* minigenes

To investigate the splicing defect observed in the PPCs in more detail, we generated 2 minigenes by PCR using control and patient 1 genomic DNAs: MG1 and MG2 (Fig 5A). The minigenes contain exon 39 and were designated -10C for the mutant and -10T for the control sequences. Sanger sequencing revealed no de novo variants in these constructs resulting from the PCR-based cloning procedure. To assess whether the minigene constructs recapitulated the splice defects observed in PPCs and whether we could pinpoint the genetic defect, HEK293T were transfected with mutant and control minigenes. Both control minigenes MG1-10T and MG2-10T showed partial skipping of exon 39 (Fig 5B, C); the mutant minigenes MG2-10C and MG2-10C showed 100% skipping of *ABCA4* exon 39 (Fig 5B, C).

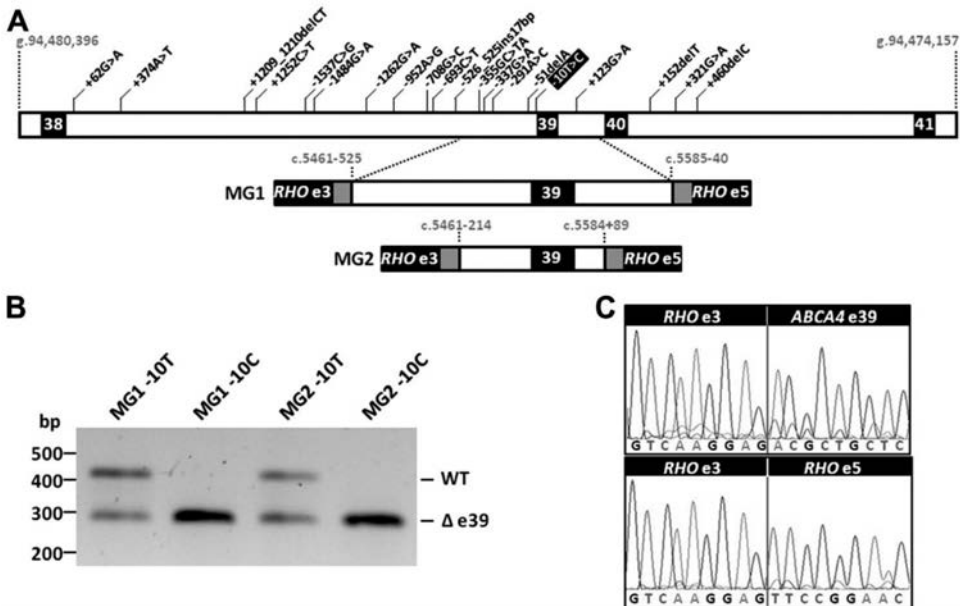


**Figure 5.** In vitro splice studies revealing that the c.5461-10T>C variant underlies exon (e) 39 skipping. **A**, Schematic representation of the *ABCA4* genomic region of patient 1 (from exons 38 to 41) and of the structure of the minigenes generated in this study (MG1 and MG2). The c.5461-10T>C variant is highlighted in the black box. The 19 additional variants in introns 38, 39, and 40 were found after Sanger sequence analysis (data not shown). **B**, Reverse-transcription polymerase chain reaction (RT-PCR) of RHO exons 3 through 5 in HEK293T cells 48 hours after transfection. The mutant MG1-10C and MG2-10C were transfected in parallel with 2 control minigenes (MG1-10T and MG2-10T). MG1-10T and MG2-10T show fragments of approximately 410 bp, corresponding to normal splicing (RHO exon 3–*ABCA4* exon 39–RHO exon 5) and a fragment of approximately 290 bp, corresponding to the size of the RHO exons spliced together without *ABCA4* exon 39. The mutant minigenes MG1-10C and MG2-10C showed 100% skipping of *ABCA4* exon 39. **C**, Sanger sequence analysis of the RT-PCR fragments confirmed the exon 39 skipping. WT = wild-type.

## Discussion

By using stem cell technology and in vitro splice assays, we showed that the frequent *ABCA4* c.5461-10T→C variant is associated with exon 39 or exons 39 and 40 skipping, which results in truncated *ABCA4* proteins. Haplotype and sequence analysis in 15 persons with STGD1 strongly suggested that this variant is part of a shared founder haplotype spanning a sizeable part of the *ABCA4* gene. In addition, no other rare single nucleotide variants were detected in this shared haplotype, which could explain the observed splice defects. The c.5461-10T→C variant is found almost exclusively in the European population (26/33243 persons vs. 1/27272 persons in non-Europeans; Exome Aggregation Consortium, available at: <http://exac.broadinstitute.org>; accessed November 10, 2015). Importantly, STGD1 or CRD patients carrying 2 c.5461-10T→C variants or 1 c.5461-10T→C variant and another causal *ABCA4* variant are now eligible for new treatments.

The clinical data of 4 homozygotes for c.5461-10T→C corroborate that this variant results in the absence of *ABCA4* activity, because all patients showed a young age of onset of STGD1 with rapid deterioration of central vision and progressive cone-rod loss of ERG responses leading to legal blindness before the age of 25 years. Moreover, in a recent study of 34 bi-allelic *ABCA4* cases with early-onset STGD1,<sup>24</sup> the c.5461-10T→C variant was found in 17 of 68 alleles (25%), and thereby was the most frequent *ABCA4* variant. The second most frequent variant in this group was c.768G→T (p.?) identified in 9 of 68 (13.2%) of alleles, which also has been deemed to have a severe effect.<sup>2</sup>

In silico predictions indicate that the c.5461-10T→C variant had a small effect on splicing ([Supplemental Fig 5](#), available at [www.aaojournal.org](http://www.aaojournal.org)). However, a strong effect of a thymine-to-cytosine change in the thymine–cytosine stretch of splice acceptor sites on splicing is not unprecedented, as shown for the *VCAN* c.4004-5T→C (p.?) variant, which has been found previously to result in exon 8 skipping in persons with autosomal dominant Wagner disease in the Netherlands.<sup>25</sup>

To explain the strong effect of the c.5461-10T→C variant, we checked for other sequence elements in or near exon 39. At position c.5461-51, the at-risk haplotype carries an adenine deletion, which is situated 5 nt downstream of the predicted branch point sequence at -56. We cannot exclude the possibility that it has a subtle effect on the strength of the exon 39 splice acceptor site. Likewise, other upstream variants could influence splicing. As depicted in [Supplemental Fig 6](#) (available at [www.aaojournal.org](http://www.aaojournal.org)), significant levels of exon 39 skipping (see

Fig 5B) in constructs with the wild-type T nucleotide suggest that *RHO* exon 3 to 5 splicing is at least as efficient as *RHO* exon 3 to *ABCA4* exon 39 to *RHO* exon 5 splicing. The splice donor site of exon 39 is predicted to be relatively strong, but it does carry a conspicuously large number of alternative splice donor sites. As shown in [Supplemental Fig 5B](#) (available at [www.aaojournal.org](http://www.aaojournal.org)), 3 additional splice donor sites are predicted very near the canonical splice donor site of exon 39. The presence of 3 alternative splice donor sites at the exon 39–intron 39 junction may render exon 39 susceptible to exon skipping. None of the other 48 splice donor sites in *ABCA4* carries more than 1 alternative splice donor site, and only 5 exons (exons 10, 15, 23, 26, and 42) contain 1 extra splice donor site residing in the last 10 nucleotides of the exons or the first 11 nucleotides of the adjacent introns. Sanger sequence analysis of introns 38, 39, and 40 in patient 1 ruled out the presence of other single nucleotide variants and deletions that could have an effect on splicing, but we cannot exclude the existence of other rare copy-number variants inside and outside of the exon 38 through exon 41 region that were missed in the Sanger and Haloplex-based sequencing.

The c.5461-10T→C variant previously was tested for its effect on splicing using the pSPL3b exon-trapping vector,<sup>3</sup> but no effect on splicing was observed. The reason may be that only 69 nt of upstream and 52 nt of downstream sequences of exon 39 were cloned into the minigene construct. Although less plausible, it is also possible that there are species-specific or cell line-specific differences in the splicing machineries, as shown for other intronic mutations.<sup>26</sup> We used HEK293T cells, derived from human embryonic kidney, whereas Rivera et al<sup>3</sup> used COS9 cells, derived from monkey kidney fibroblasts.

Finally, in the *ABCA4* cDNA of PPCs derived from patient 1, we also found exon 40 to be spliced out from part of the mRNA. This possibly can be attributed to the order of splicing. Intron 39 is relatively small and possibly is spliced out at an early stage.<sup>27</sup> Therefore, exons 39 and 40 skipping may be considered a so-called bystander effect.

*ABCA4* is a transmembrane protein situated at the rim of the photoreceptor outer segment discs and in the cell membranes.<sup>28, 29</sup> Therefore, during in vitro iPSC differentiation into PPCs, its high peak of expression is expected when the outer segments of photoreceptor cells are formed. It is interesting to note that the peak of *ABCA4* expression in iPSC-differentiated PPC cultures appeared after 1 month of differentiation. The quantitative PCR analysis after 1 month of differentiation clearly showed the expression of genes that typically are upregulated in PPCs and cone photoreceptors, indicating the presence of only these 2 types of cells. The same analysis performed after 2 months of differentiation showed an increase

of rod photoreceptor cells and a decrease of PPCs. These data suggest that ABCA4 is produced mainly by progenitor and blue cone photoreceptor cells. In the control PPCs, ABCA4 expression seemed to be derived from PPCs rather than photoreceptors ([Fig 3A](#)).

In conclusion, we found that the frequent ABCA4 c.5461-10T→C variant results in the skipping of exon 39 or exons 39 and 40. Because both splicing events result in the absence of significant parts of ABCA4 protein, the c.5461-10T→C variant can be considered to result in the absence of functional ABCA4. Accordingly, persons carrying this variant in both gene copies show an early age-of-onset form of STGD1, with a rapid progression and a poor visual prognosis in the second and third decades of life.

## References

1. Lewis RA, Shroyer NF, Singh N, et al. Genotype/Phenotype analysis of a photoreceptor-specific ATP-binding cassette transporter gene, ABCR, in Stargardt disease. *Am J Hum Genet* 1999;64:422-34.
2. Maugeri A, van Driel MA, van de Pol DJ, et al. The 2588G-->C mutation in the ABCR gene is a mild frequent founder mutation in the Western European population and allows the classification of ABCR mutations in patients with Stargardt disease. *Am J Hum Genet* 1999;64:1024-35.
3. Rivera A, White K, Stohr H, et al. A comprehensive survey of sequence variation in the ABCA4 (ABCR) gene in Stargardt disease and age-related macular degeneration. *Am J Hum Genet* 2000;67:800-13.
4. Webster AR, Heon E, Lotery AJ, et al. An analysis of allelic variation in the ABCA4 gene. *Invest Ophthalmol Vis Sci* 2001;42:1179-89.
5. Allikmets R, Singh N, Sun H, et al. A photoreceptor cell-specific ATP-binding transporter gene (ABCR) is mutated in recessive Stargardt macular dystrophy. *Nat Genet* 1997;15:236-46.
6. Maugeri A, Klevering BJ, Rohrschneider K, et al. Mutations in the ABCA4 (ABCR) gene are the major cause of autosomal recessive cone-rod dystrophy. *Am J Hum Genet* 2000;67:960-6.
7. Westeneng-van Haaften SC, Boon CJ, Cremers FP, et al. Clinical and genetic characteristics of late-onset Stargardt's disease. *Ophthalmology* 2012;119:1199-210.
8. Fritsche LG, Fleckenstein M, Fiebig BS, et al. A subgroup of age-related macular degeneration is associated with mono-allelic sequence variants in the ABCA4 gene. *Invest Ophthalmol Vis Sci* 2012;53:2112-8.
9. van Driel MA, Maugeri A, Klevering BJ, et al. ABCR unites what ophthalmologists divide(s). *Ophthalmic Genet* 1998;19:117-22.
10. Beharry S, Zhong M, Molday RS. N-retinylidene-phosphatidylethanolamine is the preferred retinoid substrate for the photoreceptor-specific ABC transporter ABCA4 (ABCR). *J Biol Chem* 2004;279:53972-9.
11. Molday RS, Zhong M, Quazi F. The role of the photoreceptor ABC transporter ABCA4 in lipid transport and Stargardt macular degeneration. *Biochim Biophys Acta* 2009;1791:573-83.
12. Shroyer NF, Lewis RA, Yatsenko AN, Lupski JR. Null missense ABCR (ABCA4) mutations in a family with stargardt disease and retinitis pigmentosa. *Invest Ophthalmol Vis Sci* 2001;42:2757-61.
13. Suarez T, Biswas SB, Biswas EE. Biochemical defects in retina-specific human ATP binding cassette transporter nucleotide binding domain 1 mutants associated with macular degeneration. *J Biol Chem* 2002;277:21759-67.
14. Sun H, Smallwood PM, Nathans J. Biochemical defects in ABCR protein variants associated with human retinopathies. *Nat Genet* 2000;26:242-6.
15. Wiszniewski W, Zaremba CM, Yatsenko AN, et al. ABCA4 mutations causing mislocalization are found frequently in patients with severe retinal dystrophies. *Hum Mol Genet* 2005;14:2769-78.
16. Bax NM, Sangermano R, Roosing S, et al. Heterozygous deep-intronic variants and deletions in ABCA4 in persons with retinal dystrophies and one exonic ABCA4 variant. *Hum Mutat* 2015;36:43-7.
17. Zernant J, Xie YA, Ayuso C, et al. Analysis of the ABCA4 genomic locus in Stargardt disease. *Hum Mol Genet* 2014;23:6797-806.
18. Bauwens M, De Zaeytijd J, Weisschuh N, et al. An augmented ABCA4 screen targeting noncoding regions reveals a deep intronic founder variant in Belgian Stargardt patients. *Hum Mutat* 2015;36:39-42.
19. Braun TA, Mullins RF, Wagner AH, et al. Non-exonic and synonymous variants in ABCA4 are an important cause of Stargardt disease. *Hum Mol Genet* 2013;22:5136-45.

20. Ahituv N, Prabhakar S, Poulin F, et al. Mapping cis-regulatory domains in the human genome using multi-species conservation of synteny. *Hum Mol Genet* 2005;14:3057-63.
21. Genome of the Netherlands C. Whole-genome sequence variation, population structure and demographic history of the Dutch population. *Nat Genet* 2014;46:818-25.
22. Livak KJ, Schmittgen TD. Analysis of relative gene expression data using real-time quantitative PCR and the 2(-Delta Delta C(T)) Method. *Methods* 2001;25:402-8.
23. Gamundi MJ, Hernan I, Muntanyola M, et al. Transcriptional expression of cis-acting and trans-acting splicing mutations cause autosomal dominant retinitis pigmentosa. *Hum Mutat* 2008;29:869-78.
24. Lambertus S, van Huet RA, Bax NM, et al. Early-onset stargardt disease: phenotypic and genotypic characteristics. *Ophthalmology* 2015;122:335-44.
25. Mukhopadhyay A, Nikopoulos K, Maugeri A, et al. Erosive vitreoretinopathy and wagner disease are caused by intronic mutations in CSPG2/Versican that result in an imbalance of splice variants. *Invest Ophthalmol Vis Sci* 2006;47:3565-72.
26. Garanto A, Duijkers L, Collin RW. Species-dependent splice recognition of a cryptic exon resulting from a recurrent intronic CEP290 mutation that causes congenital blindness. *Int J Mol Sci* 2015;16:5285-98.
27. Pulyakhina I, Gazzoli I, t Hoen PA, et al. SplicePie: a novel analytical approach for the detection of alternative, non-sequential and recursive splicing. *Nucleic Acids Res* 2015.
28. Molday LL, Rabin AR, Molday RS. ABCR expression in foveal cone photoreceptors and its role in Stargardt macular dystrophy. *Nat Genet* 2000;25:257-8.
29. Sun H, Nathans J. Stargardt's ABCR is localized to the disc membrane of retinal rod outer segments. *Nat Genet* 1997;17:15-6.

## Supplementary Material

### Supplemental methods: Patient-derived fibroblast reprogramming

Skin biopsies from two persons with STGD1, one homozygous (P1) and one heterozygous (P16) for c.5461-10T>C, as well as one control, were collected, washed in PBS (cat. no. P5493, Sigma Aldrich, St. Louis, MO, USA), dissected with a scalpel and incubated for 1-3 h at 37°C in a solution of 1000 U/ml Collagenase type II (cat. no. LS004176, Worthington Biochemical Corporation, Lakewood, NJ, USA) and Penicillin/streptomycin (cat. no. P4333, Sigma Aldrich) in DMEM (cat. no. D0819, Sigma Aldrich). The digestion was then stopped by the addition of 20% (v/v) fetal calf serum (FCS, cat. no. F7524, Sigma Aldrich) and the cell suspension was incubated in a medium containing DMEM and 20% FCS for 7 days at 37°C and 5% (v/v) CO<sub>2</sub>.

After about one month, a pure culture of fibroblasts was reprogrammed as follows. Fibroblasts were transduced at 80% confluence with four lentiviral vectors containing the pluripotency genes *OCT3/4*, *NANOG*, *KLF4* and *c-MYC*. Transduced cells were incubated for 24 h at 37°C, the lentiviruses were removed and cells washed three times with PBS. The following day, the transduced cells were transferred onto murine embryonic fibroblast (MEF)-coated plates and cultured for one month at 37°C and 5% CO<sub>2</sub> in a stem cell medium containing DMEM/Ham's F-12 (cat. no. 1445C, Sigma Aldrich), 20% (v/v) Knock-out serum replacement (KOSR, cat. no. 10828-028, Thermo Fisher Scientific), MEM Non-essential amino acids (NEAA, cat. no. M7145, Sigma Aldrich), L-glutamine (cat. no. G8541, Sigma Aldrich), β-mercaptoethanol (cat. no. M3148 Sigma Aldrich), β-FGF (cat. no. F0291, Sigma Aldrich). One month after transduction, iPSC colonies were picked and expanded on Vitronectin-coated plates (cat. no. A14700, Thermo Fisher Scientific) in Essential E8 medium (cat. no. A1517001, Thermo Fisher Scientific).

**Supplemental Table 1: ABCA4 variants in persons P1-P17**

Patient ID	Allele 1 cDNA variant	Allele 1 protein variant	Allele 2 cDNA variant	Allele 2 protein variant
P1	c.5461-10T>C	p.?	c.5461-10T>C	p.?
P2	c.5461-10T>C	p.?	c.5461-10T>C	p.?
P3	c.5461-10T>C	p.?	c.5461-10T>C	p.?
P4	c.5461-10T>C	p.?	c.5461-10T>C	p.?
P5	c.5461-10T>C	p.?	c.768G>T	p.?
P6	c.5461-10T>C	p.?	c.2588G>C	p.(Gly863Ala)/p.(Gly863del)
P7	c.5461-10T>C	p.?	c.5882G>A	p.(Gly1961Glu)
P8	c.5461-10T>C	p.?	c.2588G>C	p.(Gly863Ala)/p.(Gly863del)
P9	c.5461-10T>C	p.?	c.[1622T>C; c.2870A>G]	p.[Leu541Pro; Ala1038Val]
P10	c.5461-10T>C	p.?	c.768G>T	p.?
P11	c.5461-10T>C	p.?	c.3703A>G	p.(Asn1235Asp)
P12	c.5461-10T>C	p.?	c.[1622T>C; c.2870A>G]	p.[Leu541Pro; p.Ala1038Val]
P13	c.5461-10T>C	p.?	c.768G>T	p.?
P14	c.5461-10T>C	p.?	c.768G>T	p.?
P15	c.5461-10T>C	p.?	c.768G>T	p.?
P16	c.5461-10T>C	p.?	?	?
P17	c.1822T>A	p.(Phe608Ile)	?	?

**Supplemental Table 2: SNP analysis primer details**

Chr.1 nt. pos.	rs ID	Forward (5'->3')	Reverse (5'->3')	Product size(bp)
94115299	rs61645528	AGGCAAAATTTAACCAGAATGA	ACTTGGGGTCTTATAAATTGTTG	202
94185344	rs4847183	TAAGCACTGGTGATAAATGCTG	AAAATTCACCTTTGAGCAAATCA	202
94197193	rs11164970	TTTTATCTGAGAGGCTGGAAAG	AGAGAAAATTGCTTGATTGATCAG	211
94222858	rs4520428	ATAGTGAGGAGTGGTCTTCCAA	GTCTCAGTGGAGTGAGATGTGA	207
94435669	rs7553431	GTATGGTTGAAACAAATTGCTG	AGCCCAAACAACACCTATCTAA	244
94454018	rs12121974	CTGGTTTAGTGGGACTTGAT	TAACTCCAGTTTAGCTGGGACA	238
94469543	rs35270729	CCTATGTTGCACAGGCTAATCT	CTTAGCACTCAGGCTTTTGTCT	264
94491468	rs11165065	TTGATCTGTAATCCCCGTAG	TTTCGATGAAC TAGCTCCAGT	211
94500012	rs34541136	CCATGTTGATCCCTTCGTTT	GGGAAGTGGAGCTCACAGAGG	354
94509226	rs4147839	TTGGCAATCAAGATGCTCAC	ACCGCTGAGTTATAACATTGGT	347
94516985	rs1191231	AAAAGCTGCAAAAGTTCTTTGA	AGAGGTGGCCCTCTATGTAAA	244
94526044	rs56197337	CACGTTGGCTAAAAGGAAGG	GAAAAATCAGGGTGTCTCCAAT	247
94535174	rs2151849	TGACGTGGCATAAGAGGACA	TCAGATAGCCCAAGGCTGTT	356
94565430	rs548122	AATTTGCTCTTGGAATTTAGCAA	TACTCAGTGTCTGTCCAATGCT	396
94582227	rs4147804	GAGGTCACTGTTGTTCTAACTCTG	GAATTTCTCCCTGGGGTATG	248
94595554	rs11803430	GTGGAGTCCATATACCCAGAG	AACCTGCCTCTCATTTTGATA	399
94635986	rs12044374	GCATCATTTCTGTAGTATTGGACA	GCTGATTTTGATTGCCTCAGTA	245
94734351	rs10158261	GTGCCAGGGACACAGTAAGA	GGCTTAGCAGGAAGACAAATAG	297



**Supplemental Table 3: qPCR primers**

<b>Gene</b>	<b>Forward (5'→3')</b>	<b>Reverse (5'→3')</b>
<i>GUSB</i>	AGAGTGGTGCTGAGGATTGG	CCCTCATGCTCTAGCGTGTC
<i>OCT3/4</i>	GTTCTTCATTCACTAAGGAAGG	CAAGAGCATCATTGAACTTCAC
<i>PAX6</i>	CCGGCAGAAGATTGTAGAGC	GCCCGTTCAACATCCTTAGT
<i>CRX</i>	GCCCCACTATTCTGTCAACG	CTTCAGAGCCACCTCCTCAC
<i>CHX10</i>	GAGAAGGCATTCAACGAAGC	CATACTCCGCCATGACACTG
<i>ABCA4</i>	CATCCTGTTCCACCACCTCA	CTGTGTCTCCAACATGGCT
<i>OPN1SW</i>	ACCATTGGTATTGGCGTCTC	GGAGAGAGGCACAATGAAGC
<i>OPN1M/LW</i>	GTGGTCACTGCATCCGTCTT	ACGGTCTCTGCTAGGTCAGC
<i>RHO</i>	TCATCATGGTCATCGCTTTC	CATGAAGATGGGACCGAAGT
<i>NRL</i>	GGTCCACACCTTACAGCTC	AGCCAGTACAGCTCCTCCAG
<i>RCV1</i>	ACACCAAGTTCTCGGAGGAG	ACTTGGCGTAGATGCTCTGG

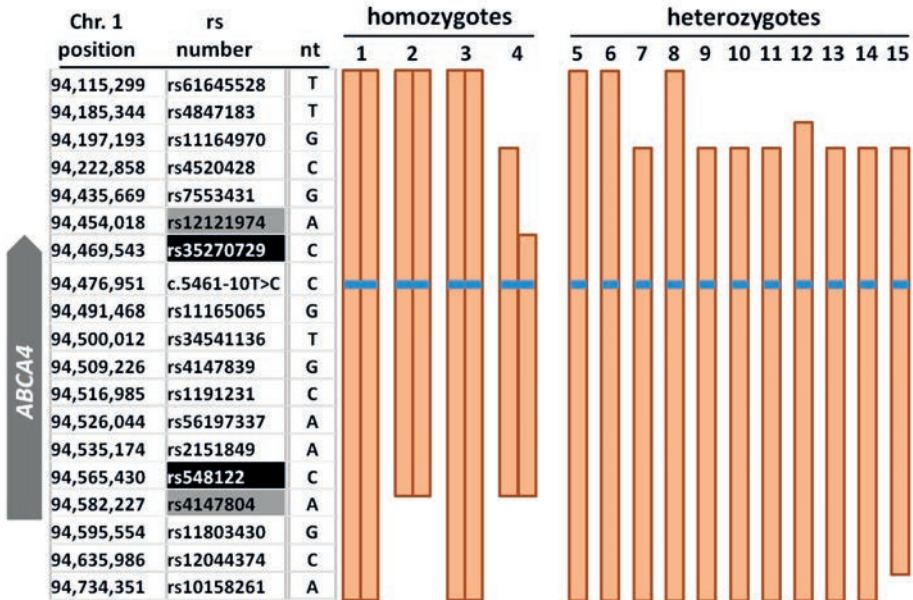
**Supplemental Table 4: Primary and secondary antibodies**

<b>Antibody</b>	<b>Host/ Type</b>	<b>Supplier</b>	<b>Cat. no.</b>
$\alpha$ -NANOG	Goat polyclonal	R&D Systems	AF1997
$\alpha$ -OCT3/4	Mouse monoclonal	Santa Cruz	SC-5279
$\alpha$ -SSEA-4	Mouse monoclonal	DSHB	MC-813-70
$\alpha$ -TRA-1-81	Mouse monoclonal	Millipore	MAB4381
$\alpha$ -ABCA4	Mouse monoclonal	Abcam	AB77285
$\alpha$ -CHX10	Sheep polyclonal	Abcam	AB16141
$\alpha$ -CRX	Sheep polyclonal	R&D Systems	AF7085
$\alpha$ -NRL	Rabbit polyclonal	Santa Cruz	SC-33183
$\alpha$ -OPN1SW	Goat polyclonal	Santa Cruz	SC-14363
$\alpha$ -OPN1M/LW	Rabbit polyclonal	Millipore	AB5405
$\alpha$ -PAX6	Mouse monoclonal	Millipore	MAB5552
$\alpha$ -RCV1	Rabbit polyclonal	Millipore	AB5585
$\alpha$ -Goat Alexa Fluor 488	Donkey polyclonal	Molecular Probes	A11055
$\alpha$ -Mouse Alexa Fluor 568	Goat polyclonal	Thermo Fisher Scientific	A11031
$\alpha$ -Mouse Alexa Fluor 488	Goat polyclonal	Invitrogen	A10680
$\alpha$ -Sheep Alexa Fluor 488	Donkey polyclonal	Molecular Probes	A11015
$\alpha$ -Rabbit Alexa Fluor 568	Donkey polyclonal	Thermo Fisher Scientific	A10042
$\alpha$ -Goat Alexa Fluor 568	Donkey polyclonal	Thermo Fisher Scientific	A11057
$\alpha$ -Sheep Alexa Fluor 568	Donkey polyclonal	Thermo Fisher Scientific	A21099

**Supplemental Table 5: Primers for minigene generation and in vitro splice assay**

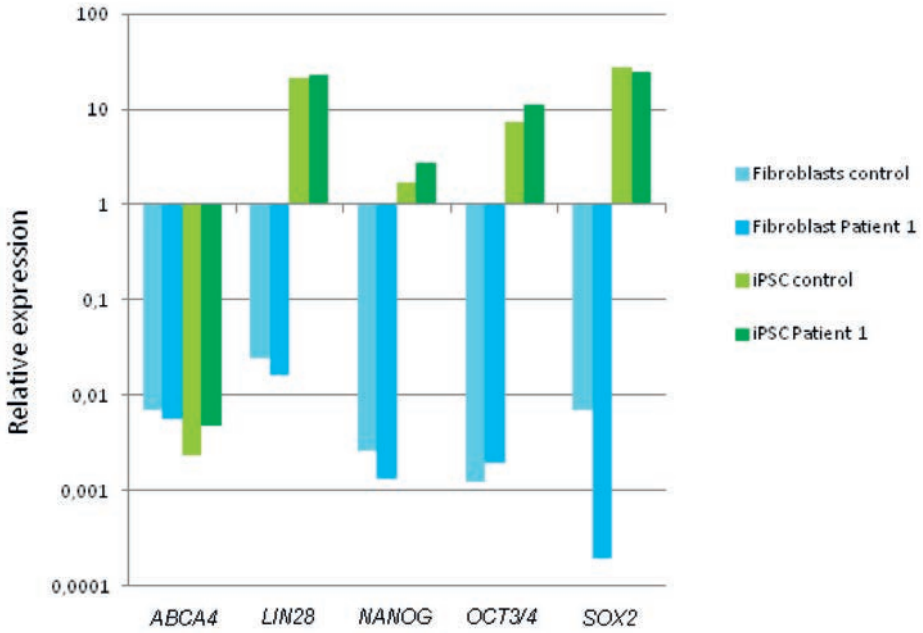
Primer	Sequence	T <sub>(ann)</sub> (-C)	Product size (bp)
MG1_F	<u>GGGGACAAGTTTGTACAAAAAAGCAGGCTTCGTGTTAACAATGCCTTGAGG</u>	58.0	942
MG1_R	<u>GGGGACCACTTTGTACAAGAAAGCTGGGTGAGCTCACCCACAGACCT</u>	58.0	
MG2_F	<u>GGGGACAAGTTTGTACAAAAAAGCAGGCTTCCTTGAGGCACTGCTTGTA</u>	58.0	427
MG2_R	<u>GGGGACCACTTTGTACAAGAAAGCTGGGTGCCACAGTCTGATGCAG</u>	58.0	
pCI-Neo-Rho-Insert_F	CGGAGGTCAACAACGAGTCT	60.0	514
pCI-Neo-Rho-Insert_R	AGGTGTAGGGGATGGGAGAC	60.0	

**Supplemental Figure 1**



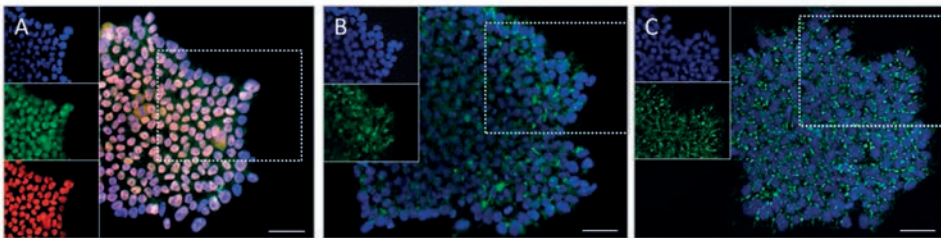
The c.5461-10T>C variant resides on an ancestral ‘founder’ haplotype spanning a large part of the ABCA4 gene. Haplotype analysis was performed in four homozygous and 11 heterozygous persons with Stargardt disease for c.5461-10T>C. All the subjects were investigated for 18 single nucleotide polymorphisms (SNPs), which are frequent variants in the Dutch population, in and outside the ABCA4 gene. Eight SNPs were present in a homozygous state in the four c.5461-10T>C homozygotes and this shared haplotype was also found in a heterozygous state in the 11 cases heterozygous for c.5461-10T>C, defining a minimal shared region of 95.9 kb between the SNPs rs35270729 and rs548122 (highlighted with black boxes). The maximum shared region, spanning 128.2 kb, was defined between the SNPs rs12121974 and rs4147804 (highlighted with grey boxes).

**Supplemental Figure 2**



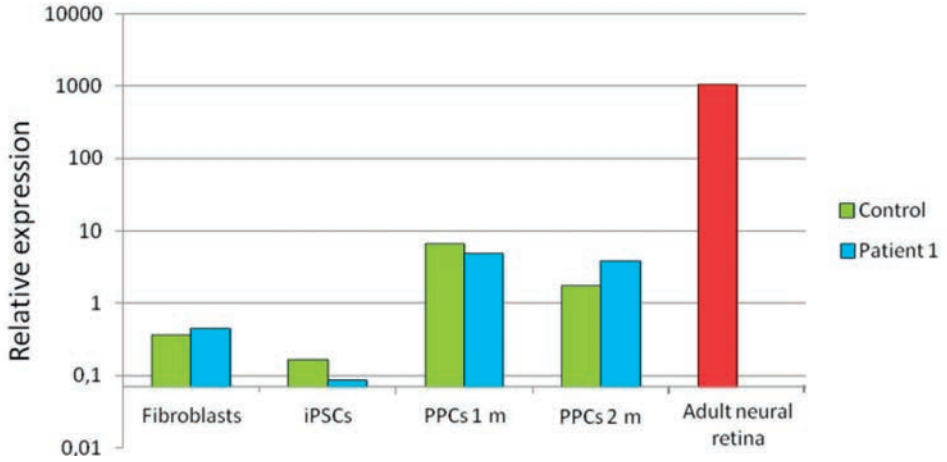
Quantitative PCR (q-PCR) analysis of cDNA derived from induced pluripotent stem cells (iPSCs). The expression of the pluripotency genes LIN28, NANOG, OCT3/4 and SOX2 (normalized against GUSB) in iPSCs was clearly increased compared with the patient fibroblasts. ABCA4 was used as a negative control of the reprogramming and its expression remained very low during the whole experiment.

**Supplemental Figure 3**



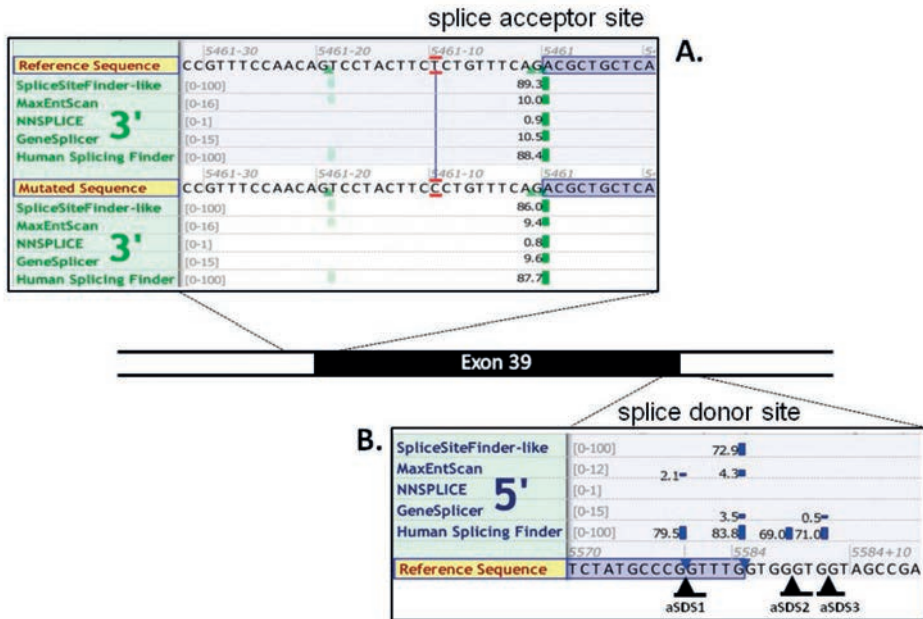
Induced pluripotent stem cells (iPSCs) show expression of pluripotency markers. Expression was observed for **A**. OCT3/4 (red) and NANOG (green), **B**. TRA-1-81 (green), **C**. SSEA4 (green). The dotted box represents the magnified area of the figures on the left side. DAPI was used for nuclear staining (blue). Scale bars 50  $\mu\text{m}$ .

Supplemental Figure 4



ABCA4 expression levels in fibroblasts, induced pluripotent stem cells (iPSCs) and photoreceptor progenitor cells (PPCs). In comparison with GUSB (expression set at 1), ABCA4 expression is very low in fibroblasts and iPSCs and consistently increased after one month (PPCs 1 m) of differentiation into PPCs. The expression slightly decreased after two months (PPCs 2 m).

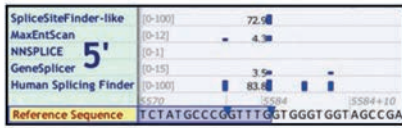
Supplemental Figure 5



In silico splice predictions of the strength of ABCA4 exon 39 splice sites. The five algorithms employed to assess the effect on splicing are depicted in green for the splice acceptor site and in blue for the splice donor site. A. The predicted effect of c.5461-10T>C on splicing is a very subtle weakening of the canonical splice acceptor site of ABCA4 exon 39. B. The canonical splice donor site of ABCA4 exon 39 and three alternative splice donor sites (aSDS 1-3).

Supplemental Figure 6

ABCA4 exon 39 splice donor site



ABCA4 exon 39 splice acceptor site



RHO exon 3 splice donor site



RHO exon 5 splice acceptor site



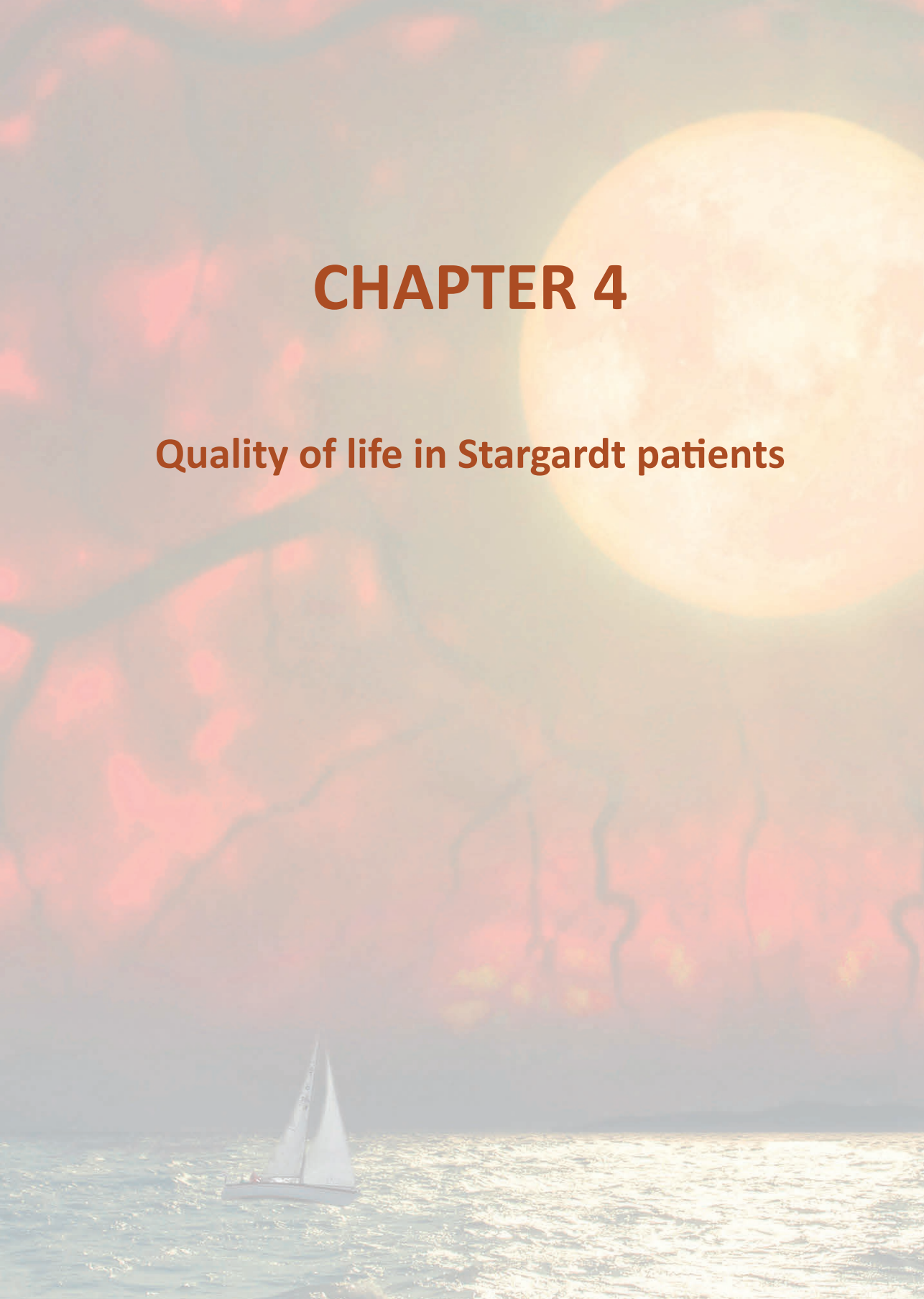
*In silico* splice prediction of the strength of ABCA4 exon 39 splice sites and RHO exon 3 donor and exon 5 acceptor splice sites. The five algorithms employed to assess the effect on splicing are depicted in green for the splice acceptor site and in blue for the splice donor site. The canonical splice donor site of RHO exon 3 is predicted to be slightly stronger than that of exon 39; the reason might be the presence of alternative splice donor sites (Supplemental Figure 5B). The splice acceptor site of RHO exon 5 is not predicted to be stronger than that of exon 39.





# CHAPTER 4

Quality of life in Stargardt patients







## CHAPTER 4

### Quality of life in Stargardt patients

*“To date, quality of life studies which assess visual impairment are mainly focused on elderly patients, and many are not specified for retinal dystrophies. Knowledge of quality of life in Stargardt disease (STGD1) patients can gain insight about the impact of the disease on daily functioning. These data are important to provide outcome measures and indicators of cost effectiveness for emerging clinical trials.*

*In this study, we provide a detailed description of our findings in social, demographic, and disease-specific characteristics, as well as general and vision-specific quality of life in patients with STGD1. The results were compared with norm groups. In general, STGD1 patients, as presented in our study, perceive good general quality of life with serious, vision-related impairments suggesting a large potential of health gain by innovative interventions to treat vision-related impairments.”*

Nathalie M. Bax  
Stanley Lambertus  
Lena Ye  
Petronella J.M. van den Wittenboer  
B. Jeroen Klevering  
Chris M. Verhaak  
Carel B. Hoyng

*Submitted for publication*

We thank Andrea W.M. Evers, Henriët van Middendorp, Gert-Jan van der Wilt, Johannes M.M. Groenewoud for their contribution without this study could not have been completed.

**PURPOSE:** This study evaluates social, demographic, and disease-specific characteristics, as well as general and vision-specific quality of life (QoL) in patients with Stargardt disease (STGD1).

**METHODS:** Our database (Department of Ophthalmology, Radboudumc, Nijmegen, the Netherlands) contains 448 patients with a clinical diagnosis of STGD1. Genetic analysis was performed in 270 patients, 260 of whom carried  $\geq 1$  *ABCA4* mutations. To those patients who had a follow-up visit between May 2013 and March 2015, we asked to participate in this study. 106 STGD1 patients participated in this study. We used three questionnaires: a patient-characteristics questionnaire, the RAND-sf36 and the VFQ-25 to evaluate the general and vision-specific QoL to obtain social, demographic, and disease-specific characteristics, as well as general and vision-specific QoL of STGD1 patients compared with norm groups.

**RESULTS:** Low vision aids were used in 86% of the patients. All patients completed education, and 43% had a part-time or full-time job.

General QoL: comparisons with norm groups revealed similar physical, social, and emotional role functioning. STGD1 patients showed better scores on mental health ( $t=5.108$   $p<=.001$ ), vitality ( $t=2.980$   $p=.004$ ), and general health perception ( $t=2.398$   $p=.019$ ) than the norm group.

Vision-specific QoL: STGD1 patients perceive less favorable vision-related QoL compared with other eye disease patients for nearly all aspects of vision-related QoL, except for general health.

**CONCLUSIONS:** STGD1 patients perceive good general QoL, but with serious, vision-related impairments suggesting a large potential of health gain by innovative interventions to treat vision-related impairments.

## Introduction

Stargardt disease type 1 (STGD1) is arguably the most common retinal dystrophy caused by a defect in a single gene, which affects 1:10,000 people worldwide [1]. This disease is caused by mutations in the *ABCA4* transporter gene and is inherited in an autosomal recessive fashion [2]. In general, patients present with progressive bilateral central vision loss, the majority of them presenting within their first two decades of life [3, 4]. Peripheral vision usually remains unaffected, but progression to peripheral loss of vision can occur, especially in patients with an early age at onset [5, 6].

The clinical heterogeneity in STGD1 is considerable with a wide variation in the age at onset and the level of visual impairment [4, 6-8]. Patients with an early age at onset show rapid retinal degeneration resulting in severe visual impairment ( $\leq 20/200$ ) before adulthood, and functional blindness between their fourth and fifth decade of life [6]. Patients with a disease onset between adolescence and middle adulthood progress slower to severe visual impairment at a median of 22 years after onset [4]. Late-onset STGD1 patients relatively preserve their visual function with only mild visual impairment ( $\geq 20/40$  Snellen) up to nine years after diagnosis, due to sparing of the central macular structures [7, 9]. To date, no treatment is available, but clinical trials are ongoing, like; gene augmentation (trial number NCT01367444, NCT01736592), and small molecule drugs (trial number NCT02402660) [10, 11].

Currently, quality of life (QoL) is determined as a significant outcome for measuring the impact of disease, and for estimating the efficacy of treatment. In general, visual impairment is related to loss in QoL [12-16]; visually impaired patients frequently have high levels of anxiety and periods of depression [14, 17, 18]. These patients are also at increased risk of accidental injuries, which can worsen existing chronic health conditions [19, 20]. Moreover, blindness is feared third most of all chronic disorders after cancer and AIDS/HIV by Americans [21]. To date, QoL studies which assess visual impairment are mainly focused on elderly patients [13, 22-25], and many are not specified for retinal dystrophies. To our knowledge, besides from retinitis pigmentosa in general, we know little about the QoL in patients with retinal dystrophies, for example STGD1.

Knowledge of QoL in STGD1 patients can gain insight about the impact of the disease on daily functioning. These data are important to provide outcome measures and indicators of cost effectiveness for emerging clinical trials [26].

This study aims to investigate general and vision-related QoL in patients with STGD1 and their relation to demographic aspects (like age and gender) and disease-specific features including disease onset and duration, and degree of visual impairment. Additionally, we provide a detailed overview of our STGD1 cohort, e.g. to obtain information about education and workability. We will present the results as explorative data.

## Methods

### Patients

The database of the Department of Ophthalmology at Radboud university medical center (Nijmegen, the Netherlands) contains 448 patients with a clinical diagnosis of STGD1. Genetic analyses was performed in 270 patients, and 260 patients were proven with one or more *ABCA4* mutations. Of these patients, which visited the outdoor clinic because of follow-up in the period from May 2013 to March 2015, we asked to participate in this study. A total of 106 STGD1 patients were willing to participate in this study. For studies on inherited retinal disease we have the certificate of approval from the central committee on Ethics and Human research (IRB). Informed consent of the research was obtained from all patients, and the study was in adherence to the tenets of the Declaration of Helsinki.

### Questionnaires

In this study, we used three questionnaires: one questionnaire to collect patient characteristics, and two standardized questionnaires to evaluate the general and vision-specific QoL. In the period from May 2013 to March 2015, the patients were interviewed individually by a trained researcher (N.M.B., S.L., L.Y.).

#### 1. Demographics and vision-related characteristics

We designed a questionnaire to acquire patient characteristics including demographics, general health (e.g., consultation of other specialists, use of medication, and presence of other diseases), life style (e.g., smoking, outdoor activities, sports, and diet), social aspects (e.g., education, work, and having a family), and vision-related characteristics (e.g., age at onset, and first complaints). We can correlate some of the social aspects to the general Dutch population ([www.CBS.nl](http://www.CBS.nl)).

The disease impact on QoL can be measured from a general perspective or from a disease-specific perspective. An assessment from a general perspective describes the perceived quality of general aspects of life, which includes physical and emotional health, and the impact of general health problems in daily life. Such an assessment enables a direct comparison of a specific patient group with healthy controls. In contrast, disease-specific QoL addresses issues related to specific

aspects of the disease. This assessment enables a comparison between one patient and another within the group of patients with the same disease. Therefore, we choose two different questionnaires to obtain general and disease-specific information:

## 2. General quality of life

General QoL was assessed with the validated 36-Item Short Form Health Survey (RAND-sf36) [24,25], of which norm scores are available. The questionnaire consists of eight subscales: physical and social functioning, role limitations due to physical health problems, role limitations due to personal or emotional problems, general mental health, energy/ fatigue, bodily pain, and general health perceptions [27, 28].

## 3. Vision-related quality of life

The Visual Function Questionnaire-25 (VFQ-25) is generally used to investigate the vision-related QoL [29]. The VFQ-25 is a 25-item version of the 51-item National Eye Visual Function questionnaire (NEI-VFQ) [30]. Norm scores are available, as well as scores from other eye diseases to compare with. The questionnaire consists of twelve subscales: overall health, overall vision, difficulty with near vision, difficulty with distance vision, driving difficulties, peripheral vision, color vision, pain and discomfort around the eyes, role limitations due to vision, dependency on others due to vision, limitations in social functioning due to vision, and mental health symptoms due to vision [29].

## Interpretation and analyses

Vision-related characteristics were described and defined as follows: age at onset was defined as the age at which the patient noticed first symptoms. When we could not identify the age of first symptoms occurred, we used the age at diagnosis. We classified clinical subtypes based on the age at onset: (1) early-onset, as described by Lambertus et al [6] ( $\leq 10$  years); (2) intermediate-onset (11-44 years); and (3) late-onset ( $\geq 45$  years), as described by Westeneng- Van Haaften et al [7]. We defined disease duration as the difference between the age at onset and the age at interview. We grouped disease duration as follows: 0-10 years, 11–20 years, 21-30 years, 31-40 years and >40 years. We measured visual acuity using an Early Treatment Diabetic Retinopathy Study (ETDRS) or Snellen chart. Disease severity was then categorized by World Health Organization (WHO) criteria as follows: mild or no visual impairment ( $\geq 20/60$ ), moderate visual impairment (20/60 - 20/200), severe visual impairment (20/200 – 20/500), and blindness ( $\geq 20/500$ ).

We compared the scores from the RAND-sf36 and the VFQ-25 questionnaires of our STGD1 population with the available norm scores and with patients with

other eye diseases (e.g., diabetic retinopathy, age-related macular degeneration, glaucoma, cataract, cytomegalovirus retinitis, and low vision in general). Detailed information of these norm groups from other eye diseases was not available. We also compared the norm scores between each subgroup (age of onset, gender, disease duration, and visual impairment) as mentioned above.

We analyzed data with SPSS version 22.0 (IBM Corp, Armonk, NY), using descriptive statistics by mean and standard deviation (SD) for continuous variables, and percentages for categorical variables. We compared two groups with independent t-tests and three or more groups with a one-way ANOVA and continuous variables in mean and SD. Comparisons with norm scores (RAND-SF36) and norm and comparison scores (VFQ-25) were assessed by an one sample t-test.

## Results

From the included 106 STGD1 patients, 60% were female. We conducted all three questionnaires in 99 patients. In the remaining seven patients, not all questionnaires could be completed, because of tiredness. The patient characteristics questionnaire was completed in 105 cases, the RAND-sf36 and the VFQ-25 both in 100 cases.

### Demographic and vision-related characteristics

An overview of the results is presented in [Table 1](#). The median age at onset was 16 years (range: 1-71). The median disease duration was 21 years (range: 2-57). 105 STGD1 patients were interviewed at a median age of 45 years (range: 16-86). The median BCVA was 20/200 Snellen (range: hand movement - 20/16). Clinical subtypes based on age at onset contained 27 (25.7%) early-onset (median 8 years), 54 (51.4%) intermediate-onset (median 17.5 years), and 24 (22.9%) late-onset (median 51.5 years) STGD1 patients. The median disease duration was 27 years (range: 7-57), 22.5 years (range: 3-51), and 9.5 years (2-31), respectively. The median BCVA in different age of onset groups was 20/600 Snellen (range: 20/6000 – 20/120) in the early onset group, 20/200 Snellen (range: 20/6000- 20/20) in the intermediate onset, and 20/50 Snellen (range: 20/600 – 20/16) in the late-onset STGD1 patients.

Patients experienced most problems with reading (95%). Reading problems occurred at a median age of 24 years (range: 6-62). Low vision aids in the broad sense, varying from a loupe to a guide dog, were used in 86% of the patients. All patients completed some kind of education, 43% of whom had finished University, and 43% had a part-time or full-time job. The majority of the patients (61%) had children.

**Table 1: Overview study cohort characteristics. Divided into demographics, general health, life style, and disease specific characteristics.**

DEMOGRAPHICS		Stargardt cohort
<b>Gender</b>	<b>Characteristics</b>	
	Male	42 (40%)
	Female	64 (60%)
<b>Nationality</b>	Dutch	106 (100%)
<b>Ethnicity</b>	Caucasian	97%
	Asian	1%
	Mixed	2%
<b>Marital status</b>	Unmarried/ Single	25%
	Married/ Cohabiting	62%
	Divorced	8%
	Widow(-er)	1%
	Other	4%
<b>Children</b>	No	39%
	Yes	61%
	1 child	9%
	2 children	30%
	3 children or more	22%
<b>Education</b>	High school	28%
	Secondary education	27%
	University	43%
	Other	2%
<b>Work situation</b>	No work	4%
	Unit for work	20%
	Full time job (>36h/week)	21%
	Part-time job (<36h/week)	22%
	School/ study	9%
	Voluntary work	11%
	Retired	13%
<b>Consanguinity</b>	No	99%
	Yes	1%
<b>Affected family members</b>	Yes	61%
	No	39%

DISEASE SPECIFIC		Stargardt cohort
<b>Age</b>	<b>Characteristics</b>	
	At examination (A/E, yrs)	16 - 86 (mean: 46)
	At onset Stargardt (A/O, yrs)	1 - 71 (mean: 24)
	Early onset (≤10 yrs)	N = 27 (25.7%)
	Intermediate (11-44 yrs)	N = 54 (51.4%)
	Late onset (>45 yrs)	N = 24 (22.9%)
	Δ = A-E/AO = Duration of complaints	2 - 57 (mean: 22.3)
	Duration of complaints (yrs)	
	First complaints (can be several)	60%
	Decreased visual acuity	33%
	Night blindness	55%
	Loss of visual field	95%
	Problems with reading	48%
	Disturbed color vision	51%
	Photophobia	
	Regular visit ophthalmologist	30%
	Yes	70%
	No	
<b>Ophthalmologic history</b>		5%
<b>Course of disease (subjective)</b>	Progressive	61%
	Stable	39%
<b>Using visual aid</b>	Yes	86%
	No	14%

LIFE STYLE		Stargardt cohort
<b>Smoking cigarettes</b>	<b>Characteristics</b>	
	Yes	18%
	No	82%
<b>Drugs</b>	Yes	0%
	No	100%
<b>Alcohol</b>	Yes	81%
	No	19%
<b>Food</b>	Fish (21x/week)	65%
	Meat (21x/week)	94%
	Fruit (21x/week)	89%
	Vegetables (21x/week)	99%
<b>Sport</b>	No	15%
	Almost never	12%
	1-2 times/week	38%
	3 times or more a week	35%
<b>Being outdoors</b>	> 8h/day	11%
	< 8h/day	85%
	Less as possible, avoid the sun	4%

GENERAL HEALTH		Stargardt cohort
<b>Characteristics</b>		
<b>Visiting other specialists</b>	Yes	37%
	No	63%
<b>Comorbidity</b>	Yes (e.g. COPD, etc.)	20%
	No	80%
<b>Allergy</b>	Yes	27%
	No	73%
<b>Medication</b>	Yes	40%
	No	60%
<b>Eye color</b>	Blue, gray (light)	58%
	Green, Hazel	19%
	Brown (dark)	23%



### General quality of life (RAND-sf36)

Results from the general QoL questionnaire RAND-sf36 are summarized in [Table 2](#). The norm scores were estimated from a Dutch population (mean age 44.1 years, range 18-89, 65% women) and had a comparable distribution of age and gender to our study cohort. Comparisons with norm groups revealed similar physical functioning, social functioning, physical role functioning and emotional role functioning compared to norms (t-values not shown). STGD1 patients showed better scores on mental health ( $t=5.108$   $p<=.001$ ), vitality ( $t=2.980$   $p=.004$ ), pain ( $t=4.241$   $p<=.001$ ), and general health perception ( $t=2.398$   $p=.019$ ) than the norm group.

Differences in aspects of QoL regarding demographic factors revealed worse mental health ( $F=9.458$ ;  $p=.003$ ) and vitality ( $F=6.576$ ;  $p=.012$ ) in women compared to men. Regarding disease characteristics, we found differences in physical functioning between groups with different ages at onset ( $F=3.622$ ;  $p=.031$ ) with less favorable perceived physical health in patients with later disease onset. In addition, we identified difference in general perceived health in patients with different duration of complaints ( $F=2.913$ ;  $p=.026$ ) with worst perceived health in patients with shorter duration of complaints. Patients also indicated differences in disease severity ( $F=5.713$ ;  $p=.001$ ) with no linear relationship between disease severity and perceived health.

### Vision-specific quality of life (VFQ-25)

The results on vision-related QoL as indicated by the VFQ-25 are reported in [Table 3](#). No differences in vision-related QoL were observed between different demographic characteristics, except for gender and mental health, indicates more mental health problems in women ( $F=4.419$ ;  $p=0.38$ ) compared to men. Differences regarding several disease characteristics were as follows: patients with a later age at onset indicated better overall vision ( $F=6.822$ ;  $p=.002$ ), distance activity ( $F=4.541$ ;  $p=.013$ ) and social functioning ( $F=7.606$ ;  $p=.001$ ) compared to those with earlier disease onset. Regarding severity of visual impairment, it was indicated that overall vision ( $F=12.164$ ;  $p<.001$ ), near vision ( $F=10.360$ ;  $p<.001$ ), distance vision ( $F=10.432$ ;  $p<.001$ ), driving ( $F=3.801$ ;  $p=.017$ ), role limitation due to vision ( $F=4.438$ ;  $p=.006$ ), color vision ( $F=2.771$ ;  $p=.046$ ), and social functioning ( $F=7.767$ ;  $p<0.001$ ) differed significantly regarding severity of visual impairment, with less favorable vision-related QoL in patients with more severe impairment. Concerning duration of disease, longer duration of disease, was related to a better vision-related QoL on every subscale ( $p<.001$  to  $p=0.02$ ), except for overall vision, ocular pain, and mental health.

Table 4 presents the scores of our STGD1 cohort compared to norm groups and other eye diseases, such as diabetic retinopathy, age-related macular degeneration, glaucoma, cataract, cytomegalovirus retinitis and low vision in general [29]. Results indicate that STGD1 patients perceive less favorable vision-related QoL compared to other patients with eye diseases, except for the group of patients with “low vision in general”. This is true for nearly all aspects of vision-related QoL except for general health which is perceived as more favorable by STGD1 patients compared to other patient groups.

**Table 2: Results of the RAND-sf36 questionnaire**

Subscale	Mean norm scores (SD)	Mean STGD1 patients (SD)	Groups of onset			Gender		Duration of disease (yrs)				Visual impairment					
			Early	Classic	Late	Male	Female	<10	11-20	21-30	31-40	40<	No or mild	Moderate	Severe	Blindness	
Physical function	81.9 (23.2)	93.5 (13.9)	<b>94.8 (14.2)</b>	<b>96.4 (7.2)</b>	<b>88.3 (15.2)</b>	94.1 (11.7)	94.3 (11.8)	92.3 (14.6)	97.7 (5.3)	90.5 (15.6)	95.9 (6.3)	96.3 (8.6)	<b>88.8 (16.2)</b>	88.2 (19.0)	<b>94.2 (10.6)</b>	<b>95.5 (12.6)</b>	<b>96.3 (7.2)</b>
Social function	86.9 (20.5)	87.5 (17.7)	84.5 (19.2)	87.8 (17.4)	90.6 (16.7)	89.4 (18.7)	86.1 (16.9)	88.0 (19.7)	90.1 (13.3)	83.0 (21.0)	83.0 (19.6)	93.8 (11.3)	88.2 (19.0)	85.4 (19.8)	87.1 (18.7)	89.8 (14.7)	
Role limitation: physical	79.4 (35.5)	79.3 (33.2)	77.0 (34.6)	82.3 (30.9)	77.4 (34.4)	81.4 (32.3)	78.6 (32.8)	75.0 (32.3)	92.7 (17.3)	67.0 (41.8)	79.5 (33.2)	87.5 (29.2)	75.0 (36.4)	71.1 (34.6)	86.2 (26.4)	86.1 (30.5)	
Role limitation: emotional	84.1 (32.3)	88.7 (27.3)	84.0 (34.9)	90.3 (25.7)	88.9 (24.3)	<b>91.5 (23.8)</b>	<b>86.1 (30.6)</b>	84.0 (33.5)	93.1 (17.0)	83.3 (33.7)	93.9 (20.1)	91.7 (28.9)	86.3 (29.0)	84.2 (28.0)	90.8 (28.0)	92.6 (23.3)	
Mental health	76.8 (18.4)	84.0 (13.5)	82.9 (13.8)	83.8 (14.2)	86.2 (13.1)	<b>89.0 (10.9)</b>	<b>80.5 (14.6)</b>	83.3 (16.4)	87.0 (11.0)	81.1 (15.7)	81.8 (12.8)	87.3 (9.9)	85.4 (15.9)	78.7 (15.8)	86.3 (12.7)	86.2 (10.1)	
Vitality	67.4 (19.9)	73.3 (19.5)	70.2 (18.8)	74.8 (18.1)	74.5 (24.7)	79.5 (19.1)	69.2 (19.1)	71.7 (26.2)	78.1 (14.5)	68.6 (19.8)	71.4 (15.4)	78.8 (15.4)	71.8 (26.3)	66.7 (18.2)	78.3 (18.6)	75.9 (15.4)	
Pain	79.5 (25.6)	88.0 (18.2)	84.9 (22.1)	90.8 (15.7)	83.6 (19.0)	85.8 (20.5)	88.8 (16.9)	87.8 (18.6)	88.5 (16.0)	83.2 (21.2)	86.5 (19.4)	95.0 (16.6)	83.9 (23.3)	89.9 (15.1)	90.0 (15.5)	87.7 (19.8)	
General health perception	72.7 (22.7)	77.9 (19.7)	<b>81.6 (12.5)</b>	<b>78.5 (20.1)</b>	<b>70.8 (26.2)</b>	79.1 (18.6)	76.7 (21.2)	<b>67.1 (27.5)</b>	<b>83.5 (13.6)</b>	<b>78.0 (19.0)</b>	<b>78.6 (11.0)</b>	<b>85.8 (14.4)</b>	<b>71.2 (26.8)</b>	<b>65.8 (22.6)</b>	<b>84.5 (12.8)</b>	<b>83.9 (12.0)</b>	

*Scores of mean and standard deviation (sd) of every subscale from different variants  
Numbers in bold = ANOVA revealed significant differences between groups (p<.05)*

**Table 3: Results of the VFQ-25 questionnaire.**

Subscale *vision specific	Mean norm scores (SD)	Mean STGD1 patients (SD)	Groups of onset			Gender		Duration of disease (yrs)					Visual impairment			
			Early	Classic	Late	Male	Female	5-10	11-20	21-30	31-40	40<	No or mild	Moderate	Severe	Blindness
General health	69 (24)	71.6 (16.9)	75.1 (15.3)	72.6 (15.9)	66.0 (19.5)	74.4 (18.2)	70.0 (15.7)	69.3 (20.1)	74.6 (17.1)	68.2 (14.6)	72.3 (15.1)	77.9 (13.8)	67.9 (20.8)	66.1 (14.8)	74.8 (16.2)	76.1 (14.4)
General vision	83 (15)	46.1 (17.9)	39.4 (17.5)	45.2 (16.4)	57.3 (17.3)	45.0 (20.4)	47.4 (16.1)	59.2 (16.6)	53.8 (16.2)	40.7 (10.9)	32.7 (13.2)	30.0 (11.5)	61.3 (19.1)	47.1 (14.8)	47.8 (12.7)	33.3 (16.5)
Near vision	92 (13)	45.7 (22.8)	39.4 (14.1)	45.2 (21.2)	54.7 (31.9)	49.6 (23.0)	43.4 (22.9)	65.5 (25.4)	43.4 (19.9)	39.2 (15.0)	29.3 (13.8)	38.9 (18.0)	65.8 (30.8)	50.0 (19.4)	42.8 (18.1)	32.9 (12.2)
Distance vision	93 (11)	51.9 (21.4)	42.3 (12.7)	53.2 (21.6)	60.3 (26.0)	53.7 (22.7)	50.9 (21.0)	70.7 (20.8)	52.4 (19.0)	45.3 (14.8)	34.5 (7.9)	42.6 (22.4)	69.4 (25.6)	54.4 (18.3)	53.1 (17.7)	38.1 (14.5)
Driving	87 (18)	28.7 (38.2)	16.7 (37.3)	26.4 (37.1)	34.5 (40.6)	33.8 (40.2)	25.8 (37.4)	47.5 (38.9)	24.2 (40.0)	6.9 (24.1)	0 (41.9)	44.4 (41.9)	51.0 (37.5)	25.0 (41.3)	13.7 (28.0)	0
Peripheral vision	97 (10)	81.8 (22.8)	76.0 (24.5)	84.0 (21.3)	84.1 (25.1)	80.1 (21.6)	83.2 (24.1)	88.0 (23.0)	77.1 (26.5)	89.1 (16.6)	82.7 (15.8)	64.6 (24.9)	79.2 (24.6)	89.3 (20.3)	84.2 (20.2)	76.9 (23.9)
Color vision	98 (8)	84.8 (22.7)	80.0 (21.7)	85.3 (23.0)	89.8 (22.7)	84.0 (24.0)	85.6 (21.9)	92.3 (18.4)	88.5 (22.1)	78.3 (25.3)	90.4 (16.3)	68.8 (24.1)	84.2 (23.9)	92.9 (14.0)	90.0 (21.4)	76.3 (23.9)
Ocular pain	90 (15)	88.6 (17.2)	86.5 (18.4)	88.5 (17.6)	93.2 (14.3)	90.1 (15.2)	88.3 (18.4)	92.8 (13.3)	91.1 (12.5)	83.7 (21.1)	85.6 (17.8)	90.6 (17.8)	90.8 (16.6)	85.1 (21.5)	90.3 (16.0)	90.3 (16.0)
Role difficulties*	93 (13)	47.8 (20.4)	44.5 (15.0)	46.3 (17.4)	56.5 (29.0)	51.6 (21.0)	45.9 (19.8)	62.7 (19.9)	50.8 (18.6)	41.0 (15.7)	33.7 (15.2)	40.6 (18.9)	60.9 (30.5)	50.0 (16.1)	40.0 (14.9)	40.0 (14.9)
Dependency*	99 (6)	75.9 (19.3)	71.8 (19.6)	75.9 (18.7)	82.7 (19.4)	80.9 (18.0)	73.3 (19.6)	87.5 (14.7)	74.7 (19.1)	69.6 (21.5)	71.2 (19.5)	74.0 (15.7)	80.9 (23.1)	76.8 (22.4)	71.3 (17.3)	71.3 (17.3)
Social function*	99 (3)	67.3 (19.3)	57.0 (16.8)	68.1 (19.0)	77.7 (17.9)	70.5 (19.8)	65.4 (19.1)	83.3 (14.5)	66.7 (17.0)	59.1 (16.1)	55.1 (23.1)	63.9 (23.1)	81.1 (19.2)	68.7 (19.7)	55.9 (16.0)	55.9 (16.0)
Mental health*	92 (12)	68.5 (19.0)	67.2 (17.1)	67.8 (20.0)	72.8 (17.4)	73.6 (17.5)	65.6 (18.9)	71.2 (18.9)	71.7 (19.7)	65.7 (20.1)	63.8 (17.3)	69.2 (15.5)	67.7 (21.7)	65.5 (19.4)	70.4 (16.8)	70.4 (16.8)

Scores of mean and standard deviation (sd) of every subscale from different variants. In bold: Anova revealed significant differences between groups (p<.05)

**Table 4:** Results of the VFQ-25 questionnaire. The results of our study cohort (Stargardt disease) are compared to the results of other eye conditions (reference: Mangione CM, Lee PP, Gutierrez PR, Spritzer K, Berry S, Hays RD, et al. Development of the 25-item National Eye Institute Visual Function Questionnaire. Archives of ophthalmology. 2001;119:1050-8, Table 4). Data are presented as mean ± standard deviation (SD).

Subscales	Stargardt disease	Diabetic retinopathy	Age-related macular degeneration	Primary open-angle Glaucoma	Age-related Cataract	Cytomegalovirus retinitis	Low vision	Reference (norm group)
General health	72 ± 17	46 ± 25 t=14.996; p<0.01	65 ± 25 t=3.829; p<0.01	62 ± 25 t=5.593; p<0.01	55 ± 25 t=9.707; p<0.01	45 ± 24 t=15.584; p<0.01	57 ± 27 t=8.531; p<0.01	69 ± 24 t=1.478; p=0.143
General vision	46 ± 18	62 ± 21 t=8.756; p<0.01	53 ± 20 t=3.781; p<0.01	71 ± 17 t=13.732; p<0.01	60 ± 17 t=7.651; p<0.01	76 ± 14 t=16.497; p<0.01	38 ± 18 t=4.512; p<0.01	83 ± 15 t=20.367; p<0.01
Near vision	46 ± 23	63 ± 30 t=7.488; p<0.01	54 ± 27 t=3.585; p<0.01	79 ± 23 t=14.426; p<0.01	73 ± 21 t=11.824; p<0.01	84 ± 20 t=16.594; p<0.01	36 ± 23 t=4.220; p<0.01	97 ± 13 t=20.063; p<0.01
Distance vision	52 ± 21	66 ± 30 t=6.511; p<0.01	56 ± 29 t=1.890; p=0.062	77 ± 25 t=11.595; p<0.01	73 ± 22 t=9.747; p<0.01	84 ± 18 t=14.830; p<0.01	38 ± 26 t=6.429; p<0.01	93 ± 11 t=18.99; p<0.01
Driving	29 ± 38	55 ± 40 t=4.813; p<0.01	39 ± 36 t=1.880; p=0.066	75 ± 28 t=8.479; p<0.01	63 ± 30 t=6.279; p<0.01	80 ± 28 t=9.395; p<0.01	10 ± 23 t=3.435; p<0.01	87 ± 18 t=10.678; p<0.01
Peripheral vision	82 ± 23	78 ± 29 t=1.679; p=0.096	77 ± 27 t=2.111; p=0.037	76 ± 27 t=2.543; p=0.013	87 ± 21 t=2.208; p=0.03	78 ± 21 t=1.679; p=0.096	59 ± 32 t=9.884; p<0.01	97 ± 10 t=6.526; p<0.01
Color vision	85 ± 23	90 ± 22 t=2.160; p<0.033	85 ± 25 t=0.045; p=0.965	93 ± 17 t=3.483; p<0.01	90 ± 20 t=2.160; p=0.033	98 ± 9 t=5.688; p<0.01	71 ± 31 t=6.218; p<0.01	98 ± 8 t=5.688; p<0.01
Ocular pain	89 ± 17	88 ± 17 t=0.439; p=0.661	87 ± 16 t=1.016; p=0.312	89 ± 14 t=0.137; p=0.891	86 ± 19 t=1.592; p=0.115	90 ± 16 t=0.713; p=0.478	85 ± 20 t=2.168; p=0.033	90 ± 15 t=0.713; p=0.478
Vision specific:								
Role difficulties	48 ± 20	69 ± 31 t=10.264; p<0.01	61 ± 31 t=6.381; p<0.01	84 ± 23 t=17.544; p<0.01	76 ± 22 t=13.661; p<0.01	78 ± 24 t=14.632; p<0.01	44 ± 29 t=1.870; p=0.064	93 ± 13 t=21.912; p<0.01
Dependency	76 ± 19	77 ± 30 t=0.476; p=0.635	72 ± 30 t=2.094; p=0.039	92 ± 19 t=8.186; p<0.01	88 ± 20 t=6.130; p<0.01	89 ± 12 t=6.644; p<0.01	51 ± 31 t=12.888; p<0.01	99 ± 6 t=11.784; p<0.01
Social functioning	67 ± 19	81 ± 26 t=6.947; p<0.01	73 ± 29 t=2.818; p<0.01	89 ± 20 t=11.066; p<0.01	87 ± 19 t=10.036; p<0.01	96 ± 9 t=14.670; p<0.01	50 ± 31 t=9.015; p<0.01	99 ± 3 t=16.215; p<0.01
Mental health	69 ± 19	66 ± 29 t=1.224; p=0.224	58 ± 27 t=5.390; p<0.01	81 ± 20 t=6.586; p<0.01	77 ± 22 t=4.505; p<0.01	74 ± 22 t=2.942; p<0.01	46 ± 27 t=11.639; p<0.01	92 ± 12 t=12.316; p<0.01

In red: scores are significantly worse for this disorder compared to Stargardt disease

In green: disorder is significantly better than Stargardt disease

## Discussion

Overall, the general QoL (RAND-sf36) in this cohort of STGD1 patients was good and comparable to norm groups. On the other hand, the vision-specific QoL as represented by the VFQ-25 reports a considerable impact of disease in vision-specific QoL. This is most obvious in the subgroup of STGD1 patients with an early age at onset, generally low visual acuity and long disease duration.

### Study cohort

In general, our study cohort has a healthy lifestyle according to diet, performing sport, not using drugs, and just a small percentage of smokers. Although, we are not able to differ the lifestyle before STGD1 was diagnosed; maybe they have altered their lifestyle after diagnosis.

According to demographics, like marital status and having children, the numbers are comparable to the general population of the Netherlands ([www.CBS.nl](http://www.CBS.nl)). Likely, these demographics are not influenced by visual impairment.

A remarkable number of cases of our cohort has finished university (43%) compared to the general Dutch population (29%). Unfortunately, we are unable to provide any explanation on this issue.

There seems to be a contrast between the education level and work participation in the labor market of our cohort. Despite that a large number of patients completed (higher) education, they did not have an equal representation on the labor market compared to the general population. A rough calculation present a harsh reality; 93% of the general population (capable for work) has a part-time or full-time job, compared to only approximately half of our STGD1 population ([www.CBS.nl](http://www.CBS.nl)). Moreover, the incidence of disqualification from work in STGD1 patients is much higher than the general Dutch population ([www.CBS.nl](http://www.CBS.nl)). Visual impairment seems to have no influence in finishing a study, but certainly gives problems in finding a job. We are not able to answer whether STGD1 patients with a part-time or full-time job were capable to find a job in the same direction of their study. To our knowledge, no registration or numbers are known for visually impaired persons and their work situation. A study of Sainohira et al indicates a strong relationship between being employed and the degree of depression in a group of visual impaired patients due to retinitis pigmentosa [31]. Therefore, we recommend better registration, counseling and guidance of institutions to help visual impaired persons to find their way on the labor market, so they could use their full capabilities.

### General quality of life

Our cohort perceive a good general health, although they have serious and persistent disabilities. An important issue explaining the good QoL in this patient group is the differences between a disability and a disease [32]. The International Classification of Functioning, Disability and Health (ICF) represents the conceptualization of disability, function, and health and indicates a significant shift from the previous image where disability was assumed to be related with miserable health [33]. This opinion nuances health from disability, and suggest that patients can be disabled as well as healthy [34]. A disease has a relationship with an illness or with feeling sick. This study shows that patients with STGD1 perceive their health as good, despite the important impairment as the result of STGD1. The impact of these limitations is better reflected in disease-specific QoL instruments, as is shown in this paper by the VFQ-25. So one could conclude that STGD1 patients, in this study, are presented as a group of patients generally perceive their health as good, with important impairments in daily life because of their visual disability. This could be explained by the flexibility to integrate these impairments in daily functioning resulting in a favourable perceived health. Several studies discuss the difficulties in interpreting health related QoL scores in people with disabilities due to the confounding between health, functioning and disability [35].

Another explanation of the good general health perception of our cohort can be related to the phenomenon that people tend to change their perception of QoL to their circumstances, also called “response shift” [36, 37]. This is a psychological mechanism of adjustment to life changing circumstances resulting in a reappraisal of new circumstances, a reappraisal of life with a disability, in this case, visual impairment [38, 39]. This is seen in cancer patients, showing QoL comparable to norm groups, and even better, explained by adjustment to and reappraisal of new life with cancer with adjusted goals resulting in a new life balance [40].

Studies on QoL in people with visual impairment predominantly focus on older people having to deal with impaired vision. These studies present less favourable QoL compared to age matched norms. This could be clarified by the important impact of visual impairment, especially in the elderly where possibilities to adjust to new life circumstances are more problematic as general functioning is normally challenged too.

Average duration of complaints in our cohort was 22 years, implicating a very long period of opportunity to adjust to disease impairments. This is also supported by the positive relationship between QoL and duration of complaints. In addition, the RAND questionnaire focuses on items related to physical condition which is not impaired in these patients. This is in line with QoL scores in patients with specific hearing as well as vision impairment: in Usher syndrome, patients also had no differences in their QoL compared to norms [41]. The patients in our sample have an average age of 46 years and nearly no co-morbidity, which could also explain the favorable scores on general QoL assessment. This implies that the vision impairment interferes with specific aspects of QoL. This, however, is reflected in the problems indicated in the vision-specific QoL assessment.

### Vision-specific quality of life

On the contrary, the vision-specific QoL indicates severe restriction on almost every subscale. This indicates that STGD1 patients suffer in their daily life, because of their visual impairment. In comparison with patients with other eye-disease, such as diabetic retinopathy, age-related macular degeneration (AMD), glaucoma, cataract, and low vision in general [29], STGD1 patients belong to the group of patients with the lowest scores, comparable to AMD and low vision patients.

From a general health perspective, STGD1 patients experience no limitation in social function or mental health. The subscales “social function” and “mental health” are represented in both questionnaires. From a disease-specific point of view, as assessed by the VFQ-25, these subscales indicate more discomforts. This discrepancy suggests concerns regarding social and mental health related to, and focused on their visual impairment, but not to their life in general. So patients indicating concerns regarding their vision related health, but do not indicate concerns regarding their health in general. That indicates that visual impairment has a significant impact on social function and mental health.

Overall, the vision-specific QoL pointed out the impact of disease that specifically arises from a low visual acuity, long disease duration and a younger age at onset.

These results are comparable with results in other studies. A better visual acuity, suggesting a better reading ability, gives a better QoL as presented in the study from Murro et al. in a group of Stargardt patients [42]. In other retinal dystrophies, such as retinitis pigmentosa, there is a relationship between QoL and the severity of visual impairment [43, 44].



### Utilization of questionnaires

Given that STGD1 patients perceive no problems in general health, a decreased score of the RAND-sf36 could suggest general problems related to well-being. This information will be helpful in tailor-made counseling beyond the scope of the direct ophthalmic care.

The VFQ-25 presents a better overview of the QoL in STGD1 patients, as it is specified to the effect of their visual impairment on their QoL. Therefore, the VFQ-25 questionnaire could be valuable as an outcome measure in clinical trials. The scale is already included in other clinical trials [45-47].

However, both Rand-sf36 and VFQ-25 questionnaires could be used to predict utility health scores. Utility health scores could be used in economic and health policy analyses and evaluations [48]. The Rand-sf36 was revised into a six dimensional health state classification called the SF-6D. This SF-6D responses could be even translated into quality-adjusted life year (QALY; i.e. one year of life in optimal health)[49]. Six items from the VFQ-25 were used to develop the visual function questionnaire – utility index health state classification, which defines visual function health states [50, 51]. Although these questionnaires may resemble useful outcome measures, the change of these outcomes doesn't always reflect the true change that clinicians need to measure. The interpretation of these subjective measurements can differ not only between patients, but also within a patient over time due to their response shift. These changes in the perception of QoL influencing the outcome of measurements present methodological challenges to reliably measure a true QoL change.

In general, STGD1 patients, as presented in our study, perceive good general QoL with serious, vision-related impairments suggesting a large potential of health gain by innovative interventions to treat vision-related impairments.

## References

- [1] Blacharski P. Retinal dystrophies and degenerations. Newsome DA (ed). 1988:135-59.
- [2] Allikmets R, Singh N, Sun H, Shroyer NF, Hutchinson A, Chidambaram A, et al. A photoreceptor cell-specific ATP-binding transporter gene (ABCR) is mutated in recessive Stargardt macular dystrophy. *Nature genetics*. 1997;15:236-46.
- [3] Stargardt K. Über familiäre, progressive Degeneration in der Maculagegend des Auges. *Graefes Arch Clin Exp Ophthalmol*. 1909:534-50.
- [4] Rotenstreich Y, Fishman GA, Anderson RJ. Visual acuity loss and clinical observations in a large series of patients with Stargardt disease. *Ophthalmology*. 2003;110:1151-8.
- [5] Klevering BJ, Deutman AF, Maugeri A, Cremers FP, Hoyng CB. The spectrum of retinal phenotypes caused by mutations in the ABCA4 gene. *Graefes Arch Clin Exp Ophthalmol*. 2005;243:90-100.
- [6] Lambertus S, van Huet RA, Bax NM, Hoefsloot LH, Cremers FP, Boon CJ, et al. Early-onset stargardt disease: phenotypic and genotypic characteristics. *Ophthalmology*. 2015;122:335-44.
- [7] Westeneng-van Haaften SC, Boon CJ, Cremers FP, Hoefsloot LH, den Hollander AI, Hoyng CB. Clinical and genetic characteristics of late-onset Stargardt's disease. *Ophthalmology*. 2012;119:1199-210.
- [8] Fujinami K, Zernant J, Chana RK, Wright GA, Tsunoda K, Ozawa Y, et al. Clinical and molecular characteristics of childhood-onset Stargardt disease. *Ophthalmology*. 2015;122:326-34.
- [9] van Huet RA, Bax NM, Westeneng-Van Haaften SC, Muhamad M, Zonneveld-Vrieling MN, Hoefsloot LH, et al. Foveal sparing in Stargardt disease. *Investigative ophthalmology & visual science*. 2014;55:7467-78.
- [10] Cohn DE, Barnett JC, Wenzel L, Monk BJ, Burger RA, Straughn JM, Jr., et al. A cost-utility analysis of NRG Oncology/Gynecologic Oncology Group Protocol 218: incorporating prospectively collected quality-of-life scores in an economic model of treatment of ovarian cancer. *Gynecologic oncology*. 2015;136:293-9.
- [11] Tosh J, Brazier J, Evans P, Longworth L. A review of generic preference-based measures of health-related quality of life in visual disorders. *Value in health : the journal of the International Society for Pharmacoeconomics and Outcomes Research*. 2012;15:118-27.
- [12] Seland JH, Vingerling JR, Augood CA, Bentham G, Chakravarthy U, deJong PT, et al. Visual impairment and quality of life in the older European population, the EUREYE study. *Acta ophthalmologica*. 2011;89:608-13.
- [13] Crews JE, Chou CF, Zack MM, Zhang X, Bullard KM, Morse AR, et al. The Association of Health-Related Quality of Life with Severity of Visual Impairment among People Aged 40-64 Years: Findings from the 2006-2010 Behavioral Risk Factor Surveillance System. *Ophthalmic epidemiology*. 2016;23:145-53.
- [14] Augustin A, Sahel JA, Bandello F, Dardennes R, Maurel F, Negrini C, et al. Anxiety and depression prevalence rates in age-related macular degeneration. *Investigative ophthalmology & visual science*. 2007;48:1498-503.
- [15] Finger RP, Kupitz DG, Holz FG, Balasubramaniam B, Ramani RV, Lamoureux EL, et al. The impact of the severity of vision loss on vision-related quality of life in India: an evaluation of the IND-VFQ-33. *Investigative ophthalmology & visual science*. 2011;52:6081-8.
- [16] Hamblion EL, Moore AT, Rahi JS. The health-related quality of life of children with hereditary retinal disorders and the psychosocial impact on their families. *Investigative ophthalmology & visual science*. 2011;52:7981-6.
- [17] van der Aa HP, Comijs HC, Penninx BW, van Rens GH, van Nispen RM. Major depressive and anxiety disorders in visually impaired older adults. *Investigative ophthalmology & visual science*. 2015;56:849-54.
- [18] Casten RJ, Rovner BW. Update on depression and age-related macular degeneration. *Current opinion in ophthalmology*. 2013;24:239-43.
- [19] Ivers RQ, Norton R, Cumming RG, Butler M, Campbell AJ. Visual impairment and risk of hip fracture. *American journal of epidemiology*. 2000;152:633-9.

- [20] Crews JE, Campbell VA. Vision impairment and hearing loss among community-dwelling older Americans: implications for health and functioning. *American journal of public health*. 2004;94:823-9.
- [21] PR L. Testimony before: Departments of Labor, Health, and Human Services, and Related Agencies. 1st U.S. Congress House Committee on Appropriations for 1993. In: Washington DCGPO, 1992, editor. pt 8A, 1317-301992.
- [22] van der Aa HP, van Rens GH, Comijs HC, Margrain TH, Gallindo-Garre F, Twisk JW, et al. Stepped care for depression and anxiety in visually impaired older adults: multicentre randomised controlled trial. *Bmj*. 2015;351:h6127.
- [23] Matamoros E, Maurel F, Leon N, Solomiac A, Bardoulat I, Joubert M, et al. Quality of Life in Patients Suffering from Active Exudative Age-Related Macular Degeneration: The EQUADE Study. *Ophthalmologica Journal international d'ophtalmologie International journal of ophthalmology Zeitschrift fur Augenheilkunde*. 2015;234:151-9.
- [24] Cimarolli VR, Casten RJ, Rovner BW, Heyl V, Sorensen S, Horowitz A. Anxiety and depression in patients with advanced macular degeneration: current perspectives. *Clinical ophthalmology*. 2016;10:55-63.
- [25] Jivraj J, Jivraj I, Tennant M, Rudnisky C. Prevalence and impact of depressive symptoms in patients with age-related macular degeneration. *Canadian journal of ophthalmology Journal canadien d'ophtalmologie*. 2013;48:269-73.
- [26] Weleber RG, Pennesi ME, Wilson DJ, Kaushal S, Erker LR, Jensen L, et al. Results at 2 Years after Gene Therapy for RPE65-Deficient Leber Congenital Amaurosis and Severe Early-Childhood-Onset Retinal Dystrophy. *Ophthalmology*. 2016.
- [27] VanderZee KI, Sanderman R, Heyink JW, de Haes H. Psychometric qualities of the RAND 36-Item Health Survey 1.0: a multidimensional measure of general health status. *International journal of behavioral medicine*. 1996;3:104-22.
- [28] Zee van der KI, Sanderman R. Het meten van de algemene gezondheidstoestand met de RAND-36, een handleiding. 2012.
- [29] Mangione CM, Lee PP, Gutierrez PR, Spritzer K, Berry S, Hays RD, et al. Development of the 25-item National Eye Institute Visual Function Questionnaire. *Archives of ophthalmology*. 2001;119:1050-8.
- [30] Mangione CM, Lee PP, Pitts J, Gutierrez P, Berry S, Hays RD. Psychometric properties of the National Eye Institute Visual Function Questionnaire (NEI-VFQ). *NEI-VFQ Field Test Investigators. Archives of ophthalmology*. 1998;116:1496-504.
- [31] Sainohira M, Yamashita T, Terasaki H, Sonoda S, Miyata K, Murakami Y, et al. Quantitative analyses of factors related to anxiety and depression in patients with retinitis pigmentosa. *PLoS One*. 2018;13:e0195983.
- [32] Schwartz CE, Andresen EM, Nosek MA, Krahn GL, Measurement REPoHS. Response shift theory: important implications for measuring quality of life in people with disability. *Arch Phys Med Rehabil*. 2007;88:529-36.
- [33] Organisation WH. *International Classification of Functioning, Disability and Health*. Geneva, Switzerland: World Health Organisation; 2001.
- [34] USDHHS. *The Surgeon General's Call to Action to Improve the Health and Wellness of Persons With Disabilities*. In: Washington DC UDoHaHS, Office of the Surgeon General, editor. 2005.
- [35] Krahn GL, Fujiura G, Drum CE, Cardinal BJ, Nosek MA, Measurement REPoH. The dilemma of measuring perceived health status in the context of disability. *Disabil Health J*. 2009;2:49-56.
- [36] Carver CS, Scheier MF. Scaling back goals and recalibration of the affect system are processes in normal adaptive self-regulation: understanding 'response shift' phenomena. *Social science & medicine*. 2000;50:1715-22.
- [37] Schwartz CE, Bode R, Repucci N, Becker J, Sprangers MA, Fayers PM. The clinical significance of adaptation to changing health: a meta-analysis of response shift. *Quality of life research : an international journal of quality of life aspects of treatment, care and rehabilitation*. 2006;15:1533-50.

- [38] Schwartz CE, Sprangers MA. Methodological approaches for assessing response shift in longitudinal health-related quality-of-life research. *Social science & medicine*. 1999;48:1531-48.
- [39] Sprangers MA, Schwartz CE. Integrating response shift into health-related quality of life research: a theoretical model. *Social science & medicine*. 1999;48:1507-15.
- [40] Ibrahim NA, Bjornsdottir I, Al Alwan AS, Honore PH. Insights about health-related quality of life in cancer patients indicate demands for better pharmaceutical care. *J Oncol Pharm Pract*. 2014;20:270-7.
- [41] Damen GW, Pennings RJ, Snik AF, Mylanus EA. Quality of life and cochlear implantation in Usher syndrome type I. *The Laryngoscope*. 2006;116:723-8.
- [42] Murro V, Sodi A, Giacomelli G, Mucciolo DP, Pennino M, Virgili G, et al. Reading ability and quality of life in Stargardt disease. *Eur J Ophthalmol*. 2017:0.
- [43] Chaumet-Riffaud AE, Chaumet-Riffaud P, Cariou A, Devisme C, Audo I, Sahel JA, et al. Impact of Retinitis Pigmentosa on Quality of Life, Mental Health, and Employment Among Young Adults. *Am J Ophthalmol*. 2017;177:169-74.
- [44] Azoulay L, Chaumet-Riffaud P, Jaron S, Roux C, Sancho S, Berdugo N, et al. Threshold Levels of Visual Field and Acuity Loss Related to Significant Decreases in the Quality of Life and Emotional States of Patients with Retinitis Pigmentosa. *Ophthalmic research*. 2015;54:78-84.
- [45] Siqueira RC, Messias A, Messias K, Arcieri RS, Ruiz MA, Souza NF, et al. Quality of life in patients with retinitis pigmentosa submitted to intravitreal use of bone marrow-derived stem cells (Reticell -clinical trial). *Stem Cell Res Ther*. 2015;6:29.
- [46] Jacobson SG, Cideciyan AV, Sumaroka A, Roman AJ, Charng J, Lu M, et al. Defining Outcomes for Clinical Trials of Leber Congenital Amaurosis Caused by GUCY2D Mutations. *Am J Ophthalmol*. 2017;177:44-57.
- [47] Varma R, Haller JA, Kaiser PK. Improvement in Patient-Reported Visual Function After Ocricplasmin for Vitreomacular Adhesion: Results of the Microplasmin for Intravitreal Injection-Traction Release Without Surgical Treatment (MIVI-TRUST) Trials. *JAMA ophthalmology*. 2015;133:997-1004.
- [48] Brazier J, Roberts J, Deverill M. The estimation of a preference-based measure of health from the SF-36. *Journal of health economics*. 2002;21:271-92.
- [49] Craig BM, Pickard AS, Stolk E, Brazier JE. US valuation of the SF-6D. *Medical decision making : an international journal of the Society for Medical Decision Making*. 2013;33:793-803.
- [50] Rentz AM, Kowalski JW, Walt JG, Hays RD, Brazier JE, Yu R, et al. Development of a preference-based index from the National Eye Institute Visual Function Questionnaire-25. *JAMA ophthalmology*. 2014;132:310-8.
- [51] Whitehead SJ, Ali S. Health outcomes in economic evaluation: the QALY and utilities. *British medical bulletin*. 2010;96:5-21.



The background of the page is a scenic photograph of a beach at sunset or sunrise. A large, bright, glowing sun or moon is centered in the upper half of the frame, partially obscured by soft, pinkish-orange clouds. The lower half of the image shows the ocean with gentle waves washing onto a sandy beach. The overall color palette is warm, dominated by oranges, pinks, and yellows.

# CHAPTER 5

## Discussion

General discussion

Clinical characteristics

Towards a useful classification of Stargardt disease

Identification, registry, and functional assessment of *ABCA4* variants

Quality of life in patients with Stargardt disease

Future perspectives

## General discussion

Stargardt disease (STGD1) is the most prevalent inherited disease that causes visual impairment in childhood and young adults [1]. STGD1 was originally considered a juvenile-onset macular degeneration, however, more recent research has shown that initial abnormalities may develop at early childhood until old age, and includes a wide range of clinical, psychophysical and imaging findings [2-5]. In recent years, considerable advances have been made in our understanding of the clinical phenotypes, natural history and molecular genetics of STGD1 and have led to the first steps in developing therapies [6-14].

This thesis provides an overview of the different clinical characteristics of STGD1, works towards unraveling genetic causes and offers detailed information about general and vision-specific quality of life in STGD1 patients.

The main goal of the studies in this thesis is to provide a better understanding of the natural course and staging of disease in order to perform better counseling, to provide an accurate diagnosis and perspective for the STGD1 patient. A STGD1 patient may potentially receive a multitude of descriptive diagnoses throughout life based on phenotypic or ERG classifications. Moreover, the present classifications offer a diagnosis at that moment, instead of a single diagnosis that is informative with respect to clinical course, which may help the patient to answer important questions like: “*Am I able to continue my present work for the next 10 years?*”, or “*Am I able to see my children growing up?*” Currently, the ophthalmologist identifies a variety of STGD1 phenotypes, and it can be difficult to provide good counseling. The main challenges in diagnosing STGD1 lie in the early-onset and late-onset spectrum. Therefore, I will discuss these cohorts in more detail.

## Clinical characteristics

### *Early-Onset Stargardt Disease (Chapters 2.1 and 2.2)*

The arbitrary cut-off point of early-onset was defined as  $\leq 10$  years of age to avoid including patients with a more typical STGD1 phenotype.

### **Visual acuity**

In all patients a fast decline in visual acuity was noted, either by the patients themselves, their parents or school physicians. Visual acuity varied greatly during the first 5 years after first ophthalmic consultation. In other studies, a wide range of BCVA at first visit was observed and in most cases visual acuity was good (20/20), suggesting that BCVA is not a proper parameter to diagnose STGD1 or to

use as an outcome measurement in therapeutic trials [4, 15]. A study of Kong et al (ClinicalTrials.gov NCT01977846), states that BCVA is not a sufficiently sensitive outcome measure for STGD1 treatment trials with 1 year follow-up [16].

### ***Retinal features and retinal imaging***

Retinal features in early-onset STGD1 patients may include: macular atrophy with macular or peripheral flecks, macular atrophy without flecks, flecks without macular atrophy, or a normal fundus appearance [4, 17]. The prevalence of a normal fundus appearance ranges from 2.5% [4] to 24% [3] in early-onset STGD1 cohorts. The absence of fundus abnormalities may leave an alarming number of patients without a correct diagnosis and can mean years of inappropriate treatment (this thesis). To minimize delay in diagnosis, I suggest that these children are screened using FAF, SD-OCT and a color vision test. Thickening of the external limiting membrane (ELM) on SD-OCT has been suggested as an early sign in the absence of other functional and structural changes to the retina [18, 19]. It may reflect a gliotic response to cellular stress at the photoreceptor level. Edges of the inner segment ellipsoid band appear to recede earlier than the ELM band in active lesions. On FA, atrophic foveal changes (sometimes appearing as a bull's eye lesion) present as hypo-autofluorescent lesions, surrounded by a hyperautofluorescent perifoveal ring and/or very subtle hyperautofluorescent flecks/dots. Hyperautofluorescence may precede the apparent atrophic changes. Abnormalities in color vision test could suggest an early-sign of a cone dysfunction.

Other studies have suggested that adaptive optics imaging could be used to study early signs in STGD1 [20-22]. Song et al. reported increased photoreceptor spacing in STGD1 patients in otherwise normal appearing areas on OCT and FAF imaging [20]. Adaptive optics imaging derived cone-density has been shown to correlate well with OCT measurements of ONL thickness and retinal sensitivity, demonstrating a valuable structure-function association, even though the extent of atrophic changes was not in correspondence with visual acuity [21]. Tanna et al. investigated the reliability and reproducibility of cone counting with adaptive optics in STGD1 patients (confocal and (nonconfocal) split-detector adaptive optics scanning light ophthalmoscopy (AOSLO) imaging), and concluded that this imaging technique is valuable for natural history studies and clinical trials [22]. This suggest that adaptive optics could be informative and a reliable follow-up measurement.

FA and ERG may be less helpful in the diagnostic phase. The rate of the dark choroid sign as seen on FA is relatively low (26%, this thesis) and full-field ERG may not be informative, as this may suggest normal retinal function. In addition, it should be realized that these are invasive tests.



If no yellow-white flecks are seen by ophthalmoscopy, patterns on full-field ERG may be helpful and can point to an isolated cone dystrophy, cone-rod dystrophy or even rod-cone dystrophy. In the early phase, optic disc pallor, hyperpigmentations, and arteriolar attenuation indicate a cone(-rod) dystrophy, but these signs may also manifest themselves not until later stages of early-onset STGD1. The progressive retinal degeneration eventually results in profound chorioretinal atrophy with retinal pigmentations. At this stage, traces of yellow-white flecks may only be seen in the far periphery. This rapid and severe retinal degeneration results in a severe visual impairment (20/200), which is usually reached before adulthood and eventually a visual acuity of about 20/500 or lower is expected at the age of about 40 years. An early-onset STGD1 patient at the age of 60 years may have the same phenotype as a retinitis pigmentosa or cone-rod dystrophy patient of the same age. Although STGD1 is due to variants in only one gene, RP and CRD can be due to variants in more than a hundred genes. These disorders are characterized by visual loss, abnormalities of color vision, visual field loss, and variable degrees of nystagmus, photophobia and night blindness. Specific genetic testing for mutations in *ABCA4* is therefore the only approach to confirm the diagnosis of STGD1.

### ***ABCA4***

The majority of the early-onset STGD1 patients carry two predicted severe *ABCA4* mutations suggesting that expression and residual activity of *ABCA4* play a major role in determining the disease severity [4, 23, 24]. A comprehensive discussion of *ABCA4* is given later.

However, it is a challenge to diagnose STGD1 in young children and further research like retinal imaging and genetic screening is necessary. Therefore, I suggest to refer children with unexplained visual complaints to a specialized ophthalmic center.

### ***Late-Onset Stargardt Disease (Chapters 2.3, 2.4 and 2.5)***

The arbitrary cut-off point of late-onset STGD1 was defined as  $\geq 45$  years of age. Patients generally present with either a mild decrease in visual acuity, metamorphopsia, oscillopsia or visual field defects. Patients can even be asymptomatic and signs of late-onset STGD1 can coincidentally be found during ophthalmologic screening for other diseases, like diabetes mellitus. A distinctive characteristic of late-onset STGD1 is so-called ‘foveal sparing’ as described in **Chapter 2.3** and by Fujinami et al [5]. Although numerous yellow-white flecks can be found throughout the retina, the fovea is somehow not affected by atrophic lesions. In contrast to early-onset patients, in late-onset STGD1 foveal structure and function are relatively preserved, until the fovea eventually becomes affected by the increasing RPE atrophy. When foveal sparing is observed, visual acuity is

preserved for a long time. Due to the extensive surrounding RPE atrophy, patients switch between central fixation with a good visual acuity, and far eccentric fixation. However, they may experience a “jack-in-the-box” effect due to large paracentral scotomas. Eventually, loss of foveal sparing will result in a sudden decrease in visual acuity.

Notably, the clinical phenotype of foveal sparing is not exclusively found in late-onset STGD1 (**Chapter 2.4**). Geographic atrophy in AMD, mitochondrial retinal dystrophy (MRD) associated with the m.3243A>G mutation, central areolar choroidal dystrophy (CACD), and pseudo-Stargardt pattern dystrophy (PSPD) should also be considered and differentiated by genetic testing. The presence of foveal sparing in retinal dystrophies with distinctly different underlying mechanisms suggests a disease-independent mechanism that prolongs the survival of the fovea. Given the development of therapies for slowing down progressive chorioretinal atrophy in IRDs, the presence of foveal sparing has implications for the design of future clinical trials, and there is a need for longitudinal studies of foveal sparing. New imaging methods like adaptive optics and OCT-angiography could be helpful. In a study of Chen et al. confocal adaptive optics demonstrated abnormal and decreased cone spacing in regions corresponding to areas of reduced and irregular FAF, in predominantly late-onset patients with foveal sparing [25].

In some recent studies, another relatively new imaging method, OCT- angiography (OCT-A), has been employed in STGD1 patients [26, 27]. OCT-A may help to understand the development of atrophy, and study disease patterns to distinguish between different entities. Guduru et al. analysed the choriocapillaris layer on OCT-A and assessed RPE changes on FAF. Areas of choriocapillaris and RPE impairment were quantified and correlated. The study presents that RPE damage on FAF appears to be significantly larger than choriocapillaris layer vessel loss on OCT-A, which suggests that RPE damage might precede choriocapillaris defects [27]. Müller et al. investigated the choroidal blood flow in areas within and adjacent to RPE atrophy secondary to late-onset STGD1 and AMD. Using OCT-A, comparison of choroidal flow signal within and outside the area of RPE atrophy revealed distinct differences between STGD1 and AMD, potentially implicating a differential role of the choroid in the pathogenesis of RPE atrophy in these two diseases [26].

Contrary to early-onset STGD1 patients, the late-onset phenotype is at the mild end of the STGD1 spectrum. Mainly, patients with late-onset STGD1 are diagnosed with one severe and one mild *ABCA4* variant. Mild variants described in late-onset cases often include c.5603A>T (p.Asn1868Ile), c.[2588G>C; 5603A>T]

(p.[Gly863Ala, Gly863del; Asn1868Ile]) or other mild coding or intronic variants such as c.5882G>A (p.Gly1961Glu) and c.4253+43G>A (p.[=, Ile1377Hisfs\*3]), respectively [11, 28-30].

The misunderstanding persists that patients with an age at onset of 50 years or above could not develop an inherited retinal dystrophy, and are thus usually diagnosed with age-related macular degeneration (AMD). Therefore, knowledge on these phenotypes is essential in order to have well diagnosed cohorts for therapeutic trials, both for AMD and STGD1. In addition, *ABCA4* mutation screening may be essential, as Vitamin A supplements are recommended for AMD patients, but are contra-indicated in STGD1 patients.

In upcoming and ongoing trials: profound inter-eye differences in disease progression has impact on the statistical power of clinical trials; treated and untreated eyes must demonstrate a larger difference than do the inter-eye differences by their natural course. However, lower inter-eye correlations are more likely found in late-onset STGD1 patients carrying combinations of variants that more often show a large difference in disease expression between siblings (**Chapter 2.5**). Therefore, in therapeutical trials, inter-eye discordance may be an exclusion criterion.

### **Towards a useful classification of Stargardt disease.**

Already in 1909, Duane described the necessity of a useful classification in (eye) diseases [31]. In general, from many points of view it is of great importance to have a correct and uniform arrangement, classification, and nomenclature of diseases. The arrangement and classification of diseases is crucial in the selection of statistics on morbidity (causes of illness) and mortality (causes of death). If the nomenclature is not uniform, the consequence may be that medical doctors use different terms to denote the same condition. To develop a classification that will be universally acceptable is a difficult task. A classification which is suitable for the purposes of a general practitioner is not usually the best for a medical specialist [31].

Classification of a specific disease has the same challenges. In our opinion a good classification needs first of all a good understanding of the natural course of disease. There is a need for clarifying staging of disease and understanding the natural course of STGD1 in order to obtain an widely accepted, useful and correct classification. In addition, the classification must be manageable and understandable for clinicians worldwide, to obtain a better counseling, to provide a more accurate diagnosis and prognosis for the patient. Consequently, for STGD1

patients it will be better to understand their disease and future perspectives. Additionally, a widely accepted classification will be helpful to evaluate efficacy of upcoming treatments.

Several classifications of STGD1 have been proposed, however, they include just a small aspect of the disease. Van Driel et al. and Maugeri et al. introduced a classification based on the expected residual function of the ABCA4 protein by the severity of mutations [32, 33]. However, this classification will only work when the genetics of STGD1 are totally elucidated and we have accurate quantitative data on the effect of mutations on ABCA4 protein function. Additionally, information about phenotype and course of disease is lacking. Especially the course of disease represents important information for the patient.

Fishman et al. differentiated three clinical phenotypes based on flecks and atrophic lesions [34]. Still, the phenotypes of STGD1 are numerous. Furthermore, genotyping and functional assessment are missing and the patients may be diagnosed with several stages of diseases during life; this will be confusing.

Lois et al. recognized three patterns based on electrophysiological attributes [35]. Based on this classification, patients may get the diagnosis “cone dystrophy” which during life can develop into a “cone-rod dystrophy”. Besides, the present classifications lack information about clinical course. Also it is time consuming and burdensome for the patients to undergo ERG measurements. Nowadays, more efficient and patient-friendly imaging is available to evaluate the progression and stage of STGD1.

Therefore, this thesis proposes a more useful classification to provide a better understanding and perspective of natural course of disease, which includes ABCA4 function, clinical presentation and functional assessment.

What kind of “work-flow” do we advise? First, refer a patient with unexplained visual loss to a specialized ophthalmic center. Second, ask patients for family history, initial symptoms, age of onset, medical history and use of medication. Third, perform clinical examination of best-corrected visual acuity, ophthalmoscopy, fundus photography, fundus autofluorescence, and spectral-domain optical coherence tomography. Color vision tests could be helpful in children. All these examinations are non-invasive and a good baseline for further follow-up. Fourth, when any abnormalities and/or a positive family history are noted, we advise to perform genetic testing. When no abnormalities are seen and a negative family history exists, but the patient has still complaints of vision loss, we advise to make an appointment for follow-up.

Based on results from earlier studies and studies described in this thesis, we roughly classify STGD1 based on age-at-onset, which is now divided in three main subtypes:

1. Early-onset STGD1 (disease onset  $\leq 10$  years, Chapters 2.1, 2.2). STGD1 patients with an early-onset of disease are at the most severe spectrum of STGD1 phenotypes. They have a fast decline of visual acuity and in most cases are legally blind around the age of 20 years.
2. The “classic” or intermediate STGD1 as typically described in literature with fishtail flecks and age of onset between 11-44 years.
3. Late-onset STGD1 with an age of onset  $\geq 45$  years (Chapters 2.3, 2.4 and 2.5). STGD1 patients with a late-onset are at the mild spectrum of STGD1 disease. Typically, patients present with a foveal sparing phenotype and consequently a good visual acuity. However, due to atrophic lesions surrounding the fovea, they experience a “jack-in-the-box” effect, which can give problems in daily life.

In addition, whenever a spectrum of disease contains overlapping phenotypes as the rule rather than the exception, any cut-off point used to define a particular disease within that spectrum will be arbitrary. Natural history studies in combination with statistical analyses, like multinomial logistic regression calculation may be necessary to determine a more exact cut-off point.

**Table 1** gives an overview of the three subtypes, including typical fundus abnormalities at presentation of disease at the ophthalmologist, acceleration of visual decline, end stage of visual acuity, ERG abnormalities and combination of *ABCA4* mutations. Examples of clinical presentation of the classification based on age-at onset, is demonstrated in **Figure 1**. [36]

Age at onset	Typical abnormalities at fundoscopy	Visual acuity decline	End stage visual acuity (Snellen)	ERG abnormalities	<i>ABCA4</i> mutations
Early (mean, 7 yrs)	None/ Bull's eye/ Central atrophy	Fast	Hand movement	Cone - Rod	2 severe
Intermediate (mean, 23 yrs)	Yellowish flecks/ Fundus flavimaculatus	Moderate	20/1200 - 20/200	Cone	1 severe, 1 mild
Late (mean, 55 yrs)	Foveal sparing	Slow	20/100 – 20/40	None	1 severe, 1 mild*

**Table 1** Overview of types of STGD1. \*The definition of mild variants is currently not well established as they can have an effect on the mRNA and protein or both. In addition, non-*ABCA4* factors may play a role.

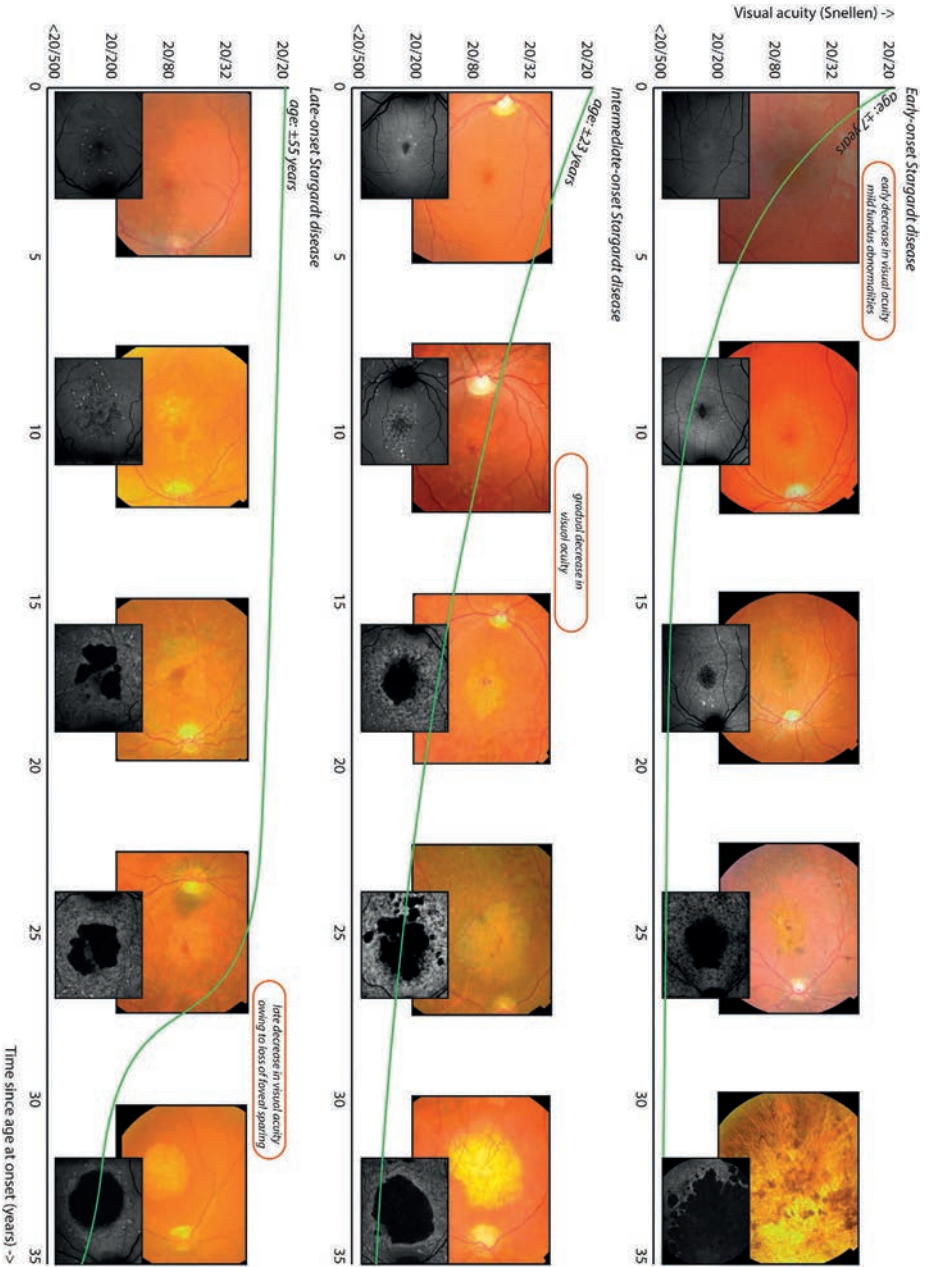


**Figure 1.** Overview of disease progression in subtypes of STGD1. Subtypes have distinctive disease onsets, indicating the severity of disease. The visual acuity decline is fast in early-onset STGD1, whereas in late-onset STGD1, visual acuity is affected only several years after disease onset.

## Identification, registry and functional assessment of *ABCA4* variants

Until recently, approximately 25% of STGD1 patients were missing a complete genetic diagnosis [33, 37-39]. Identification, registry and functional assessment of reported variants is essential to elucidate the missing heritability in STGD1. Van Driel et al. [32] and Maugeri et al. [33] first proposed a classification based on the expected residual function of the *ABCA4* protein by the severity of mutations. In this model, patients showed a spectrum of clinical phenotypes, from classical STGD1 when carrying a severe and mild (or two moderately severe) variant, to more severe phenotypes such as CRD (when carrying a severe and moderately severe variant), and RP (when carrying two severe *ABCA4* variants). To better understand the impact of individual variants and to elucidate the missing heritability in STGD1, we provided several studies in this thesis.

### Identification and registry of *ABCA4* variants (Chapter 3.1)

Till date, 7,447 *ABCA4* variants are described in the Leiden Open (source) Variation Database (LOVD). We collected all up to 2016 published *ABCA4* variants from 3,928 retinal dystrophy cases, which included 5,962 *ABCA4* variants (this thesis). This was the first comprehensive collection of *ABCA4* variants AND STGD1 cases. In rare diseases, like STGD1, combining genetic data is important to increase statistical power which can aid in the classification of variants, whether they are pathogenic or benign. Allele frequencies were compared between the STGD1 patient cohort and ~33,370 non-Finnish European controls in ExAC, because till now this is the best comparison as no other sizeable validated database is available. The assumed effect of the missense variants was verified by PhyloP, Grantham and CADD scores. The odds ratio contributes to support the hypothesis of the classification of a variant.

The study also proposes five variants (p.[Gly863Ala, Gly863del], p.(Gly1961Glu), p.(Ala1038Val), c.5714+5G>A, p.(Arg2030Gln)) to have a mild pathogenic effect in most cases based on their low or absent homozygous occurrence in STGD1 cases, while having a relatively high allele frequency. It was also proposed that in a small percentage of cases the p.(Gly1961Glu) allele can act as a moderate to severe variant. Recently, it was proposed that only ~10% of p.[Gly863Ala, Gly863del] alleles present in the general population result in STGD1 when found in *trans* with a severe variant, i.e. when p.[Gly863Ala, Gly863del] is in *cis* with p.(Asn1868Ile) [28, 29]. The p.(Asn1868Ile) variant, despite its unprecedented high allele frequency (i.e. 7%) in the normal population for an autosomal recessive variant, in

other studies was also found as a single mutation in *trans* with loss-of-function mutations, in ~10% of STGD1 cases [28, 29]. It was strongly associated with late onset STGD1, often due to foveal sparing. The mean ages at onset for STGD1 cases carrying p.(Asn1868Ile) and a severe variant in *trans* were 42 years [29] and 36.3 years [28]. Runhart et al. also found 3/10 bi-allelic siblings to be unaffected and calculated that a combination of p.(Asn1868Ile) with a loss-of-function variant in *trans* is penetrant in ~2% of individuals [29]. Although this finding was challenged [40], Cremers and colleagues strengthened earlier findings by using *ABCA4* variant allele frequency data from ~21,559 Dutch control persons [41]. Their conservative estimate is that the penetrance of p.(Asn1868Ile), when in *trans* with a severe variant, is ~5%. These findings suggest an important role for environmental or genetic modifiers in STGD1.

What is clearly lacking in these genotype-phenotype studies is a trustworthy functional classification of protein and RNA defects. “*In vivo*” analysis of variants in more suitable models, e.g. patient-derived retinal organoids, may be used to confirm pathogenicity as well as to assess expression levels.

### **Functional assessment of *ABCA4* variants (Chapter 3.2 and 3.3)**

In [Chapter 3.2](#), we elucidated the functional effect of one of the most frequent *ABCA4* variants associated with STGD1, i.e. c.5461-10T>C. Based on splice strength prediction algorithms this variant was predicted to have a very small effect on the strength of the splice acceptor site of exon 39. However, mRNA analysis of patient-derived PPCs revealed full exon(s) 39 or 39/40 skipping, which essentially means no *ABCA4* function. Our hypothesis was that a “weak” splice donor site of exon 39, probably explains the large effect of this predicted mild splice acceptor site variant. Follow-up studies have proven this to be true: strengthening of the splice donor site by mutagenesis of the c.5584+4 position from G>A nullifies the splice defect due to c.5461-10>C (S.S. Cornelis, M. Khan, F.P.M. Cremers, unpublished data).

We investigated the presence of the first five identified deep-intronic *ABCA4* variants [42] in 45 (monoallelic) genetically unsolved STGD1 cases, as described in [Chapter 3.3](#). We identified c.5196+1137G>A (a.k.a. V1) and c.4539+2001G>A (a.k.a. V4), in two and five probands of 45 cases (this thesis) [43]. The V4 variant also was very frequent in Belgian STGD1 cases as it explained 18/70 monoallelic probands [44]. For three of the five deep-intronic variants, i.e. V1-V3, it was shown that they resulted in aberrant mRNA in patient-derived keratinocytes, due to the insertion of pseudoexons [42]. Pseudoexons are small intronic segments that in the normal genome are not recognized by the splicing machinery as exons. STGD1-associated deep-intronic variants often strengthen the splice acceptor or donor site, and thereby result in the definition of a pseudoexon which will



subsequently be inserted in the mRNA. Almost invariably, pseudoexon insertions result in the introduction of a stopcodon or a frameshift into the reading frame. These will lead to nonsense-mediated decay of the mRNA and/or to ABCA4 protein truncation, thereby leading to the absence of ABCA4 activity, if the splicing defect affects 100% of the mRNA.

Two neighboring intron 30 variants, c.4539+2001G>A (V4) and c.4539+2028C>T (V5), were not functionally tested previously. In a recent study by Albert et al. [45], the effect of these variants could not be shown *in vitro*, using a splice assay, nor in patient-derived fibroblasts. Fibroblasts therefore were reprogrammed into induced pluripotent stem cells, which were subsequently differentiated into photoreceptor progenitor cells (PPCs). RNA analysis of PPCs revealed partial insertion of a 345-nt pseudoexon for V4 and V5. Both variants do not affect the splice acceptor or donor site of this pseudoexon, but create exonic splice enhancers that apparently act in a retina-specific manner.

Variants V1 to V5 were identified after a targeted search for intronic variants located in or close to predicted ultralow expressed pseudoexons [42]. In follow-up studies, the complete 128-kb ABCA4 gene was sequenced in mono-allelic STGD1 cases, which revealed another 13 causal deep-intronic variants. Together with copy number variants and the above-mentioned low-penetrant p.Asn1868Ile variant, these non-coding variants currently explain ~84% (Bauwens et al. 2019) and ~95% (Sangermano et al. 2019) of STGD1 probands [11, 30]. The relatively high occurrence of deep-intronic ABCA4 variants partially can be explained by the fact that many of them have a mild effect as only a proportion of mRNA is defective. Intermediate and late-onset STGD1 in most cases are due to a combination of a severe with a mild variant, explaining why intronic variants are relatively abundant in STGD1.

## Quality of life

Therapeutic trials for STGD1 are ongoing and new therapies are emerging. Currently, quality of life (QoL) is considered a significant outcome to measure the impact of disease, to estimate the efficacy of treatment, and an indicator of cost effectiveness for emerging clinical trials [46]. Additionally, knowledge of QoL in STGD1 patients can provide insight into the impact of the disease on daily functioning. But at the same time, we know little about the QoL in patients with STGD1. Therefore we performed a study on general and disease specific QoL in STGD1 in [Chapter 4](#).

Remarkably, the general QoL was even better for STGD1 patients than for norm groups. We discussed a good general health, “response shift”, and the difference between “disability” and “disease” as possible explanation. However, will this help us determine a significant outcome to measure the impact of disease? In my opinion: no. The results are just to confirm if a patient is generally healthy. It does not measure the burden or limitations of being visually impaired. In other words: it does not measure the visual disease impact, so it is not suitable as an outcome measurement in trials.

The vision-specific QoL was reduced in STGD1 patients. The vision-specific QoL was comparable or even worse than in patients with AMD or diabetic retinopathy. Studies of QoL in AMD patients reflect high levels of anxiety and depression. In our study we did not measure these aspects. In follow-up or future studies, this needs more attention to demonstrate if these psychological problems are present in STGD1 patients.

In general, STGD1 patients, as presented in our study, perceive good general QoL with serious, vision-related impairments suggesting a large potential of health gain by innovative interventions to treat vision-related impairments. Although treatments are currently lacking, there is a need for health improvement illustrated by the fact that only 43% of the STGD1 patients has a part-time or fulltime job, despite the fact that 100% of the STGD1 patients received a high school education.

What questionnaires do I recommend for ongoing and upcoming trials? Both Rand-sf36 and VFQ-25 outcomes could be used to predict utility health scores. Utility health scores could be used in economic and health policy analyses and evaluations [47]. The Rand-sf36 was revised into a six dimensional health state classification called the SF-6D. The SF-6D responses can be translated into quality-adjusted life year (QALY; i.e. one year of life in optimal health) [48]. Six items from the VFQ-25 were used to develop the visual function questionnaire – utility index health state classification, which defines visual function health states [49, 50]. Although these questionnaires may seem like useful outcome measures, a change in these outcomes does not always reflect a true change in the clinical condition. A questionnaire to evaluate the capabilities of a patient may be a better outcome measure, than the questionnaires I discussed.

In my opinion, counseling and capabilities of STGD1 patients needs more attention and further research. For example, we need to evaluate why STGD1 patients are less likely to be employed, even though they obtained a proper education and to

investigate whether they are depressed or anxious, as shown in other studies on visually impaired patients [51-53]. Better counseling and finding the bottleneck of unused capabilities may be beneficial for better quality of life in STGD1 patients.

## Future perspectives

### *Phenotyping STGD1*

STGD1 is not only a disease which starts in adolescence and young adulthood, but could appear from early childhood to old age. Good classification is essential to understand the wide clinical spectrum of STGD1. The classification must be manageable and understandable for all clinicians worldwide, to obtain a better counseling, to provide a more accurate diagnosis and prognosis for the patient. Consequently, for STGD1 patients it will be better to understand their disease and future perspectives. Additionally, universal accepted classification will be helpful to evaluate efficacy of upcoming treatments. Therefore, further studies on the natural course of disease are mandatory.

### *Elucidating the missing heritability in STGD1*

Identification, registry and functional assessment is essential to elucidate the missing heritability in STGD1. A worldwide variant and patient database, like LOVD-*ABCA4*, will help to identify and register all published *ABCA4* variants and cases. The next challenge will be to also include unpublished *ABCA4* variants and STGD1 cases known in diagnostic centers. Sharing genetic data is important to increase statistical power and can aid in the classification of pathogenic and benign variants.

New techniques, like mRNA analysis of patient-derived PPCs or fibroblasts, could study the functional effect of *ABCA4* variants. To investigate the effect of a variant, *in vivo* analysis of variants in more suitable models, e.g. patient-derived retinal organoids, can be used to confirm pathogenicity as well as to assess expression levels.

Eventually to expand the collection of *ABCA4* variants we must combine these with cases, in order to understand the genotype-phenotype correlation and prediction of disease outcome.

### *Quality of life*

Less is known about QoL in STGD1 patients. The standardized available questionnaires to measure visual impairment and QoL do not specify the exact problems STGD1 patients face in daily life. These questionnaires need to be improved and specify the reason WHY someone needs help and not IF someone

needs help. Counseling and capability of STGD1 patients needs more attention and further research. Better counseling and finding the bottleneck of unused capabilities may be beneficial for better QoL in STGD1 patients.

**Upcoming therapies**

Since the first description of Stargardt disease in 1917 by Karl Stargardt [54], more than a century has passed and we still have no cure. Trials are ongoing, but for STGD1 patients who are visiting our clinic at this moment, we still have no treatment to offer. Although frustrating, there is some perspective.

Currently, gene therapy, stem cell therapy, and pharmacotherapy with visual cycle modulators and complement inhibitors are being studied as potential treatments. Figure 2 presents the working mechanisms of the potential treatments for STGD1 in the visual cycle:

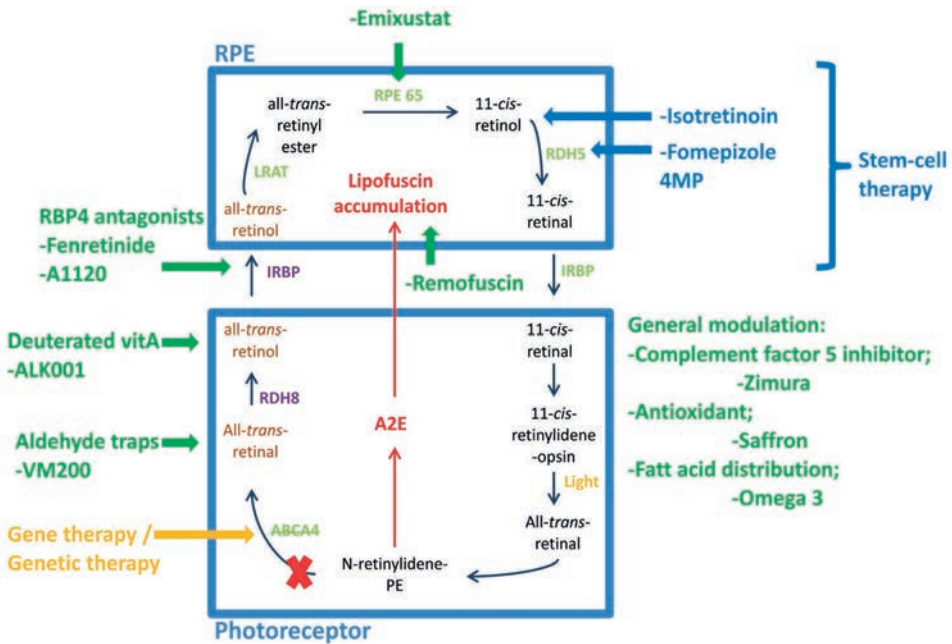


Figure 2: After Sears AE, Bernstein PS, Cideciyan AV, et al.[55]

**Gene therapy** aims to augment the mutated *ABCA4* gene, nevertheless the outcomes of a phase I/II trial are pending (SAR422459; ClinicalTrials.gov, Identifier: NCT01367444). However gene therapy is rapidly developing and more targeted techniques like CRISPR/CAS9-facilitated DNA editing and antisense oligonucleotides (AON)-based RNA modulation are potentially effective strategies targeting specific mutated regions of the *ABCA4* gene or RNA.

[Stem cell therapy](#) has been explored as an option to regenerate or replace damaged RPE cells. Stem cells can be derived from human embryonic stem cells (hESCs), induced pluripotent stem cells (iPSCs), and adult stem cells. Currently, stem cell therapy suggests potential biologic plausibility in a phase I/II trial. ClinicalTrials.gov Identifier: NCT01469832.

[Drug treatments](#) for STGD1 aim to reduce toxic bisretinoids and lipofuscin in the retina and retinal pigment epithelium (RPE). These agents include C20-D3-vitamin A (ALK-001), isotretinoin, VM200, emixustat, and A1120 [14, 56-63]. Avacincaptad pegol is a C5 complement inhibitor that may reduce inflammation-related RPE damage. Animal models of STGD1 show promising data for these treatments, although proof of efficacy in humans is lacking. Fenretinide and emixustat are visual cycle modulators for dry AMD and STGD1 that failed to halt geographic atrophy progression or improve vision in trials for AMD. A1120 prevents retinol transport into RPE and may spare side effects typically seen with VCMs (night blindness and chromatopsia).

All these treatment options offer biologically plausible treatments for STGD1. Further trials are warranted to assess efficacy and safety in humans.

### **My thoughts for the near future**

Investigation of knowledge of the metabolic dimensions critical to the pathogenesis of retinal dystrophies in general, is crucial. Further research of this topic needs attention. Suitable human eye-models may help, because most studies are now performed on rodents, that do not possess a macula. For instance primates, like Marmosets, or human donor eyes. Another future perspective on human eye-models might be *in vitro* retina models.

New imaging techniques, like adaptive optics and OCT-A may help to understand etiologic features like foveal sparing, all in order to elucidate the disease. Multimodal imaging studies are necessary to study the natural history and provide biomarkers to monitor the efficacy of treatment(s).

To determine efficacy of treatments, international cooperation is necessary to obtain cohorts of sufficient subjects. In the Netherlands the RD5000 database contains all clinical and essential genetic data of Dutch STGD1 cases [64]. In this system detailed standardized phenotyping is essential.

We have to be aware that STGD1 (but also other retinal dystrophies), is a rare disease. Collecting cohorts and information is essential to obtain detailed

information about e.g. the course of disease. However, selecting patients for therapeutical trials may be a problem. A well phenotyped study cohort is crucial to determine the effect of a treatment, but candidates are rare. Most of them are not eligible for clinical trials, because the disease is already too far progressed to measure any treatment effect. On the other hand, considering lots of upcoming and ongoing therapeutical trials, we have to be very selective which trial we select STGD1 patients for.

Hopefully, treatment will be available for STGD1 patients within 10 years, based on the latest developments. In the meantime, good counseling of STGD1 patients is crucial. Finally, it is also important to support patients to function optimally in their daily life.

## References

1. Blacharski, P., *Retinal dystrophies and degenerations*. Newsome DA (ed), 1988: p. 135-159.
2. Westeneng-van Haaften, S.C., et al., *Clinical and genetic characteristics of late-onset Stargardt's disease*. *Ophthalmology*, 2012. **119**(6): p. 1199-210.
3. Lambertus, S., et al., *Early-onset stargardt disease: phenotypic and genotypic characteristics*. *Ophthalmology*, 2015. **122**(2): p. 335-44.
4. Fujinami, K., et al., *Clinical and molecular characteristics of childhood-onset Stargardt disease*. *Ophthalmology*, 2015. **122**(2): p. 326-34.
5. Fujinami, K., et al., *Clinical and molecular analysis of Stargardt disease with preserved foveal structure and function*. *Am J Ophthalmol*, 2013. **156**(3): p. 487-501 e1.
6. Charbel Issa, P., et al., *Rescue of the Stargardt phenotype in Abca4 knockout mice through inhibition of vitamin A dimerization*. *Proc Natl Acad Sci U S A*, 2015. **112**(27): p. 8415-20.
7. McClements, M.E., et al., *An AAV Dual Vector Strategy Ameliorates the Stargardt Phenotype in Adult Abca4(-/-) Mice*. *Hum Gene Ther*, 2018.
8. Lambertus, S., et al., *Asymmetric Inter-Eye Progression in Stargardt Disease*. *Invest Ophthalmol Vis Sci*, 2016. **57**(15): p. 6824-6830.
9. Strauss, R.W., et al., *The Natural History of the Progression of Atrophy Secondary to Stargardt Disease (ProgStar) Studies: Design and Baseline Characteristics: ProgStar Report No. 1*. *Ophthalmology*, 2016. **123**(4): p. 817-28.
10. Kong, X., et al., *Visual Acuity Change Over 24 Months and Its Association With Foveal Phenotype and Genotype in Individuals With Stargardt Disease: ProgStar Study Report No. 10*. *JAMA Ophthalmol*, 2018. **136**(8): p. 920-928.
11. Sangermano, R., et al., *Deep-intronic ABCA4 variants explain missing heritability in Stargardt disease and allow correction of splice defects by antisense oligonucleotides*. *Genet Med*, 2019.
12. MacDonald, I.M. and P.A. Sieving, *Investigation of the effect of dietary docosahexaenoic acid (DHA) supplementation on macular function in subjects with autosomal recessive Stargardt macular dystrophy*. *Ophthalmic Genet*, 2018. **39**(4): p. 477-486.
13. Mehat, M.S., et al., *Transplantation of Human Embryonic Stem Cell-Derived Retinal Pigment Epithelial Cells in Macular Degeneration*. *Ophthalmology*, 2018. **125**(11): p. 1765-1775.
14. Saad, L. and I. Washington, *Can Vitamin A be Improved to Prevent Blindness due to Age-Related Macular Degeneration, Stargardt Disease and Other Retinal Dystrophies?* *Adv Exp Med Biol*, 2016. **854**: p. 355-61.
15. Khan, K.N., et al., *Early Patterns of Macular Degeneration in ABCA4-Associated Retinopathy*. *Ophthalmology*, 2018. **125**(5): p. 735-746.
16. Kong, X., et al., *Visual Acuity Change over 12 Months in the Prospective Progression of Atrophy Secondary to Stargardt Disease (ProgStar) Study: ProgStar Report Number 6*. *Ophthalmology*, 2017. **124**(11): p. 1640-1651.
17. Fujinami, K., et al., *Fine central macular dots associated with childhood-onset Stargardt Disease*. *Acta Ophthalmol*, 2014. **92**(2): p. e157-9.
18. Lee, W., et al., *The external limiting membrane in early-onset Stargardt disease*. *Invest Ophthalmol Vis Sci*, 2014. **55**(10): p. 6139-49.
19. Burke, T.R., et al., *Abnormality in the external limiting membrane in early Stargardt disease*. *Ophthalmic Genet*, 2013. **34**(1-2): p. 75-7.
20. Song, H., et al., *Cone and rod loss in Stargardt disease revealed by adaptive optics scanning light ophthalmoscopy*. *JAMA Ophthalmol*, 2015. **133**(10): p. 1198-203.
21. Razeen, M.M., et al., *Correlating Photoreceptor Mosaic Structure to Clinical Findings in Stargardt Disease*. *Transl Vis Sci Technol*, 2016. **5**(2): p. 6.

22. Tanna, P., et al., *Reliability and Repeatability of Cone Density Measurements in Patients With Stargardt Disease and RPGR-Associated Retinopathy*. Invest Ophthalmol Vis Sci, 2017. **58**(9): p. 3608-3615.
23. Garces, F., et al., *Correlating the Expression and Functional Activity of ABCA4 Disease Variants With the Phenotype of Patients With Stargardt Disease*. Invest Ophthalmol Vis Sci, 2018. **59**(6): p. 2305-2315.
24. Fakin, A., et al., *Phenotype and Progression of Retinal Degeneration Associated With Nullizigosity of ABCA4*. Invest Ophthalmol Vis Sci, 2016. **57**(11): p. 4668-78.
25. Chen, M., et al., *Multi-modal automatic montaging of adaptive optics retinal images*. Biomed Opt Express, 2016. **7**(12): p. 4899-4918.
26. Muller, P.L., et al., *Choroidal Flow Signal in Late-Onset Stargardt Disease and Age-Related Macular Degeneration: An OCT-Angiography Study*. Invest Ophthalmol Vis Sci, 2018. **59**(4): p. AMD122-AMD131.
27. Guduru, A., et al., *Comparative analysis of autofluorescence and OCT angiography in Stargardt disease*. Br J Ophthalmol, 2018. **102**(9): p. 1204-1207.
28. Zernant, J., et al., *Frequent hypomorphic alleles account for a significant fraction of ABCA4 disease and distinguish it from age-related macular degeneration*. J Med Genet, 2017. **54**(6): p. 404-412.
29. Runhart, E.H., et al., *The Common ABCA4 Variant p.Asn1868Ile Shows Nonpenetrance and Variable Expression of Stargardt Disease When Present in trans With Severe Variants*. Invest Ophthalmol Vis Sci, 2018. **59**(8): p. 3220-3231.
30. Bauwens, M., et al., *ABCA4-associated disease as a model for missing heritability in autosomal recessive disorders: novel noncoding splice, cis-regulatory, structural, and recurrent hypomorphic variants*. Genet Med, 2019.
31. Duane, A., *A Classification of Eye Diseases: With the Outline of a Universal Morbidity List Based on the Nomenclature of Diseases of the Royal College of Physicians, of London*. Trans Am Ophthalmol Soc, 1909. **12**(Pt 1): p. 31-61.
32. van Driel, M.A., et al., *ABCR unites what ophthalmologists divide(s)*. Ophthalmic Genet, 1998. **19**(3): p. 117-22.
33. Maugeri, A., et al., *The 2588G-->C mutation in the ABCR gene is a mild frequent founder mutation in the Western European population and allows the classification of ABCR mutations in patients with Stargardt disease*. Am J Hum Genet, 1999. **64**(4): p. 1024-35.
34. Fishman, G.A., et al., *Variation of clinical expression in patients with Stargardt dystrophy and sequence variations in the ABCR gene*. Arch Ophthalmol, 1999. **117**(4): p. 504-10.
35. Lois, N., et al., *Phenotypic subtypes of Stargardt macular dystrophy-fundus flavimaculatus*. Arch Ophthalmol, 2001. **119**(3): p. 359-69.
36. Hoyng C.B., L.S., Bax N.M. , *Macular dystrophies, Chapter 3, Stargardt disease*. 2016.
37. Allikmets, R., et al., *A photoreceptor cell-specific ATP-binding transporter gene (ABCR) is mutated in recessive Stargardt macular dystrophy*. Nat Genet, 1997. **15**(3): p. 236-46.
38. Lewis, R.A., et al., *Genotype/Phenotype analysis of a photoreceptor-specific ATP-binding cassette transporter gene, ABCR, in Stargardt disease*. Am J Hum Genet, 1999. **64**(2): p. 422-34.
39. Webster, A.R., et al., *An analysis of allelic variation in the ABCA4 gene*. Invest Ophthalmol Vis Sci, 2001. **42**(6): p. 1179-89.
40. Allikmets, R., J. Zernant, and W. Lee, *Penetrance of the ABCA4 p.Asn1868Ile Allele in Stargardt Disease*. Invest Ophthalmol Vis Sci, 2018. **59**(13): p. 5564-5565.
41. Cremers, F.P.M., et al., *Author Response: Penetrance of the ABCA4 p.Asn1868Ile Allele in Stargardt Disease*. Invest Ophthalmol Vis Sci, 2018. **59**(13): p. 5566-5568.
42. Braun, T.A., et al., *Non-exomic and synonymous variants in ABCA4 are an important cause of Stargardt disease*. Hum Mol Genet, 2013. **22**(25): p. 5136-45.
43. Bax, N.M., et al., *Heterozygous deep-intronic variants and deletions in ABCA4 in persons with retinal dystrophies and one exonic ABCA4 variant*. Hum Mutat, 2015. **36**(1): p. 43-7.



44. Bauwens, M., et al., *An augmented ABCA4 screen targeting noncoding regions reveals a deep intronic founder variant in Belgian Stargardt patients*. Hum Mutat, 2015. **36**(1): p. 39-42.
45. Albert, S., et al., *Identification and Rescue of Splice Defects Caused by Two Neighboring Deep-Intronic ABCA4 Mutations Underlying Stargardt Disease*. Am J Hum Genet, 2018. **102**(4): p. 517-527.
46. Weleber, R.G., et al., *Results at 2 Years after Gene Therapy for RPE65-Deficient Leber Congenital Amaurosis and Severe Early-Childhood-Onset Retinal Dystrophy*. Ophthalmology, 2016. **123**(7): p. 1606-20.
47. Brazier, J., J. Roberts, and M. Deverill, *The estimation of a preference-based measure of health from the SF-36*. J Health Econ, 2002. **21**(2): p. 271-92.
48. Craig, B.M., et al., *US valuation of the SF-6D*. Med Decis Making, 2013. **33**(6): p. 793-803.
49. Rentz, A.M., et al., *Development of a preference-based index from the National Eye Institute Visual Function Questionnaire-25*. JAMA Ophthalmol, 2014. **132**(3): p. 310-8.
50. Whitehead, S.J. and S. Ali, *Health outcomes in economic evaluation: the QALY and utilities*. Br Med Bull, 2010. **96**: p. 5-21.
51. Rovner, B.W. and R.J. Casten, *Activity loss and depression in age-related macular degeneration*. Am J Geriatr Psychiatry, 2002. **10**(3): p. 305-10.
52. Brody, B.L., et al., *Depression, visual acuity, comorbidity, and disability associated with age-related macular degeneration*. Ophthalmology, 2001. **108**(10): p. 1893-900; discussion 1900-1.
53. Horowitz, A., J.P. Reinhardt, and G.J. Kennedy, *Major and subthreshold depression among older adults seeking vision rehabilitation services*. Am J Geriatr Psychiatry, 2005. **13**(3): p. 180-7.
54. K., S., *Über familiäre Degeneration in der Makulagegend des Auges mit und ohne psychischen Störungen*. Arch f Psych und Nervenkr, 1917(58): p. 852-887.
55. Sears, A.E., et al., *Towards Treatment of Stargardt Disease: Workshop Organized and Sponsored by the Foundation Fighting Blindness*. Transl Vis Sci Technol, 2017. **6**(5): p. 6.
56. Kaufman, Y., L. Ma, and I. Washington, *Deuterium enrichment of vitamin A at the C20 position slows the formation of detrimental vitamin A dimers in wild-type rodents*. J Biol Chem, 2011. **286**(10): p. 7958-65.
57. Radu, R.A., et al., *Treatment with isotretinoin inhibits lipofuscin accumulation in a mouse model of recessive Stargardt's macular degeneration*. Proc Natl Acad Sci U S A, 2003. **100**(8): p. 4742-7.
58. Maeda, A., et al., *Primary amines protect against retinal degeneration in mouse models of retinopathies*. Nat Chem Biol, 2011. **8**(2): p. 170-8.
59. Yehoshua, Z., et al., *Systemic complement inhibition with eculizumab for geographic atrophy in age-related macular degeneration: the COMPLETE study*. Ophthalmology, 2014. **121**(3): p. 693-701.
60. Dugel, P.U., et al., *Phase ii, randomized, placebo-controlled, 90-day study of emixustat hydrochloride in geographic atrophy associated with dry age-related macular degeneration*. Retina, 2015. **35**(6): p. 1173-83.
61. Kong, J., et al., *Correction of the disease phenotype in the mouse model of Stargardt disease by lentiviral gene therapy*. Gene Ther, 2008. **15**(19): p. 1311-20.
62. Kubota, R., et al., *Safety and effect on rod function of ACU-4429, a novel small-molecule visual cycle modulator*. Retina, 2012. **32**(1): p. 183-8.
63. Dobri, N., et al., *A1120, a nonretinoid RBP4 antagonist, inhibits formation of cytotoxic bisretinoids in the animal model of enhanced retinal lipofuscinogenesis*. Invest Ophthalmol Vis Sci, 2013. **54**(1): p. 85-95.
64. van Huet, R.A., et al., *The RD5000 database: facilitating clinical, genetic, and therapeutic studies on inherited retinal diseases*. Invest Ophthalmol Vis Sci, 2014. **55**(11): p. 7355-60.





# CHAPTER 6

## Epilogue

**Summary**

**Samenvatting**

**List of publications**

**PhD portfolio**

**Curriculum Vitae**

**Acknowledgements/ Dankwoord**

## SUMMARY

This thesis contains studies on clinical, genetic and psychological characteristics of Stargardt disease (STGD1). The general introduction in **Chapter 1** provides information about the retina, retinal dystrophies, and an overview of all aspects of STGD1. At the end of the introduction, I summarize the aims of this thesis.

Clinical characteristics of STGD1 are described in **Chapter 2**. This chapter contains several studies on different subtypes of STGD1:

**Chapter 2.1** gives a detailed description of early-onset STGD1 patients. In its natural course, early-onset STGD1 initially presents with variable full-field electro-retinographic abnormalities and fundusoscopic findings. As this retinal degeneration progresses, the spectrum of phenotypes eventually converges, causing profound chorioretinal atrophy and severe vision loss. Thus, early-onset STGD1 lies at the severe end of the spectrum of *ABCA4*-associated retinal phenotypes.

We notice in early-onset STGD1 patients a delay of diagnosis, because they initially present without fundus abnormalities. Therefore, we analyzed this group of patients in **Chapter 2.2**. A lack of obvious fundus abnormalities left an alarming number of children with STGD1 without the correct diagnosis. We propose that greater awareness of this subtype avoids misdiagnosis and years of inappropriate treatment.

In **Chapter 2.3** I switch to late-onset STGD1. A typical phenotype in late-onset STGD1 patients is called “foveal sparing”. In this chapter, we provide a detailed description of our clinical findings in this interesting vision-preserving retinal phenomenon, which mainly occurs in patients with late-onset STGD1 and characterizes the mild end of the clinical variations in STGD1. Long-term follow-up data provided insights in the natural course of foveal sparing. Although the etiology is unclear, we hypothesize on possible underlying factors.

The intriguing phenomenon of foveal sparing is not only a feature in late-onset STGD1. In several other retinal dystrophies, like central areolar choroidal dystrophy (CACD), mitochondrial retinal dystrophy (MRD), and pseudo-Stargardt pattern dystrophy (PSPD), foveal sparing is noticed.

In **Chapter 2.4**, we provide a detailed description of our clinical findings in these distinct retinal dystrophy patients with a clearly recognizable foveal sparing

phenotype. Long-term follow-up data provided insights into the natural course of foveal sparing. The presence of foveal sparing in retinal dystrophies with distinctly different underlying mechanisms suggests a disease-independent mechanism that prolongs the survival of the fovea. The associated preservation of visual acuity is important for the individual prognosis and has implications for the design of future therapeutic trials for inherited retinal disease.

**Chapter 2.5** presents the results of our study in asymmetry in disease progression between left and right eyes in STGD1 patients. Asymmetric inter-eye progression in STGD1 is most likely observed in patients with a later disease onset and patients carrying combinations of *ABCA4* variants that only partially affect *ABCA4* function. This needs to be considered in novel therapeutic trials with a fellow-eye paired controlled design to optimize the power of a study.

Studies on identification, registry and functional assessment of *ABCA4* variants are provided in **Chapter 3**. The clinical outcome in STGD1 depends on the severity of two *ABCA4* variants. To provide an accurate prognosis and to select patients for novel treatments, it is important to assess the functional significance of non-truncating *ABCA4* variants. All published *ABCA4* variants were collected in a Leiden Open (source) Variant Database (LOVD) in **Chapter 3.1**. *In silico* meta-analysis of 5,962 variants in 3,928 *ABCA4*-associated retinal dystrophy cases was performed, which allowed us to predict the functional effects. Based on their prevalence in patients vs controls, we hypothesized that five variants (c.2588G>C; p.[Gly863Ala, Gly863del], c.5882G>A; p.(Gly1961Glu), c.3113C>T; p.(Ala1038Val), c.5714+5G>A; p.[=, Glu1863Leufs\*33] (Cornelis et al 2016, Sangermano et al 2017), and c.6089G>A; p.(Arg2030Gln)) act as mild alleles. These studies will facilitate the pathogenicity assessment of variants with unknown significance found in diagnostics.

In **Chapter 3.2** we investigated the presence of five deep-intronic *ABCA4* variants identified previously by Braun et al. (2013). We analyzed 45 maculopathy cases with one causal *ABCA4* variant for the presence of these deep-intronic variants, and in addition tested a subset of these patients for the presence of heterozygous deletions encompassing one or several exons. In this way we found six probands with heterozygous deep-intronic mutations, two probands with sizeable heterozygous deletions, and one proband with a heterozygous deep-intronic mutation and a sizeable deletion. As antisense oligonucleotide-based therapies are being development, patients with deep-intronic variants are eligible for this novel treatment.

Furthermore, **Chapter 3.3** aimed to elucidate the functional effect of the *ABCA4* variant c.5461-10T>C, one of the most frequent variants associated with STGD1. Splice site strength prediction programs predicted a very small effect of this variant on the splicing of exon 39. This variant is located on a 'founder' haplotype lacking other disease-causing rare sequence variants. Employing patient-derived photoreceptor progenitor cells, we found mRNA exon(s) 39 or 39/40 skipping and predicted *ABCA4* protein truncation if the mutant RNA escapes nonsense-mediated decay. Given the severe phenotype in persons homozygous for this variant, we concluded that this variant results in the absence of *ABCA4* activity. This work not only sheds light on the significance of this frequent variant, but also serves as an excellent example for the study and classification of similar non-canonical splice site variants with unknown effects on splicing.

Currently, quality of life is determined as a significant outcome for measuring the impact of disease, and for estimating the efficacy of treatment. With upcoming therapies in STGD1, we provide in **Chapter 4** a research of quality of life in STGD1 patients. We used three questionnaires to provide information on demographics, general quality of life, and vision-specific quality of life. In general, STGD1 patients, as present in our study, perceive good general quality of life, but serious vision-related impairments. This suggests a large potential of health gain by innovative interventions to treat STGD1 patients.

A general discussion on clinical, genetics and psychological characteristics in patients with STGD1 is given in **Chapter 5**.

## SAMENVATTING

Dit proefschrift bevat onderzoek naar de klinische, genetische en psychologische aspecten van de ziekte van Stargardt (STGD1). Het eerste hoofdstuk bevat de inleiding van het proefschrift. Het beschrijft de bouw en functie van het netvlies, erfelijke netvlies aandoeningen, en de klinische, genetische en psychologische aspecten van STGD1. Tenslotte worden de leerdoelen van dit werk benoemd. Het proefschrift is opgedeeld in drie delen (Hoofdstukken 2, 3 en 4) met ieder zijn eigen aandachtsgebied.

**Hoofdstuk 2** bevat verschillende studies naar de verschillende subtypen binnen STGD1:

**Hoofdstuk 2.1** geeft een uitgebreide beschrijving van het vroeg optredende STGD1 type. Er is een groot verschil in fundoscopische afwijkingen tussen kinderen bij eerste klinische presentatie. Maar als de ziekte verder vordert, dan vormt het zich meer een duidelijk fenotype dat zich presenteert als centrale chorioretinale atrofie leidend tot ernstig visus verlies. Wij scharen daarom het vroeg optredende fenotype tot een ernstige vorm binnen het *ABCA4*-geassocieerde spectrum.

STGD1 patiënten waarbij de ziekte zich al vroeg openbaart krijgen vaak de diagnose pas laat gesteld, ondanks dat zij soms al jaren visuele klachten hadden. Bij hen werden in eerste instantie geen fundoscopische afwijkingen waargenomen. Daarom hebben wij deze groep patiënten bestudeerd en de resultaten zijn te vinden in **Hoofdstuk 2.2**. Wij hopen dat door middel van een groter bewustzijn van dit subtype binnen STGD1 het aantal verkeerde diagnoses en jaren van inadequate behandeling kan worden vermeden.

In **Hoofdstuk 2.3** maak ik de switch naar laat optredende STGD1. Een typisch kenmerk binnen de laat optredende STGD1 patiënten is “foveal sparing”. In dit hoofdstuk worden de klinische bevindingen en natuurlijk beloop beschreven van dit interessante fenomeen. Ondanks dat de etiologie van foveal sparing (nog) onbekend is, doen wij hierin wel een aantal hypothesen over mogelijke onderliggende factoren.

Het fenomeen foveal sparing wordt niet alleen in (laat optredende) STGD1 gezien, maar ook in een aantal andere retinale dystrofieën, zoals: centrale areolaire choroidale dystrofie (CACD), mitochondriële retinale dystrofie (MRD) en pseudo-Stargardt patroon dystrofie (PSPD).

In **Hoofdstuk 2.4** beschrijven wij uitgebreid de overeenkomsten en verschillen



tussen de verscheidene aandoeningen met foveal sparing om zo een beter beeld te krijgen van het natuurlijk beloop van de aandoening. Aangezien foveal sparing in verschillende retinale dystrofieën voor komt suggereert dat er een onafhankelijke onderliggende factor of mechanisme is, welke er voor zorgt dat juist de fovea gespaard blijft. Het daarmee samenhangende resterend gezichtsvermogen is belangrijk voor de patiënt, maar kan mogelijk ook een rol spelen in toekomstige mogelijkheden voor therapie bij retinale dystrofieën.

In **Hoofdstuk 2.5** wordt onze studie ten aanzien van asymmetrie in ziekte progressie tussen het linker en rechter oog van de STGD1 patiënten beschreven. Asymmetrie van ogen zien we met name bij patiënten die STGD1 op een latere leeftijd ontwikkelen, of bij degenen die een combinatie van *ABCA4* varianten dragen die maar deels de *ABCA4* functie beïnvloeden. Dat er asymmetrie tussen ogen is van eenzelfde patiënt is een belangrijk gegeven bij mogelijke therapieën die in trials worden geëvalueerd, want dit kan de uitkomsten beïnvloeden, dus een goede selectie van patiënten in trials is essentieel en asymmetrie tussen ogen kan dus een exclusie criteria zijn.

Studies ten aanzien van het identificeren, registeren en functioneel testen van *ABCA4* varianten worden weergegeven in **Hoofdstuk 3**. De ernst van de aandoening correleert met de ernst van de twee *ABCA4* varianten. Om een juiste prognose te kunnen stellen en om patiënten te kunnen selecteren voor klinische trials, is het belangrijk om de functionele significantie van *ABCA4* varianten te bepalen die niet leiden tot een premature translatie stop. Alle gepubliceerde *ABCA4* varianten werden verzameld en ingevoerd en de “Leiden Open (source) Variant Database (LOVD)”. De resultaten zijn te lezen in **Hoofdstuk 3.1**. *In silico* meta-analyse van 5,962 varianten in 3,928 *ABCA4*-geassocieerde retinale dystrofie patiënten werd verricht, waardoor wij het functionele effect konden voorspellen. Wij konden hieruit afleiden dat 5 varianten (c.2588G>C; p.[Gly863Ala, Gly863del], c.5882G>A; p.(Gly1961Glu), c.3113C>T; p.(Ala1038Val), c.5714+5G>A; p.[=, Glu1863Leufs\*33] (Cornelis e.a. 2016, Sangermano e.a. 2017) en c.6089G>A; p.(Arg2030Gln)) zich als een milde variant voordoen, gebaseerd op de prevalentie van deze varianten in STGD1 patiënten ten opzichte van niet-aangedane personen. Deze studies geven handvaten om de geschatte pathogeniciteit te voorspellen van *ABCA4* varianten die in DNA diagnostiek gevonden worden met een onduidelijke betekenis.

In **Hoofdstuk 3.2** onderzochten wij de aanwezigheid van vijf diep-intronische *ABCA4* varianten, die eerder werden beschreven door Braun e.a. (2013) bij 45 patiënten met een maculopathie waarbij maar één oorzakelijke *ABCA4* variant bekend was. Tevens werd gekeken naar de aanwezigheid van heterozygote deleties die één

of meerdere exonen omvatten. Op deze manier vonden wij zes probanden met een heterozygote diep-intronische mutatie, twee probanden met heterozygote deleties en één proband met een heterozygote diep-intronische mutatie en een heterozygote deletie. Wanneer op antisense oligonucleotide gebaseerde therapieën beschikbaar komen, dan zijn de patiënten met diep-intronische varianten zeer geschikt voor deze therapie.

In **Hoofdstuk 3.3** wordt het functionele effect van c.5461-10T>C, één van de meest voorkomende *ABCA4* varianten, beschreven. Predictie programma's voorspelden een klein effect op de inclusie van exon 39 in het mRNA. Door de toepassing van 'patient-derived photoreceptor progenitor cells' vonden we dat exon(en) 39 of 39/40 in het mRNA werden overgeslagen, waardoor er een korter voorspeld *ABCA4* eiwit wordt gemaakt, vooropgesteld dat het mutante mRNA niet wordt afgebroken door 'nonsense-mediated decay'. De patiënten bij wie deze variant homozygoot aanwezig was, hadden een zeer ernstig fenotype. Wij concludeerden dat deze variant resulteert in de afwezigheid van *ABCA4* activiteit. Deze studie beschrijft niet alleen de significantie van deze veelvoorkomende variant, maar is ook een goed voorbeeld voor het onderzoeken en classificeren van vergelijkbare varianten in de splice site consensus sequenties met een nog onbekend effect op de splicing.

In **Hoofdstuk 4** stappen wij over van de genetica naar de kwaliteit van leven van STGD1 patiënten. Momenteel wordt kwaliteit van leven als een significante parameter gebruikt om de impact van de ziekte en de effectiviteit van een mogelijke therapie te meten. Wij hebben drie vragenlijsten gebruikt om de algemene patiënt karakteristieken, de algemene kwaliteit van leven en de ziekte specifieke kwaliteit van leven te meten. In het algemeen ervaren STGD1 patiënten een goede algemene kwaliteit van leven, maar ondervinden zij wel veel hinder van hun visuele handicap. Deze uitkomst geeft aan dat er veel gezondheidswinst te behalen is als STGD1 patiënten kunnen worden behandeld voor hun visuele handicap.

Het manuscript wordt afgesloten met een algemene discussie, waarin klinische, genetische en psychologische aspecten bij STGD1 uiteengezet worden in **Hoofdstuk 5**.

## LIST OF PUBLICATIONS

### *Publications related to this thesis:*

#### **“Early-onset Stargardt disease”**

Stanley Lambertus, Ramon A.C. van Huet, *Nathalie M. Bax*, Lies H. Hoefsloot, Frans P.M. Cremers, Camiel J.F. Boon, B. Jeroen Klevering, and Carel B. Hoyng.  
Ophthalmology, 2015;122(2):335-44

#### **“The absence of fundus abnormalities in Stargardt disease”**

*Nathalie M. Bax*, Stanley Lambertus, Frans P.M. Cremers, B. Jeroen Klevering, and Carel B. Hoyng.  
Graefe’s Archive for Clinical and Experimental Ophthalmology, 2019;257(6):1147-1157

#### **“Foveal sparing in Stargardt disease”**

Ramon A.C. van Huet\*, *Nathalie M. Bax\**, S. Carla Westeneng-Van Haften, Muhamed Muhamed, Marijke N. Zonneveld-Vrieling, Lies H. Hoefsloot, Frans P.M. Cremers, Camiel J.F. Boon, B. Jeroen Klevering, and Carel B. Hoyng.  
Investigative Ophthalmology and Visual Science 2014;55(11):7467-78  
\*Shared first authors

#### **“Foveal sparing in retinal dystrophies”**

*Nathalie M. Bax*, Dyon Valkenburg, Stanley Lambertus, B. Jeroen Klevering, Camiel J.F. Boon, Frank G Holz, Frans P.M. Cremers, Monika Fleckenstein, Moritz Lindner\*, and Carel B. Hoyng\*.  
Investigative ophthalmology and Visual Science, In press  
\*Shared last authors

#### **“Asymmetric inter-eye progression in Stargardt disease”**

Stanley Lambertus, *Nathalie M. Bax*, Joannes M.M. Groenewoud, Frans P.M. Cremers, Gert Jan van der Wilt, B. Jeroen Klevering, Thomas Theelen, and Carel B. Hoyng.  
Investigative Ophthalmology and Visual Science 2016;57(15):6824-6830

#### **“In silico functional meta-analysis of 5,962 ABCA4 variants in 3,928 retinal dystrophy cases.”**

Stéphanie S. Cornelis, *Nathalie M. Bax*, Jana Zernant, Rando Allikmets, Lars G. Fritsche, Johan T. den Dunnen, M. Ajmal, Carel B. Hoyng, and Frans P.M. Cremers.  
Human Mutation, 2017;38(4):400-408

#### **“ Heterozygous deep-intronic variants and deletions in ABCA4 in persons with retinal dystrophies and one exonic ABCA4 variant.”**

*Nathalie M. Bax\**, Riccardo Sangermano\*, Susanne Roosing\*, Alberta A. Thiadens, Lies H. Hoefsloot, L. Ingeborgh van den Born, Milan Phan, B. Jeroen Klevering, S. Carla Westeneng-van Haften, Terry A. Braun, Marijke N. Zonneveld-Vrieling, Ilse J. de Wijs, Merve Mutlu, Ed M. Stone, Anneke I. den Hollander, Caroline C.W. Klaver, Carel B. Hoyng, and Frans P.M. Cremers.  
Human mutation 2015;36(1):43-7  
\*Shared first authors

**“Photoreceptor progenitor mRNA analysis reveals exon skipping resulting from the ABCA4 c.5461-10T → C mutation in Stargardt disease.”**

Riccardo Sangermano, *Nathalie M. Bax*, Miriam Bauwens, L. Ingeborgh van den Born, Elfride de Baere, Alex Garanto, Rob W. Collin, AS Goercharn-Ramlal, AH den Engelsman-van Dijk, Karl Rohrschneider, Carel B. Hoyng, Frans P.M. Cremers, and Silvia Albert. *Ophthalmology*, 2016;123(6):1375-85

**“Quality of life in Stargardt patients.”**

*Nathalie M. Bax*, Stanley Lambertus, B. Jeroen Klevering, Chris M. Verhaak, and Carel B. Hoyng. Submitted for publication

**Other publications:**

**“Stargardt disease”**

Carel B. Hoyng, Stanley Lambertus, and *Nathalie M. Bax*

“Macular Dystrophies”, Chapter 3, pages 25-30, Editors: Giuseppe Querques, Eric H. Souied, 2016

**“Non-syndromic retinitis pigmentosa due to mutations in the mucopolysaccharidosis type IIIC gene, heparan-alpha-glucosaminide N-acetyltransferase (HGSNAT).”**

Haer-Wigman L, Newman H\*, Leibur R\*, *Bax NM\**, Baris HN, Rizel L, Banin E, Massarweh A, Roosing S, Lefeber DJ, Zonneveld-Vrieling MN, Isakov O, Shomron N, Sharon D, Den Hollander AI, Hoyng CB, Cremers FP, Ben-Yosef T. *Human Molecular Genetics*, 2015;24(13):3742-51

\*Shared second authors.

**“Mutations in the polyglutamylase gene TLL5, expressed in photoreceptor cells and spermatozoa, are associated with cone-rod degeneration and reduced male fertility.”**

Bedoni N, Haer-Wigman L, Vaclavik V, Tran VH, Farinelli P, Balzano S, Royer-Bertrand B, El-Asrag ME, Bonny O, Ikonomidis C, Litzistorf Y, Nikopoulos K, Yioti GG, Stefanidou MI, McKibbin M, Booth AP, Ellingford JM, Black GC, Toomes C, Inglehearn CF, Hoyng CB, *Bax N*, Klaver CC, Thiadens AA, Murisier F, Schorderet DF, Ali M, Cremers FP, Andréasson S, Munier FL, Rivolta C.

*Human Molecular Genetics*, 2016;25(20):4546-4555

**“Progression of late-onset Stargardt disease.”**

Lambertus S, Lindner M, *Bax NM*, Mauschitz MM, Nadal J, Schmid M, Schmitz-Valckenberg S, den Hollander AI, Weber BH, Holz FG, van der Wilt GJ, Fleckenstein M, Hoyng CB; Foveal sparing Atrophy Study Team (FAST).

*Investigative Ophthalmology and Visual Science*, 2016;57(13):5186-5191

**“Differential disease progression in atrophic age-related macular degeneration and late-onset Stargardt disease.”**

Lindner M, Lambertus S, Mauschitz MM, *Bax NM*, Kersten E, Lünig A, Nadal J, Schmitz-Valckenberg S, Schmid M, Holz FG, Hoyng CB, Fleckenstein M; Foveal sparing Atrophy Study Team (FAST).

*Investigative Ophthalmology and Visual Science*, 2017;58(2):1001-1007

**“Highly sensitive measurements of disease progression in rare disorders: Developing and validating a multimodal model of retinal degeneration in Stargardt disease.”**

Lambertus S, *Bax NM*, Fakin A, Groenewoud JM, Klevering BJ, Moore AT, Michaelides M, Webster AR, Van der Wilt GJ, Hoyng CB.

Plos One, 2017;12(3):e0174020

**“Antisense oligonucleotide-based splicing correction in individuals with Leber congenital amaurosis due to compound heterozygosity for the c.2991+1655A>G mutation in CEP290.”**

Duijkers L., Van den Born L.I., Neidhardt J., *Bax N.M.*, Pierrache L.H.M., Klevering B.J., Collin R.W.J., Garanto A.

International Journal of Molecular Sciences, 2018;19(3). pii: E753.

**“Identification and rescue of splice defects caused by two neighboring deep-intronic ABCA4 mutations underlying Stargardt disease.”**

Albert S., Garanto A., Sangermano R., Khan M., *Bax N.M.*, Hoyng C.B., Zernant J., Lee W., Allikmets R., Collin R.W.J., Cremers F.P.M.

American Journal of Human Genetics, 2018;102(4):517-527

**“The common ABCA4 variant p.Asn1868Ile shows nonpenetrance and variable expression of Stargardt disease when present in trans with severe variants.”**

Runhart EH\*, Sangermano R\*, Cornelis SS, Verheij JBG, Plomp AS, Boon CJF, Lugtenberg D, Roosing S, *Bax NM*, Blokland EAW, Camps-Jacobs M, Van der Velde-Visser SD, Pott JWR, Rohrschneider K, Thiadens A, Klaver C, Van den Born LI, Hoyng C, Cremers FPM\*shared first authors

Investigative Ophthalmology and Visual Science, 2018;59(8):3220-3231

**“Deep-intronic ABCA4 variants explain missing heritability in Stargardt disease and allow correction of splice defects by antisense oligonucleotides.”**

Riccardo Sangermano, Alejandro Garanto, Mubeen Khan, Esmee H. Runhart, Miriam Bauwens, *Nathalie M. Bax*, L. Ingeborgh van den Born, Muhammad Imran Khan, Joke B.G.M. Verheij, Jan-Willem R. Pott, Alberta A.H.J. Thiadens, Caroline C.W. Klaver, Bernard Puech, Isabelle Meunier, Sarah Naessens, Ellen A.W. Blokland, Duaa M. Elmelik, Gavin Arno, Ana Fakin, Keren J. Carss, F. Lucy Raymond, Andrew R. Webster, Claire-Marie Dhaenens, Heidi Stöhr, Felix Grassmann, Bernhard H.F. Weber, Carel B. Hoyng, Elfride De Baere, Silvia Albert, Rob W.J. Collin, and Frans P.M. Cremers

Genetics in Medicine, 2019 Jan 15. doi: 10.1038/s41436-018-0414-9. [Epub ahead of print]

**“Highly variable disease courses in siblings with Stargardt disease.”**

Dyon Valkenburg, Esmee Runhart, *Nathalie Bax*, Bart Liefers, Stanley Lambertus, Clara I Sánchez, Frans PM Cremers, Carel B. Hoyng.

Ophthalmology, In Press

**“Late-onset Stargardt disease due to mild deep-intronic ABCA4 alleles.”**

Esmee Runhart, Dyon Valkenburg, Stéphanie Cornelis, Mubeen Khan, Riccardo Sangermano, Silvia Albert, *Nathalie Bax*, Galuh Astuti, Christian Gilissen, Jan Willem Pott, Joke Verheij, Ellen Blokland, Frans Cremers, Ingeborgh van den Born, and Carel Hoyng.

Submitted for publication

**“The RD5000 Database: Facilitating Clinical, Genetic, and Therapeutic Studies on Inherited Retinal Diseases.”**

Ramon A.C. van Huet, Clasien J. Oomen, Astrid S. Plomp, Maria M. van Genderen, B. Jeroen Klevering, Reinier O. Schlingemann, Caroline C.W. Klaver, L. Ingeborgh van den Born, Frans P.M. Cremers, and the RD5000 Study Group

*Members of the RD5000 Study Group:*

Nathalie M. Bax, Carel B. Hoyng, Stanley Lambertus, Wendy A. van Zelst-Stams, Arthur A. B. Bergen, José Schuil, Mary J. van Schooneveld, Laurence Pierrache, Magda A. Meester-Smoor, Camiel J. F. Boon, Jan Willem R. Pott, Redmer van Leeuwen, Hester Y. Kroes, Yvonne de Jong-Hesse, and F. Nienke Boonstra.

*Investigative Ophthalmology and Visual Science, 2014;55(11):7355-60.*

**“Development of Refractive Errors-What Can We Learn From Inherited Retinal Dystrophies?”**

Michelle Hendriks, Virginie J.M. Verhoeven, Gabriëlle H.S. Buitendijk, Jan Roelof Polling, Magda A. Meester-Smoor, Albert Hofman, RD5000 Consortium, Maarten Kamermans, L. Ingeborgh van den Born, Caroline C.W. Klaver

*Members of the RD5000 Consortium:*

Nathalie M. Bax, Carel B. Hoyng, Stanley Lambertus, Wendy A. van Zelst-Stams, Arthur A. B. Bergen, José Schuil, Mary J. van Schooneveld, Laurence Pierrache, Magda A. Meester-Smoor, Camiel J. F. Boon, Jan Willem R. Pott, Redmer van Leeuwen, Hester Y. Kroes, Yvonne de Jong-Hesse, and F. Nienke Boonstra. \* *shared first authors; † contributed equally.*

*American Journal of Ophthalmology, 2017;182:81-89.*

**Abstract on Stargardt disease, Orphanet**

[http://www.orpha.net/consor/cgi-bin/OC\\_Exp.php?lng=EN&Expert=827](http://www.orpha.net/consor/cgi-bin/OC_Exp.php?lng=EN&Expert=827)

## PhD PORTFOLIO

Name PhD candidate: Nathalie Martine Bax Department: Department of Ophthalmology Graduate school: Radboud Institute for Health Sciences (RIHS)	PhD period: 1-5-2013 to 15-6-2016 Promotors: Prof. dr. C.B. Hoyng Prof. dr. F.P.M. Cremers	
	Year(s)	ECTS
<b>TRAINING ACTIVITIES</b>		
<b>Courses &amp; Workshops</b>		
RUNMC introduction course for PhD students	2013	0.5
How to write a medical scientific paper	2013	0.2
Basiscursus Regelgeving en Organisatie voor Klinisch onderzoekers (BROK)	2013	1.25
How to prepare your poster presentation	2013	0.2
Endnote	2014	0.2
Stress management	2014	0.2
NIHES EWP Survival analysis for Clinicians	2014	1.8
SPSS	2014	0.2
Certificate in Advanced English, Radboud in'to Languages	2014-2015	3.0
Art of presenting science, Artesc course	2015	1.5
Academic writing	2015	3.0
LEGO Serious Play	2015	0.2
Scientific writing: A-Z	2015	0.2
Adobe InDesign and Illustrator workshop	2015	0.4
Personal Team role profile	2016	0.2
Basics of networking	2016	0.2
How to write a medical scientific abstract	2016	0.2
Mindfulness for PhD students	2016	2.0
Applying visual electrophysiology for clinical evaluation and vision research	2016	0.4
Dissertation first aid: How to prepare and print your thesis	2016	0.1
<b>Seminars &amp; Lectures</b>		
Radboud Research Round Sensory Disorders (n=5) <sup>#</sup>	2014-2016	0.75
Ophthalmology referring evenings (n=6) <sup>#</sup>	2013-2016	0.6
PhD defences (n=6)	2013-2016	0.6
Orations (n=2)	2015-2016	0.2
An editor's perspective on scientific publishing	2016	0.1
Donders Lecture John O'Keefe	2016	0.1
<b>Symposia &amp; Conferences</b>		
Novel therapies for inherited retinal dystrophies	2014	0.25
Macula Symposium Rotterdam	2014	0.25
Nederlands Oogheelkundig Gezelschap conference (n=1)	2014	0.25
International DOG-symposium AMD, Baden-Baden	2015	1.0
Juvenile Macular Dystrophy symposium	2013, 2015	0.5
Publieksavond 'Therapie in Zicht'	2015	0.1
OOG/ZOG (n=3) <sup>#</sup>	2013-2015	0.3
Association for Research in Vision and Ophthalmology Annual Meeting (ARVO) (n=3) <sup>***</sup>	2014-2016	4.5
Dutch Ophthalmology PhD Students conference (n=3) <sup>###</sup>	2014-2016	1.5
Medische retina en imaging symposium, Nijmegen	2016	0.25
<b>Other</b>		
RD5000 database development/ meetings	2013-2016	0.75
Taskforce genetic therapy meetings	2014-2015	0.6
Open Dag Blindheidsonderzoek	2014	0.2
Open Dag Radboudumc	2015	0.2

**TEACHING ACTIVITIES (LECTURING, SUPERVISION AND OTHER)**

DNA Diagnostiek Oogheelkunde	2013-2015	30.0
Organisatie Publieksdag "Juvenile Macula Degeneratie"	2013 en 2015	4.0
Documentaire film "Met het oog op morgen"	2014	1.0
Organisatie Open dag Blindheidsonderzoek "Waarom ziet Arco slecht?"	2014	2.0
Supervision research internship Master students Medicine	2014-2016	1.5
Consultant Gene therapy (Sanofi)	2014-2016	1.0
Education Bachelor students	2015	0.25
50+ Beurs - Education patients	2015	0.5
Scientific publication reviews (n=3)	2015-2016	0.3
"Onderzoeker in de klas" wetenschapseducatie voor basisonderwijs	2016	0.6
<b>TOTAL</b>		<b>70.1 ECTS</b>

# Oral presentation; \* Poster presentation

1 ECTS (European Credit Transfer System) equals a workload of 28 hours



## CURRICULUM VITAE



Nathalie Martine Bax was born on May 14th, 1984 in Gouda, The Netherlands. In 2002, she graduated from secondary school at the “Coornhert Gymnasium” in Gouda, and started her medical training at the Erasmus University in Rotterdam.

Her interest in research and foreign countries was combined when writing her master thesis. For her thesis entitled ‘Genotype and phenotype correlation studies in epilepsy syndromes in children’, she participated in a research project at the Department of Pediatrics in Siena, Italy.

After finishing her medical study in 2010, she worked for 2 years as a resident at the Intensive Care Unit of the Albert Schweitzer hospital in Dordrecht, followed by a residency in Surgery and Orthopedics at the “Havenziekenhuis” in Rotterdam.

In May 2013, she joined the research group of prof. dr. C.B. Hoyng and started her PhD project on Stargardt disease at the Department of Ophthalmology in the Radboudumc in Nijmegen. Her research results are presented in this thesis.

In September 2016, she started her residency in Ophthalmology at the same institute under the supervision of prof. dr. J.E.E. Keunen and prof. dr. B.J. Klevering.

## ACKNOWLEDGEMENTS/ DANKWOORD

Toen ik een jaar of 8 was, won ik mijn eerste zwemwedstrijd. Ik keek erg uit naar de prijsuitreiking: Wat zou mijn prijs zijn? Een beker, of een gouden medaille? Ik hoopte op een mooie kampioensbeker. Helaas voor mij had men dat jaar wat anders verzonnen. Het waren de jaren '90 en "de smiley" vierde zijn hoogtijdagen. Ik kreeg dan ook een grote kartonnen smiley met daarop de tekst "nummer één word je nooit alleen". Destijds was ik teleurgesteld dat ik geen gouden medaille of beker won, maar een rond, geel karton. En waarom had ik het niet alleen gedaan? Wie had mij dan geholpen tijdens het zwemmen? Nooit gedacht dat ik als volwassen vrouw aan juist dit moment terug heb moeten denken tijdens mijn promotie. Want ondertussen weet ik: je doet het niet alleen en je kan het niet alleen. En daarin spelen sommige mensen een grote rol, sommigen een bijrol en/of ondersteunende rol, maar ieder met een aandeel. Daarom wil ik hier de personen bedanken zonder wie ik dit werk niet had kunnen doen en volbrengen.

Allereerst de grote groep zonder wie dit proefschrift en onderzoek naar de ziekte van Stargardt in het algemeen niet mogelijk was geweest: "de patiënten". Voor mij zijn velen bekenden geworden, maar in dit boek anoniem en als nummers weergegeven. Nu de eerste klinische trial in het Radboudumc van start is gegaan, komt er dan hopelijk toch zicht op een behandeling. Dank voor uw onzelfzuchtige medewerking, want voor de meesten zal een therapie te laat zijn. Door uw medewerking kan het hopelijk wel snel mogelijk worden voor de volgende generatie.

Dan de man zonder wie ik dit werk niet had kunnen doen; Prof. dr. Hoyng, Beste Carel, of ook wel gekscherend "De Grote Nul". Dankjewel voor jouw vertrouwen in mij, al heeft het ons beider afgelopen jaren wat grijze haren gekost. Ik bewonder jouw enthousiasme, jouw oprechtheid om daadwerkelijk een therapie te vinden voor oogaandoeningen, en dat je mensen probeert te verbinden. Om jouw doel te bereiken wals je soms over zaken heen of merk je wat er op de achtergrond gebeurd niet altijd op, maar je hart zit meer dan op de goede plek. Jouw humor werkt soms aanstekelijk. Er zijn weinigen met wie (en ook om...) je zo kan lachen als met jou: de trip naar Moorfields, de vergadering over gentherapie bij ARVO, in jouw Porsche naar Bonn, en dat je gewoon in je gypak met witte sportsokken de afdeling opkomt, et cetera. Je kan trots zijn op de onderzoeksgroep en het werk dat je hebt neergezet. Zonder jou was er nu geen trial in Nederland gaande voor een therapie voor de ziekte van Stargardt. Nogmaals, dank.

En natuurlijk mijn andere promotor: prof. dr. Cremers, beste Frans. Mijn dank dat je mijn tweede promotor wilde zijn. Jij kan de ingewikkeldste nieuwste ontwikkelingen in genetica-land in 30 seconden uitleggen, alsof het niets is. Je bent echt briljant op genetica vlak, maar desondanks ben je nooit naast je schoenen gaan lopen en erg bescheiden. Erg leuk dat je ook interesse hebt getoond in het klinisch werk en samen met mij de polikliniek oogheelkunde bent rond geweest. Je hebt mij veel geleerd over genetica, ABCA4 (cursief!!), maar ook dat je soms gewoon moet doorpakken. Ik waardeer het erg dat ik altijd bij je terecht kon voor advies of gewoon een kleine peptalk. Ook jij hebt een onderzoeksgroep neergezet waar je trots op kan zijn, en waar ik je nog veel succes mee wens.

Prof. dr. Klevering, Beste Jeroen, of “gewoon” BJ: jou zie ik toch een beetje als mijn onofficiële derde promotor. Niet alleen door het onderwerp van destijds jouw promotie waar ik toch grotendeels op verder heb geborduurd, maar met name door je betrokkenheid tijdens mijn PhD en “laatste loodjes”. Dankjewel voor je eerlijkheid, maar vooral ook je sturing, kennis, helderheid en pragmatische instelling. Soms heb ik wel eens gedacht dat je een klein extra X-chromosoom hebt, want je hebt een geheugen waar een vrouw jaloers op kan zijn. Je vergeet echt niets en je houdt ook tig ballen tegelijk in de lucht (spreekwoordelijk). Dankjewel voor je altijd goedbedoelde bemoeienis, uiteindelijk heb ik het altijd gewaardeerd.

Prof. dr. Klaver, Beste Caroline: Rotterdam vs Nijmegen, wij kennen het beiden. Dank dat je destijds mij getipt hebt bij Carel. Ik vind het erg leuk dat je nu ook grotendeels in het Radboudumc werkt en deelneemt in mijn corona. Ik heb ontzettend veel bewondering voor je hoe je alles combineert, van top onderzoek tot je gezin, en dat met alle reisafstanden. Tevens sta je als vrouw meer je mannetje dan de meeste mannen. Chapeau!

Dr. Lambertus, Beste Stanley, Stargardt-maatje: onze (grote) verschillen hebben wij optimaal benut door elkaar juist aan te vullen in het Stargardt onderzoek. Daardoor hebben wij een grote database weten op te bouwen om het Stargardt onderzoek zo veel mogelijk van de grond te krijgen en mooie projecten kunnen doen. Ook de vele congressen en reizen die wij hebben gemaakt waren onvergetelijk. Nu wij beiden weer wat extra tijd hebben, kunnen wij eindelijk BBQ'en in onze tuinen. Terima kasih banyak!

De vele co-auteurs van alle artikelen: dank u allen wel! Dear co-authors: thank you all!

In het bijzonder:

Leden van het RD5000 consortium: een goede landelijke samenwerking om alle retinale dystrofieën in Nederland in kaart te brengen en daardoor ook betere samenwerking op onderzoeksgebied.

Dear German colleagues from the Universitäts-Augenklinik Bonn, especially prof. dr. Frank Holz, prof. dr. Monika Fleckenstein, prof. dr. Schmitz-Valckenberg and of course Moritz. I think we all appreciate that Carel was overruled in the brainstorm session about the name of our consortium “FAST”. Thank you all for the great and pleasant teamwork!

Many thanks to our collaborators at the Moorfields Eye Hospital in London for our successful collaboration: prof. dr. Webster, prof. dr. Moore, prof. dr. Michaelides, and Ana.

Also many thanks to other international collaborators: prof. dr. Stone, prof. dr. Braun, prof. dr. Fritsche, prof. dr. Alikmets, and dr. Zernant.

Tevens dank voor de “genetische” samenwerking met prof. dr. De Baere en Miriam Bauwens van het Universitair Ziekenhuis Gent.

Dr. Oomen, Beste Clasiën, dank voor al jouw inzet op het Stargardt project, van aanvragen schrijven tot overleggen met de ethische commissie. Je bent een onmisbaar manusje-van-alles geweest! Daarnaast kon ik altijd even bij je terecht voor een praatje en loop je over van tips over flora en fauna. Sinds kort heb je een nieuwe baan, ik wens je veel plezier en succes. Dat gaan we nog vieren met de al lang geplande BBQ, die er nu echt van gaat komen.

Prof. Boon, Beste Camiel, dank voor je samenwerking op verschillende projecten. Wat ga jij als een speer! Helaas heb je Nijmegen verlaten voor een mooie carrière in het Westen van het land. Gelukkig houd je door de samenwerkingen nog wel goed contact met Nijmegen. Zo bewijst je deelname in mijn corona dan ook. Ik wens je veel succes (al lijkt je dat bijna niet nodig te hebben) met je verdere carrière en hoop dat je het plezier in je werk weet vast te houden.

Dr. Van Huet, Beste Ramon, over “als een speer gaan” gesproken... dat kan ik ook over jou zeggen! Dank voor het inwerken in het Stargardt onderzoek waar jij toen net aan was begonnen. Van het vertalen van “dinges, dingen, dingetje, ding, je-weet-wel.. dinges” tot databases bouwen. Altijd gezellig met een kopje thee. Blijf vooral zoals je bent, veel plezier en succes als stafarts!

Voor al het statistisch werk kon ik altijd terecht bij “ons Hans”, drs. Groenewoud. Wat een monnikengeduld heb jij. Helaas werd een van je collega’s gedurende het onderzoek ook echt monnik en kwamen daardoor sommige projecten in wat zwaarder weer, waardoor jij veel extra werk op je hebt genomen. Dank voor al je geduldige uitleg en statistisch werk.

Prof. dr. Van der Wilt, beste Gert Jan, dank voor de samenwerking. Tevens gaf jouw kritische blik op het kwaliteit van leven artikel net dat extra zetje dat het nodig had.

Dr. Verhaak, beste Chris, psychologie en oogheelkunde..... het is een gebied waar nog veel in te winnen valt. Dank voor je geduld en samenwerking.

Prof. dr. Den Dunnen, Beste Johan, dank voor je laagdrempelig overleg met betrekking tot de LOVD database.

Ellen en Jelina, “De Stargardt- meisjes”: dank voor het mede opzetten van het Stargardt onderzoek. Ondertussen zijn jullie nu al werkzaam als oogarts (gelukkig in de regio). Het wordt snel weer tijd voor een etentje.

Stéphanie: ik ben blij dat je uit de sollicitatie naar voren rolde als degene die we zochten voor het genetisch database project. Wat een werk heb jij in korte tijd verzet! Er is een mooi artikel uitgekomen en dankzij je inzet werk je nu ook bij de genetica! Veel succes in je verdere carrière.

De collegae van de afdeling genetica: Susanne, Lonneke D, Lonneke HW, Saskia, Alex, Galuh, Mahesh, Imran en Shazia, dank voor de fijne samenwerking en extra uitleg over GGUGAAAUGAAACUAUUUGUGCU.

Marijke: ondertussen ben je van een welverdiend pensioen aan het genieten, maar ik mocht nog op de valreep kennis maken met jouw ervaring in het genetisch lab. Dank voor je begeleiding.

Dr. Collin, Beste Rob, ondertussen weet ik dat je niet de secretaresse bent van Frans... (hoe lang heb ik dat geloofd??). Je doet fantastisch werk op de afdeling, hopelijk komt de AON therapie snel van de grond. Veel succes!

Prof. dr. Den Hollander, Beste Anneke, dank voor je interesse en laagdrempeligheid. Ongelofelijk hoe succesvol jij onderzoek doet. Hopelijk komt er snel een antwoord op de etiologie van leeftijds- gebonden macula degeneratie.

Dr. Albert, Cara Silvia, grazie mille per tutto il lavoro genetico svolto. Ora finalmente avrò piu' tempo per migliorare il mio italiano con te. In bocca al lupo con la tua futura ricerca.

Dr. Sangermano, Caro Riccardo, grazie per la tua collaborazione con "ABCA4". Ti auguro tanto piacere e successo nella tua futura carriera. A presto!

Bert en Bjorn: dank dat ik veelvuldig gebruik kon maken van jullie kamer. En Bert: ik kom snel langs bij de atletiekvereniging om weer aan mijn hardloop skills te werken (op de Pegasus!).

De samenwerking met de afdeling radiologie: dankjewel Mark en Freerk; naast het werk natuurlijk ook voor alle gezelligheid! Dr. Sánchez, Dear Clarisa, thank you for your collaboration. Finally, we can go to Madrid!! Vamos!

De afronding van mijn proefschrift heb ik gedaan tijdens mijn opleiding tot oogarts en daarom ook dank naar mijn opleider: prof. dr. Keunen, beste Jan, dank voor je steun en begrip. Tevens kan jij als de beste iemand een hart onder de riem steken en afsluiten met een high-five. Eind dit jaar ga je met welverdiend pensioen, geniet er van! Of ga je toch kiezen voor een politieke carrière?

Dr. Keijser, Beste Sander, als nieuwbakken opleider maak je zo nog het einde van mijn proefschrift mee. Dank voor je interesse en luisterend oor. Veel succes en plezier met het opleider-schap.

Dr. Tilanus, Caro Mauk, grazie per essere stato il mio mentor. Sono contenta di aver sempre potuto contare su di te e sui tuoi consigli. Ora finalmente avrò il tempo di rispolverare il mio italiano con te.

Dr. Theelen, Beste Thomas, dank voor je laagdrempelig overleg over imaging en wat daar nu precies op te zien is. Helaas hebben we met de "bearfoot" niet gewonnen, misschien weer tijd voor een nieuwe wedstrijd?

Uiteraard ook alle andere stafleden van de afdeling Oogheelkunde in het Radboudumc die ik hierboven niet specifiek heb genoemd: dank voor jullie wijze lessen in het dagelijkse oogheelkunde-leven.

Het ondersteunend personeel, jullie zijn wel de Atlas van de afdeling:

Lief stafsecretariaat; Berna, Francis en Bart in het bijzonder. Jullie zijn echt onmisbaar voor alle planningen, technische zaken, het organiseren van alles, als luisterend oor etc. etc. etc. Ik ben blij dat ik de nieuwe opzet van het secretariaat niet heb meegemaakt, want er valt nu minder te kletsen haha.

Lieve optometristen, Jack en Liesbeth in het bijzonder, dank voor het ondersteunen op de patiënten dagen en dat ik van jullie het oogheelkundig onderzoek van ERG tot fundus foto's maken heb geleerd.

Dames en heren van de administratie: dank voor het altijd weer opspuren van dossiers en andere ondersteunende taken.

Lieve dames van "de VP": tijdens mijn onderzoek hebben wij niet heel veel met elkaar te maken gehad, maar tijdens mij opleiding des te meer. Dank voor het luisterend oor en alle dropjes waardoor ik weer even door kon.

Tijdens mijn onderzoek hebben ook verschillende studenten geholpen. Dankjewel Cécile, veel succes bij je opleiding tot SEH-arts! Lieve Mara, regelen stelt voor jou niks voor. Wat je ook gaat doen, met jou komt het wel goed! En Dyon: blijkbaar heb ik je niet afgeschrikt, maar je zelfs enthousiast genoeg kunnen krijgen om ook een PhD traject te volgen waarin je veel van het Stargardt werk over hebt kunnen nemen. Ik wens je veel succes bij het afronden van je eigen proefschrift en bij je opleiding tot oogarts.

Ook de PhD's die later zijn gestart: Sanne, Vivian, Tom en Anita, bedankt voor de gezelligheid. Esmée en Patty: dank voor het overnemen van het "Stargardt werk". Het is bij jullie in goede handen en fijn te weten dat al het werk door kan gaan en niet verloren gaat. Zet 'm op en veel succes!

PhD's van andere Nederlandse centra: dank voor jullie gezelligheid op cursussen en congressen!

De AIOS oogheelkunde: Carla, John, Dzenita, Anita, Stefan, Jelina, Ellen, Ramon, Artin, Nicole, Yara, Myrte, Mustapha, Martijn, Stanley, Elise, Eveline, Linde, Robert, Freekje, Vivian en Sanne; dank voor jullie gezelligheid en fijne samenwerking. Vooral "team Sesame". Fijn dat wij tegelijk zijn gestart en alles kunnen delen!

Mijn mede PhD's: dank voor het welkom voelen in Nijmegen! Het was een warm bad waarin ik terecht kwam. Wij zijn allemaal erg verschillend, maar desondanks konden wij het allemaal goed met elkaar vinden en hebben wij met elkaar een mooie tijd gehad. Dear "Connie", thank you for your discussions on almost everything. You have a very creative mind, so your career as photographer will be fine! I wish you a lot of success in your new career. Michel, je deed me vaak denken aan de zin "het is een bijzonder kind, en dat is-ie!" Dank voor je soms totaal andere kijk op dingen, maar dat geeft andere mensen dan weer stof tot nadenken. Ik denk dat je in Heidelberg op een mooie plek zit en wens je daar veel succes. Dear Laura, Guapa, thank you for your nice talks, you are a very kind person. I am

happy that you are continuing your work as post-doc in Nijmegen. Lieve Myrte, je bent ontzettend collegiaal en kan jezelf soms totaal wegcijferen voor ‘het grote goed’. Dank voor je scherpzinnigheid en gezelligheid zowel binnen als buiten het werk. Ik denk dat de nieuwe bewoners nog steeds confetti tegenkomen (ik vond het een goed idee, haha). Lieve Yara, je bent een fijne collega, ook buiten het werk kunnen we het goed met elkaar vinden en dat waardeer ik. Ik wens je veel succes in je verdere (academische) carrière! Lieve Nicole, ik bewonder je doelgerichtheid en effectiviteit. Ik denk dat weinig mensen weten dat achter jou “als machine”, juist een hele lieve persoonlijkheid schuilt. Dankjewel voor je fijne samenwerking. Lieve Roos, dank voor wie je bent. Ik heb denk ik nooit zo met iemand gelachen tijdens het winkelen als met jou in de Victoria’s Secret en dankzij jou heb ik Mickey Mouse sneakers in mijn kast. Blijf wie je bent en veel succes in je verdere loopbaan! En dan “mijn” Zwelgjes: dankjulliewel voor jullie vriendschap. Als mijn PhD klaar is (als laatste van het stel), dan is er weer tijd voor veel leuke dingen: escape room, eten, drinken, feestjes, eten, drinken, winkelen, eten, drinken. Lieve Maartje, dank voor je fijne aanwezigheid en dat ik bij je terecht kan. Lieve Freekje, gelukkig hebben wij dezelfde humor, dan vindt iemand het ten minste nog leuk. Ik ben blij dat je weer terug bent uit Amerika en nu ook bent begonnen aan de opleiding tot oogarts. Lieve Eveline, “dat-dacht-ik-ook!”, wat fijn dat we samen hetzelfde traject doorlopen. Dank voor je steun en gezelligheid.

“Oogappeltjes”: fijn om het met elkaar buiten het werk, alsnog over oogheelkunde te hebben, haha.

Linda en Ann Laure: dank voor jullie gezelligheid, jullie steun toen het even niet lekker liep en de introductie in HET hockeyteam.

Het hockeyteam was (en is) in Nijmegen toch mijn grote afleiding buiten het ziekenhuis. Bedankt meidties (+ “Tabata” Joost) van het allerleukste hockeyteam: Union Dames “11”. Ik ben ontzettend blij dat ik in dit team terecht ben gekomen. We zijn een echt vriendinnen-team, we hebben veel samen gelachen en gehuild (maar gelukkig vooral het eerste, dat laatste doen nu de vele baby’s). Komend seizoen zal ik weer een stuk fitter aanwezig zijn en mij vaker op feestjes kunnen melden! Ik hoop dat we nog lang naar festivals gaan, eten, feesten, vakanties samen vieren, nog meer lekker eten etc. etc.

Mijn vrienden uit “de goeie ouwe tijd”. Lieve Charlotte, Erik, Anne Fleur, Joost, Renske, Gijs, Pauline, Annelieke, Heleen, Freija, Esther, Jan Maarten, Jacqueline, Aimée en Karmijn: dank voor jullie vriendschap. Altijd fijn dat in de periode van mijn sociale afwezigheid, jullie er toch gewoon zijn en blijven. Er moet weer wat quality time worden ingehaald!



Ik ben blij dat op deze dag 2 lieve vriendinnen die ik al zo lang ken mij bij staan. Jullie kennen mij door-en-door, heb ik aan een blik of half woord genoeg, kan ik mijzelf zijn en we hebben elkaar altijd gesteund en gesupporterd.

Lieve Charlotte: als klinisch geneticus begrijp jij hoofdstuk 3 als de beste, haha. Ondanks ons drukke leven hebben wij gelukkig nog oog en tijd voor elkaar. Hoe jij de balans houdt van jouw werk en privéleven is erg knap. Je bent een topper!

Lieve Anne Fleur: “niet lullen, maar poetsen” is je op het lijf geschreven. Daarnaast sta je altijd voor ieder klaar die je lief is (en ook niet lief), en heb je ook in moeilijke tijden je altijd staande gehouden. Je ouders zullen, net als ik, trots op je zijn!

Mijn familie: dank voor jullie aanhoudende belangstelling en support. Ik heb heel wat visites en feestjes de laatste tijd moeten laten schieten, maar vanaf nu kan ik er weer gezellig bij zijn!

Lieve pap en mam, ik had niet verwacht dat ik jullie zo zou missen. Ik beschouwde mijzelf wel als een globetrotter, maar werken en wonen aan de andere kant van het land en niet zomaar even langs kunnen gaan, viel toch wat zwaarder dan ik van tevoren in had geschat. Gelukkig zijn jullie beiden met pensioen en toen jullie merkten dat ik het toch wel erg fijn vond om jullie vaker te zien, zijn jullie vaak deze kant op gekomen. Bedankt voor jullie onvoorwaardelijke steun en hulp. Jullie hebben mij nooit gepusht of gestuurd, maar altijd vertrouwen in mij gehad in wat ik wilde doen. Ik ben blij dat ik jullie nog “heb” en hoop dat jullie er nog heel lang zijn in goede gezondheid.



